



2017

# GENE EXPRESSION PROFILES REVEAL ALTERNATIVE TARGETS OF THERAPEUTIC INTERVENTION FOR THE TREATMENT OF DRUG-RESISTANT NON- SMALL CELL LUNG CANCERS

Madeline J. Krentz Gober

University of Kentucky, madeline.krentz@uky.edu

Author ORCID Identifier:

 <https://orcid.org/0000-0001-7761-6741>

Digital Object Identifier: <https://doi.org/10.13023/ETD.2017.309>

**[Click here to let us know how access to this document benefits you.](#)**

---

## Recommended Citation

Krentz Gober, Madeline J., "GENE EXPRESSION PROFILES REVEAL ALTERNATIVE TARGETS OF THERAPEUTIC INTERVENTION FOR THE TREATMENT OF DRUG-RESISTANT NON-SMALL CELL LUNG CANCERS" (2017). *Theses and Dissertations--Pharmacy*. 78.

[https://uknowledge.uky.edu/pharmacy\\_etds/78](https://uknowledge.uky.edu/pharmacy_etds/78)

**STUDENT AGREEMENT:**

I represent that my thesis or dissertation and abstract are my original work. Proper attribution has been given to all outside sources. I understand that I am solely responsible for obtaining any needed copyright permissions. I have obtained needed written permission statement(s) from the owner(s) of each third-party copyrighted matter to be included in my work, allowing electronic distribution (if such use is not permitted by the fair use doctrine) which will be submitted to UKnowledge as Additional File.

I hereby grant to The University of Kentucky and its agents the irrevocable, non-exclusive, and royalty-free license to archive and make accessible my work in whole or in part in all forms of media, now or hereafter known. I agree that the document mentioned above may be made available immediately for worldwide access unless an embargo applies.

I retain all other ownership rights to the copyright of my work. I also retain the right to use in future works (such as articles or books) all or part of my work. I understand that I am free to register the copyright to my work.

**REVIEW, APPROVAL AND ACCEPTANCE**

The document mentioned above has been reviewed and accepted by the student's advisor, on behalf of the advisory committee, and by the Director of Graduate Studies (DGS), on behalf of the program; we verify that this is the final, approved version of the student's thesis including all changes required by the advisory committee. The undersigned agree to abide by the statements above.

Madeline J. Krentz Gober, Student

Dr. Esther P. Black, Major Professor

Dr. Dave Feola, Director of Graduate Studies

---

GENE EXPRESSION PROFILES REVEAL ALTERNATIVE TARGETS OF  
THERAPEUTIC INTERVENTION FOR THE TREATMENT OF DRUG-  
RESISTANT NON-SMALL CELL LUNG CANCERS

---

DISSERTATION

---

A dissertation submitted in partial fulfillment of the  
requirements for the degree of Doctor of Philosophy  
in the College of Pharmacy at the  
University of Kentucky

By:

Madeline J. Krentz Gober  
Lexington, Kentucky

Director:

Dr. Esther P. Black, Ph.D., Professor of Pharmaceutical Science  
Lexington, Kentucky

2017

Copyright © Madeline Krentz Gober, 2017

## ABSTRACT OF DISSERTATION

### GENE EXPRESSION PROFILES REVEAL ALTERNATIVE TARGETS OF THERAPEUTIC INTERVENTION FOR THE TREATMENT OF DRUG-RESISTANT NON-SMALL CELL LUNG CANCERS

More than 80% of lung cancer patients die from drug-resistant, metastatic disease. Our focus is to identify new drug targets and alternative therapeutic strategies to improve outcomes for this majority of lung cancer patients. We aimed to satisfy the need for new treatment approaches by leveraging the information gained from the development of two multigene biomarker predictors of Epidermal Growth Factor Receptor Inhibitors (EGFRI) response in Non-Small Cell Lung Cancer (NSCLC). From these data, we first identified TGF $\beta$  signaling as a possible modulator of EGFRI resistance and I hypothesized that TGF $\beta$  signaling participates in the development and maintenance of erlotinib-resistance and -sensitivity and regulates the gene expression of the miRNA comprising the signature of response. To identify novel putative treatment strategies for overcoming EGFRI resistance, we leveraged the raw data used to build the EGFRI-response predictors of NSCLC cells with divergent EGFRI responses using mathematical and protein-protein interaction modeling to identify a network of deregulated proteins in EGFRI-resistant cells. From this analysis, we identified a drug combination that is kills EGFRI-resistant NSCLC cells and further study will confirm if this novel strategy translates into a clinically utilizable option for the treatment of EGFRI-resistant NSCLC.

KEYWORDS: Pharmacogenomics; EGFR; TGF $\beta$ ; Non-Small Cell Lung Cancer; Casein Kinase 2; CK2 and MEK combination treatment.

Madeline Krentz Gober

---

Student's Signature

July 10<sup>th</sup> 2017

---

Date

GENE EXPRESSION PROFILES REVEAL ALTERNATIVE TARGETS OF  
THERAPEUTIC INTERVENTION FOR THE TREATMENT OF DRUG-  
RESISTANT NON-SMALL CELL LUNG CANCERS

By:

Madeline Krentz Gober

Dr. Esther P. Black

Director of Dissertation

Dr. Dave Feola

Director of Graduate Studies

July 10<sup>th</sup> 2017

Date

## ACKNOWLEDGEMENTS

This dissertation could not have been completed without the dedication and support of many friends, colleagues, mentors, and family.

First, I thank my advisor, Dr. Penni Black for encouraging and allowing me to grow as a well-rounded individual rather than just a bench top scientist. Thank you for forcing me to face the things I was afraid of and allowing me to embrace my creativity, develop my own directions and make this body of work my own.

To my committee, thank you each for sharing your unique backgrounds, expertise and styles with me. To Dr. Dave Feola, thank you for being warm and supportive, but also judicious. To Dr. Sylvie Garneau-Tsodikova, thank you for being inviting, and sensible but ambitious. Thank you for also sharing my love of civil service and helping me develop new community-based programs here at UK. To Dr. Rina Plattner, thank you for being honest and kind but critical.

To our collaborators, Dr. Katherine Thompson and Dr. Robert Flight, thank you for helping me see, model and analyze our data in new ways. Without your input, a substantial fraction of this work would not have been possible.

I would like to thank my family for being so supportive. I thank my parents, Kim and Doug Krentz, who encouraged me to be determined and creative and taught me that I could achieve anything I was willing to work hard enough for.

I thank my husband, Redding Gober, for encouraging me to pursue anything that makes me happy and always daring me to dream bigger. I asked a lot when I asked you to move this far with me, but I think we're both happy that you did and we're better for it. I firmly believe that together we can accomplish anything we want to and I'm happy you share my life ambitions. Thank you also for tolerating that horses are the key to my sanity and for embracing my passion.

Finally, to my friends, lab mates, and department colleagues, thank you for all that you've done to make this possible. It truly takes a village to raise a successful PhD student, and I can't thank you all enough for helping me troubleshoot my problems, sharing your reagents and instruments, participating in my adventures teaching third grade science, and for simply listening when I needed to gripe. I solved more problems than I can count by simply walking down the hall and asking someone and I can't thank you all enough for being there when I needed you most.

## TABLE OF CONTENTS

---

ACKNOWLEDGMENTS.....	iii
LIST OF TABLES.....	viii
LIST OF FIGURES.....	ix
CHAPTER 1 .....	1
A LUNG CANCER OVERVIEW.....	1
Overview of Cancer .....	1
Lung Cancer Epidemiology .....	3
Common Driver Mutations in Lung Tumors .....	4
Targeted Therapies in NSCLC.....	12
B EPIDERMAL GROWTH FACTOR RECEPTOR (EGFR) .....	17
EGFR Activation and Signaling.....	17
EGFR Mutations in Non-Small Cell Lung Cancers (NSCLC).....	20
Inhibition of EGFR in Lung Cancer Therapy.....	22
C TRANSFORMING GROWTH FACTOR BETA (TGF $\beta$ ) BIOLOGY AND SIGNALING.....	26
TGF $\beta$ Signaling .....	26
The Role of TGF $\beta$ in Lung Cancer .....	30
Targeting TGF $\beta$ Signaling in Cancer: A Paradox Problem .....	34

D	CASEIN KINASE 2 (CK2) BIOLOGY .....	35
	The Kinase .....	35
	CK2 in Cancer .....	38
	Therapeutic Targeting of CK2 in Cancer .....	43
E	PROJECT OVERVIEW .....	44
CHAPTER 2	.....	49
A	OVERVIEW .....	49
B	METHODS .....	51
C	RESULTS .....	54
	Most Signature miRNA Promoters Contain Smad Binding Elements.....	54
	TGF $\beta$ -mediated Smad Signaling has an Opposing Phenotype in Erlotinib Resistant and -Sensitive Cell Lines.....	55
	TGF $\beta$ Treatment Induces an EMT Protein Expression Switch in A549 but not in PC9.....	56
	TGF $\beta$ Induces Smad 4 Binding to Putative SBEs in the Promoter of mir-141/200c in Erlotinib-Sensitive Cells.....	57
	Time, Not Treatment, Alters the Expression of the Candidate microRNAs.....	57
	Time, Not Treatment, Alters the Cell Cycle Position of A549 and PC9 Cells .....	58
	TGF $\beta$ Activation of Non-Canonical Effectors ERK1/2 and AKT Differs Between A549 and PC9 .....	59
D	DISCUSSION .....	60
E	CONCLUSIONS .....	64
CHAPTER 3	.....	96
A	OVERVIEW .....	96

B	METHODS .....	97
C	RESULTS.....	99
	TGF $\beta$ Treatment Has Opposing Effects on Migration in Erlotinib-Sensitive versus Erlotinib-Resistant NSCLC Cells .....	100
	TGF $\beta$ Inhibition Significantly Impairs Wound Healing Ability in PC9 Cells.....	100
	TGF $\beta$ Influences Erlotinib Resistance Differently between A549 and PC9 Cells .....	100
D	DISCUSSION.....	101
E	CONCLUSIONS .....	102
CHAPTER 4 .....		109
A	OVERVIEW .....	109
B	METHODS .....	110
C	RESULTS.....	113
	CK2 Connects the miRNA and mRNA Signatures of EGFR1 Sensitivity.....	114
	CK2 Inhibition Induces Greatest Cell Death in KRAS Active NSCLC.....	115
	CK2 and the Members of the EGFR-MAPK-ERK Signaling Cascade Appear to Function Exclusively of one Another .....	115
	Combinatorial Targeting of CK2 and MEK Induces Apoptosis in KRAS Active NSCLC Cells .....	116
D	DISCUSSION .....	117
E	CONCLUSIONS .....	120
CHAPTER 5 .....		129
A	OVERVIEW .....	129
B	METHODS .....	130
C	RESULTS.....	131

CX-4945 increases erlotinib-sensitivity in PC9 but not in A549 cells.....	131
D DISCUSSION .....	132
E CONCLUSIONS .....	132
CHAPTER 6 .....	136
A SUMMARY OF RESULTS.....	136
B EXPERIMENTAL LIMITATIONS .....	142
Genomic Modeling of the Deregulation of EGFR- Resistant NSCLC.....	142
Biological and Pharmacological Testing of the Hypotheses Identified <i>in silico</i> .....	143
C CONTRIBUTION TO THE FIELD.....	143
D CONCLUSIONS .....	146
APPENDIX I: SUPPLEMENTARY FIGURES FOR CHAPTER 2.....	147
APPENDIX II: SUPPLEMENTARY FIGURES FOR CHAPTER 4.....	154
APPENDIX III: SUPPLEMENTARY FIGURES FOR CHAPTER 5.....	225
REFERENCES.....	234
VITA.....	279

## LIST OF TABLES

---

Table 1.1: Targeted therapies in NSCLC. ....	16
Table 4.1: G1-X-G2 Analysis-Induced EGFR1 Resistance Network Members that interact with CK2 $\alpha$ or CK2 $\alpha'$ within one edge and are pharmacologically actionable. ....	124
Supplementary Table I-1: Output of 5-way ANOVA analysis. (Data pairs with Supplementary figures I-4 and I-5).....	147
Supplementary File I-1: Experimental Ct Averages. ....	150
Supplementary Table II-1: Interacting mRNA:miRNA genes (100) from the Feasible Solutions (FS) analysis. ....	154
Supplementary Table II-2: Initial FS candidates that interact with EGFR. ....	159
Supplementary Table II-3: G1-X-G2 Analysis-Induced EGFR1 Resistance Network Members. ....	162
Supplementary Table II-4: G1-X-G2 Analysis-Induced EGFR1 Resistance Network Members that interact with CK2 $\alpha$ or CK2 $\alpha'$ within one edge.....	180
Supplementary Table II-5: G1-X-G2 Analysis-Induced EGFR1 Resistance Network Members that interact with CK2 $\alpha$ or CK2 $\alpha'$ within one or two edges. ....	183
Supplementary Table II-6: G1-X-G2 Analysis-Induced EGFR1 Resistance Network Members that do not interact with CK2 $\alpha$ or CK2 $\alpha'$ .....	199
Supplementary Table II-7: Induced network members sorted by putative collective activity of community members. ....	200

## TABLE OF FIGURES

---

Figure 1.1: Oncogenic driver mutations and percentage of occurrence in lung adenocarcinomas.....	6
Figure 1.2: Tumor suppressors that are commonly lost in lung adenocarcinomas. ....	11
Figure 1.3: EGFR Signaling Pathways.....	19
Figure 1.4: TGF $\beta$ Signaling Pathways. ....	28
Figure 1.5: CK2 Signaling Pathways.....	37
Figure 1.6: Cross talk amongst TGF $\beta$ , EGFR, and CK2 Signaling. ....	47
Figure 2.1: Signature microRNA genes contain SBE elements .....	66
Figure 2.2: Total Smad expression, Smad activation and EMT program marker expression varies with TGF $\beta$ or inhibitor treatment. ....	67
Figure 2.3: TGF $\beta$ induces Smad 4 binding to SBEs in the promoter of mir-200/141 in PC9 cells.....	70
Figure 2.4: Time of TGF $\beta$ treatment reflects changes in endogenous miRNA gene expression.....	72
Figure 2.5: A549 and PC9 cells exit the cell cycle regardless of treatment with TGF $\beta$ or SB-431542 .....	74
Figure 2.6: TGF $\beta$ modulation differentially impacts ERK and AKT activation between A549 and PC9 .....	76
Figure 2.7: Signature microRNA genes contain SBE elements. ....	77
Figure 2.8: TGF $\beta$ induces a mesenchymal phenotype in A549, but inhibition generates an EMT-intermediate phenotype in erlotinib-sensitive, PC9 cells. ....	78
Figure 2.9: E-cad expression in response to treatment.....	79
Figure 2.10: Normalized Ct values demonstrate that time change, not individual treatment, affects endogenous miRNA expression changes in A549 and PC9 cells. ....	81
Figure 2.11: Time of treatment has the most significant influence on miRNA expression changes.....	82
Figure 2.12: A549 cell counts following corresponding treatments and time points comparing growth in 1% and 10% serum media.....	83

Figure 2.13: PC9 cell counts following corresponding treatments and time points comparing growth in 1% and 10% serum media.....	87
Figure 2.14: Densitometry of Figure 2.6 western blots. (A).....	91
Figure 2.15: Signature microRNA genes contain both putative SBE elements and putative ELK1 binding sites. ....	95
Figure 3.1: TGF $\beta$ treatment influences the migratory ability of A549 and PC9 cells.....	104
Figure 3.2: LY-2109761 alters wound healing capabilities of A549 and PC9 cells. ....	105
Figure 3.3: TGF $\beta$ treatment alters erlotinib response in A549 and PC9 cells. ....	107
Figure 4.1: The G1-X-G2 expanded network links nearly every EGFR1 resistance described to date.....	122
Figure 4.2: NSCLC cells resistant to EGFR1 are most sensitive to CK2 inhibition. ....	125
Figure 4.3: Co-treatment with CX-4945 and MEK inhibitor, AZD6244, induces cell death in KRAS active NSCLC. ....	127
Figure 4.4: Screening for synergistic interactions between the CK2 inhibitor, CX-4945, and the MEK inhibitor, AZD6244.....	128
Figure 5.1: TGF $\beta$ treatment in combination with CX-4945 alters erlotinib response in A549 and PC9 cells. ....	134
Figure 6.1: The Impact of Co-Targeting MEK and CK2 on Cancer Signaling Pathways. ....	145
Supplementary Figure II-1: NSCLC cells most sensitive to CX-4945 have decreased CSNK2B expression. ....	222
Supplementary Figure II-1.....	223
Supplementary Figure II-1.....	224
Supplementary Figure III-1: Comparison of CX-4945 treatment on erlotinib response.	225

# CHAPTER 1

## A. LUNG CANCER OVERVIEW

### Overview of Cancer

Cancer is a group of genetic diseases that are caused by DNA damage and epigenetic changes. These changes result in cells that are characterized by uncontrolled growth, unchecked survival, and invasion into surrounding and distant tissues.

Cancers are classically characterized by six hallmarks with an additional two hallmarks and two tumor-enabling characteristics that are increasingly recognized (1):

- 1) Growth signal autonomy: Normal cells require direction of external growth factors to drive replication. Cancers circumvent this need by mutational loss of growth factor pathway regulation and sometimes autonomous secretion of and response to growth factors.
- 2) Genomic instability: This is a tumor-enabling characteristic. Tumor cells gain increasing numbers of mutations and epigenetic changes that are selected for by pressure over successive generations.
- 3) Evasion of growth and proliferation inhibitory signals: The majority of the body's healthy cells are not actively dividing. This is due to their response to growth inhibitory signals that are required to maintain homeostasis and prevent unwanted growth. Cancers develop acquired mutations to evade these inhibitory signals.
- 4) Tumor promoting inflammation: This is another tumor-enabling characteristic. Pathways that respond to signals from the immune system that are intended to induce cell death are co-opted by tumors to enhance tumorigenesis and progression.
- 5) Evasion of apoptosis, or programmed cell death: Normal cells undergo apoptosis in response to events like DNA damage. Cancer cells evade apoptosis generally through loss of apoptotic regulators.
- 6) Avoiding immune destruction: The immune system can play a role of identifying and destroying emerging neoplasias. Tumors develop methods of locally disabling immune surveillance mechanisms.

## CHAPTER 2

- 7) Gain of unlimited replication potential: Normal cells are programmed to stop dividing (senesce) or undergo apoptosis following too many rounds of DNA replication and subsequent cell division events.
- 8) Angiogenesis, or the formation of new blood vessels: All cells require blood vessels to supply oxygen and nutrients and cancer cells induce the formation of new blood vessels in order to supply their rapidly growing numbers.
- 9) Deregulated cellular energetics: The perpetual proliferation of tumor cells requires increased energy metabolism from a variety of sources (e.g., carbohydrates or lipids) to produce additional ATP demand to fuel growth. They also require larger amounts of cellular building blocks like nucleotides. Tumor cells adjust cellular metabolism pathways to meet increased energy requirements by the tumor.
- 10) Invasion and metastasis: The healthy cells only migrate for the purposes of development and wound healing. Cancer cells exploit the pathways that regulate these processes in order to invade surrounding tissues with the ultimate goal of colonizing tissues at distant sites from the initial, primary tumor site.

Cancers are driven by a series of two types of mutations: 1) gain-of-function mutations including amplification events resulting in oncogenic drivers, also known as oncogenes, and 2) loss-of-function mutations resulting in loss of genes responsible for regulating proliferation and survival, known as tumor suppressors (1). Proto-oncogenes, or genes that can become oncogenic with a gain-of-function mutation in one copy of the gene, are often involved in growth and proliferation pathways. Tumor suppressor genes require the loss-of-function of at least one (for haploinsufficiency and lower gene dose), but more often two copies of the gene (complete loss) in the genome. Tumor suppressors are most often growth inhibitors, responsive to growth inhibitors, or related to DNA repair or cell cycle check points (2). Cancers were initially described as having an “oncogene addiction” when cell survival is dependent on the constant over-activation of oncogenic signaling pathways (3, 4). However, it is growing increasingly evident that tumors are incredibly heterogeneous. Therapeutically targeting only the “oncogene addiction” leads to resistance arising from the selection of tumor cells that have alternative means of functioning around the inhibited oncogene (4). Moreover, not all tumors have an evident single “oncogenic addiction” and it is clear that successful tumor treatment will require the therapeutic-targeting of multiple oncogenic drivers and sources of resistance

## CHAPTER 2

simultaneously or sequentially (4). These specific aberrations in the cancer genome are paramount to cancer genesis, adaptability and progression and will be described in depth later in this chapter.

Cancer progression is marked by the extent of primary tumor invasion into the surrounding tissues. In the later stages, after heavily invading surrounding tissues, tumor cells gain the potential to survive beyond the stroma. This process primes them to enter nearby blood vessels (intravasation) and be transported to distant organs via the circulatory or lymphatic system (5). Following transport, cancer cells exit blood vessels by a process called extravasation and either lie dormant or begin colonizing near the site of exit (5). The colonization of distant organs is called metastasis and is a hallmark of the latest stages of the disease most often resulting in death (1, 5). Lung cancers are particularly deadly because the majority of patients present in the later stages of the disease where metastatic colonization is already in progress or distant lesions have already been confirmed (6).

### **Lung Cancer Epidemiology**

Lung and bronchial cancers represent a significant health issue both in the United States as well as abroad and are the number one cancer killer in the world (7). Around 14% of cancer diagnoses each year are lung and bronchial cancers (6, 8). Lung and bronchial cancers are second in the number of diagnoses in both men and women in the U.S. each year behind the gender specific cancers, prostate and breast (6, 8). However, 26-28% of the cancer deaths each year are attributable to lung and bronchial cancers in both men and women, which exceeds that of any other cancer (6, 8). The high incidence of lung cancer mortality correlates with the fact that 80-85% of patients present in the later stages of the disease (6, 8).

The Commonwealth of Kentucky has one of the highest incidences of lung cancer in the U.S. with an exceptionally high rate of lung cancer diagnoses in the rural, underserved, Appalachian communities (9). Eighty-two percent of lung cancer deaths are directly attributable to smoking (10). Frequent indirect smoke exposure also contributes to lung cancer development (10). The Commonwealth of Kentucky has one of the highest smoking rates in the U.S. (6, 7). Kentucky agriculture has historically relied heavily on

## CHAPTER 2

tobacco as a major state crop. The federal deregulation of tobacco occurred in the mid-2000s causing many local farmers to stop growing the crop while the local economy suffered accordingly. Many Kentucky smokers still consider smoking to be a form of boosting the local economy despite the decrease in working tobacco farms. Other environmental sources of carcinogen exposure leading to lung cancer include radon, chloromethyl ethers, asbestos, arsenic and other outdoor pollution namely by industry and vehicles (11). Of these, high radon levels are also commonly seen in Kentucky (12). Moreover, reliance on the rural industry of coal mining exposes many residents of underserved Appalachia to additional industrial carcinogens including increased radon levels and heavy metal exposure at jobsites (11, 13). The mining industry also introduces these carcinogens into the environment where they are commonly found in the air, soil and in water runoff further compounding the problem (13).

Lung cancers present as different histological subtypes that are broken down into two broad categories: 1) Small Cell Lung Cancers (SCLC) and 2) Non-Small Cell Lung Cancers (NSCLC) which encompass adenocarcinomas, bronchioalveolar carcinomas, squamous cell carcinomas, and large cell carcinomas. Adenocarcinomas represent the largest percentage of lung cancer cases (14).

### **Common Driver Mutations in Lung Tumors**

Tobacco smoke is the main contributing factor to DNA mutagenesis leading to lung cancer pathogenesis, but other environmental factors including radon, occupational lung carcinogens and indoor and outdoor pollution contribute to lung cancer development (11). The carcinogenic activity of tobacco smoke is largely caused by three specific groups of chemicals: 1) tobacco-specific nitrosamines, 2) polycyclic aromatic hydrocarbons, and 3) aromatic amines (15). As lung cancers are largely driven by carcinogen exposure resulting in DNA damage and epigenetic alterations, they are highly heterogeneous and have one of the highest numbers of somatic mutations among cancers (16, 17). This high level of heterogeneity among lung tumors complicates molecular testing efforts for drug assignment and leads to quick cancer evolution in response to treatment (18).

In recent years, an increasing number of driver mutations in lung cancers have been identified. Growth promoting drivers of lung cancers currently known include Kirsten

## CHAPTER 2

rat sarcoma viral oncogene homolog (KRAS), the epidermal growth factor receptor (EGFR), BRAF, MEK-1, HER2, MET, multiple members of the PI3K/AKT/mTOR pathways, ALK, ROS1, and rearranged during transfection (RET) (19). Prominent tumor suppressors found to be inactivated in lung cancers that are currently known include p53, phosphatase with tensin homology (PTEN), members of the p16<sup>INK4A</sup>/RB pathway and STK11. Other less prevalent oncogenes currently being studied in NSCLC include fibroblast growth factor receptor 1 (FGFR1), discoidin domain receptor 2 (DDR2), MYC family member amplification, and amplification of BCL2 (19).

### *The Oncogenic Drivers of the Hallmarks of Cancer in Lung Tumors*

Most lung adenocarcinomas harbor known oncogenic driver mutations (20). The activation of proto-oncogenes into oncogenes often occurs by gene amplification, structural rearrangements forming fusion proteins with other genes, deletions and point mutations (19). Signaling by oncogenes often results in “oncogene addiction”, making those proteins ideal candidates for targeted therapy (3, 4). Unfortunately, the signaling pathways regulated by oncogenes and tumor suppressors are commonly interconnected and the mutational evolution of tumors in response to disease progression and/or therapeutic selection pressure adds complexity to this increasingly intricate relationship (19).

KRAS is a member of the RAS family of proto-oncogenes that include KRAS, NRAS, and HRAS. RAS family members encode G-proteins that bind guanosine diphosphate (GDP) in inactive form. Upon activation of an upstream receptor tyrosine kinase (RTK), they switch to bind guanosine triphosphate (GTP) allowing the activation of many downstream pathways (19). These pathways include the mitogen-activated protein kinase (MAPK) pathway through ERK and phosphoinositol-3-kinase (PI3K)/AKT/mTOR pathway (21). Activation mutations in KRAS are the result of mutations that alter the GTPase function of the protein hindering KRAS-GTP from being inactivated into KRAS-GDP (19, 21). KRAS activation mutations occur in 25-40% of lung adenocarcinoma tumors making them the most common oncogenic alterations in lung adenocarcinomas (19, 22). Meta-analyses have shown that KRAS mutated tumors are resistant to EGFR inhibitors (EGFRI) as KRAS signaling is downstream of the EGFR RTK (23). Mutations in HRAS

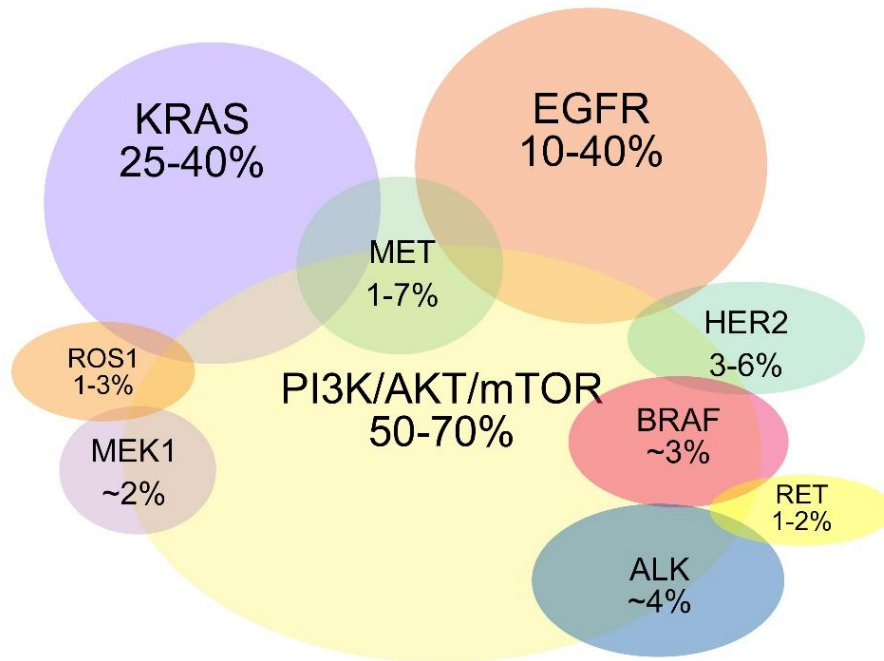


**Figure 1.1: Oncogenic driver mutations and percentage of occurrence in lung adenocarcinomas.**

## CHAPTER 2

and NRAS are rare in lung adenocarcinomas (24). KRAS mutations are more common in western populations, males and smokers (25, 26). KRAS driver mutations very rarely occur in lung adenocarcinomas concurrently with EGFR activation mutations (27).

BRAF is a serine/threonine protein kinase that is downstream of KRAS signaling in the MAPK-ERK signaling pathway (28). Activated BRAF activates MEK1/2, and MEK1/2 subsequently activates ERK1/2 which regulates transcription factors including c-Jun and ELK1 (28). BRAF mutations only occur in about 3% of NSCLC with mutual exclusivity from KRAS and EGFR mutations (19, 27). Similar to what is observed in melanoma and colorectal cancers, 50-75% of BRAF mutations in lung adenocarcinomas are the V600E activation mutation in the kinase domain of the protein (19, 29). Other BRAF mutations observed in the kinase domain include D594G and L596R and mutations also occur in the activation domain (G-loop) of the protein including G465V and G468A (28, 30).

MEK1 (also known as MAPK1) is a serine/threonine kinase downstream of RAS in the MAPK-ERK signaling cascade (31). Somatic mutations resulting in activation of MEK1 are rare and found in less than 2% of lung adenocarcinomas. MEK mutations are most often activation mutations in exon 2 that is not part of the kinase domain (32). Importantly, NSCLC harboring these MEK1 mutations have been shown to be sensitive to anti-MEK therapies (32).

Human epidermal growth factor receptor 2 (HER2/ERBB2) is a member of the ERBB/EGFR family of receptor tyrosine kinases. HER2 does not commonly bind ligand directly as most ligands have a low affinity for the HER2 receptor (33). Instead, HER2 binds to other ligand bound receptors of the same family and is a preferential heterodimerization partner by other ERBB family receptors (33, 34). HER2 signals through a variety of downstream signaling pathways including STAT, PI3K/ATK/mTOR, and MAPK-ERK (35). HER2 mutations in NSCLC are observed as an overexpression in 20% of cases, as an amplification in 2%, and activation mutations are only observed in 1-4% of NSCLC (36, 37).

MET, also known as hepatocyte growth factor receptor, is a proto-oncogene that encodes a membrane-spanning tyrosine kinase receptor (38). Like many other RTKs, MET binds its ligand and homodimerizes, which results in the activation of the tyrosine

## CHAPTER 2

kinase domain. It is able to activate Ras-MAPK-ERK, PI3K-AKT, and c-SRC pathways (38). MET amplification is a common mechanism of acquired resistance to EGFR inhibitor (EGFRI) treatment and is observed in ~20% (39, 40). MET amplifications are observed in treatment naïve patients in approximately 1-7% of tumors (40, 41). MET amplification occurrence has been reported as high as 21% in one study of a treatment-naïve cohort of western Europeans (all non-Asian), 93% of whom were smokers (42). MET amplification leading to acquired EGFRI resistance occurs by aberrant or unregulated PI3K-AKT signaling. Tumors harboring a MET amplification have been shown to drive and maintain the PI3K/AKT signaling cascade thereby bypassing EGFRI blockade (19). For this reason, one of the mechanisms proposed to overcome acquired EGFRI resistance in NSCLC is co-treatment with EGFRI and MET inhibitors (39).

The phosphoinositol-3-kinase (PI3K)/AKT and mTOR signaling pathways are responsible for cell survival, proliferation, differentiation, adhesion and motility and are also frequently mutated in NSCLC (43). Many of the receptor tyrosine kinases are able to activate this pathway including EGFR, MET, HER2, insulin-like growth factor receptor, platelet-derived growth factor receptor, and transforming growth factor receptor beta (TGF $\beta$ ) (44). Activated RTKs recruit PI3K to the membrane where it is responsible for the phosphorylation of phosphatidylinositol 4,5-bisphosphate (PIP<sub>2</sub>) into phosphatidylinositol 3,4,5-triphosphate (PIP<sub>3</sub>). Active PIP<sub>3</sub> recruits AKT to the membrane where it can be phosphorylated by PI3K and/or mTOR (45). RAS family members have been shown to be able to activate PI3K directly contributing to the cross talk between PI3K/AKT/mTOR and MAPK-ERK signaling cascades (45). The PI3K/AKT/mTOR signaling pathway is commonly deregulated in NSCLC, and other cancers, with 50-70% of NSCLC harboring PI3K pathway member mutations (22, 44). Oncogenic mutations in PI3K and AKT have been reported with amplification of the PIK3CA gene, which encodes the alpha isoform of the PI3K catalytic subunit, most commonly observed (44). PIK3CA mutations largely involve the catalytic domain and occur in 1-3% of NSCLC (22). Mutations in AKT are rare, only being reported in 0.5-2% of NSCLC (22). Loss of PI3K regulation by the tumor suppressor component, PTEN, also occurs and will be discussed further below (45).

ALK is a receptor tyrosine kinase found commonly with a gain-of-function mutation in NSCLC resulting in constitutively active ALK signaling (46). ALK mutations are most commonly rearrangement mutations resulting in a fusion of the intracellular kinase domain

## CHAPTER 2

with a different gene, echinoderm microtubule associated protein-like 4 (EML4) (47, 48). ALK-EML4 fusion proteins come in a number of variants, but the most commonly described is the fusion of exons 1-13 of EML4 joined to ALK exons 20-29 (47, 49). Other partner genes besides EML4 have been described recently, but are less common (50). Active ALK signaling results in cell proliferation and apoptotic evasion mediated by JAK3/STAT3, RAS/MAPK-ERK, and PI3K/AKT signaling pathways (51). Oncogenic ALK mutations are susceptible to ALK inhibition by crizotinib (52) and have been found in approximately 4-8% of NSCLC (53). ALK rearrangements generally occur exclusively from EGFR and KRAS alterations, but instances of ALK rearrangements occurring concomitantly with EGFR mutations have been reported as a mechanism for EGFR resistance (20, 47).

ROS1 is a proto-oncogene encoding a transmembrane receptor tyrosine kinase. Its kinase domain has high homology with that of ALK (54). Similar to ALK, ROS1 mutations are most commonly gene rearrangements resulting in fusion proteins and are found in 1-3% of NSCLC (55, 56). A variety of fusion partners have been identified including, FIG, KDELR2, TPM3, SDC4, LRIG3, EZR, SLC34A2, and CD74 (50, 56). Early clinical evidence has suggested that NSCLC harboring ROS1 rearrangements are sensitive to the ALK/MET kinase inhibitor, crizotinib (55).

Rearranged during transfection (RET) is a proto-oncogene activated by chromosomal rearrangement resulting in oncogenic fusion RTK signaling (57). RET is most commonly found fused with KIF5B and RET fusions have been identified in 1-2% of NSCLC (58). Tumors harboring RET rearrangements are sensitive to several multi-kinase inhibitors, and recent in vitro evidence suggests that tumors harboring KIF5B-RET fusions are sensitive to RET inhibition (59).

### *The Tumor Suppressors Commonly Lost in Lung Cancer*

Tumor suppressor genes are important negative regulators of cell growth and proliferation, and a normal functioning cell requires two copies of these genes to function (60). Tumor suppressor genes were famously described as “anti-oncogenes” by Alfred Knudson in 1993 where he outlined a “two-hit” hypothesis describing how the loss of two

## CHAPTER 2

copies of a tumor suppressor gene resulted in carcinogenic activity (60). The first allele is most often lost by an inactivation mutation, epigenetic silencing or other aberrations, while the second allele is most commonly lost by loss of heterozygosity (LOH) when a region of a chromosome is lost by deletion, mitotic recombination, or non-reciprocal translocation (19). The most common tumor suppressor genes inactivated in NSCLC are TP53, PTEN, the p16<sup>INK4A</sup>/RB cell cycle regulating pathway, and serine/threonine kinase 11 (STK11). Others have been noted, FHIT and RASSF1A, but they are less prevalent in NSCLC than those listed and are discussed elsewhere.

The most commonly occurring gene mutation found in lung cancers is TP53. TP53 mutations are found in up to 80-100% of small cell lung carcinomas and in up to 65% in non-small cell lung cancers, although a consensus on frequency varies (19, 61, 62). p53, the protein product of the TP53 gene, is responsible for making cell fate decisions in response to damaged DNA by upregulating genes responsible for DNA repair or apoptosis accordingly (63). It is also a transcription factor for a host of other genes (19). In healthy cells, DNA damage or other carcinogenic stress induces p53 expression, which promotes DNA repair or cell cycle arrest by inducing the expression of cyclin-dependent kinase inhibitors (64). For this reason, p53 plays a crucial role in determining cell fate between whether to repair DNA damage or undergo apoptosis (65). TP53 loss is most commonly due to a hemizygous deletion of the chromosomal locus in which it resides (19). TP53 loss of function also occurs when missense mutations in the DNA binding domain occur (62). TP53 mutations in NSCLC correlate with a history of smoking or environmental exposure to smoke (64, 66). TP53 mutations can occur concomitantly with EGFR and KRAS mutations (67).

A second commonly mutated tumor suppressor is phosphatase with tensin homology (PTEN). As discussed earlier, PTEN is a lipid and protein phosphatase responsible for inhibiting PI3K/AKT/mTOR signaling. It does this by dephosphorylating PIP3 back into PIP2 (68).

STK11 (also known as LKB1) is a serine/threonine kinase responsible for inhibiting mTOR (69). As described above, components of the AKT/mTOR signaling pathway have been found to be deregulated in around 30% of lung adenocarcinomas (22). STK11 activity is inhibited by a variety of deletion or other somatic mutations leading to inactive,

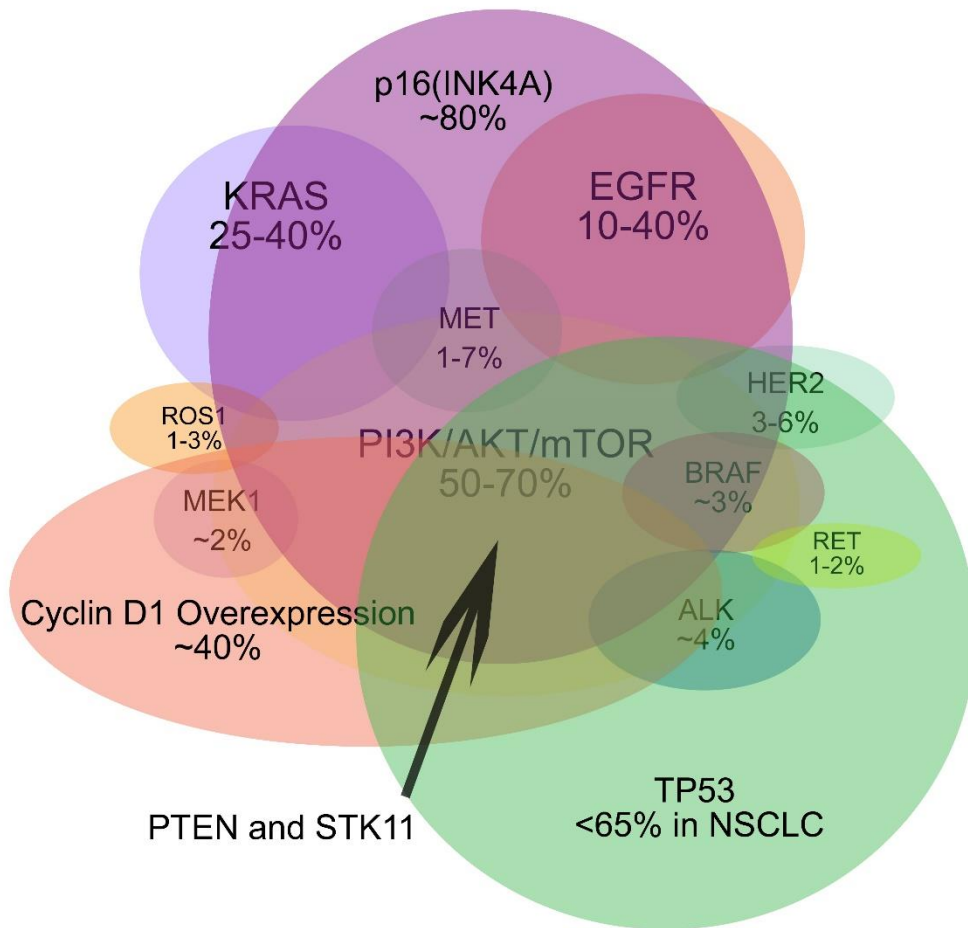


**Figure 1.2: Tumor suppressors that are commonly lost in lung adenocarcinomas.** Percentage of lung adenocarcinomas with each tumor suppressor loss. Occurrence laid over the oncogenic driver mutations in lung adenocarcinomas.

## CHAPTER 2

truncated proteins (70). Inactivation of STK11 specifically occurs in 11-30% of lung adenocarcinomas (22, 70, 71). STK11 inactivation mutations comprise the third most common mutation observed in lung adenocarcinomas behind p53 and KRAS (19, 70). It has been suggested that STK11 mutations correlate to smoking history. STK11 loss has also been correlated with the existence of KRAS mutations. Smoking status, KRAS mutations, and STK11 mutations are mutually exclusive of EGFR mutations (70, 71).

The p16<sup>INK4A</sup>/cyclin D1/CDK4/RB pathway is responsible for cell cycle progression between G1 and S phase and members of the pathway are commonly mutated in lung cancers (19). Retinoblastoma protein (Rb), encoded by the RB1 gene, mediates the G1/S transition of the cell cycle by sequestering the E2F1 transcription factor required for S-phase entry until its phosphorylation (72). RB1 was the first tumor suppressor gene described in lung cancer (73). It is found to be inactivated in around 90% of lung carcinomas, but it is only inactivated in 10-15% of NSCLC (17). In NSCLC, perturbations in this pathway most commonly come from members upstream of RB resulting in hyperphosphorylation of the protein leaving the G1-S transition to occur unchecked. In NSCLC, these alterations occur in cyclin D1, CDK4 and the cyclin-dependent kinase inhibitor, p16<sup>INK4A</sup> (74). In normal signaling, p16<sup>INK4A</sup> is responsible for inhibiting phosphorylation of RB by cyclin D1 halting the cell cycle. p16<sup>INK4A</sup> is inactivated in approximately 80% of NSCLC (75, 76). Overexpression of cyclin D1 by gene amplification, epigenetics, or transcriptional upregulation is found in ~40% of NSCLC (77).

### **Targeted Therapies in NSCLC**

Targeted therapies are quickly becoming standard of care for lung cancers harboring oncogenic mutations. The majority of NSCLC patients present with tumors in the advanced stages of the disease (78). Until very recently, patients with advanced stage NSCLC were most often placed onto platinum-based chemotherapy regimens (29). Clinical trials examining the efficacy of various platinum-doublet combinations have revealed that improving the therapeutic benefit of conventional chemotherapies has hit a plateau. This has spurred forward the development of therapies that target specific oncogenic mutations to improve outcomes (29, 79). Several targeted therapies have become the standard of care for advanced NSCLC harboring specific mutations and they are described below. When paired with the development of diagnostic or companion

## CHAPTER 2

biomarkers, these targeted therapies have greatly improved treatment for some patients while the remainder are treated with the appropriate cytotoxic agents (29). Importantly, EGFR is commonly targeted in lung adenocarcinomas and will be covered more in depth in the EGFR section of this chapter. A discussion of the hallmarks of cancer with current FDA-approved drugs targeting them in lung cancer is presented below.

### *Targeting Growth and Proliferation in NSCLC*

Oncogenic KRAS mutations occur in 25-40% of NSCLC and are common in pancreatic, colorectal, serous ovarian and thyroid cancers, making them a desirable therapeutic target (80). Mutant KRAS is also an attractive target because it tends to occur exclusively of other driver mutations (e.g., EGFR, ALK) (81). Over the last three decades, attempts at targeting KRAS have been largely unsuccessful, and there are currently no KRAS inhibitors approved or in trials. Current methods of “targeting” mutant KRAS involve targeting the members of downstream pathways to eliminate oncogenic KRAS signal through them (81). These include inhibitors of MAPK-ERK and PI3K/AKT/mTOR pathways among others, and the FDA approved inhibitors of each of these targets are outlined below (81).

Oncogenic ALK rearrangement mutations (described in the oncogenes discussion above) were first described in 2007 and have been found to occur in around 4-8% of adenocarcinoma patients (82). The first generation ALK inhibitor, crizotinib, was approved in 2011 for use in patients with advanced NSCLC harboring a confirmed ALK rearrangement mutation (83). A second generation ALK inhibitor, ceritinib, is 20 times more potent than crizotinib and has demonstrated promise in patients who progressed on crizotinib or were intolerant of crizotinib. It has also performed well in ALK-inhibitor-naïve patients (84). The other second generation ALK inhibitor, alectinib, has shown activity against the crizotinib resistance mutation (L1196M), reducing the size of both previously treated and untreated brain metastases (29). Both of the second generation ALK-inhibitors are indicated for use in patients who progressed on or were intolerant of crizotinib (29). Importantly, NSCLC that harbor ROS1 rearrangements have also been shown to be sensitive to crizotinib treatment, which suggests a possible dual role for the ALK inhibitor although it is not currently FDA-approved for use in ROS1 rearrangements (29).

## CHAPTER 2

BRAF mutations occur in approximately 2-3% of NSCLC and are also a therapeutic target in lung cancers. Approximately 50-75% of the BRAF mutations observed in lung cancer are the V600E mutation that also occurs commonly in melanoma (85). V600K also occurs in 6-30% of melanomas (86), but it is very uncommon in NSCLC. Of the approved BRAF inhibitors, vemurafenib and dabrafenib have demonstrated significant activity in BRAF V600E and V600K mutant melanomas, so they are being explored for efficacy in NSCLC both alone and in conjunction with the MEK inhibitor, trametinib (29). Initial Phase II trials of trametinib combined with dabrafenib revealed an overall response rate of 63% (29). Vemurafenib has also demonstrated activity in NSCLC patients harboring a BRAF V600E mutation as a single agent (87, 88). While vemurafenib and dabrafenib are in trials, none are currently FDA approved specifically for the treatment of NSCLC.

The tissue-type specific drug approval by the FDA for targeted therapies has limited our ability to best match patients to targeted therapies (e.g., BRAF in lung). Off-label use occurs, but this limits payment options leaving the majority of patients unable to receive these therapies unless they have been specifically designated for their specific tumor type and mutation status. An ongoing NCI trial, Molecular Analysis for Therapy Choice (MATCH), is currently working to identify whether actionable variants of 143 genes associated with cancer that match to 20 drugs in the study work in a non-tissue-specific manner (89). The study specifically aims to assign targeted therapies independent of anatomical tumor locations in any advanced or solid tumors or lymphomas that are refractory or with no standard therapy (89). Of the drugs described above, crizotinib is included for ALK and ROS1 rearrangements, while dabrafenib in conjunction with trametinib and trametinib alone are included for BRAF mutations. The EGFR/HER2 inhibitor, afatinib (described in depth below), is also included for the treatment of EGFR/HER2 mutations (89). Other oncogenic mutations found commonly in lung cancers that are included are AKT and PIK3CA. Hopefully, this endeavor will end the “off-label” use of targeted therapies across tissue types. This would allow patients whose tumors harbor specific mutational statuses responsive to targeted therapies to receive them.

### *Targeting Angiogenesis in NSCLC*

As stated earlier, loss of growth and proliferation regulation is not the only commonality between tumors that allow them to grow and invade unchecked. One of the

## CHAPTER 2

drivers of lung cancer currently being targeted clinically is angiogenesis. Angiogenesis is the process by which cancer cells stimulate surrounding blood vessels to grow into and around a tumor supplying the oxygen and nutrients rapidly proliferating cells need to grow – it is also imperative for the development of metastatic lesions (1). The development of anti-angiogenesis therapies have been aimed at inhibiting the vascular endothelial growth factor (VEGF) receptor on local endothelial cells. These inhibitors intentionally target normal tissues is to prevent them from responding to stimuli coming from the tumor. Importantly, the opportunity to target the healthy cells to minimize tumor growth is a promising option because healthy cells are significantly less likely to develop resistance to a drug. There are currently two FDA-approved drugs that target the VEGF receptor in lung cancers: bevacizumab and ramucirumab. Both are monoclonal antibodies targeting the extracellular, ligand-binding domain of the VEGF receptor (29).

### *Targeting the Immune Evasion Mechanisms of NSCLC*

Immune evasion is also a commonality among tumors. In the past few decades, it has grown increasingly evident that the role of the tumor microenvironment, namely the interaction of the tumor cells with circulating immune cells, is critical for cancer growth and progression (90). Therapeutic targeting of tumor cell immune evasion has recently gained a lot of momentum as a first-line clinical option for patients with high PD-L1 expression (90). Inhibiting both of these interactions between the tumor and its surroundings are imperative to cutting tumors off from their resources and self-preservation methods. Evasion of the immune system is a key step in cancer development, specifically for NSCLC. Tumors overcome the immune responders (activated T cells, B cells, natural killer cells monocytes and dendritic cells) by over-expressing PD-L1 or PD-L2 ligand on their cell surface (90). The immune responder cells, CD4, CD8 and pro-B cells, express the receptor (PD-1) on their surface. The interaction between the receptor on the immune cell and the ligand on the tumor cell suppresses the anti-tumor immune response. This process is also known as T-cell exhaustion (90). By blocking the interaction of PD-L1 with the PD-1 receptor on immune cells, T-cell exhaustion is overcome allowing immune cells to maintain their tumor-cell killing function (91).

There are currently three approved monoclonal antibodies targeting this interaction between immune cell receptors and the tumor cell blockade of immune response:

<b>Drug</b>	<b>Target</b>	<b>Specific Mutations</b>	<b>Stage</b>
<b><i>Drugs Targeting Growth and Proliferation</i></b>			
<b>Crizotinib</b>	ALK/ROS1	Rearrangements in both	Approved for ALK
<b>Ceritinib</b>	ALK	Rearrangements	Approved
<b>Alectinib</b>	ALK	Rearrangements	Approved
<b>Vemurafenib</b>	BRAF	V600E and V600K	Clinical trials
<b>Dabrafenib</b>	BRAF	V600E and V600K	Clinical trials alone and in combination with trametinib (MEK inhibitor)
<b>Gefitinib</b>	EGFR	EGFR Exon 19 Deletion or L858R	Approved
<b>Erlotinib</b>	EGFR	EGFR Exon 19 Deletion or L858R	Approved
<b>Afatinib</b>	EGFR/HER2/HER4	EGFR Exon 19 Deletion or L858R/EGFR T790M	Approved
<b>Dacomitinib</b>	EGFR/HER2/HER4	EGFR T790M	Clinical trials
<b>Neratinib</b>	EGFR/HER2	EGFR T790M	Clinical trials
<b>Osimertinib</b>	EGFR T790M	EGFR T790M	Approved
<b>Necitumumab</b>	EGFR	None	Approved in combination with gemcitabine and cisplatin
<b>Cetuximab</b>	EGFR	None	Clinical trials
<b><i>Drugs Targeting Angiogenesis</i></b>			
<b>Bevacizumab</b>	VEGFR	None	Approved
<b>Ramucirumab</b>	VEGFR	None	Approved
<b><i>Drugs Targeting Immune Evasion Mechanisms</i></b>			
<b>Nivolumab</b>	PD-1	High PD-L1 Expression	Approved
<b>Pembrolizumab</b>	PD-1	High PD-L1 Expression	Approved
<b>Atezolizumab</b>	PD-L1	High PD-L1 Expression	Approved

**Table 1.1: Targeted therapies in NSCLC.**

## CHAPTER 2

nivolumab, pembrolizumab, and atezolizumab. Pembrolizumab (marketed as Keytruda) is an IgG4 isotype humanized monoclonal antibody targeting PD-1 molecules expressed on the surfaces of the immune cells (92). Nivolumab (marketed as Opdivo) is also a monoclonal antibody targeting PD-1 molecules on immune cell surfaces. It is a fully humanized IgG4 isotype antibody (93). The final immune checkpoint inhibitor currently approved for use in NSCLC is atezolizumab (marketed as Tecentriq) (90). Atezolizumab is a fully humanized IgG1 isotype monoclonal antibody targeting the PD-L1 ligand on the tumor surface rather than the PD-1 receptor on the surface of the immune cells (94). PD-L1 expression levels are being investigated as a predictive biomarker with success in some tumor subgroups, but it does not appear that PD-L1 levels have prognostic value (90).

### **B. EPIDERMAL GROWTH FACTOR RECEPTOR (EGFR)**

As stated earlier, EGFR is a common oncogenic driver of NSCLC. This body of work stems from the Black laboratory's work in identifying predictive biomarkers of EGFR inhibitor success in NSCLC, and for this reason I have described it in depth below.

#### **EGFR Activation and Signaling**

EGFR is a transmembrane, receptor tyrosine kinase (RTK) that includes an extracellular ligand binding domain and an intracellular tyrosine kinase domain (95). EGFR is a member of the ErbB family of RTKs that are structurally similar. They consist of an extracellular, ligand binding domain, a lipophilic membrane-spanning domain, and a cytoplasmic tyrosine kinase domain (96). EGFR and other members of the ErbB RTK family have varying affinities for multiple ligands. The extracellular growth factors with which they interact include epidermal growth factor (EGF), transforming growth factor alpha (TGF $\alpha$ ), heparin-binding epidermal growth factor (HB-EGF), amphiregulin (AREG), epiregulin (97), and betacellulin (BTC) (98). Binding of the ligand results in receptor homodimerization or heterodimerization with other members of the EGFR/ErbB family of receptors resulting in autophosphorylation of the tyrosine residues of the kinase domain (96, 99, 100).

## CHAPTER 2

EGFR signal transduction occurs through MAPK-ERK, PI3K/AKT/mTOR, and STAT signaling pathways (99, 100). Importantly, signal transduction through these signaling pathways is not exclusively driven by EGFR in normal cells. Rather, EGFR belongs to a network of other RTKs that can activate common effectors (101). The complexity of these networks is growing constantly and the phenomenon is being described as 'crosstalk' amongst the signaling pathways and RTKs (102). This improves our understanding of compensatory signaling routes and the development and maintenance of targeted therapy-resistance. However, it also underscores the need for developing novel methodologies targeting multiple sources of tumor driving and drug resistance generating pathways.

One of the pathways stimulated by EGFR activation is the MAPK-ERK pathway, with members RAS/RAF/MEK/ERK. The MAPK/ERK signaling pathway is specifically responsible for growth and proliferation, which is why it is commonly mutated in cancer (28, 67). EGFR activates this cascade by phosphorylating the KRAS GTPase using mediator proteins (e.g., SOS and GRB2) (103). Phosphorylated KRAS then phosphorylates BRAF, which in-turn phosphorylates MEK1/2, and finally MEK1/2 phosphorylates ERK1/2. Phosphorylated ERK then translocates into the nucleus where it activates transcription factors associated with growth and proliferation (e.g., ELK1 and ETS1) (104). The MAPK-ERK pathway is ultimately responsible for regulating the expression of genes that drive growth and proliferation of the cell (e.g., MYC and JUN) (105, 106).

EGFR signaling also activates the PI3K/AKT signaling pathway. The initial steps in PI3K/AKT signaling are described more in depth in the oncogenes and tumor suppressor sections above. The important thing to note about this signaling pathway is that AKT is able to activate a number of independent downstream pathways. In normal signaling, one role of AKT is the phosphorylation of the Bcl-2 family member, Bad, which ultimately leads to caspase activation and the induction of apoptosis (107). AKT can also signal through the mammalian target of rapamycin (mTOR), sometimes referred to as mechanistic target of rapamycin, which is responsible for regulating cell size and proliferation in non-cancerous cells (108).

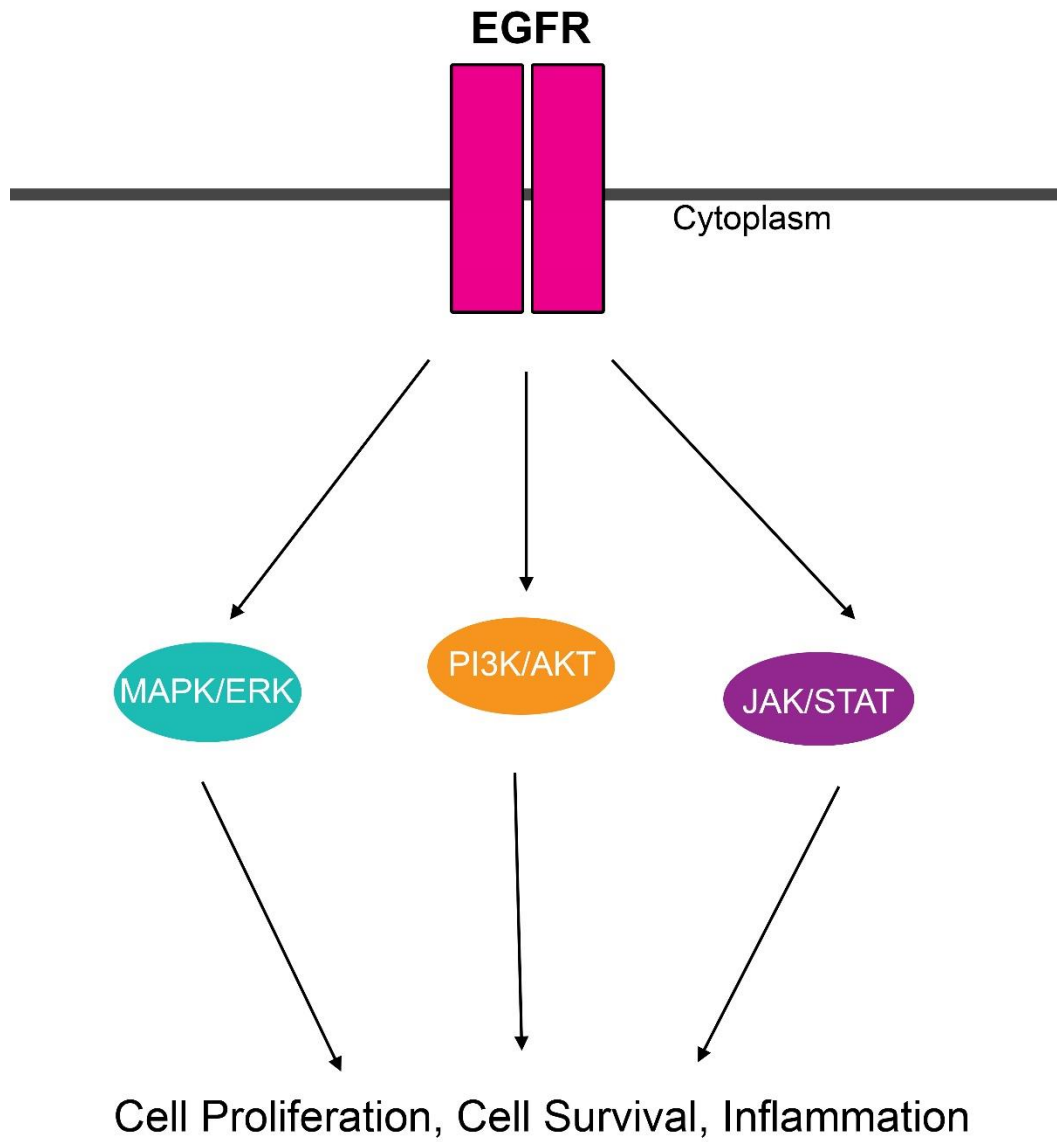


**Figure 1.2: EGFR Signaling Pathways.**

## CHAPTER 2

A third signaling pathway driven by EGFR is the signal transducers and activators of transcription signaling pathway mediated by a family of STAT molecules (109). Until rather recently, STAT signaling was believed to be activated only by cytokine signals (e.g., interferon and interleukin family members) with its activation being mediated by the Janus Kinase (JAK) (110, 111). We now know that STAT proteins can also be indirectly activated by EGFR via SRC-mediated phosphorylation (112). Phosphorylation of a STAT molecule results in a homodimerization with a STAT family member of the same type, resulting in translocation of the complex into the nucleus and gene expression regulation (112). STAT family members are responsible for regulating the expression of genes promoting survival, growth and proliferation, immune response, angiogenesis and wound healing (113, 114).

Importantly, these three signaling pathways do not encompass all of the signaling events regulated by EGFR, just those that are best characterized and are relevant to the contents of this dissertation.

### **EGFR Mutations in Non-Small Cell Lung Cancers (NSCLC)**

EGFR action as an oncogene impacts many cellular functions including proliferation, differentiation, invasion, survival, neovascularization and metastasis (100). EGFR mutations are found in a number of tumor types including NSCLC (19). In lung cancers, the majority of EGFR mutations occur in lung cancers of the adenocarcinoma histological subtype (25, 67) and are also most commonly found in younger patients who are female with no history of smoking (22, 115, 116). EGFR activation mutations have been identified in 10-15% of unselected western patients (20, 25). However, EGFR activating mutations occur more commonly in Asian populations and are observed in 30-40% of lung tumors (67, 115). EGFR oncogenic mutations result in constitutive tyrosine kinase activation (117).

In NSCLC, oncogenic mutations in the EGFR gene occur in the exons (18-24) that, when translated, comprise the tyrosine kinase domain of the protein (19). The most common of these mutations are the exon 19 frame deletion mutations, of which there are over twenty different variants that account for around 45% of the EGFR mutations in NSCLC (19). The second most common type of EGFR mutations are missense mutations, most commonly L858R in exon 21, accounting for approximately 40% of EGFR mutations

## CHAPTER 2

in NSCLC (67). Less common EGFR mutations (~5-10% of EGFR mutations in NSCLC) leading to EGFR inhibitor (EGFRI) resistance often involve in-frame duplications or insertions into exon 20 (26). Variant-III (EGFRvIII) mutations also occur (~3% of NSCLC) where the extracellular binding domain of EGFR is deleted, which prevents the EGF ligand from binding, but still results in aberrant downstream signaling (118). EGFRvIII, gene duplication mutations, and over-expression of EGFR protein occur more commonly in squamous cell carcinomas than in adenocarcinomas (119).

Acquired resistance mutations are most often selected for in patients undergoing EGFRI treatments which lead to resistance. The most common of these is the T790M point mutation in exon 20, which results in an amino acid change from a threonine to a methionine. This interferes with the binding of reversible EGFRI (120). The T790M mutation is found in approximately 50-60% of patients who develop acquired resistance to EGFRI (120). Importantly, T790M mutations have been observed in treatment-naïve patients, so they are not exclusively driven by EGFRI treatment (20). Other common routes of EGFRI resistance occur through the activation of PI3K-AKT signaling pathway and this is most commonly achieved by amplification of MET (39).

Mutations in EGFR are not the only mechanism by which aberrant EGFR signaling occurs in lung cancer. EGFR has also been found to be over-expressed, generally as a result of a genomic amplification event, with increased EGFR copy number observed in up to 50% of lung cancers (121). EGFR over-expression can also occur as a result of increased promoter activity or a decrease or loss of transcriptional or translational regulation mechanisms (122). EGFR over-expression results in increased EGFR activity with and without activating mutations present suggesting that the increased activity is likely due to the high volume of receptors in the membrane spontaneously dimerizing with one another at the cell surface (122, 123). Increased expression or cleavage-processing to mature form of ErbB family ligands has also been linked to increased EGFR stimulation through autocrine (cell to self) and paracrine (cell to immediate surrounding cells) dosing of growth-inducing ligands (124, 125). Finally, it has been suggested that EGFR heterodimerization to other ErbB RTK family members could be a contextual contribution to oncogenic signaling in tumors (122). Specifically, EGFR-ErbB3 heterodimerization has been described in NSCLC as a possible source of EGFR targeted therapy resistance (39, 126). EGFR-ErbB3 dimers are imperative for EGFR regulation of PI3K/AKT. Specifically,

## CHAPTER 2

the ErbB3 tyrosine kinase domain differs from EGFR which allows the docking of PI3K directly to the kinase (127). EGFR-ErbB3 dimers are dissociated by EGFRIs, but the resultant under-activation of AKT signaling leads to compensatory over-expression of ErbB3. This shifts the receptor equilibrium, thereby reducing EGFRi response (127).

### **Inhibition of EGFR in Lung Cancer Therapy**

There are currently two main classes of drugs targeting EGFR (EGFRi) in cancer: 1) small molecule inhibitors of the tyrosine kinase domain of EGFR (EGFR-TKIs) and 2) monoclonal antibodies that bind the extracellular ligand binding domain preventing the binding of EGF or other ErbB family ligands and activation of the receptor. Currently, only the small molecule inhibitors of EGFR are used in lung cancers and a review of EGFR-targeting monoclonal antibodies in lung cancer and why they are not currently used is provided below.

#### *Small Molecule Inhibitors of EGFR*

Preclinical work in the development of EGFR inhibitors demonstrated that point mutations in the ATP binding pocket of EGFR could eliminate its tyrosine kinase activity (128-130). This led to the development of two competitive, reversible, ATP binding pocket-targeting small molecules as the first generation of EGFR-TKI inhibitors: gefitinib (Trade name: Iressa) and erlotinib (Trade name: Tarceva) (130, 131). Early trials of the first generation EGFR-TKIs revealed that patients with no smoking history, Asian ethnicity and a tumor of adenocarcinoma histology were most likely to respond to treatment (132). It was determined later that patients exhibiting these clinical characteristics most often harbored the EGFR exon 19 deletion or exon 21 L858R activation mutations (3, 133). Due to these observations, the prospective Phase 3 trial was performed specifically in patients exhibiting these clinical characteristics in Asia (134). Mok *et al.* demonstrated that patients with a confirmed EGFR mutation had a significantly higher overall response rate and longer progression free survival when treated with gefitinib compared to the platinum-based chemotherapy arm (134). They also demonstrated the gefitinib treatment arm of patients without an EGFR mutation had significantly lower overall response and a shorter progression free survival (134). This study established EGFR mutation status as a biomarker for EGFR-TKI patient selection (29, 135). Since then, a number of studies

## CHAPTER 2

comparing the first generation EGFR-TKIs, gefitinib and erlotinib, as well as second generation, afatinib, to platinum-doublet chemotherapies have consistently demonstrated superior overall response rates, progression-free survival, and quality of life in the targeted therapy arm (136-140). Retrospective analysis of some of these studies suggested that afatinib treatment offered greater overall survival in exon 19 deletion tumors over L858R tumors. However, the more recent LUX-Lung 7 trial designed to confirm prior study results did not observe the same effect (141, 142). Erlotinib was FDA-approved in 2004 for the treatment of NSCLC as a second or third line therapy. It was most recently redesignated in October 2016 for the treatment of locally advanced or metastatic NSCLC harboring EGFR exon 19 deletions or exon 21 L858R substitution mutations (143, 144). Notably, gefitinib received conditional FDA approval following Phase II trials in 2003, but approval was later withdrawn after negative Phase III results in unselected patients (145). In 2015, gefitinib was FDA-approved a second time, but only as a first line therapy in patients with metastatic, EGFR mutant NSCLC, and not in populations harboring other mutations (146). Importantly, a majority of patients on first-line EGFR-TKIs do progress between 10-15 months following the start of treatment (29, 147).

The most common reason for progression is the development of secondary resistance mutations in EGFR. For this reason, the second generation of EGFR-TKI development has been largely centered around overcoming secondary mutations in EGFR. Selecting the treatment following progression on EGFR-TKI relies heavily on being able to identify the source of resistance (147). Importantly, not all EGFR-TKI resistance mechanisms arise due to mutations in EGFR. Bypass-signaling by other RTKs (e.g., HER2 and ALK), downstream mutations (e.g., BRAF and PIK3CA), and phenotypic changes (e.g., EMT) are also sources of EGFR-TKI resistance (147, 148). As previously stated, T790M mutations are the most common acquired EGFR-TKI resistance mutations in NSCLC accounting for 50-60% of treatment-induced resistance (120). Because of this, the second generation of EGFR-TKIs aimed to comprehensively target this acquired resistance mutation (T790M) and other resistance sources (e.g., HER2, HER4) (145). Second generation small molecule inhibitors, afatinib, dacomitinib, and neratinib, are each irreversible inhibitors of the EGFR tyrosine kinase domain (147). Each targeted T790M mutations, had some overlap in the EGFR sensitivity conferring mutations, and all include some binding to the HER2/HER4 receptors which represent an additional source of potential resistance (147). While the *in vitro* study of each of these three drugs appeared

## CHAPTER 2

promising, clinical trials of the second-generation EGFR-TKIs in patients resistant to either of the first generation EGFR-TKIs only demonstrated a response rate of around 10% (149-151). Additionally, adverse side effects were observed at drug concentrations too low to inhibit T790M mutated EGFR molecules *in vivo* (149-151). Currently, afatinib is the only second generation, small-molecule EGFR-TKIs approved for the treatment of advanced NSCLC harboring an exon 19 deletion mutation or an exon 21 L858R EGFR activation mutation (152).

The third generation of small molecule EGFR-TKIs are being designed specifically to target the T790M mutation more effectively than the second generation small molecules. Rather than targeting both mutant and wild-type EGFR and other conserved receptors (e.g., HER2 and HER4), these specifically target mutant EGFR (T790M, exon 19 deletion, and exon 21 L858R substitution) with minimal impacts on wild-type EGFR (147). Importantly, this would theoretically limit adverse events, but minimal activity against wild-type EGFR highlights that these inhibitors will not be utilizable in patients with amplified/overexpressed EGFR. All third generation EGFR-TKI small molecule inhibitors are irreversible inhibitors of EGFR (147). Of them, only one (osimertinib) has been approved for the treatment of metastatic NSCLC with the EGFR T790M mutation (153). The rocletinib study has been paused in Phase II/III trials due to side effects, and olmutinib is only approved in Asia. ASP8273 is in Phase III trials, and nazartinib, PF-06747775, avitinib, and HS-10296 are all in Phase I/II trials (147). As with first and second generation small molecule EGFR-TKIs, third generation inhibitors select tumor cells with novel or rare point mutations (e.g., C797S in exon 20 or L798I/Q *in cis* with T790M) leading to resistance (154-156). Most importantly, additional mechanisms of EGFR-independent resistance to third generation EGFR-TKIs are being reported (147). Activating mutations in NRAS (e.g., E63K) as well as amplification of wild-type NRAS and KRAS have been reported in osimertinib resistance. These mutations were also observed in gefitinib and afatinib resistance (157). It has been suggested that loss of the T790M population of cells led to the over-growth of cell populations with HER2 amplifications, PIK3CA mutations or BRAF V600E at the time of progression (158). Amplifications of HER2 and MET genes have also been described as mechanisms for overcoming T790M-targeting EGFR-TKIs (155). All of the resistance mechanisms described above in response to single-agent EGFR-TKIs underscore the need to target other pathways concurrently or sequentially with EGFR-TKIs to minimize or eliminate resistance mechanisms. Very importantly, the

## CHAPTER 2

third generation of EGFR-TKIs are much better tolerated than the first and second generations and this observation has opened them to be explored as co-therapeutics with new studies and clinical trials currently in the planning stages (147).

### *Targeting EGFR with Monoclonal Antibodies*

Another therapeutic route for antagonizing EGFR signaling in NSCLC is the use of EGFR-targeting monoclonal antibodies. Anti-EGFR monoclonal antibodies work by targeting the ligand binding domain of EGFR and competitively block the interaction of EGFR with any of its ligands (159). Complexes of EGFR and anti-EGFR monoclonal antibodies are then internalized and degraded leading to a decrease in cell surface EGFR (160). It has also been suggested that this action could lead to antibody-dependent cellular cytotoxicity (161). EGFR-directed monoclonal antibodies currently being investigated are cetuximab, matuzumab, panitumumab, and necitumumab, but others are in development (160).

Cetuximab has been studied in Phase II and III trials in combination with first-line chemotherapy in advanced NSCLC (162-164). Two Phase III trials, FLEX and BMS099, were opened to compare the combination of chemotherapy with cetuximab. The FLEX trial demonstrated improved overall survival with the combination treatment versus chemotherapy alone whereas BMS099 did not demonstrate an improvement in progression free survival (165, 166). Importantly, only the FLEX trial analyzed and considered EGFR expression levels as a point of comparison in survival computations. Patients expressing high EGFR levels that were treated with the combination of cetuximab and chemotherapy had a median survival of 12 months compared to 9.8 months in patients expressing low levels of EGFR, although this difference was not found to be statistically significant (121, 167). Though demonstrated in colorectal cancers, KRAS mutation status does not predict response rate, progression-free survival, or overall survival in NSCLC (168, 169). Necitumumab was analyzed in two Phase III trials as well: INSPIRE tested activity in advanced non-squamous cell NSCLC, and SQUIRE tested efficacy in squamous NSCLC (170, 171). The INSPIRE trial was prematurely closed due to an increased number of adverse events, grade 3 or higher, including fatal thromboembolic events and sudden/unexplained death (170). The SQUIRE trial demonstrated improved overall survival in the combination necitumumab arm compared

## CHAPTER 2

to chemotherapy alone (171). Currently, only necitumumab in combination with gemcitabine and cisplatin is FDA approved for use in lung cancer, specifically only in squamous histological subtype NSCLC (172, 173).

### **C. TRANSFORMING GROWTH FACTOR BETA (TGF $\beta$ ) BIOLOGY AND SIGNALING**

As stated before, the Black laboratory's efforts have been centered on identifying predictive biomarkers for EGFR-TKI therapies. We also aim to leverage the genes comprising the biomarkers to identify novel treatment options for overcoming both inherent and acquired resistance to EGFR-TKIs in NSCLC. As will be described in more detail later, one of our gene signatures indicated TGF $\beta$  as a putative source of EGFR-TKI resistance. For this reason, I've included an in-depth look at TGF $\beta$  signaling and its role in cancer below.

TGF $\beta$  is a ubiquitous cytokine that is active in a number of cell processes, and the majority of cell types contain the ability to secrete the ligand as well as the receptors to respond to it (174). TGF $\beta$  signaling is essential for development, cell differentiation, homeostasis and wound healing in adult tissues (175). TGF $\beta$  belongs to the TGF $\beta$  superfamily of receptors and transcription factors that has over thirty members. The TGF $\beta$  superfamily can be subdivided into two distinct signaling families: 1) TGF $\beta$ , activin, nodal and other factors and 2) growth and differentiation factors including the bone morphogenic proteins (BMPs) and the anti-muellerian hormone (AMH/MIS) (176-178). Other members of the TGF $\beta$  superfamily are responsible for embryonic stem cell differentiation, organogenesis, body axis formation and symmetry establishment during development (179). In the developed adult, TGF $\beta$  superfamily members are responsible for functions like gonadal regulation, muscle development, and bone growth and repair (179). TGF $\beta$  superfamily expression and signaling behavior is largely tissue-specific limiting their signaling in adult tissues (176).

#### **TGF $\beta$ Signaling**

## CHAPTER 2

### *The Receptors*

TGF $\beta$  canonical signaling has three receptor types (T $\beta$ R-I (type 1), T $\beta$ R-II (type 2), and T $\beta$ R-III (type 3)), three ligands (TGF- $\beta$ 1, TGF- $\beta$ 2, and TGF- $\beta$ 3), and three transcription factors (Smads 2, 3, and 4) (178, 180, 181). Importantly, T $\beta$ R-III expression is tissue-specific and lung tissues and tumors have very low levels of the type 3 receptor expression (182). Outlined below are the activities of the T $\beta$ R-I/II receptor complexes. The TGF- $\beta$ 1 ligand isoform has been specifically shown to activate canonical Smad (2,3,4) signaling via T $\beta$ R-I and T $\beta$ R-II interactions (183). TGF- $\beta$ 1 activates signaling by binding the type 2 receptor (175). The active, ligand-bound type 2 receptor then binds a type 1 receptor forming a heterodimer where the type 2 receptor can transphosphorylate the type 1 receptor (175). The active heterodimer then binds to a second type 1 and type 2 receptor resulting in a tetrameric complex of TGF $\beta$  receptors that can recruit, bind and activate Smad transcription factors (180).

### *Canonical TGF $\beta$ Signaling*

The term 'Smad' is derived from embryonic development work in *Drosophila* on Mothers against decapentaplegic (MAD) and from SMA in *C. elegans*. In humans, the conserved equivalent is called SMA and MAD related protein, hence the name Smad. Smads 2 and 3, also known as the receptor Smads (R-Smads) due to their direct interaction with the TGF $\beta$  receptor complex, are phosphorylated by the active type 1 receptor on the C-terminal SSXS motif contained within the MAD homology (MH) 2 domain (181). Phosphorylation of Smads 2 and 3 results in a conformational change of the protein. This reveals the MH1 domain containing the nuclear localization signal (NLS) and linker region by which the R-Smads can complex with Smad 4 (181). Unbound Smad 4 traffics between the cytoplasm and nucleus, and is the only Smad with a nuclear export signal (NES) (181). Active Smad heterocomplexes accumulate in the nucleus, presumably due to the masking of the NES on Smad 4 by the R-Smads (181, 183). Nuclear localization of active Smad complexes enables them to interact with various co-activators and co-repressors resulting in either the induction or repression of TGF $\beta$  signaling pathway responsive genes respectively (183). Smad regulation of genes occurs specifically by their binding to Smad Binding Elements (SBEs) contained in the promoters of TGF $\beta$  signaling pathway responsive genes (181, 184).

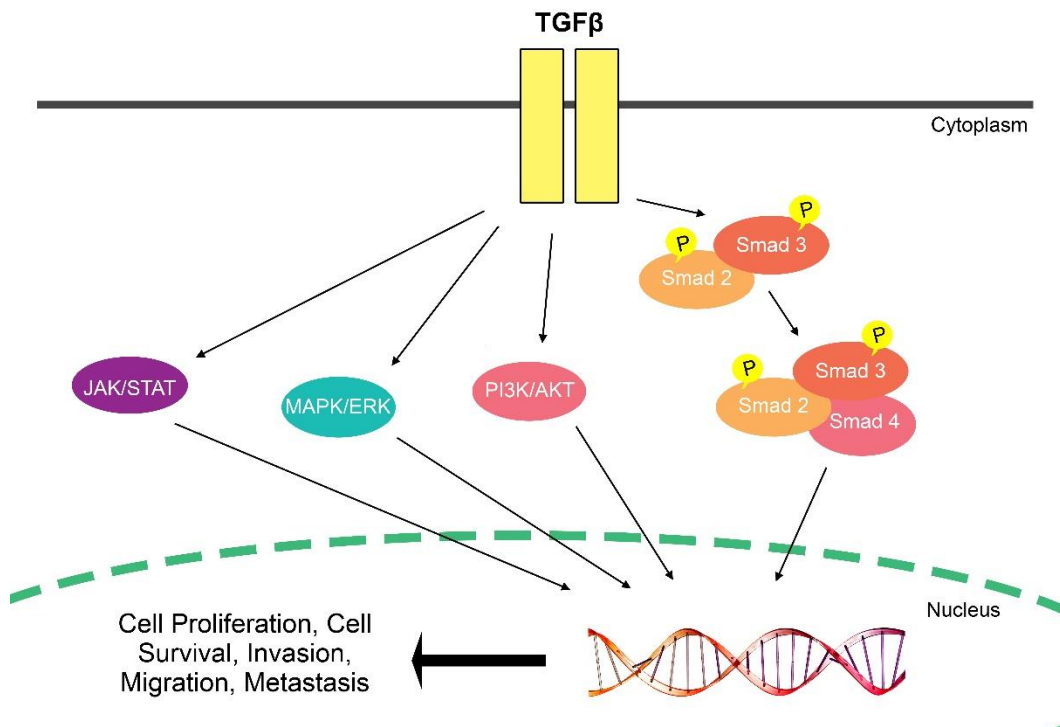


**Figure 1.3: TGFβ Signaling Pathways.**

## CHAPTER 2

TGF $\beta$  signaling via the Smads is regulated by a variety of cellular mechanisms. Smad 2 and 3 must dock with the receptor for activation by T $\beta$ R-I and the process of docking relies on several adaptor proteins including SARA, Hgs, and Dab2 (185-187). Activation of Smads 2 and 3 can also be blocked by the inhibitory Smad (Smad7) that impedes the phosphorylation of the R-Smads. Smad7 can do this with two mechanisms: 1) It can physically bind T $\beta$ R-I blocking the binding of the R-Smads (188), and 2) it recruits Smurf 1/2 (E3 ubiquitin ligase) to facilitate TGF $\beta$  receptor degradation (189). The R-Smads also undergo linker region phosphorylation by other signaling effectors (e.g., ERK 1/2, JNK, p38, Casein Kinase 1, and CDKs) that results in stabilization of active Smad signals (175, 190). Finally, Smad 2/3/4 complexes are disabled and disassembled by PPM1A phosphatase, followed by Smurf 1/2 polyubiquitination, and proteosomal degradation (191, 192). The TGF $\beta$  receptor complex can also be regulated by proteins that associate with it. One of these, TGF $\beta$ -receptor-interacting protein 1 (TRIP-1), interacts with ligand bound TGF $\beta$  complexes and is phosphorylated by them (181). Increased levels of TRIP-1 represses TGF $\beta$  signaling and mutants of TRIP-1 have been shown to enhance TGF $\beta$  signaling (193).

Normal TGF $\beta$  canonical signaling is involved in the regulation of cytotaxis and autonomous growth suppression (175). TGF $\beta$  mediates cytotaxis in the G<sub>1</sub> Phase of the cell cycle by specifically initiating the downregulation of c-Myc (180, 194). Myc downregulation results from a complex of Smad 3, E2F4/5, and p107 bound to an SBE in the Myc promoter (194, 195). Smad 3 also regulates ID1 via a complex of Smad 3 and ATF3 bound to an ID1 promoter region SBE (196). In this context, this is a self-enabled activity of Smad 3 as it is also responsible for the induction of ATF3 expression (196). TGF $\beta$  also negatively influences cell proliferation by regulating the cyclin dependent kinase inhibitors p15<sup>INK4b</sup> and p21<sup>CIP</sup> (180, 194). Specifically, Smad 3 downregulation of Myc prevents the complex of Myc and Miz-1 from forming and thereby blocks p15 transcription that is reliant on the Myc/Miz-1 complex (197). Then Smad 3 complexes with free Miz-1 and Sp1 to stimulate p15 transcription (197). TGF $\beta$  activation also results in the formation of Smad 2:3/Sp1/FoxO complexes that are responsible for transactivating the promoter of p21 (198).

### *Non-Canonical TGF $\beta$ Signaling*

## CHAPTER 2

Like many RTKs, the TGF $\beta$  receptor is able to modulate a network of signaling pathways in addition to the canonical effectors. It is specifically able to activate the growth and proliferation pathways MAPK-ERK, MAPK-p38, and MAPK-JNK (199, 200). The role of TGF $\beta$  in MAPK-ERK signaling came to light after it was observed that Ras was rapidly activated by TGF $\beta$  ligand treatment in epithelial cells (201). The T $\beta$ R-I/II complex can activate the MAPK-JNK and MAPK-p38 pathways via TGF $\beta$ -activated kinase 1 (TAK1). TAK1 can also activate the growth and survival kinases PI3K/AKT/mTOR and AKT/PKB as well as GTP binding effectors like RhoA, and Rac (202, 203). TGF $\beta$  signaling is known to repress NF $\kappa$ B signaling in non-cancerous cells (204). It has also been implicated in mediating the activation of other kinases, including the focal adhesion kinase (FAK), Abl, and Src, by either direct activation or transcriptional control (205-207).

Activated TGF $\beta$  receptors can also influence signaling in many of these pathways via the Smads, which complicates our understanding of the TGF $\beta$  signaling network. Smad-mediated activation of the MAPK-p38 signaling cascade has been shown to induce Caspase-8 and Bid activation, resulting in apoptosis (208). TGF $\beta$  signaling can also induce apoptosis through other members of the mitochondrial Bcl-2 family, as well as via NF $\kappa$ B, AKT, and MAPK-JNK intracellular moderators (209).

### **The Role of TGF $\beta$ in Lung Cancer**

#### *TGF $\beta$ Signaling Pathway Mutations in NSCLC*

Mutations in the TGF $\beta$  signaling pathway members (e.g., Smads) do occur, but most are not commonly observed in lung cancers. Loss of T $\beta$ R-III expression is commonly observed in lung cancers, which is not surprising as signaling via the T $\beta$ R-III receptor has been shown to block cell motility and invasiveness in NSCLC (210). Smad 2 mutations are observed in 7% of lung cancers and are most commonly missense mutations impacting the Smad-complex-forming region of the MH2 domain or the DNA binding domain within the MH1 domain (211, 212).

#### *The “TGF $\beta$ paradox”*

## CHAPTER 2

As previously stated, TGF $\beta$  signaling plays an imperative role in cellular homeostasis and genomic stability by inducing cell cycle arrest, differentiation and apoptosis of cells. In the early stages of tumor development, TGF $\beta$  signaling maintains these roles, thus serving as a potent anti-cancer agent (213). In the later stages of tumor development, TGF $\beta$  signaling activity switches to promote cell growth, invasive ability, and ultimately metastasis. This dichotomous activity of TGF $\beta$  signaling has been rightly dubbed the “TGF $\beta$  paradox” (175). While many theories exist on how this switch occurs mechanistically, it is increasingly evident that the means by which the shift in TGF $\beta$  signaling activity occurs likely happens on a case-by-case contextual basis adding further complexity to this already enigmatic problem. Some of the mechanisms proposed to explain the shift in TGF $\beta$  signaling include the changes in miRNA expression such as the miR-106b-25 cluster (214, 215). Others have suggested that epigenetic changes altering TGF $\beta$  signaling activity (e.g., TGF $\beta$  receptor methylation or promoter over-activation depending on tissue-specific context) and target (e.g., ID1) expression result in the shift from anti- to pro-tumorigenic TGF $\beta$  signaling (179, 216). As further described below, TGF $\beta$  signaling results in the secretion of cytokine-stimuli into the tumor microenvironment and is activated in response to stimuli in the tumor microenvironment as well. The positive feedback loop between tumor cell TGF $\beta$  signaling and tumor-infiltrating immune cells that amplify the stimuli have also been described as a possible mechanism for the signaling switch to occur (217, 218). Finally, mutations in TGF $\beta$  signaling family members or regulators (e.g., p15<sup>INK4b</sup> deletion eliminating TGF $\beta$  regulation) have been suggested as a possible mechanism (213). What is evident is that there is neither a specific consensus across tumor models or TGF $\beta$ -paradox arms as to how the paradox arises, nor a methodology for accurately determining which arm is at play. This is incredibly important because while pro-tumorigenic TGF $\beta$  seems to be an obvious and promising target, unintentional targeting of anti-tumorigenic TGF $\beta$  signaling in unselected patient populations may be detrimental (179, 219).

### *The Roles of TGF $\beta$ Driving the Hallmarks of Cancer*

- 1) *Growth Signal Autonomy*: While there is no known mechanism underlying the shift in TGF $\beta$  activity from growth suppressor to growth promoter, it has been postulated that it may be coupled to TGF $\beta$ 's ability to induce the expression of many cytokines, growth factors, and their receptors (175). TGF $\beta$  signaling

## CHAPTER 2

promotes the production of EGFR and PDGFR receptors as well as cytokines and ligands including: connective tissue growth factor (CTGF), bFGF, PDGF, and TGF $\alpha$  (175). The phosphorylation of the Smad 2/3 linker region by pERK1/2 is another source driving prolonged TGF $\beta$  signaling (175).

- 2) *Genomic Instability*: The role of TGF $\beta$  signaling in the accumulation of genomic instability is more of an unintentional consequence than a direct action. Specifically, tumors overcome the regulation of cell cycle progression via Smad 3 regulation of Myc, p15 and p21, which in turn impacts the DNA damage recognition and repair pathways as well as the cell fate decision (197, 220). TGF $\beta$  has also been shown to influence changes in the epigenome, which also lead to accumulating genomic instability. Specifically, Smad 2 has also been shown to complex with HDAC resulting in the silencing of targets such as p15 (221).
- 3) *Evasion of Growth Suppressors*: As stated earlier, normal TGF $\beta$  signaling plays a role in negative cell cycle regulation. Neoplastic mechanisms for overcoming cytostatic TGF $\beta$  activity include deregulated Myc expression, methyltransferase inactivation of p21 transcription, and aberrant PI3K/AKT signaling (197, 220, 222, 223). It has also been suggested that T $\beta$ R-III and TGF- $\beta$ 3 likely play a role in suppressing unregulated TGF $\beta$  signaling (210).
- 4) *Tumor Promoting Inflammation*: TGF $\beta$  ligands produced by cancer cells serve as an attractant for tumor-infiltrating monocytes and macrophages (224). These immuno-species are known for their ability to promote tumor invasion and metastasis in response to TGF $\beta$  signals from the tumor cells. They do this by stimulating angiogenesis and the breakdown of the extracellular matrix (225). They also secrete additional TGF $\beta$  ligand into the tumor microenvironment further stimulating the tumor and in turn more immuno-species (225). Many other tumor microenvironment species also secrete and respond to TGF $\beta$  ligands (e.g., myeloid-derived suppressor cells) amplifying the TGF $\beta$  signal and driving TGF $\beta$ -metastasis (226).

## CHAPTER 2

- 5) *Evasion of Apoptosis*: TGF $\beta$  signaling is specifically involved in the induction of apoptosis in normal cells through both caspase-dependent and caspase-independent means discussed above (209). Many of the aberrations characteristic of in the “TGF $\beta$  paradox” shift to pro-tumorigenic activity (e.g., p15<sup>INK4b</sup> loss) specifically lead to a loss in growth suppression activity by TGF $\beta$  (174).
- 6) *Avoiding Immune Destruction*: TGF $\beta$  activity has been shown to suppress immunosurveillance by specifically inhibiting NK and cytotoxic T lymphocyte differentiation resulting in a decrease in the cytotoxic effectors they secrete, including: Fas ligand, perforin/granzyme, lymphotoxin- $\alpha$ , and interferon- $\gamma$  (218, 227-229). Moreover, TGF $\beta$  further inhibits the tumor-targeting ability of these two immune cell types by stimulating regulatory T cells in the tumor microenvironment (230).
- 7) *Unlimited Replication Potential*: The shift of TGF $\beta$  signaling to pro-tumorigenic activity results in cell cycle regulation loss and is important to the acquisition of unlimited replication in cells (213). The shift also overcomes the ability of TGF $\beta$  to induce apoptosis using a variety of means (209). While these hallmarks of the “TGF $\beta$  paradox” shift do not truly result in unlimited replication potential (by means like telomerase overexpression), they do contribute by deregulation of the cell cycle and evasion of apoptosis.
- 8) *Angiogenesis*: TGF $\beta$  signaling enhances tumor vascularization in a number of ways including the direct induction of key angiogenic factors including VEGF and CTGF (231, 232). TGF $\beta$  also plays a role in the maturation of new blood vessels. Smad 2/3 activation in response to TGF $\beta$  has been shown to correlate with genes involved in blood vessel maturation, including plasminogen activator inhibitor 1 (PAI-1) and fibronectin (233).
- 9) *Deregulating Cellular Energetics*: TGF $\beta$  signaling plays a role in deregulating cellular energetics indirectly. TGF $\beta$  is specifically associated with the development of rigid tumor microenvironments that allow for the enhancement of cell selection and metastatic expansion (234). TGF $\beta$  signaling alters cellular

energetics to meet the need of a growing and changing tumor by regulating the expression of Lysyl oxidase (LOX) family members that are responsible for cross-linking extracellular matrix building-block proteins like collagen and elastin (175). In normal tissues, LOX family members play a role in embryonic development and organogenesis. Importantly, their pro- or anti-tumorigenic activity with respect to TGF $\beta$  signaling appears to correlate with the “TGF $\beta$  paradox”.

10) *Invasion and Metastasis*: One of the best characterized role of TGF $\beta$  signaling in cancer is its ability to induce EMT, one of the initiating steps of metastasis. During EMT, cells lose their cellular polarity and adhesive properties and gain enhanced migratory and invasive capabilities. It has been shown that the induction of EMT by TGF $\beta$  relies on both Smad-dependent and Smad-independent signals (174). TGF $\beta$ -driven EMT is associated with the expression of E-cadherin repressors Zeb1 and Zeb2 (235). Specifically, the Zeb proteins associate with other corepressors, including Smad 3 to repress the transcription of epithelial genes such as E-cadherin (E-cad) (236). Moreover, many non-canonical pathways downstream of TGF $\beta$  activation contribute to EMT induction in response to TGF $\beta$  signaling directly or pathway collaboration with TGF $\beta$  signaling. The downstream signaling pathways shown to be responsive to TGF $\beta$  or work in collaboration with TGF $\beta$  include MAPK-ERK, PI3K/AKT, Rho/ROCK, Hedgehog, and WNT signaling pathways (190, 237).

### **Targeting TGF $\beta$ Signaling in Cancer: A Paradox Problem**

Effectively targeting TGF $\beta$  signaling therapeutically in cancer without inducing side effects has been the unachievable goal of the TGF $\beta$  community for decades. TGF $\beta$  clearly plays a role in tumor progression by driving growth. However, more important when considering therapeutic value are the roles of TGF $\beta$  in vascularization, reciprocal immunostimulatory activities within the tumor microenvironment, as well as invasion and metastasis. As stated earlier, EMT is a process that not only complicates EGFR sensitivity, but also complicates cancer treatment across tumor types (1, 147). In lung cancer alone, between 80-85% of patients present with a tumor that has already invaded nearby tissues or distally metastasized. This high percentage of advanced tumors is the

## CHAPTER 2

foremost reason why lung cancer treatments have such poor outcomes (6). For this reason, it is understandable why the field would aim to target one of the premiere drivers of tumor metastasis. Progress has been made in the last decade and a half towards understanding the enigma of the “TGF $\beta$  paradox” and the role TGF $\beta$  plays in driving tumor progression and metastasis will certainly keep it an attractive target moving forward (213). Unfortunately, many attempts have been made to target TGF $\beta$  clinically, and while they show promise in treating some tumors, they have devastating off-target effects in others (219). This is likely attributable to the role of TGF $\beta$  in normal cells. As stated earlier, TGF $\beta$  is specifically responsible for preventing cell growth, proliferation and survival in normal tissues following appropriate completion of development processes (175). Delineating the pro-tumorigenic activities of TGF $\beta$  from the anti-tumorigenic behaviors and determining how to identify and target them clinically is paramount to the success of TGF $\beta$  inhibitors (179).

Identifying which arm of the TGF $\beta$ -paradox is occurring continues to be enigmatic, so we need to seek out means of targeting pro-tumorigenic TGF $\beta$  signaling activities without targeting TGF $\beta$  directly. Recently, the activity of protein kinase CK2, also known as Casein Kinase 2 (CK2), has been linked to TGF $\beta$ -induced EMT as well as the development of acquired EGFR1 resistance (238, 239). Initial clinical studies of its orally-available inhibitor, CX-4945, suggest that treatment is well tolerated by patients unlike TGF $\beta$  inhibitors (240). For this reason, I explored it as an alternative avenue for overcoming EGFR1 resistance and have compiled an overview of it below.

### **D. CASEIN KINASE 2 (CK2) BIOLOGY**

#### **The Kinase**

Casein Kinase 2 (CK2) is a protein kinase that is ubiquitously expressed in both healthy and cancerous cells (241). CK2 consists of two catalytic subunits ( $\alpha$  and  $\alpha'$ ; gene IDs CSNK2A1 and CSNK2A2, respectively) and two regulatory subunits (both CK2 $\beta$ ; gene ID CSNK2B) (241). The complete protein kinase CK2 holoenzyme can be any tetrameric arrangement of two  $\alpha$  subunits and two  $\beta$  subunits (i.e.  $\alpha_2\beta_2$ ,  $\alpha'\beta_2$ ,  $\alpha'\beta_2$ ) (242). There is

## CHAPTER 2

also mounting evidence that CK2 $\alpha$  and CK2 $\alpha'$  subunits have kinase activity in their monomeric forms, but the holoenzyme has a substantially higher affinity for substrates (243, 244). Live-cell fluorescent imaging revealed that the majority of CK2 subunits are not contained in holoenzyme, but are dispersed as single subunits throughout the cell (245). Once the formed holoenzyme, subunits are predicted to remain associated as the dissociation constant for the holoenzyme is incredibly low (246).

CK2 $\alpha$  and CK2 $\beta$  subunits have been shown to be essential for viability using murine knock-out studies. CK2 $\alpha'$  knock out mice are viable, but males of this genotype are sterile (247). This suggests that while CK2 $\alpha$  may be functionally distinct from CK2 $\alpha'$ , it is able to partially compensate for its loss (241). Loss of the CK2 $\beta$  subunit results in early embryonic lethality in mice (248). CK2 has been shown to play a role in spermatogenesis (247), organ development (248, 249), and it has been suggested that its function is imperative during embryogenesis (250). In adult tissues, CK2 levels have also been shown to increase during times of cell proliferation and return to basal expression levels following proliferation events (242). While CK2 is constitutively expressed in nearly all tissues, its basal levels are considered to be sparse compared to other kinases (251). Importantly, unlike CK2, most kinases are regulated by expression levels and, more specifically, by activation events like ligand binding. Since CK2 is constitutively active, low expression levels are likely important to moderating CK2 activity.

What makes CK2 so unique is that unlike other proto-oncogenic kinases, CK2 is constitutively active without the aid of a gain-of-function mutation in both normal and cancer cells (252). Because CK2 $\alpha$  subunits are constitutively phosphorylated, the source of regulation must be something other than an upstream kinase. One of the known mechanisms of CK2 regulation comes from the CK2 $\beta$  “regulatory” subunits, which have been shown to act in a stimulatory fashion unlike the name suggests in most cases (253). However, in very specific cases (e.g., calmodulin and MDM2), CK2 $\beta$  subunits have been shown to be potent inhibitors of CK2 $\alpha$  phosphorylation of the substrate protein and, thereby, regulating the kinase activity of the  $\alpha$  subunits (254, 255). The CK2 holoenzyme has very high affinity for most of its substrates compared to free subunits and it has been suggested that this ability to complex tightly with many of its substrates is bridged by the CK2 dimer portion of the enzyme (256, 257). For this reason, decreases in CK2 $\beta$  expression might lead to an imbalance of active substrates of CK2 $\alpha$  monomeric activation

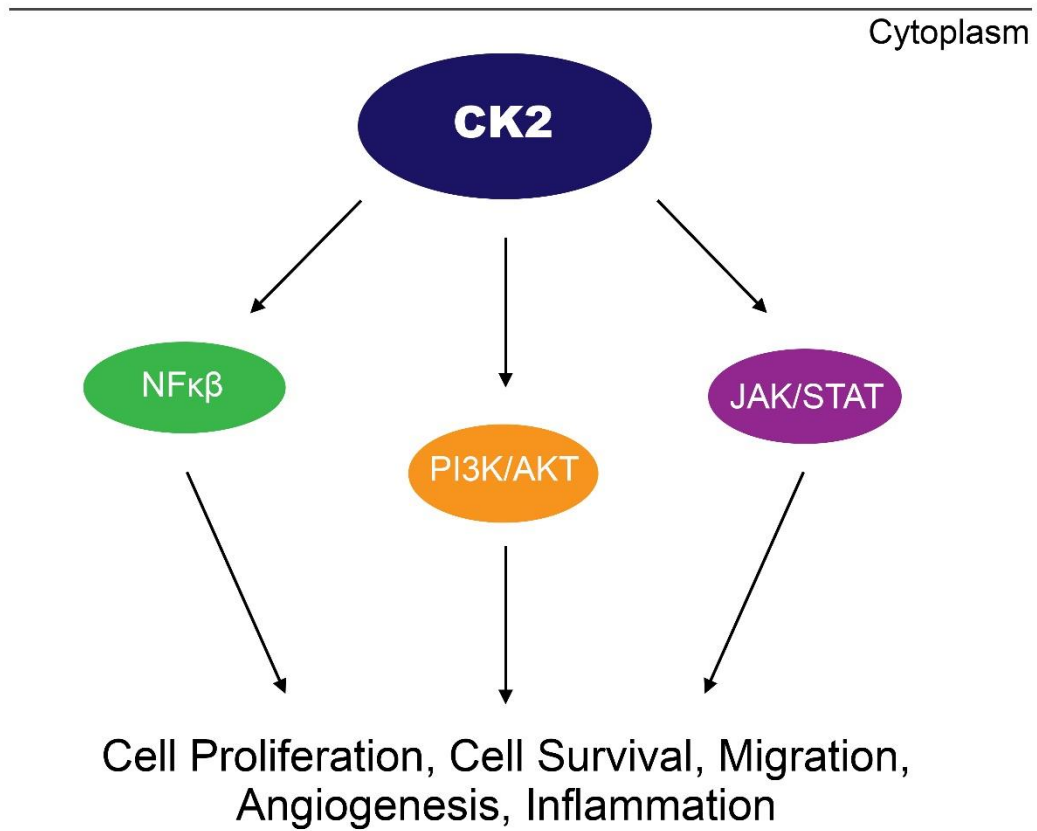


**Figure 1.4: CK2 Signaling Pathways.**

## CHAPTER 2

versus active substrates by the holoenzyme. CK2 is believed to be regulated by a combination of its subcellular location as well as its binding to other proteins or non-protein factors (255, 258). CK2 dynamically localizes to a variety of specific cellular compartments and/or organelles based on a diverse set of cellular conditions (259-261). Specifically, CK2 has been shown to shuttle between nuclear structures such as the chromatin and nuclear matrix in response to changes in growth stimuli (262, 263). It is also known to be dispersed throughout the cell during mitosis, which lends to the observation that its aberrant signaling is occurring in cancer cells where the mitotic process is recurring far more frequently than in normal cells (264). The protein degradation pathway has also been implicated in regulating its action (265).

### **CK2 in Cancer**

As stated earlier, CK2 expression levels are relatively stable and very small changes in its protein expression heavily impact the regulation of cellular homeostasis (242). Prior work has shown a link between CK2 subunit expression changes and the transformation of cells (266-268). CK2 subunits are upregulated in all cancers that have been profiled for its expression, including lung and bronchial, prostate, breast, colorectal, ovarian and pancreatic cancers (269). Increased CK2 activity from overexpression of the constitutively active kinase has been associated with aggressive tumor behavior (269, 270). Additionally, CK2 has no known gain-of-function mutations that would drive neoplastic transformation (252). For this reason, the reigning opinion is that overexpression of CK2 subunits leads to malignant transformation of cells, and this mechanism has been described as a “non-oncogene addiction” (271).

Perhaps most fascinating is that, across the literature, CK2 has been implicated for playing a role in the genesis and maintenance of every one of the classic as well as the emerging “hallmarks of cancer” (1):

#### *1) The Role of CK2 in Growth Signal Autonomy*

The global role of CK2 in cell signaling has been described as acting “horizontally” across a number of “vertical” signaling pathways both in cancer and in healthy cell signaling, thereby representing a means of pathway integration in

cancer cells (271, 272). CK2 has been shown to regulate common developmental signal transduction cascades known to be adulterated in tumorigenesis. Specifically, PTEN is phosphorylated by CK2 altering its stability and limiting its ability to regulate AKT signaling (273, 274). Similarly, CK2 drives AKT activation by phosphorylating it at a specific serine residue, Ser129, leading to hyperactivation of AKT signaling (275, 276). CK2 has also been shown to interact with the kinase suppressor of RAS (KSR) molecular scaffold required for the spatial regulation of MAPK-ERK signaling and its loss from that complex results in impaired RAF, MEK, and ERK activation (277). CK2 also influences a number of other signaling pathways responsible for aberrant growth and proliferation in tumors including JAK/STAT (278), NF $\kappa$ B (279), fibroblast growth factor (FGF) (280, 281), AKT/PKB signaling (275), Wnt signaling (279, 282), and Hedgehog signaling (283). Importantly, CK2 has been shown to connect many of these pathways acting as an intermediary effector in the network. Specifically, EGFR/ERK has been shown to stimulate WNT/ $\beta$ -catenin through CK2 $\alpha$  (284).

### *2) The Role of CK2 in Genomic Instability*

CK2 has been well described for its role in regulating the response to DNA damage. Perhaps the best described role of CK2 in the cell cycle is that it regulates the tumor suppressor, p53. It does so by CK2-mediated phosphorylation at serine 392 in response to UV induced DNA damage (268, 285-287). Specifically, UV-induced DNA damage induces the assembly of the CK2-hSPT16-SSRP1 complex (288). CK2 has also been shown to phosphorylate MDM2, which decreases its binding affinity for pRB and reduces its ability to direct p53 degradation (285, 289). Another important feature of CK2 activity that promotes the genomic instability fueling oncogenic transformation is that it would appear to play a crucial role in transcription and chromatin remodeling (290, 291). CK2 activity is also connected to all three RNA polymerase functions, DNA topoisomerase II, as well as a number of pre-mRNA transcription and splicing factors suggesting a further role in mRNA translation (292-295). It is believed that phosphorylation of transcription and splicing factors by CK2 likely changes their activity as well (296). CK2 has also been shown to facilitate DNA repair through phosphorylation of the XRCC1 scaffolding protein required for single-strand break repair and base excision repair

## CHAPTER 2

(297) and plays a role in many cellular mechanisms that recognize and repair DNA damage and strand breaks (251).

### *3) The Role of CK2 in the Evasion of Growth Suppressors*

CK2 also plays a role in the evasion of growth suppression by the negative regulation of tumor suppressors like PTEN and PML. PML is a tumor suppressor responsible for moderating the pathways involved in growth suppression, apoptosis and senescence, and it is most frequently lost in tumors by post-translational mechanisms (298). CK2 promotes ubiquitin-mediated degradation of PML by phosphorylating it at Ser517 (298). CK2 has also been shown to phosphorylate the tumor suppressor PTEN at its C-terminus tagging it for proteasome-mediated degradation (274). Importantly, the CK2 phospho-site on PTEN is not the only one influencing the fate of PTEN (299). CK2 has also been recently identified for its ability to phosphorylate and inhibit the action of another member of the p53 tumor suppressor family, the TAp73 variant, promoting a cancer stem cell phenotype in head and neck cancers (300).

### *4) The Role of CK2 in Tumor Promoting Inflammation*

CK2 has been shown to play a role in tumor-promoting inflammation pathways. Specifically, it has been shown to respond to reactive oxygen species (ROS) by interactions with p38, ultimately inducing NF $\kappa$ B activation (301). Platelet activating factor (PAF) and tumor necrosis factor  $\alpha$  (TNF $\alpha$ ) also drive the activation of p38/CK2/NF $\kappa$ B in response to ROS (301). CK2 has also been shown to modulate IL-6 expression in breast cancer. It has been suggested that IL-6 stimulation induces CK2 to phosphorylate the EMT effector, TWIST, thereby stabilizing it (302, 303). This is an example of how CK2 can influence and respond to tumor microenvironment inflammation signals that promote tumor development. It has also been shown that CK2 interaction with JAKs is necessary for the induction of JAK/STAT signaling in response to inflammatory cytokines (278), and inhibition of CK2 prevents constitutive STAT signaling (304). Interestingly, CK2 maintains epithelial characteristics in patients with chronic colitis preventing inflammation-driven apoptosis (305).

### *5) The Role of CK2 in the Evasion of Apoptosis*

CK2 has been implicated for globally regulating apoptotic pathways influencing Bid, Bad, Max, Faf1, Bcl-2 and Bcl-xL, caspase 2, caspase-inhibiting protein ARC, and the inhibitor of apoptosis proteins (IAPs), which include survivin (242, 263). Specifically, the activation of AKT/PKB signaling by CK2 has been shown to upregulate survivin expression by  $\beta$ -catenin (306). It has also been demonstrated that CK2 inhibition can sensitize breast tumor cells to TRAIL-induced apoptosis mediated by the Apo2 ligand (307, 308). Moreover, targeting overexpressed CK2 in glioblastoma results in the suppression of pro-survival signaling pathways including PI3K/AKT, JAK/STAT, HSP90, Wnt, Hedgehog, and NF $\kappa$ B (309).

### *6) The Role of CK2 in Avoiding Immune Destruction*

The role of CK2 in the ability of cancer cells to avoid immune response is only coming to light very recently. Rather than a function in the cancer cells themselves, CK2 activity in regulatory T-cells (T<sub>reg</sub> cells) has been implicated for its role in helping tumor cells hide from immune responses. Specifically, it has been shown that CK2 $\beta$  ablation in the T<sub>reg</sub> cells of mice results in the induction of a cancer-killing inflammatory response called T helper type 2 (T<sub>H2</sub>) by dendrites responding to the differentiated T<sub>reg</sub> cells (310). CK2 is overexpressed in T<sub>reg</sub> cells, and its function specifically suppresses T-cell antigen receptor signaling in T<sub>reg</sub> cells. Ultimately, this results in the induction of the T<sub>H2</sub> inflammatory response in the lungs (311). It has been suggested that global targeting of CK2 in cancer treatment could possibly have the secondary impact of inducing the T<sub>H2</sub> response and eliciting an impactful anti-tumor immune response (311).

### *7) The Role of CK2 in Replicative Immortality*

CK2 has been described as interacting with and/or phosphorylating many of the proteins involved in the regulation of the G1/S cell cycle checkpoint as described above. To date, CK2 interactions with p53 have not been shown to

differentiate between normal and mutant p53 as well, so it is not surprising that its action plays a role in replicative immortality in cancer cells expressing mutant p53 (312, 313). It has been demonstrated in glioblastoma cells that CK2 inhibition is sufficient to induce p53-dependent cell cycle arrest and also results in sensitization of cells to TNF $\alpha$ -driven apoptosis (314). CK2 inhibition also resulted in increased telomerase activity and increased p53-dependent senescence, but importantly, these functions by CK2 inhibition were only observed in p53 wild-type cells (314).

### *8) The Role of CK2 in Angiogenesis*

CK2 has been well described for its role in promoting angiogenesis in tumors. CK2 regulates hypoxia inducible factor-1 $\alpha$  (HIF-1 $\alpha$ ), the main angiogenesis inducing pathway, in a variety of ways (315). It has been shown that inhibition of CK2 results in lower expression of HIF-1 $\alpha$  during times of hypoxia because of increased p53 levels (316, 317). CK2 has also been shown to specifically phosphorylate Proline-Rich-Homeodomain protein (PRH) specifically blocking its ability to bind DNA. This action prohibits PRH from repressing VEGF and other components of VEGF signaling (318). FGF has also been implicated in angiogenesis and it is also a known binding partner of CK2 $\beta$ . The complex of FGF-2 and CK2 has also been shown to drive CK2 kinase to act on nucleolin which is responsible for the synthesis and maturation of ribosomes (281). This relationship suggests that CK2 activity is likely also important for the production of FGF and VEGF signaling components (e.g., ligands, receptors). Finally, it has also been shown that PDGF signaling, a common growth factor player in angiogenesis, induced the expression of CK2 $\alpha'$  subunits.

### *9) The Role of CK2 in Deregulating Cellular Energetics*

CK2 plays such an extensive role in the other hallmarks of cancer, so it is no surprise that it also may play a role in the metabolic reprogramming of cells required to compensate for the increased energy demands of developing tumors. Specifically, CK2 kinase activity has been described as regulating the purinosome, a multi-subunit complex responsible for purine synthesis in cells in response to changes in available nucleotides (319). CK2 has also been directly linked to the

## CHAPTER 2

hormonal regulation of carbohydrate metabolism as well as the regulation of other enzymes involved in carbohydrate storage and metabolism (320). Finally, CK2 activity has been implicated in upregulating cytosolic levels of zinc, a secondary messenger implicated in many growth and proliferation pathways including AKT and ERK1/2 activation. CK2 phosphorylates the ZIP7 channel on the endoplasmic reticulum simulating it to open, thereby releasing stored zinc levels into the cytosol (321).

### *10) The Role of CK2 in Invasion and Metastasis*

Recently, the greatest interest in CK2 as a tumor driver has been in its role in invasion and metastasis. CK2 has been shown to be an intermediate effector linking pERK activation by EGFR to the phosphorylation of  $\alpha$ -catenin and the subsequent transactivation of  $\beta$ -catenin leading to invasiveness of tumor cells (284). CK2 $\beta$  down-regulation has been observed concurrently with dramatic changes in cell migration and adhesive properties (322). A genome-wide characterization of mRNA expression in CK2 $\beta$ -depleted breast cancer cells highlighted the upregulation of the core mesenchymal genes (CDH2, VIM, SNAIL1, TWIST1, ZEB1, ZEB2, etc.), and a down-regulation of the core epithelial genes (CDH1, CDH3, MUC1, etc.) (322). CK2 $\beta$ -depleted breast cells also demonstrated changes in a number of genes responsible for the necessary extracellular matrix and cytoskeletal alterations required for EMT (e.g., ADAM19, ADAM23, FN1, COL6A1) (322).

### **Therapeutic Targeting of CK2 in Cancer**

The initial trepidation in targeting CK2 came from the revelations that it interacts with a large fraction of the kinome, and when inhibited, might logically result in adverse events in patients. It has also been shown that knockouts of two of the three subunit types results in embryonic lethality (248, 249, 252). Despite this, the growing knowledge of the role of CK2 in tumorigenesis of many types of cancer led to the development of the orally-available CK2 inhibitor, CX-4945 (Silmitasertib), in 2010 (252). CX-4945 is in clinical Phase 1/2 trials in cholangiocarcinoma (240) (323). However, CK2 inhibition is currently not being investigated in lung cancers.

## CHAPTER 2

CX-4945 treatment has been largely inconsequential as a single agent, likely because the majority of its roles in cancer can be compensated for by other kinases (252). Importantly, Franchin *et al.* demonstrated that CK2 null cells ( $\alpha/\alpha^{(-/-)}$ ) still demonstrate pAKT S129 levels despite the fact that the Serine 129 residue is a specifically known CK2 phosphosite (252, 324). This reinforces the notion that single-agent CK2 inhibition may continue to have poor efficacy as an anti-tumor therapy because compensatory signaling is readily activated. It also highlights that CK2 is a logical secondary signaling source that may be responsible for drug-resistance to current targeted therapies. A Phase 1/2 trial in cholangiocarcinoma is examining the combination of CX-4945 with gemcitabine and cisplatin (323) and combinations of CX-4945 and other targeted agents are currently being explored pre-clinically.

### E. PROJECT OVERVIEW

The aim of our lab is to use pharmacogenomics to improve the clinical care of lung cancer patients. Specifically, we have used high-density genomic data generated from NSCLC cell lines with known sensitivities to EGFR1 to do three things:

- 1) *Develop predictors of EGFR1-response in order to accurately stratify NSCLC patient response to EGFR1 therapy.* As stated earlier, clinically-utilized small molecule inhibitors of EGFR1 are specifically designated for the treatment of tumors harboring specific EGFR mutations. Using single-gene mutation statuses to identify patient response does not encompass all putative responders, nor does it account for non-responders harboring the mutation of interest. Developing more robust predictors is paramount to accurately stratifying responders from non-responders. It can also identify the potential for resistance development in patients.
- 2) *Interrogate the deregulated genes and signaling pathways identified by gene expression predictors to gain a greater understanding of the biology governing response to EGFR1 in NSCLC.* Exploring the genes and pathways that indicate

## CHAPTER 2

drug-sensitivity provide essential knowledge for identifying the mechanisms by which resistance to therapy develops. We might also identify possible secondary targets for the treatment of EGFR-resistant NSCLC.

- 3) *Leverage deregulated mRNA and miRNA genes to determine putative interactions that might be exploited to identify novel drug targets and methodologies for treating EGFR-resistant NSCLC.* We have developed a methodology for expanding the network in a disciplined manner to identify nodes connecting deregulated signaling pathways and cellular processes. Using this multi-faceted approach to identify deregulated networks, we are able to filter much of the “noise” generated by the heterogeneity among NSCLC lines in the genomic studies. From a translational standpoint, this is a particularly difficult hurdle in identifying novel drug targets and treatment strategies for lung tumors that harbor immense amounts of somatic mutations and expression level changes.

The history of targeting EGFR and managing EGFR resistance has been built on the philosophy of targeting “oncogene addictions” exclusively. While many NSCLC are reliant on overactive EGFR signaling, almost all eventually develop resistance to EGFR inhibitors because subpopulations of cells not requiring constitutively active EGFR signaling or with mutant, drug-resistant EGFR arise (29, 147). The second and third generations of EGFR inhibitors were built to overcome some of the resistance mechanisms that are acquired, but have essentially continued to monotherapeutically target EGFR (147). This strategy does not impact the development of other resistance mechanisms through other kinases and oncogenes (e.g., MET, ALK and ROS1), phenotypic changes (e.g., EMT), and alterations in downstream effectors (e.g., BRAF) (147, 148). Moreover, consecutive generations of EGFR inhibitors have also allowed the selection of novel resistance polymorphisms in well-characterized EGFR antagonists (e.g., NRAS E63K and EGFR L798I/Q) (147, 154-156). Mechanisms of drug-resistance across every biological model from antibiotic-resistance in bacteria to anti-retroviral resistance among HIV/AIDS patients highlight that drug-resistance results from the selection of cells/organisms that have evolved means of bypassing drug efficacy. Complex eukaryotic organisms like humans have cells that possess many more avenues of circumventing specific nodes while achieving the same results in response to situations like genetic loss

## CHAPTER 2

or damage. While this behavior of compensatory signaling is imperative for human growth, development, and survival despite genetic defects, it is also exploited by tumor cells to overcome both innate and pharmacological anti-cancer strategies. Continuing our current method of simply modifying EGFR inhibitors with a focus on targeting only EGFR will likely always be met with resistance mechanisms that will continually evolve to overcome the newest anti-EGFRI.

Early EGFRI-TKI efficacy prediction relied on the presence of EGFR activation mutations and KRAS activation status (3, 133, 143, 166, 169, 325, 326). This method of identifying responders did not segregate responders completely. To address this, our lab hypothesized that multivariate biomarkers could be used to better capture the EGFRI-resistant and -sensitive phenotypes (327, 328). In line with our first aim to produce biomarker signatures of drug efficacy, the lab produced two different polygenic biomarkers predictive of EGFRI sensitivity, one of 180-mRNA and one of 13-miRNA genes (327, 328). Importantly, both are the product of larger lists of deregulated genes that distinguish the EGFRI-resistant and -sensitive phenotypes.

The second goal of our lab is to interrogate the list of deregulated genes that stratify EGFRI-resistant and -sensitive cells. We do this to better understand the biology driving each phenotype, thereby rationally seeking alternative methods for targeting EGFRI-resistance. Of the mRNA that were found to be deregulated for the generation of the 180-mRNA signature, MAPK-ERK and PI3K/AKT/mTOR signaling were prominently represented (328). Because of this, our lab members have systematically interrogated the value of MEK and EGFR combinatorial therapy (329), the regulation of downstream ERK by deregulated dual-specificity phosphatases (DUSPs) (330), and the role of p110 $\alpha$  isoform compensation in PI3K inhibitor compensation (331).

The desire for a new perspective on the cellular deregulation stratifying EGFRI-resistant and -sensitive cells led to the development of the second signature identifying response to the EGFR-TKI, erlotinib. Comprised of 13- deregulated miRNA genes, the additional signature was not only able to discriminate between EGFRI-resistant and -sensitive cells, but was also able to distinguish clinical samples as primary or metastatic lesions (327). Bioinformatic analysis of the 13-miRNA genes comprising the signature revealed that they functionally converged on the TGF $\beta$  signaling pathway (327). As stated

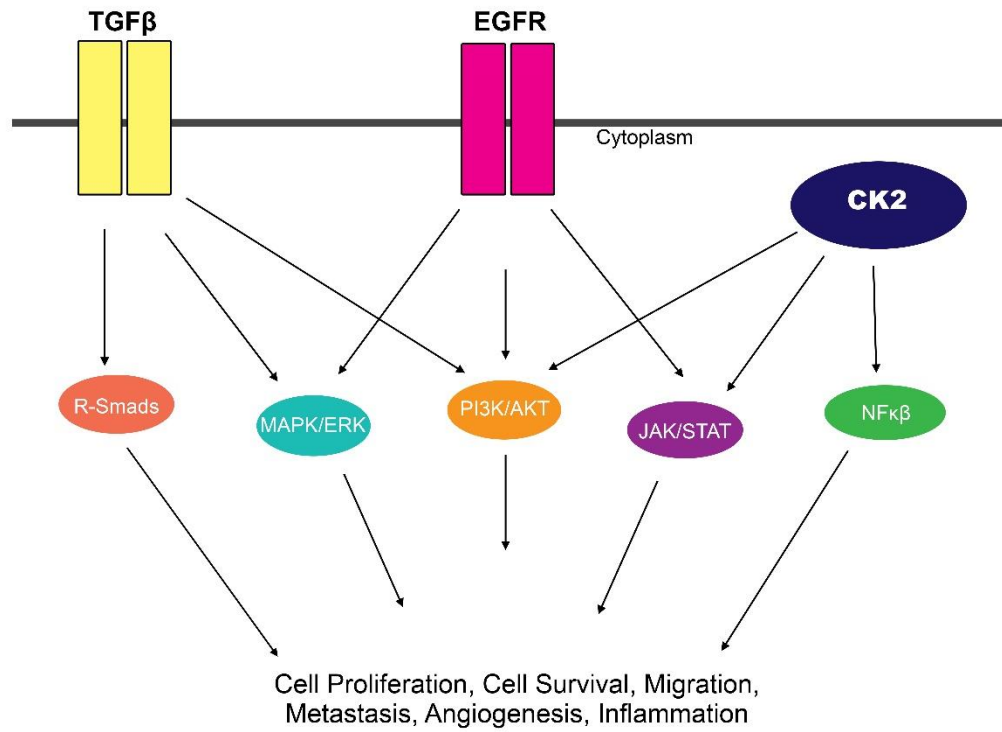


**Figure 1.5: Cross talk amongst TGFβ, EGFR, and CK2 Signaling.**

## CHAPTER 2

earlier, phenotypic changes, like EMT, are sources of EGFR1 resistance (148) and TGF $\beta$  is a known driver of the EMT program (332, 333). Moreover, many of the signature miRNA putatively control expression of EMT-related proteins (327). For this reason, **the first hypothesis I proposed and tested was that the miRNA comprising the signature of response were transcriptionally regulated by canonical TGF $\beta$  signaling by Smad activation/repression (Chapter 2)**. Canonical TGF $\beta$  signaling by Smad activity could be responsible for controlling the expression of the miRNA that distinguish EGFR1-resistant from -sensitive cells.

**The second hypothesis I proposed and tested was that TGF $\beta$  signaling impacted EGFR1-resistance differently between EGFR1-resistant and -sensitive NSCLC (Chapter 3).**

The third aim of our lab is to leverage the gene expression data generated over time that is descriptive of the fundamental cellular differences between EGFR1-resistant and -sensitive cells using novel mathematical and computational methods. The two expression signatures were culled from larger lists of 1495 deregulated mRNA and 23 deregulated miRNA genes. We chose to bolster current studies by considering inversely related miRNA:mRNA pairs. **The third aim I proposed and tested was whether mRNA and miRNA gene expression data interactions, whether physical or not, would identify nodes of cell signaling. These interactions and their protein-protein interacting partners may indicate new targets for novel treatment options (Chapter 4).**

This work is a study of what we can learn about the biology of a tumor phenotype (e.g., EGFR1 resistance status) by interrogating gene expression differences. I will demonstrate the value of cross-examining multiple levels of genomic data to identify meaningful networks of deregulated signaling. I will also demonstrate that meaningful therapeutic targets can be captured using basic mathematical characterization of “significantly deregulated genes”. Finally, I will propose a method for the targeted treatment of EGFR1-resistant lung tumors as identified by this new method of network analysis.

## CHAPTER 2

### A. OVERVIEW

Lung cancers are frequently diagnosed in later stages of disease progression with few treatment options available for patients. In the last decade, a number of targeted therapies have been developed against impactful oncogenic targets in lung cancer (e.g., EGFR, ALK, and ROS), but many tumors either lack an actionable oncogenic mutation or harbor an inherent resistance mutation (e.g., KRAS). Therefore, most patients receive a cytotoxic agent to which they may not respond (55, 83). Unfortunately, many patients with a targetable mutation eventually develop resistance to targeted therapy enforcing the need to couple or stage therapies to combat resistance.

Genome scale sequencing and gene expression technologies have provided scientists and clinicians the tools to gather increasingly more specific insight on tumor heterogeneity thereby allowing for tumor-specific therapeutic decisions to be made. While the ability to characterize tumors at this level has revolutionized the concept of personalized cancer care, the breadth of information presents the dilemma of how to interpret molecular characteristics that are biologically relevant for treatment decisions. Recently, The Cancer Genome Atlas (TCGA) conducted genomic, transcriptomic, and proteomic profiling of 230 lung adenocarcinomas revealing that 73% of the tumors studied showed activation of the Ras/Raf cascade downstream of a Receptor Tyrosine Kinase (RTK) at the level of genomic alterations and gene expression, but only a subset of those tumors showed aberrant activation of this cascade at the protein level (334). This observation underscores the diversity within and between tumors reinforcing the need for multivariate predictors of drug response to overcome the failings of single biomarker methods of response prediction.

One of the more commonly targeted oncogenic RTKs in Non-Small Cell Lung Cancers (NSCLC) is the Epidermal Growth Factor Receptor (EGFR). The EGFR inhibitor,

## CHAPTER 2

erlotinib, is indicated for use in patients harboring an EGFR-activating mutation (10-15% of patients) and is contraindicated for use in patients with mutated KRAS (25-30% of patients) (335). Using only these two markers to assign erlotinib treatment in NSCLC has yielded results that are modest at best (336). To augment the short-comings of KRAS and EGFR mutation status as the sole predictive metric, the Black laboratory showed that microRNA (miRNA) expression patterns in different cell lines could predict erlotinib resistance, reporting that a 13-miRNA gene signature could be used for these purposes (327). Our 13-miRNA gene signature of response is not only able to stratify NSCLC cells and tumor samples into erlotinib-sensitive and -resistant groups, but was also able to discriminate between primary and metastatic lesions. Understanding why the expression of these small RNA molecules can distinguish response to anti-EGFR therapy and discriminate metastatic lesions has implications for both prognostic and predictive clinical applications.

MicroRNA are non-coding, small, RNA that regulate gene expression by pairing with complementary mRNA resulting in translation inhibition or degradation of the mRNA (337). miRNA play a role in a number of biological processes (e.g., growth, differentiation, and proliferation), so it is not surprising that endogenous expression levels are deregulated in cancer (338). Bioinformatic analysis of the 13-gene miRNA signature showed that many of the proposed target genes functionally converge on the TGF $\beta$  signaling pathway (327). For this study, we specifically focused on signature members miR-140, miR-141, and miR-200c due to their opposing expression between erlotinib-sensitive and -resistant cell lines. The miR-200 family, including miR-200c and miR-141, is well-characterized for preventing EMT onset by targeting transcription factors (e.g., Zeb1 and 2) responsible for suppressing expression of epithelial characteristics, such as the E-cadherin (E-cad) adhesion proteins (332, 339-341). High expression of these two miRNA correlate with erlotinib-sensitivity in the 13-miRNA gene signature. Conversely, miR-140 is highly expressed in erlotinib-resistant cells and is predicted to target the TGF $\beta$  receptor and Smad 2 (327, 342). Importantly, these data demonstrate that opposing expression profiles and activities are necessary for EMT.

The TGF $\beta$  signaling pathway is well documented for its role in the induction and potentiation of the mesenchymal phenotype in tumor cells (343). TGF $\beta$  is a ubiquitous cytokine that is active in a number of cell processes, and many of cell types secrete the

## CHAPTER 2

ligand and express the receptors to bind it (174). Activation of TGF $\beta$  signaling is accomplished by TGF $\beta$  ligands binding to the extracellular domain of TGF $\beta$ II receptors. This allows it to recruit the TGF $\beta$ I receptor and then bind a second pair of activated TGF $\beta$ II/I receptors resulting in transautophosphorylation within the tetramer (179).

TGF $\beta$  canonical signaling is mediated by Smads 2, 3, and 4, which bind to Smad Binding Elements (SBE) on DNA eliciting a transcriptional response (344). TGF $\beta$  potentiates the Epithelial to Mesenchymal Transition (EMT) in some cancer cells by signaling through a variety of other non-canonical pathways including PI3K/AKT and MAPK/ERK (190). Interestingly, several groups have noted that erlotinib sensitivity tends to correlate with the epithelial phenotype (345). Since TGF $\beta$  upregulates genes responsible for the activation of the EMT program (346), and because the miRNA signature is capable of stratifying between primary and metastatic lesions *ex vivo* (327), we hypothesize that TGF $\beta$  supports differential expression of the signature miRNA between erlotinib-resistant and -sensitive NSCLC.

## B. METHODS

### Cell Culture, Protein harvest, Immunofluorescence, and Western Blot

A549, PC9, H460, and H1650 cell lines (NSCLC) were purchased from ATCC. They were cultured in RPMI 1640 supplemented with 10% FBS (USA Scientific) and maintained in a humidified incubator at 37 °C at 5% CO<sub>2</sub>. Cells were seeded in 6-well plates and were allowed to grow under maintenance media conditions for 48 hours prior to treatments. Cells undergoing 24 hours of treatment were plated 4 x 10<sup>4</sup> cells/well, and 72- and 168-hour treated samples were plated at 1 x 10<sup>4</sup> cells. Cells were treated with SB-431542 (3  $\mu$ M) (Selleck Chem) and/or TGF $\beta$  (5 ng/ml) (Cell Signaling Technologies) under minimal serum (1%) conditions for time frames specified. If treatment times exceeded 72 hours, treatment media was replenished at the 72-hour time point. Whole-cell extracts were collected using RIPA buffer (50 mM Tris-HCl, 1% NP-40, 150 mM NaCl, 1 mM EDTA, 0.25% DOC, 10% glycerol, in ddH<sub>2</sub>O) and protein content was quantified

## CHAPTER 2

using a BCA kit (ThermoFisher) prior to western blotting. Proteins were separated using SDS-PAGE and were transferred to a nitrocellulose membrane. Expression and/or activation of specific proteins (pSmad 2, tSmad 2, pSmad 3, tSmad 3, tSmad 4,  $\alpha$ -tubulin, pERK1/2, tERK1/2, pAKT, tAKT, E-cad, Vimentin, N-cad, Zeb1) was assessed by western analysis using antibodies purchased from Cell Signaling Technologies. Immunofluorescence was performed using Alexa Fluor-conjugated antibodies of the specific clone of E-cad and vimentin used for western blotting (Cell Signaling Technologies). Immunofluorescence was measured using the AMG EVOS microscope with built-in EVOS software (Thermo Fisher). Cell morphology images were recorded using the Zeiss AxioObserver Microscope and processed using the AxioVision software.

### **Chromatin Immunoprecipitation (ChIP)**

ChIP assays were carried out with the Simple ChIP Plus Enzymatic Chromatin IP Kit (Cell Signaling Technologies) to measure Smad 4 binding to two putative SBE sites in the shared promoter of miRNA-141 and miR-200c at -1645/-1247 and -1793/-1395 from each transcriptional start site, respectively. Cells were plated at  $5 \times 10^5$  cells per dish in 10 cm dishes for 48 hours prior to a media change to 1% FBS-containing RPMI +/- 5 ng/ml TGF $\beta$ 1 treatment for 24 hours. After treatment, cells were cross-linked, processed, and digested as described in the Simple ChIP protocol (Cell Signaling Technologies). Samples were divided following digestion and chromatin complexes were immunoprecipitated with Smad 4 antibody (20  $\mu$ l/ChIP) against a non-specific rabbit IgG (1  $\mu$ l/ChIP) overnight and then pulled down with magnetic ChIP-grade protein G beads for 2 hours (Cell Signaling Technologies). Immunoprecipitated samples were washed, uncrosslinked, and DNA was prepared as described in the Simple ChIP protocol (Cell Signaling Technologies). SYBR Green qRT-PCRs (Applied Biosystems) were performed with negative-control  $\alpha$ -Satellite and positive-control ID1 Smad 4-specific control primers against the experimental region containing the two putative SBEs in the shared promoter of miR-141/-200c (Forward: GCATTACTCAGCAAATCCTTAC; Reverse: CCCGACAGGTGATTGCC. Primers designed in-house and produced by IDT). Data was analyzed using the Percent Input method where signals from ChIP samples are represented as a percentage of the total chromatin input. Each individual experiment was replicated in triplicate for each primer set and processed using the 2% input method described in the Cell Signaling Technologies protocol. Data represented is for three biological replicates (n = 3). P-values were

## CHAPTER 2

generated using paired t-tests comparing each TGF $\beta$  treated sample to its respective untreated sample.

### **Real-Time PCR Analysis of miRNA Expression**

Total small RNA was harvested from the cells using the mirVANA™ miRNA isolation kit (Life Technologies). cDNA was synthesized for U6, miR-140, miR-141, and miR-200c using the TaqMan MicroRNA Reverse Transcription kit and corresponding reverse transcription TaqMan primers for U6, miR-140, miR-141, and miR-200c (Life Technologies). cDNA was then subjected to quantitative Real Time PCR (qRT-PCR) using TaqMan Mastermix II with no UNG, and corresponding TaqMan microRNA assay primers (Life Technologies). qRT-PCR were performed by a 7900HT Fast Real-Time PCR system (ABI) and all reactions were run in duplicate with corresponding positive and negative controls. The data was analyzed using a 5-way ANOVA following internal normalization of raw Ct values to the internal U6 as the normalization probe.

### **Propidium Iodide (PI) and Flow Cytometry**

A549 and PC9 cells were subjected to the same treatments and time points as previously described. Specifically, cells were rinsed in PBS at point of harvest, trypsinized, and collected in a 15 ml conical tube. Cells are centrifuged at 1500 rpm and the supernatant is removed. Cells are washed once with cold PBS, pelleted, and the supernatant removed. Finally, the cell pellet was resuspended in 400  $\mu$ l of cold PBS and then 1 ml of cold, 100%, molecular biology grade ethanol was added to each sample dropwise while gently vortexing and then samples were placed on ice for 30 minutes. Cells were pelleted by centrifugation and the supernatant removed, and then washed in cold PBS/1%BSA. The pellet was resuspended in 0.3 ml of PI solution (1X PBS/1% BSA/50  $\mu$ g/ml PI/0.5 mg/ml RNase A). Samples were incubated in the PI solution for at least 30 minutes at 4 °C protected from light. Samples were assayed on the Attune Flow Cytometer acoustic focusing cytometer, and 10,000 cells from each sample were profiled for PI emission, and data was collected with the Attune-specific software provided (Applied Biosystems/ThermoFisher). Percentage of total cells in each phase of the cell cycle was determined using the cell cycle analysis platform in the FlowJo V10 software (FlowJo).

### **Statistics**

To analyze changes in endogenous gene expression data generated by qRT-PCR described above, a five-way ANOVA was performed using the following variables: treatment with TGF $\beta$ , treatment with SB-431542, time point, expression as internally normalized Ct values, and cell line, along with all interaction terms. The overall F-test, followed by partial F-tests were used to determine significant effects. Following the ANOVA, post-hoc comparisons were made for significant terms in the ANOVA using two-sample *t*-tests to compare subgroups of interest. Tests were determined to be significant if p-values were less than 0.05. All analyses were performed in SAS Version 9.3 or above (SAS Institute Inc., Cary, NC).

### **C. RESULTS**

#### **Most Signature miRNA Promoters Contain Smad Binding Elements**

The promoter of each of the 13 signature miRNA was analyzed using chipMAPPER (347, 348) for putative SBEs (344, 349). Predicted SBEs were retained if they had conservative E-values ( $\leq 25$ ) and a score greater than 3.0. SBEs matching these criteria were found in the promoter regions of twelve of the thirteen signature miRNA (Figure 2.7). The three signature miRNA genes we focused on in this study (miR-140, miR-141, and miR-200c) have multiple predicted SBEs within -2000 base pairs of transcriptional start site (Figure 2.1) (184, 344, 350).

The activity of complexes containing Smad 2 and Smad 3 along with the DNA-binding member, Smad 4, have been shown to have both positive and negative effects on transcription (351, 352). Since the signature miRNAs are differentially expressed among cell lines, the majority of their promoters contain putative SBEs, and the known dual behavior of TGF $\beta$  activity on gene expression, we hypothesized that the canonical TGF $\beta$  signaling pathway likely controls opposing expression levels of signature miRNA between erlotinib-sensitive and -resistant NSCLC lines.

## **TGF $\beta$ -mediated Smad Signaling has an Opposing Phenotype in Erlotinib Resistant and -Sensitive Cell Lines**

A549 and PC9 cell lines were selected as representative NSCLC cell lines due to their opposing erlotinib responses and opposing expression levels of the 3 candidate miRNA. A549 are inherently erlotinib-resistant because they harbor a KRAS activation mutation, and PC9 are erlotinib-sensitive treatment because they contain an activating exon 19 deletion in EGFR (328).

We first examined the expression and activation of the Smad molecules, Smad 2, Smad 3, and Smad 4, after treatment with exogenous TGF $\beta$  ligand, an inhibitor of TGF $\beta$ RII, SB-431542, or the combination in these cell lines (Figure 2.2A) by western blot to determine if these effectors could be responsible for signature miRNA regulation. In both A549 and PC9 after 24 hours of treatment, pSmad 2 and pSmad 3 levels are elevated in cells treated with TGF $\beta$ , and the effect was diminished in cells treated with SB-431542 or the combination of SB-431542 and TGF $\beta$ . Total Smad 2, Smad 3 and Smad 4 levels appear to be consistently expressed across treatments at 24 hours. There were no obvious levels of pSmad 2 or pSmad 3 in either cell line or in any treatment condition at the 72-hour treatment time point. Total Smad 2 and Smad 4 levels appear to be consistently expressed in both cell lines across both treatments. However, in both cell lines, tSmad 3 levels were diminished in cultures treated with TGF $\beta$ .

At 168 hours, pSmad 2 levels were seen only in A549 treated with TGF $\beta$ . Phospho-Smad 3 levels were not observed in either line at 168 hours. tSmad 2, tSmad 3, and Smad 4 appear diminished in PC9 treated with TGF $\beta$  alone, and this phenotype was not observed in any other condition. A549 demonstrated similar expression of total Smad molecules across all treatment conditions.

We observed the cyclical activation of Smad 2 in A549 while activation of Smad 3 was observed early following initial stimulation, but did not return. In PC9, a different phenotype emerged with diminished levels of all Smad 2, Smad 3, and Smad 4 molecules by 168 hours. Taken together, these data suggest that the TGF $\beta$  canonical signals are managed differently in A549 and PC9.

### **TGF $\beta$ Treatment Induces an EMT Protein Expression Switch in A549 but not in PC9**

Like many, we observed that A549 cells treated with TGF $\beta$  undergo a morphological change with treatment and appropriately activate R-Smad proteins - a phenotype consistent with EMT. PC9 cells did not undergo these changes with TGF $\beta$  treatment, but interestingly, PC9 cells treated with the TGF $\beta$  inhibitor displayed an EMT intermediate phenotype known as “Metastable” (Figure 2.8) (353). For this reason, we assessed a panel of EMT protein markers to determine if the morphological changes observed were indicative of EMT progression and correlated with signature miRNA endogenous expression changes.

A549 and PC9 were plated, treated, and harvested as described for protein measured by BCA assay prior to western blotting. Lysates were assessed for mesenchymal markers N-Cadherin (N-cad), Zeb1, and vimentin as well as the epithelial marker, E-cadherin (E-cad) to confirm if the morphological changes were consistent with EMT occurring (Figure 2.2B). As a comparison, we also profiled A549 and PC9 cells for E-cad and vimentin expression by immunofluorescence at 24- and 168-hour (7 days) time points (Figure 2.2C-F). mRNA levels of E-cadherin were examined in both cell lines at 24-, 72- and 168-hour time points to fully capture the change in expression of this epithelial marker across time points (Figure 2.9I).

In A549, TGF $\beta$  suppressed E-cad expression across each of the time points in the experiment, as expected. Conversely, vimentin expression increased over the time course of TGF $\beta$  treatment. N-cad and Zeb1 appear in the 72- and 168- hour time points, respectively, in TGF $\beta$ -treated A549. The immunofluorescence profile of E-cad expression at the 24 hour and 7 day –treated time points in A549 cells was consistent with the levels observed by western analysis. Vimentin levels increased in A549 cells also mirrored the western blot results (Figure 2.2C,D).

In PC9, neither TGF $\beta$  stimulation nor its inhibition decreased E-cad expression or induced expression of the mesenchymal markers assessed. E-cad expression was consistent between the western and immunofluorescent assays. Vimentin expression was not observed by western or immunofluorescence assays (Figure 2.2E,F). Since PC9 responded unexpectedly to treatment, we sought to determine if TGF $\beta$  directly regulated

## CHAPTER 2

the expression of two candidate miRNA genes in both A549 and PC9 by assessing if Smad 4 directly binds a shared putative SBE.

### **TGF $\beta$ Induces Smad 4 Binding to Putative SBEs in the Promoter of mir-141/200c in Erlotinib-Sensitive Cells**

To test the impact of the observed deregulation of R-Smad activity in A549 and PC9 on candidate miRNA expression, we asked whether Smad 4 was directly binding the promoters of our miRNA genes. Smad 4 is the only member of the canonical-Smad family with a nuclear localization signal, and others have shown that it is required for any active Smad complex to translocate into the nucleus to regulate transcription. Direct regulation of gene expression by TGF $\beta$ -activated Smad complexes is expected to occur within 24 hours of treatment (184). For these reasons, we only tested Smad 4 binding to the SBE locus after 24 hours of treatment by Chromatin Immunoprecipitation (ChIP).

In A549 cells, TGF $\beta$  treatment induced a significant enrichment of the positive control, the ID1 promoter SBE, bound to Smad 4 ( $p = 0.0171$ ). The mir-141/-200c promoter region was not significantly enriched in A549 cells in any treatment or antibody combination (Figure 2.3A). In PC9 cells, TGF $\beta$  treatment enriched both the positive control, ID1 ( $p = 0.0035$ ), and the mir-141/-200c promoter containing the SBE locus ( $p = 0.0006$ ), suggesting that Smad 4 is bound to the shared promoter region in PC9 cells and not in A549 cells treated with TGF $\beta$  (Figure 2.3B). This observation led us to ask whether the observed DNA interaction between the Smad 4- containing complex and the SBE resulted in changes in endogenous levels of miR-141 or miR-200c.

### **Time, Not Treatment, Alters the Expression of the Candidate microRNAs**

Activated Smad 2 and Smad 3 were present in both lines at 24h post-TGF $\beta$  treatment and pSmad 2 returned at 168h after treatment in A549. We have also shown that Smad 4 is expressed in all conditions and binds mir-141/200c promoter at 24 hours post-TGF $\beta$  treatment in PC9. For these reasons, we anticipated that differential expression of the signature miRNA genes would occur under these conditions as a result of TGF $\beta$  treatment. To explore this, A549 and PC9 were cultured and harvested as described and assessed for endogenous expression changes of three signature miRNA

## CHAPTER 2

genes, miR-140, miR-141, and miR-200c by qRT-PCR. Importantly, these experiments were performed in 1%-serum media to minimize the impact of exogenous cytokines. We tested each of the three miRNA profiled in the conditions indicated here in both 1% serum and 10% serum treatment conditions to confirm that the changes observed are not due to serum levels. Importantly, miRNA expression does not significantly differ between the two serum levels for any of these three miRNA (Figure 2.13).

The miRNA expression trends did not differ significantly among treatment conditions, but differences across time points were observed (Figure 2.10). An initial 2-way ANOVA comparing endogenous miRNA expression changes as internally-normalized Ct values within each cell line indicated that the most impactful variable governing endogenous expression change was the time of treatment. The 2-way ANOVA was not able to compare whether the expression changes correlated with other miRNA tested or the erlotinib- sensitivity status of a cell line. In order to capture this complexity, we used a 5-way ANOVA to identify significant interactions between five variables: 1) miRNA expression (Ct values), 2) time point sample was taken, 3) TGF $\beta$  treatment addition, 4) SB-431542 treatment addition, and 5) cell line. All combinations of factors were simultaneously calculated (5-way ANOVA Input in Supplementary Table 1, Ct averages in supplementary file 1, Appendix I). The 5-way ANOVA revealed that treatments and miRNA expression levels are not related, and that the most influential experimental component was the time of treatment (Figure 2.4A and Figure 2.11). Figure 2.11 shows that individual miRNA expression follow the same trends across treatments over time. For simplicity, since expression trends did not differ drastically between treatments, we chose to present the overarching miRNA expression trends generated as averages of treatments in each individual cell line at each time point (Figure 2.4A). The table highlights the significance of endogenous expression changes among time points separated by miRNA gene in each cell line (Figure 2.4B). Taken together, these data demonstrate that treatment was not impactful in the changes in endogenous miRNA expression, but the time of treatment was. Importantly, individual miRNA expression changes did not correlate with the erlotinib sensitivity of each cell line. From these data, we hypothesized that the impact of the time of treatment may be directly related to the cell cycle position of the cells.

### **Time, Not Treatment, Alters the Cell Cycle Position of A549 and PC9 Cells**

## CHAPTER 2

To assess whether observed changes in miRNA expression correlate with cell cycle position, as a measure of time, A549 and PC9 cells were assessed for percentage of cells in each cell cycle position at each of the time points. Cells were treated and harvested as described for cell cycle analysis using propidium iodide staining and flow cytometry. For each sample, 10,000 events were counted to ensure percentages were not skewed by the differing number of cells present in each sample at the end of treatment. Overall proliferation following respective treatment times is shown in Figures 2.12 and 2.13 as cell counts.

Irrespective of treatment, the percentage of A549 cells in the  $G_0$ - $G_1$  phase of the cell cycle increased over time of treatment. PC9 cells behaved similarly (Figure 2.5). However, PC9 cells treated with TGF $\beta$  failed to continue to proliferate after 72 hours while the percentage of cells in  $G_0$ - $G_1$  changed. To understand the impact of time and treatment on percentage of cells in the  $G_0$ - $G_1$  phase of the cell cycle, a 2-way ANOVA was performed within each individual cell line to capture the most impactful factor influencing the trends. The ANOVA confirmed that the most important factor governing the increasing number of cells in of  $G_0$ - $G_1$  phase was cumulative time of treatment. In A549 cells, time of treatment significantly explained cells in the  $G_0$ - $G_1$  phase of the cell cycle ( $p < 0.0001$ ). In PC9, both treatment conditions ( $p < 0.0001$ ), time of treatment ( $p = 0.0002$ ), and the interaction of the two variables ( $p = 0.0168$ ) had a significant impact on the percentage of cells in the  $G_0$ - $G_1$  phase of the cell cycle. Because cell cycle position interacted with time of treatment, we wondered whether a specific non-canonical signal transduction cascade downstream of TGF $\beta$  was activated that might impact cell cycle progression.

### **TGF $\beta$ Activation of Non-Canonical Effectors ERK1/2 and AKT Differs Between A549 and PC9**

Since miRNA endogenous expression changes appeared to correlate with changes in the cell cycle rather than TGF $\beta$  treatment, we endeavored to understand the impact of TGF $\beta$  treatment on non-canonical effectors known to drive growth and proliferation, Ras/MAPK and PI3K/AKT pathways. The same protein lysates profiled for the R-Smad effectors and EMT marker proteins in Figure 2.2 were assessed for both pERK1/2 and pAKT expression. Corresponding total protein expression of each across

## CHAPTER 2

the same treatments and time points described above were measured by western blot (Figure 2.6). In A549, pERK1/2 levels increase with TGF $\beta$  treatment across the time points while total protein levels remained constant. pAKT levels in A549 increased at the 24-hour time point, but then diminish across time points while total levels of the protein were constant. In PC9, pERK1/2 and pAKT levels were elevated at the 24-hour time point, but both diminish over time without a decrease in total protein levels in the cells treated with SB-431542 with and without co-treatment with TGF $\beta$ . Densitometry performed on these blots can be seen in Figure 2.14. These data suggest that the relationship between TGF $\beta$  and non-canonical growth and proliferation pathways and may explain why the changes in endogenous miRNA expression correlated with an increasing percentage of cells in the G<sub>0</sub>-G<sub>1</sub> phase of the cell cycle.

### D. DISCUSSION

In early stages of tumor development, TGF $\beta$  acts as a tumor suppressor preventing the proliferation, differentiation, and overall survival of the impacted cells. In later stages of tumor development, TGF $\beta$  shifts from tumor suppressive functions to promotion of tumorigenesis by driving the transcription of pro-EMT genes, which stimulate tumor cells to invade and metastasize (354, 355). The role of TGF $\beta$  signaling in EMT is of particular interest to our group because the 13-gene miRNA signature not only stratified NSCLC into erlotinib-sensitive and erlotinib-resistant groups, but was also able to discriminate between primary and metastatic tumors (327), and multiple members of the miRNA signature have been shown to play either a promoting or repressing role in EMT in NSCLC (332, 356, 357). For this reason, we endeavored to understand the role of TGF $\beta$  signaling on the expression of microRNA genes dysregulated in erlotinib-sensitive compared with erlotinib-resistant cell lines.

TGF $\beta$  drives EMT by using the canonical signaling pathway, mediated by the R-Smads, which upregulate transcription responsible for the repression of epithelial characteristics (190). Analysis of the TGF $\beta$ -driven R-Smad family members, showed a differential response to TGF $\beta$  treatment between the erlotinib-resistant, A549 cells, and erlotinib-sensitive, PC9 cells. Activated Smad 2 and Smad 3 expression was observed in

## CHAPTER 2

both cell lines at similar levels at early time points of treatment. At the 168-hour time point, activated Smad 2 levels return in A549 cells treated with TGF $\beta$ , compared to unchanging total Smad 2, Smad 3 and Smad 4 levels across treatments. In PC9 cells after 168 hours of TGF $\beta$  treatment, the total expression of all TGF $\beta$  effectors tested was reduced suggesting the impact of some negative feedback mechanism. TGF $\beta$  is known for promoting EMT in late stages of tumor development, but in the early stages, it functions in an anti-EMT capacity (355). We believe this cyclical pattern of TGF $\beta$  activation and R-Smad molecule repression to be indicative of TGF $\beta$  acting in an anti-EMT capacity in these cells.

To delve further into whether TGF $\beta$  treatment acted by different mechanisms between the two lines tested, we explored TGF $\beta$ -driven morphological changes and EMT marker protein expression changes. It is known that TGF $\beta$  treatment induces a very long, fibroblast-like phenotype in A549 cells (Figure 2.8) and western blot analysis of the EMT markers E-cad, vimentin, N-cad, and Zeb1 shows that TGF $\beta$  treatment induced a protein expression phenotype consistent with EMT (Figure 2.2B) (358). However, this study is the first to demonstrate biological differences in “epithelial” NSCLC cell lines, like PC9 cells, treated with TGF $\beta$ . In PC9 cells, the morphology after TGF $\beta$  treatment is unchanged. Interestingly, PC9 cells treated with the TGF $\beta$  inhibitor, SB-431542, with and without co-stimulation with TGF $\beta$  develop a morphology consistent with an EMT-intermediate phenotype known as “metastable” suggesting that the inhibition of TGF $\beta$  in PC9 cells may play a role in the induction of EMT (Figure 2.8) (353, 359). This observation, as well as that of the change in expression of the R-Smads in these cells, is consistent with the TGF $\beta$ -paradox theory and also correlates with the signature’s ability to stratify primary and metastatic lesions. To test whether TGF $\beta$  inhibition induced EMT initiation in PC9 cells, we profiled EMT protein markers to determine if the morphological change was indeed indicative of an EMT intermediate. While PC9 cells treated with the TGF $\beta$  inhibitor, SB-431542, undergo a morphological change consistent with EMT initiation, the western blot and immunofluorescence analyses revealed that the cadherin switch, that is essential for full-EMT, did not occur in response to treatment (360). Taken together, these data suggest that while TGF $\beta$  may act as a pro-tumorigenic, pro-EMT fashion in A549 cells, it may play an anti-EMT and protective role in PC9 cells because the inhibition of TGF $\beta$  did not induce a complete EMT transition in these cells.

## CHAPTER 2

Since A549 and PC9 cells appeared to represent either side of the TGF $\beta$  paradox, we sought to elucidate whether TGF $\beta$  directly regulated the expression of the candidate signature miRNA genes to understand whether the differing impact of TGF $\beta$  observed by R-Smad and EMT marker expression was also differentially regulating the expression of some of the signature miRNA genes. We expected TGF $\beta$  to directly regulate the expression of the signature miRNA and from there we expected to be able to triangulate a relationship between erlotinib- sensitivity, TGF $\beta$  signaling, and the 13-miRNA gene signature to determine therapeutically-relevant, secondary targets for overcoming inherent or acquired erlotinib-resistance. To test if TGF $\beta$  was directly influencing the expression of miR-200c and miR-141, we performed a ChIP assay to determine whether TGF $\beta$  induced the binding of Smad 4 to an SBE site in the shared promoter of mir-200c/mir-141. These two miRNA genes have very different baseline expression profiles between the mesenchymal, A549, and epithelial, PC9, cell lines. We showed that TGF $\beta$  treatment induced Smad 4 interaction with the shared mir-141/mir-200c promoter only in PC9 cells. However, in PC9 cells endogenous miR-141 and miR-200c expression at 24 hours after treatment showed no impact of any treatment condition, suggesting that TGF $\beta$  signaling may not be important in this context. Importantly, Smad 4 must be bound to activated Smad 2 or Smad 3 to carry out transcriptional control, and we did not test whether pSmad 2/3 was present with Smad 4.

While we did not observe a change in endogenous expression of any of the three miRNA in response to treatment, we did observe that the change in expression of miR-200c and miR-141 in response to changes in the time of treatment, and we believe that time is reflective of cell cycle position. Importantly, miR-200c and miR-141 are thought to be under coordinated transcriptional regulation because of an overlapping promoter region (361). Our data suggests that, at least in these treatment conditions and cell lines tested, miR-141 and miR-200c are not commonly regulated as is expected of genes that share a promoter region. We also observed that the trends in expression changes did not segregate the two erlotinib-resistant lines, A549 and H460 cells, from the two erlotinib-sensitive lines, PC9 and H1650 cells, suggesting that changes in the expression of these miRNA did not correlate with erlotinib-resistance or EMT status (Figure 2.4 and Figure 2.11).

Using a 5-way ANOVA, we discovered that that the most important factor

## CHAPTER 2

governing the changes in endogenous miRNA expression was the time of treatment. Thus, we investigated whether cell cycle stage could impact the expression of these genes. In Figure 2.15, we interrogated the putative transcription factor binding sites of one cell cycle regulated effector, ELK1, using the ChipMAPPER algorithm (347, 348). The analysis revealed putative ELK1 sites in the promoters of 12 out of 13 of the miRNA genes profiled, supporting our hypothesis that cell cycle progression may control the expression of the candidate miRNA genes. Analysis of the cell cycle position of A549 and PC9 cells across the same treatments and time points revealed that as time of treatment increased, the percentage of cells in the G<sub>1</sub>-G<sub>0</sub> phase of the cell cycle increased, except in TGFβ treated cells at the final time point (Figure 2.5). Importantly, the impact of treatment alone on cell cycle stage was only significant in PC9 cells (Figure 2.5). Figures 2.12 and 2.13 illustrate cell counts, reflective of doublings, in both 1% and 10% serum across treatment conditions. PC9 cells failed to continue to grow in the presence of TGFβ and 1% serum which may explain the reduction of cells in G<sub>1</sub>-G<sub>0</sub> phase of the cell cycle at 168 hours. Further experimentation will be necessary to understand this modest but significant decline.

Finally, because of the observation that cell cycle position may be important in expression of the miRNA examined in this study, we interrogated the activation of TGFβ non-canonical growth and proliferation pathways, Ras/MAPK and PI3K/AKT, to determine if they may play a role in the relationship of cell cycle position and endogenous miRNA expression. pERK activation increased across the time points in A549 cells, and its activation may influence the re-emergence of pSmad 2 levels at 168 hours because pERK is known to phosphorylate the linker region of Smad 2 to stabilize the signal (190). pERK signaling is also required for TGFβ- driven EMT, consistent with the increase in pERK signal in A549 cells undergoing TGFβ-induced EMT (353). PC9 cells harbor an EGFR-activating mutation resulting in the constant expression of pERK and pAKT. Perhaps most interestingly, treatment with the TGFβ receptor inhibitor, SB-431542, resulted in the reduction of both signals regardless of co-treatment with TGFβ ligand. SB-431542 is a competitive ATP binding site kinase inhibitor and has been shown to disallow ERK, JNK, or p38 pathway activation from other signals or their response to serum (362). These data suggest that, at least in PC9 cells, the perpetual activation of ERK and AKT signals from active EGFR signaling may rely on basal activation from TGFβRII in order to persist. We anticipate testing this using a TGFβ-receptor knock-down to observe whether the same

## CHAPTER 2

impact on ERK and AKT signals is observed.

Our future experiments will attempt to fill the gaps noted from this work. We will determine whether the remaining erlotinib-sensitive cell lines used to generate gene expression data have a similar response to long term TGF $\beta$  treatment even though we know that erlotinib-sensitive tumors also have metastatic capability. We will also determine if erlotinib response is altered by time in treatment as miRNA expression and cell cycle position were. We will test whether the expression of ELK1 in cells is important for cell cycle progression in this context because the shared promoter of mir-141 and mir-200c contains an ELK1 binding site. We might also determine if E2F sites are present and active because TGF $\beta$ -driven, DNA-binding Smad complexes have been shown to interact with cell cycle regulating elements (363, 364). Therefore, it is possible that Smad 4 binding to the SBE in PC9 cells does requires coordinate cell cycle regulation, through ELK1, to regulate the expression of miR-141. The presence of known cell cycle responsive elements in the promoters of most of the 13-signature miRNA suggests that the cell cycle may play a role in governing the expression levels of these miRNA genes. Understanding the mechanism of regulation of the signature miRNA genes might help us further understand whether TGF $\beta$  signaling is a driver of EMT and metastasis or a passenger alongside cell cycle-dependent regulation of these genes.

### **E. CONCLUSIONS**

Our original hypothesis that TGF $\beta$  directly regulated the expression of the microRNA gene signature and that it modulated gene expression differently in erlotinib-resistant versus erlotinib-sensitive cells was founded on a bioinformatics analysis of these genes with little regard for cellular context. We found that TGF $\beta$  is likely not directly responsible for control of the expression of the microRNA genes we tested. However, we still find it an attractive therapeutic target if we can understand the cellular or tumoral context wherein targeting this cytokine impacts NSCLC patient survival.

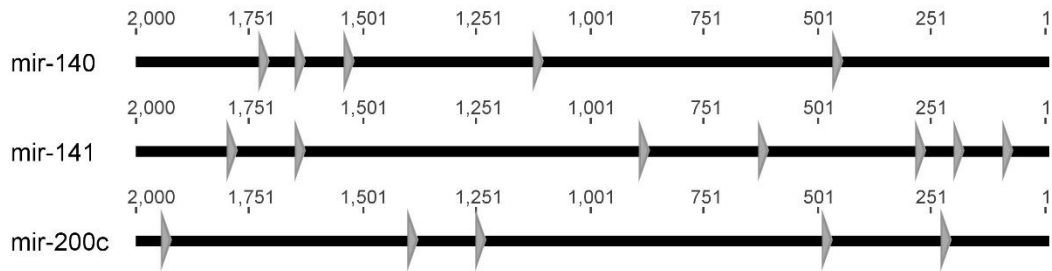
## CHAPTER 2

ADAPTED FROM: Krentz Gober, M., *et al.* A microRNA signature of response to erlotinib is descriptive of TGF $\beta$  behaviour in NSCLC. *Scientific Reports*. 2017

Copyright © Madeline Krentz Gober, 2017

## CHAPTER 2

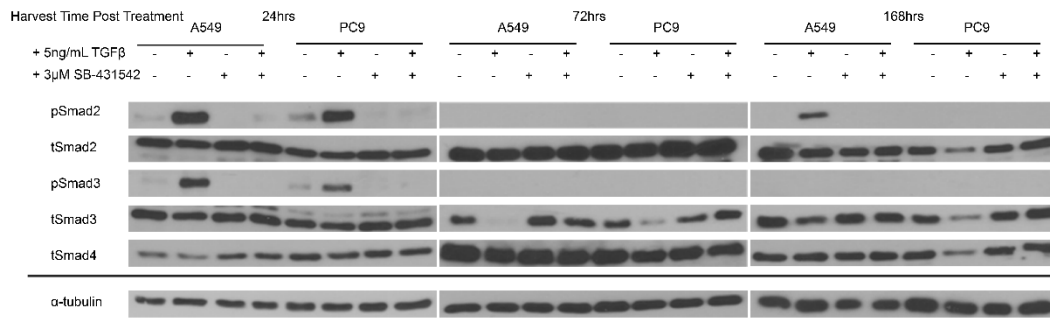
**Figure 2.1: Signature microRNA genes contain SBE elements.** Promoter analysis was conducted using the ChipMAPPER algorithm (347, 348). microRNA genes -140, -141, and -200 contain putative SBE elements as represented by the triangle with conservative E-values less than or equal to 25 and a score greater than 3.0.



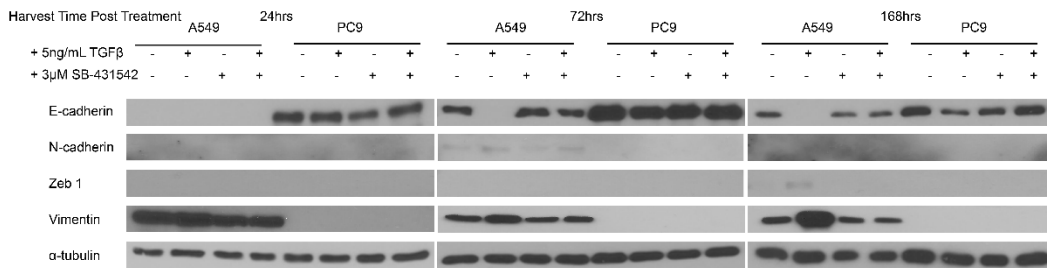
CHAPTER 2

**Figure 2.2: Total Smad expression, Smad activation and EMT program marker expression varies with TGFβ or inhibitor treatment.** Erlotinib-resistant, A549 cells, and erlotinib-sensitive, PC9 cells were plated, treated and harvested as described. Proteins were visualized by western blotting. All blots from the same samples; α-tubulin levels are representative controls for each sample. **(A)** Profiling of Smad family member expression and activation across time demonstrates changes in TGFβ canonical signaling. **(B)** EMT protein markers demonstrate program initiation and progression among treatment conditions. **(C)** A549 cells treated for 24 hours for E-cadherin and vimentin expression by immunofluorescence **(D)** A549 cells treated for 7 days for E-cadherin and vimentin expression by immunofluorescence **(E)** PC9 cells treated for 24 hours for E-cadherin and vimentin expression by immunofluorescence **(F)** PC9 cells treated for 7 days for E-cadherin and vimentin expression by immunofluorescence.

**A**

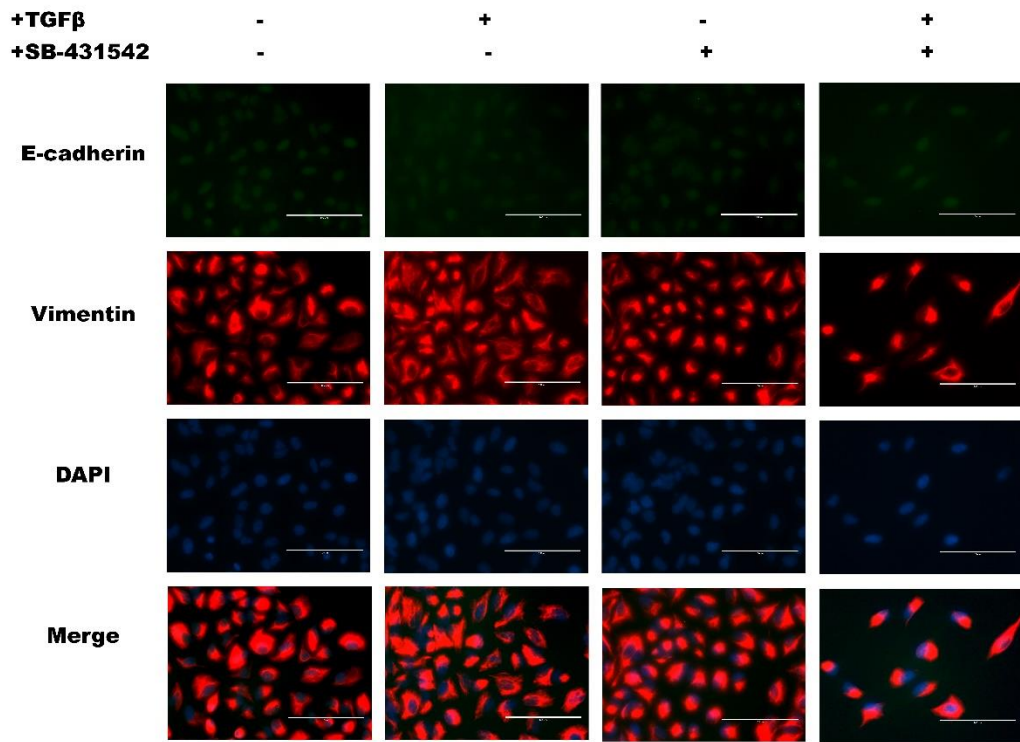


**B**

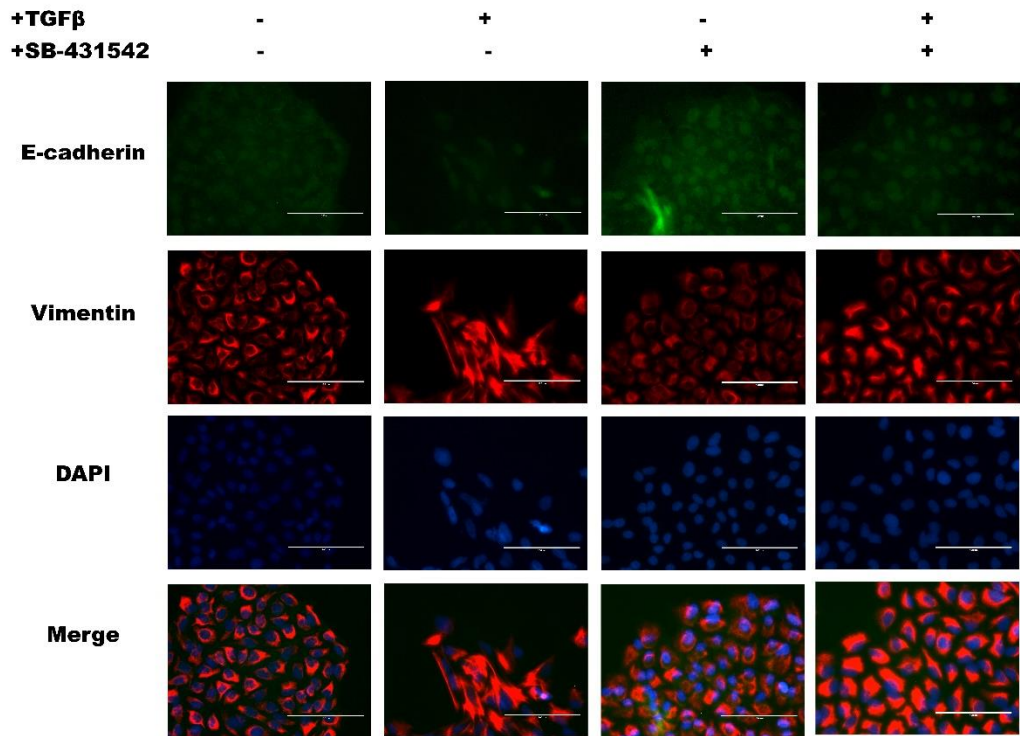


CHAPTER 2

C

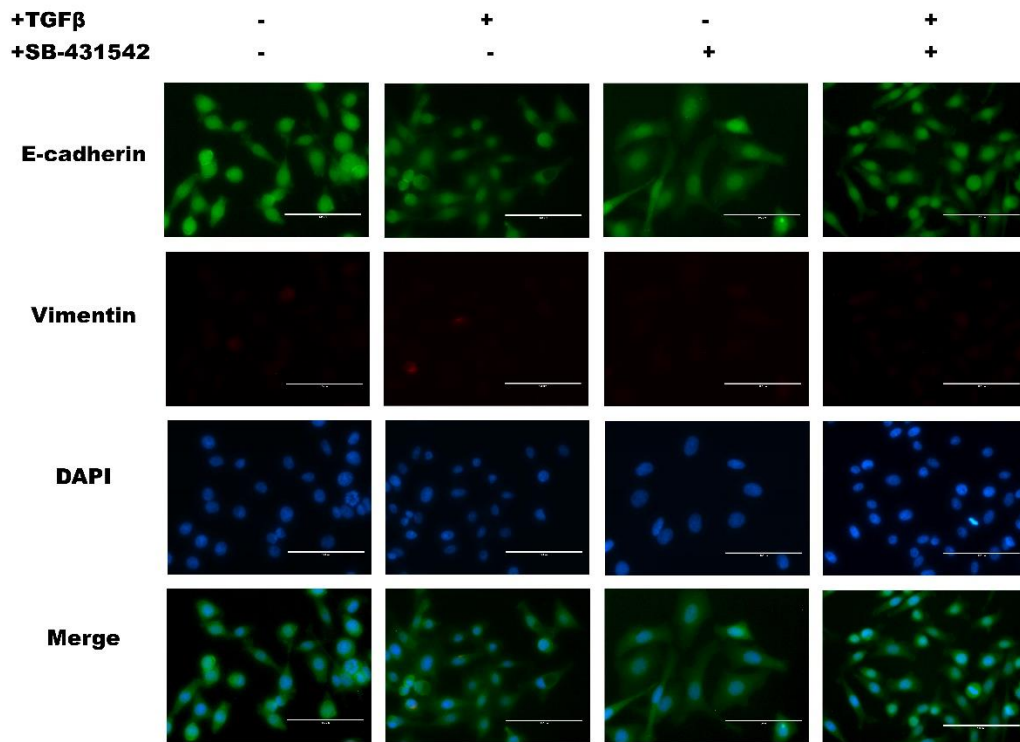


D

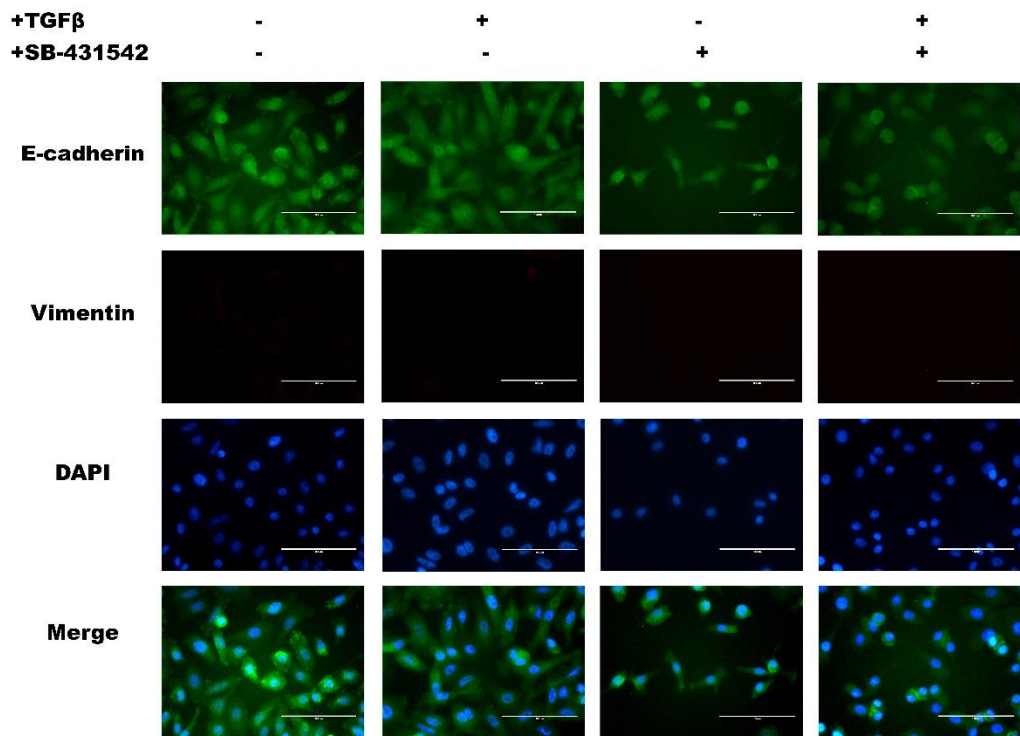


CHAPTER 2

E

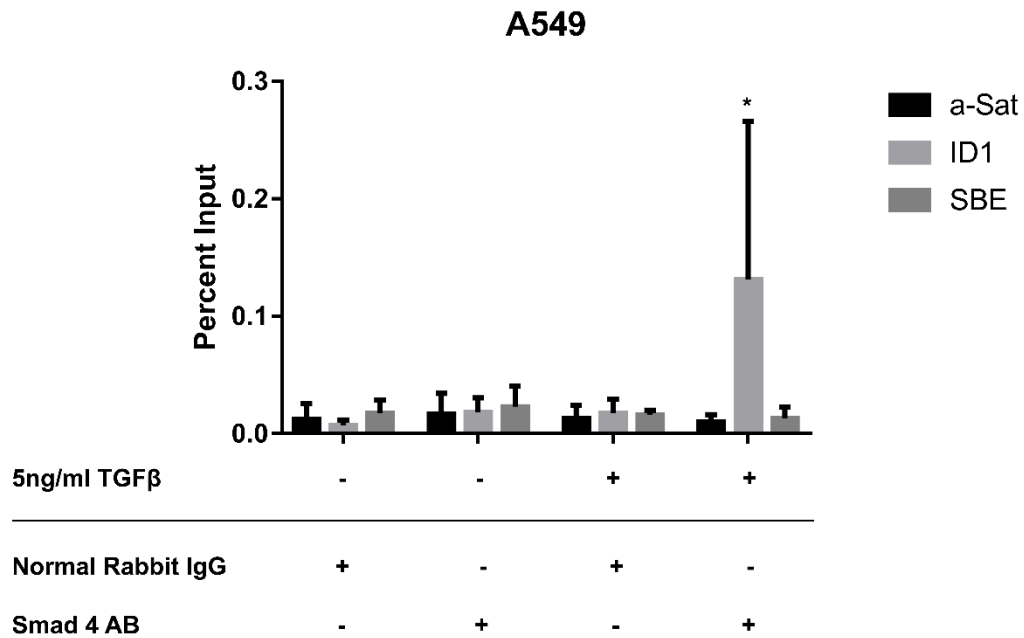


F



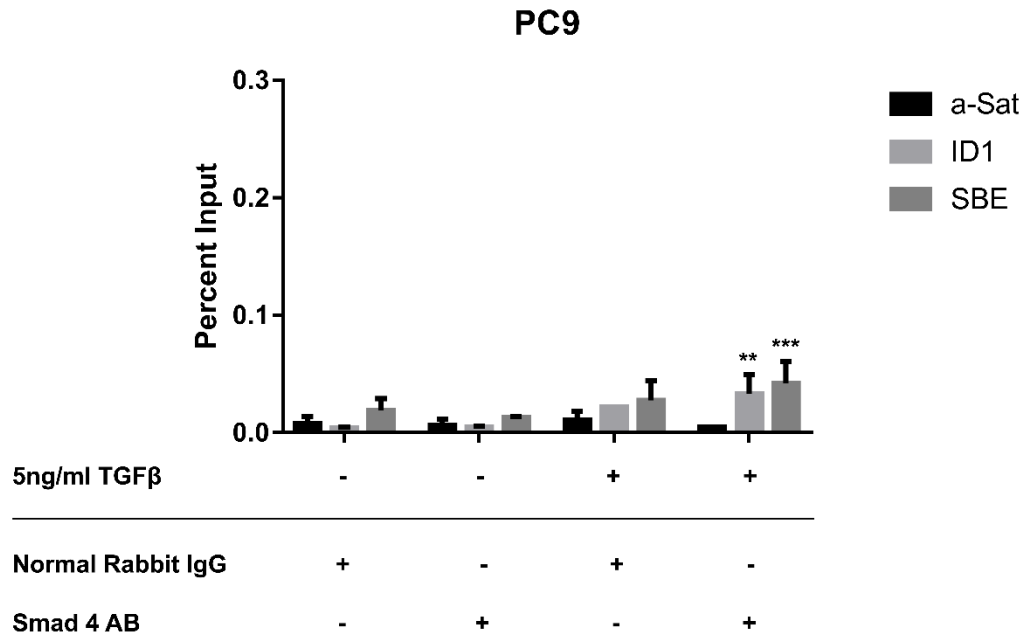
**Figure 2.3: TGFβ induces Smad 4 binding to SBEs in the promoter of mir-200/141 in PC9 cells.** Chromatin immunoprecipitation was performed to identify whether a physical interaction between Smad 4 and a predicted SBE locus in the shared promoter of mir-200c/-141 resulted from TGFβ treatment. Normal rabbit IgG served as the antibody negative control and α-Satellite primers as the negative PCR control. ID1 locus immunoprecipitation was the positive control for Smad 4 binding. **(A)** In A549, positive Smad 4-ID1 association is observed with TGFβ treatment, but an Smad 4-SBE interaction is not. **(B)** In PC9, both Smad 4-ID1 and Smad 4-SBE interaction is observed. Significance was calculated using an unpaired t-test comparing TGFβ-treated cells and -untreated samples with the same primer set. (n=3)

**A**



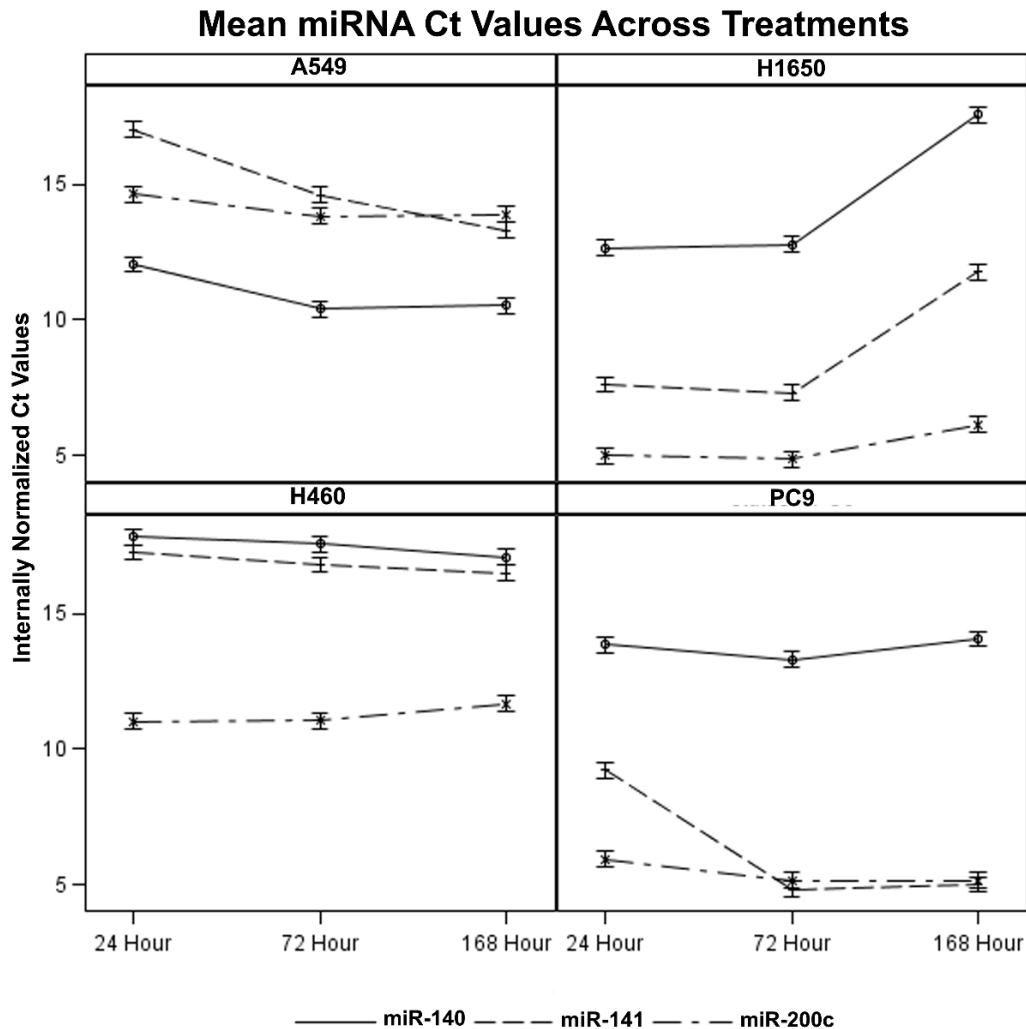
**Figure 2.3 (continued): TGFβ induces Smad 4 binding to SBEs in the promoter of mir-200/141 in PC9 cells.**

**B**



**Figure 2.4: Time of TGFβ treatment reflects changes in endogenous miRNA gene expression.** Changes in endogenous gene expression were analyzed using a five-way ANOVA considering the variables: TGFβ treatment, SB-431542 treatment, time point, expression as internally normalized Ct values, and cell line, along with all interaction terms. **(A)** Data presented here is aggregated by averaging over treatments in order to capture overarching trends in miRNA and cell line patterns at multiple time points. Fine-scale trends were broken down by individual treatments as presented in Figure 2.10. **(B)** Comparison of the significance of endogenous expression changes between time point's samples and by individual miRNA genes in each cell line.

A

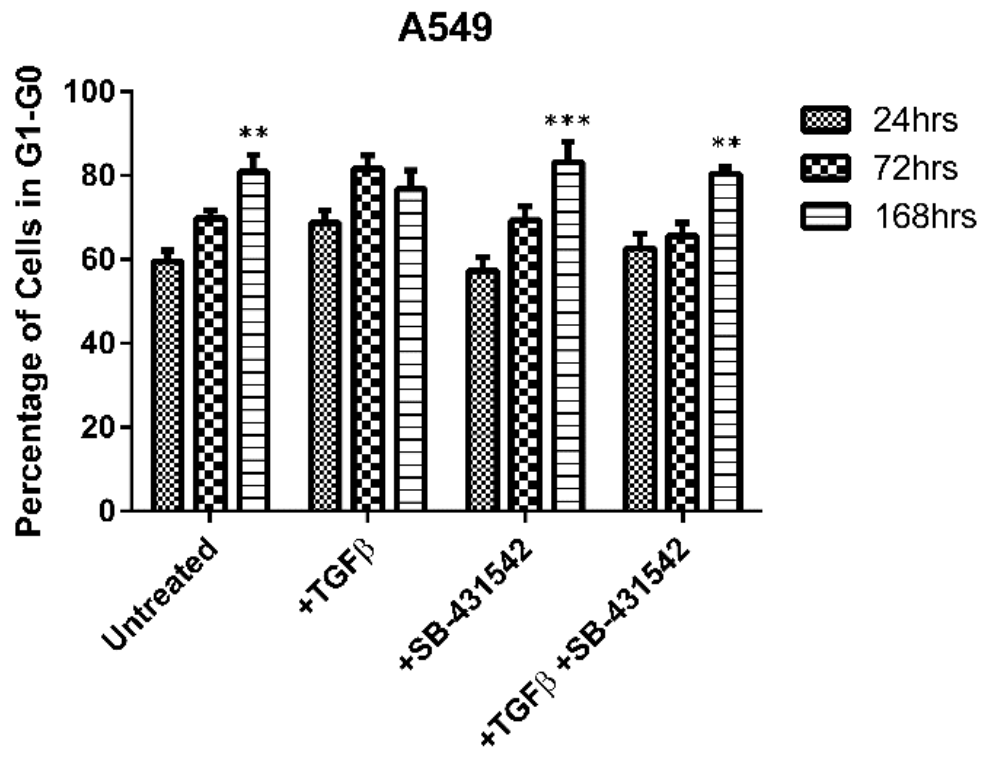


**Figure 2.4 (Continued): Time of TGF $\beta$  treatment reflects changes in endogenous miRNA gene expression.**

**B**

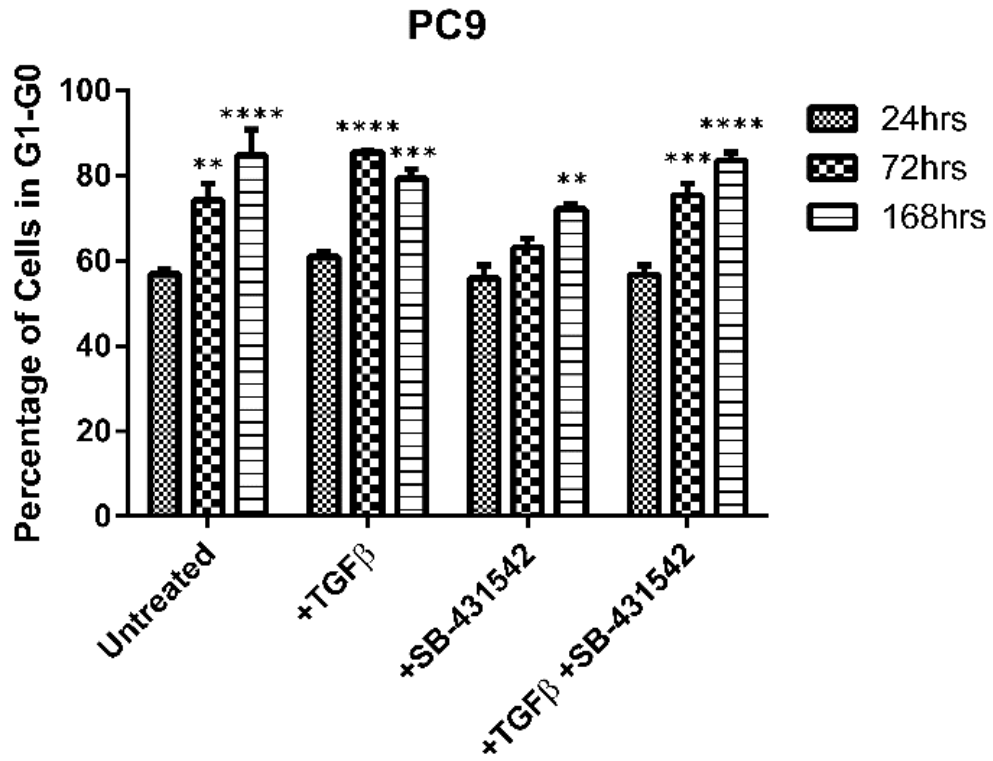
	Cell Line	miRNA	24 vs 72 hours	24 vs 168 hours
<b>Resistant</b>	<b>A549</b>	miR-140	<0.0001****	0.0002***
		miR-141	<0.0001****	<0.0001****
		miR-200c	0.0471*	0.0675
	<b>H460</b>	miR-140	0.5221	0.0656
		miR-141	0.2548	0.0605
		miR-200c	0.9663	0.1077
<b>Sensitive</b>	<b>PC9</b>	miR-140	0.1875	0.5760
		miR-141	<0.0001****	<0.0001****
		miR-200c	0.0561	0.0500*
	<b>H1650</b>	miR-140	0.7751	<0.0001****
		miR-141	0.4358	<0.0001****
		miR-200c	0.7586	0.0051***

**Figure 2.5: A549 and PC9 cells exit the cell cycle regardless of treatment with TGF $\beta$  or SB-431542.** The graph reflects the percentage of **A) A549** or **B) PC9** cell populations in G<sub>0</sub>-G<sub>1</sub> phase of the cell cycle at 24, 72, and 168 hours following treatment. Significance was determined using an unpaired t-test comparing the 72- and 168-hour time points individually to the 24-hour time point of the same treatment. **(C)** A two-way ANOVA was utilized to determine the significance of treatment and/or time point reflective of the percentage of cells in the G<sub>0</sub>-G<sub>1</sub> phase of the cell cycle.

**A**

**Figure 2.5 (Continued): A549 and PC9 cells exit the cell cycle regardless of treatment with TGFβ or SB-431542.**

**B**

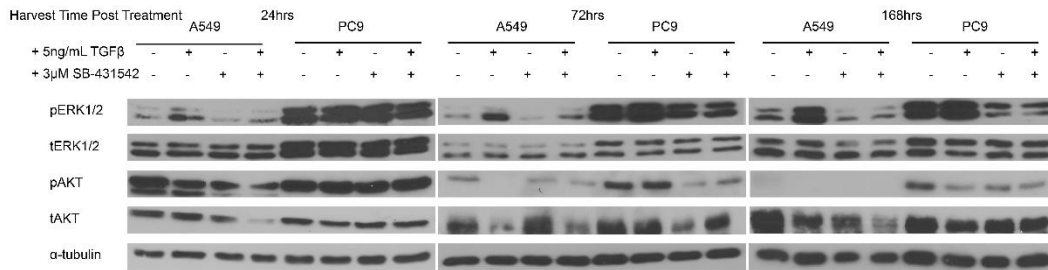


**C**

Source of Variation	A549	PC9
<i>Interaction</i>	0.0583	0.0168*
<i>Time</i>	<0.0001****	<0.0001****
<i>Treatment</i>	0.1042	0.0002***

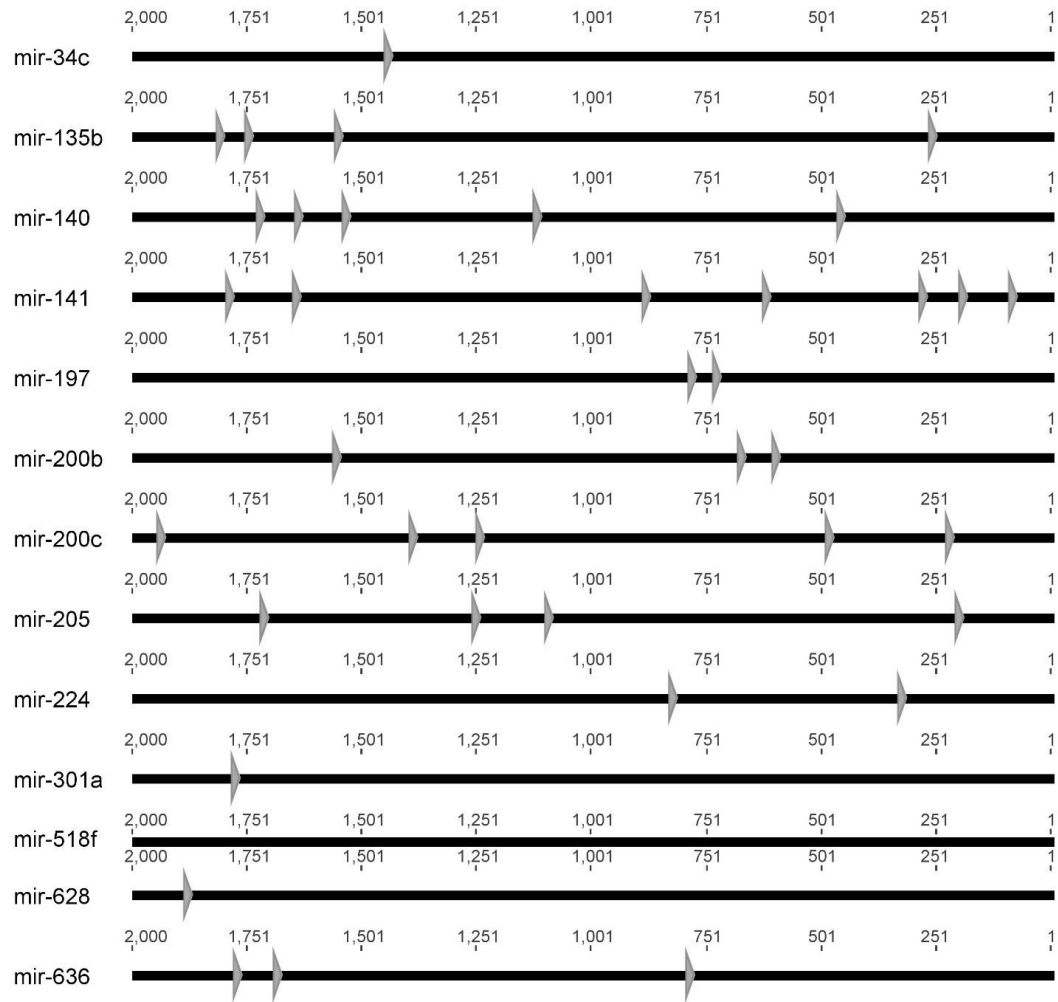
CHAPTER 2

**Figure 2.6: TGF $\beta$  modulation differentially impacts ERK and AKT activation between A549 and PC9.** A549 and PC9 cells were plated, treated, and harvested as described in the methods.  $\alpha$ -tubulin levels are representative of an individual lysate pool. Lysates profiled here are the same as in figure 2.2. ERK-MAPK and PI3K-AKT signaling are non-canonical signaling effectors of the TGF $\beta$  signaling pathway. All blots from the same samples;  $\alpha$ -tubulin levels are representative of each sample.



CHAPTER 2

**Figure 2.7: Signature microRNA genes contain SBE elements.** Promoter analysis was conducted using the ChipMAPPER algorithm (347, 348). Twelve out of thirteen of the signature microRNA genes contain putative SBE elements as represented by the triangle with conservative E-values less than or equal to 25 and a score greater than 3.0 (181, 184).



## CHAPTER 2

**Figure 2.8:** *TGF $\beta$  induces a mesenchymal phenotype in A549, but inhibition generates an EMT-intermediate phenotype in erlotinib-sensitive, PC9 cells.* A549 and PC9 cells were treated as described in the methods. Bright field images of cell morphology were acquired using the microscope and software described in the methods. **(A)** Shows full-sized bright-field images taken at 5X magnification, and **(B)** shows a closer representation of the morphology changes. Time is in hours.

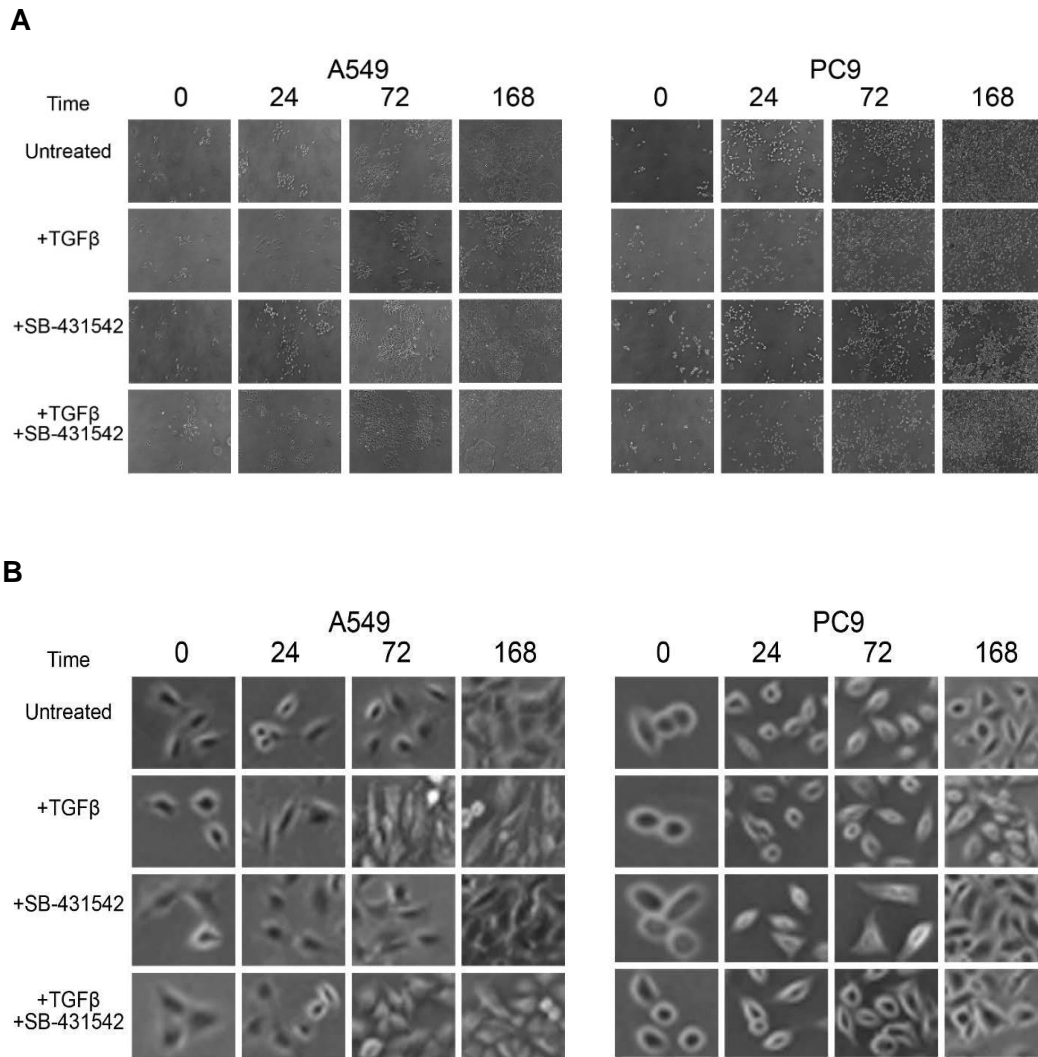


**Figure 2.9: E-cad expression in response to treatment. (A)** E-cad mRNA levels quantified by qRT-PCR in A549 (n=1). **(B)** E-cad mRNA levels quantified by qRT-PCR in PC9 (n=1). mRNA levels are demonstrated as fold change relative to respective untreated samples which are standardized to a fold change of 1.

A

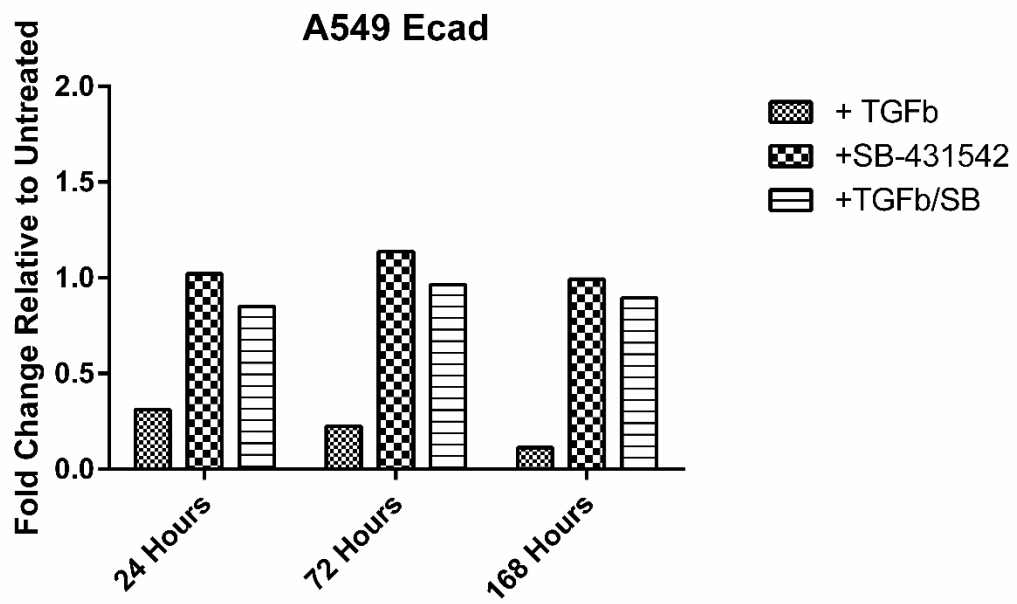


**Figure 2.9 (continued): E-cad expression in response to treatment. (A)** E-cad mRNA levels quantified by qRT-PCR in A549 (n=1). **(B)** E-cad mRNA levels quantified by qRT-PCR in PC9 (n=1). mRNA levels are demonstrated as fold change relative to respective untreated samples which are standardized to a fold change of 1.

**B**

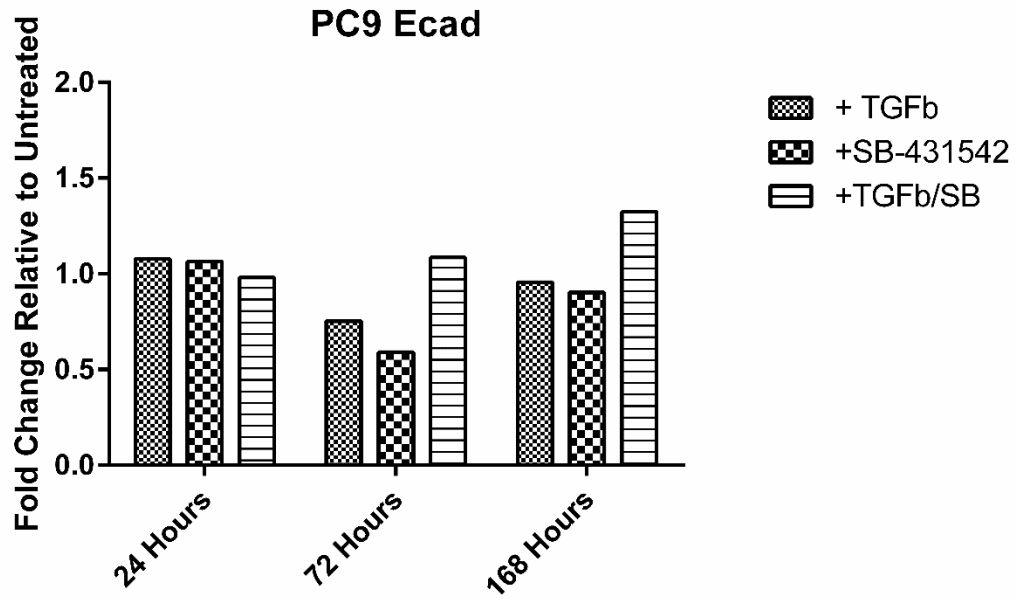


**Figure 2.10: Normalized Ct values demonstrate that time change, not individual treatment, affects endogenous miRNA expression changes in A549 and PC9 cells.**

(A-F) Raw miRNA expression levels using qRT-PCR experiments as described in Figure 4 and Supplemental Figure 5.

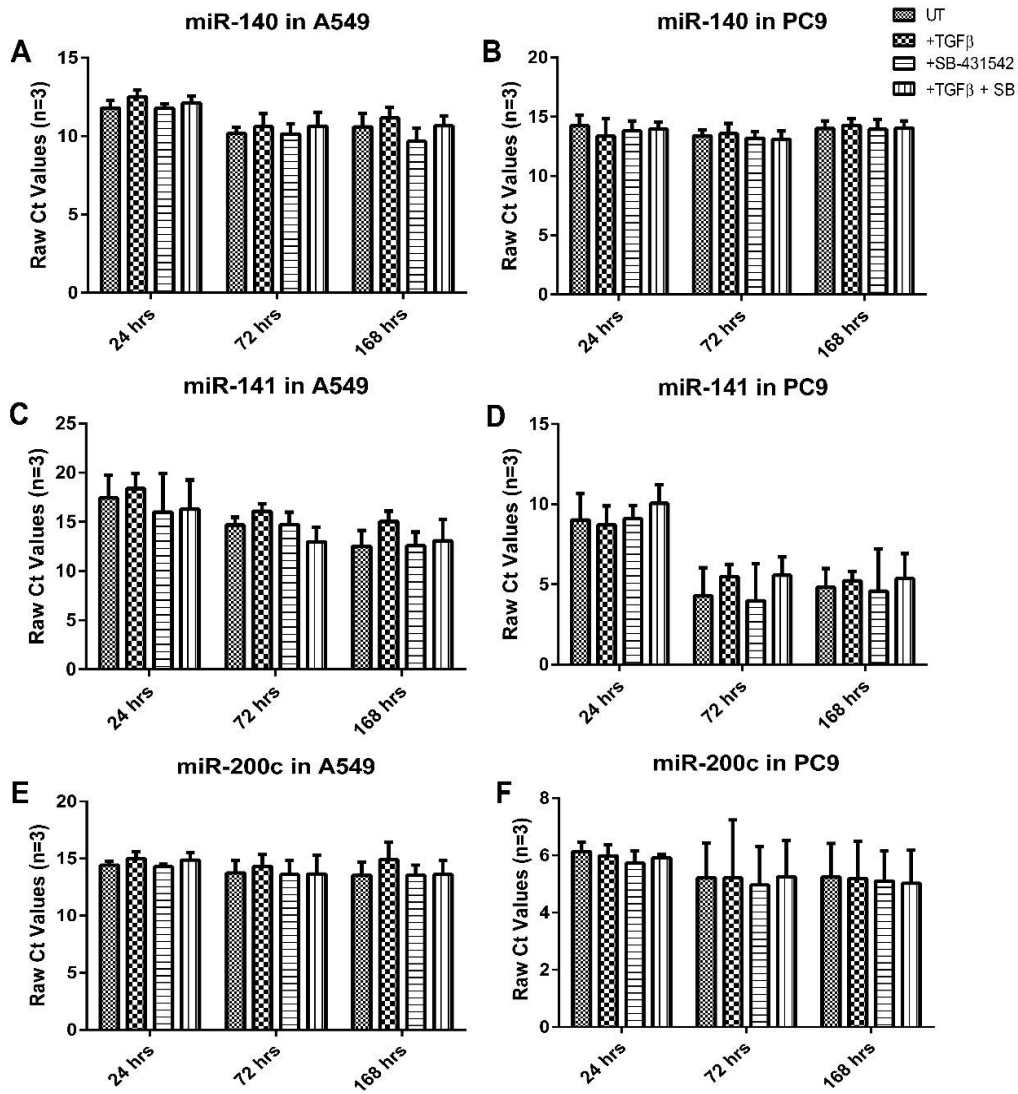
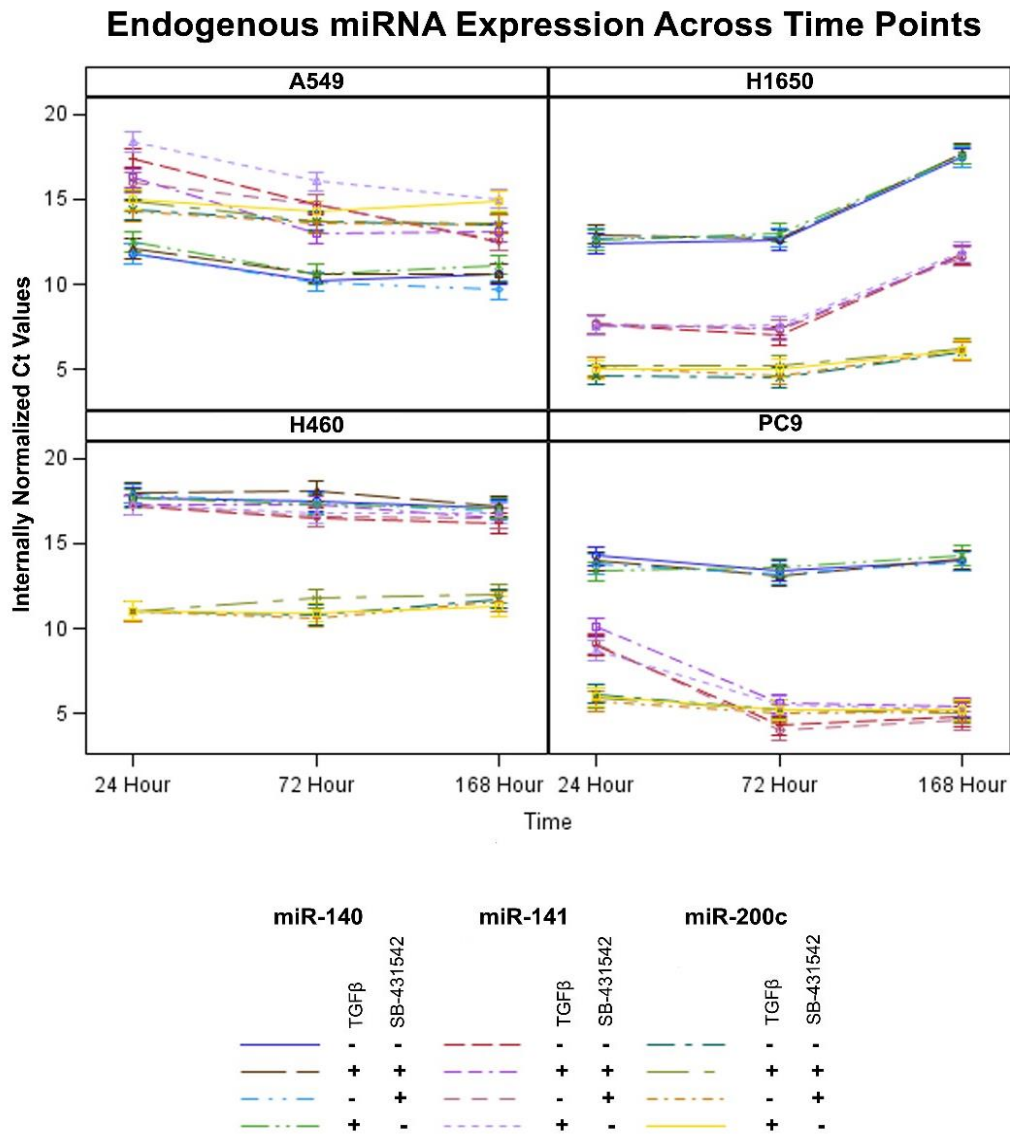


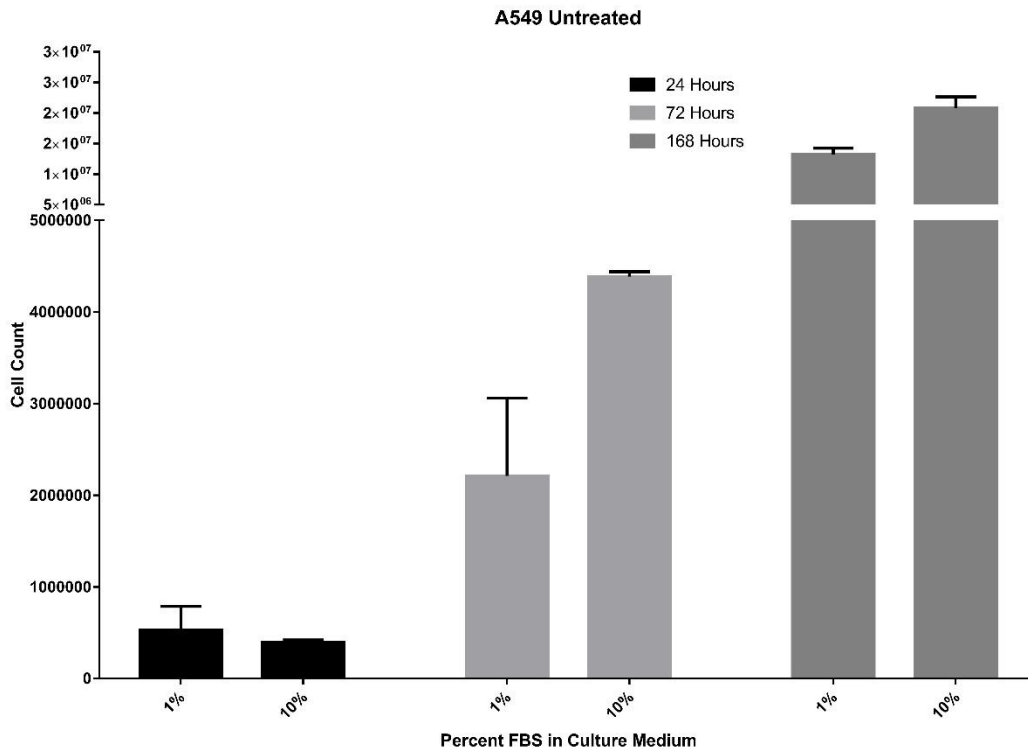
**Figure 2.11: Time of treatment has the most significant influence on miRNA expression changes.** Changes in endogenous gene expression were analyzed using a five-way ANOVA considering the variables: TGFβ treatment, SB-431542 treatment, time point, expression as internally normalized Ct values, and cell line, along with all interaction terms.



CHAPTER 2

**Figure 2.12: A549 cell counts following corresponding treatments and time points comparing growth in 1% and 10% serum media. (A) Untreated (B) +5ng/ml TGF $\beta$  (C) +3 $\mu$ M SB-431542 (D) +5ng/ml TGF $\beta$  +3 $\mu$ M SB-431542. Cells were plated at  $1 \times 10^4$  cells/well in a 6-well dish 48 hours prior to 0 hour treatment introduction and counted at the appropriate harvest time using a hemocytometer. (n=2)**

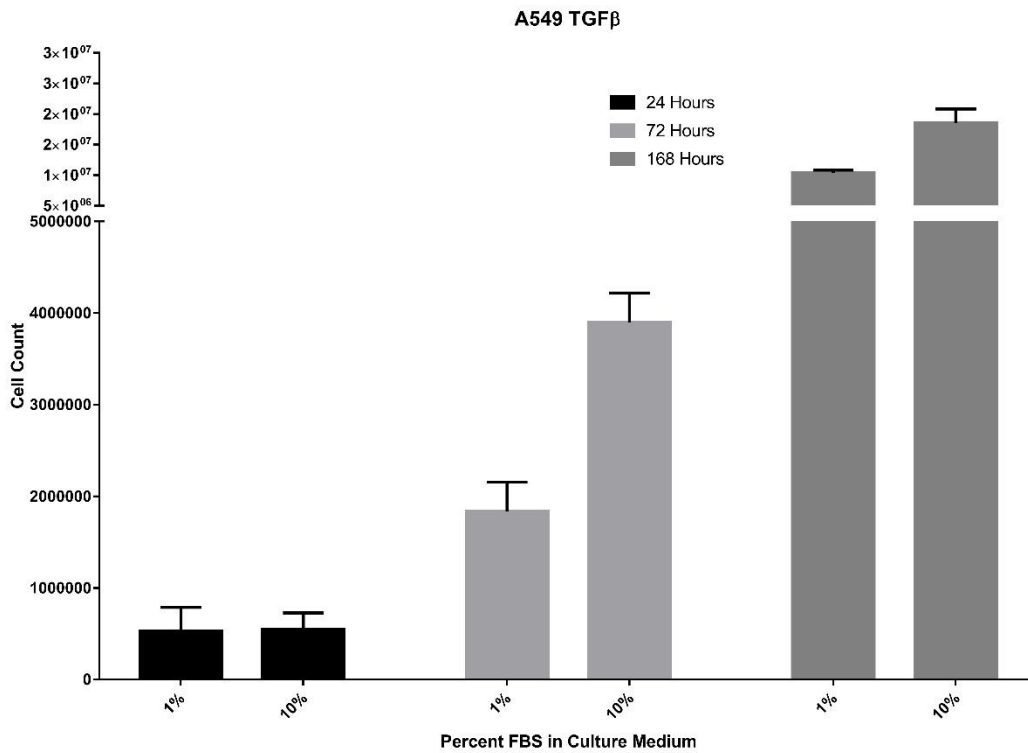
**A**



CHAPTER 2

**Figure 2.12 (continued): A549 cell counts following corresponding treatments and time points comparing growth in 1% and 10% serum media. (A) Untreated (B) +5ng/ml TGF $\beta$  (C) +3 $\mu$ M SB-431542 (D) +5ng/ml TGF $\beta$  +3 $\mu$ M SB-431542. Cells were plated at  $1 \times 10^4$  cells/well in a 6-well dish 48 hours prior to 0 hour treatment introduction and counted at the appropriate harvest time using a hemocytometer. (n=2)**

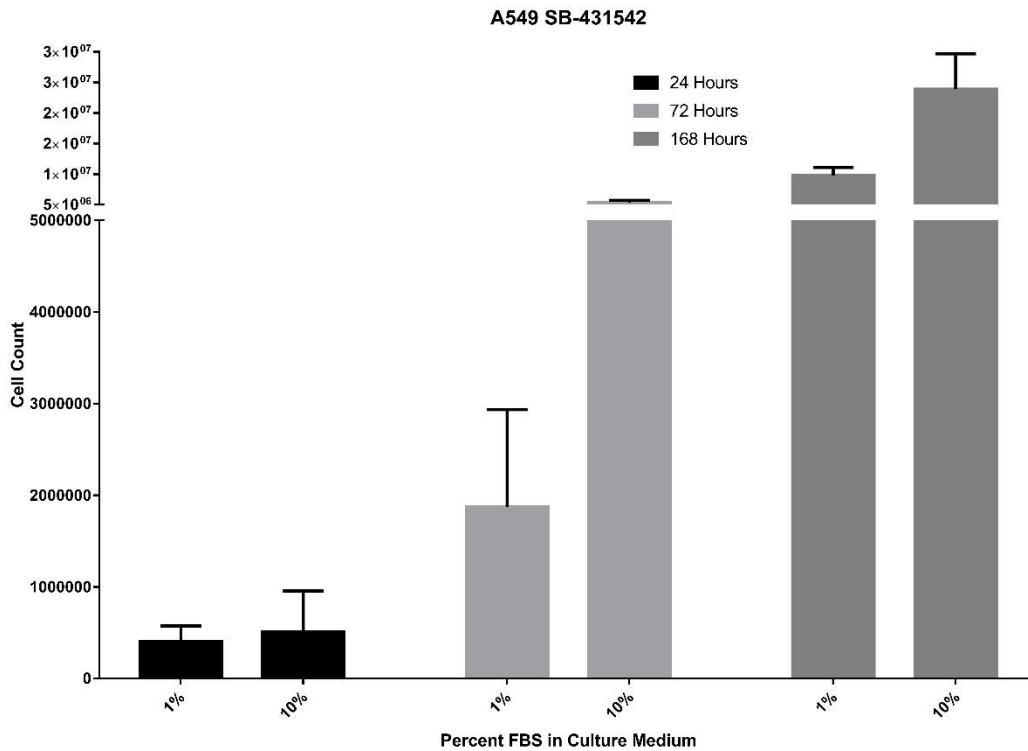
**B**



CHAPTER 2

**Figure 2.12 (continued): A549 cell counts following corresponding treatments and time points comparing growth in 1% and 10% serum media. (A) Untreated (B) +5ng/ml TGF $\beta$  (C) +3 $\mu$ M SB-431542 (D) +5ng/ml TGF $\beta$  +3 $\mu$ M SB-431542. Cells were plated at  $1 \times 10^4$  cells/well in a 6-well dish 48 hours prior to 0 hour treatment introduction and counted at the appropriate harvest time using a hemocytometer. (n=2)**

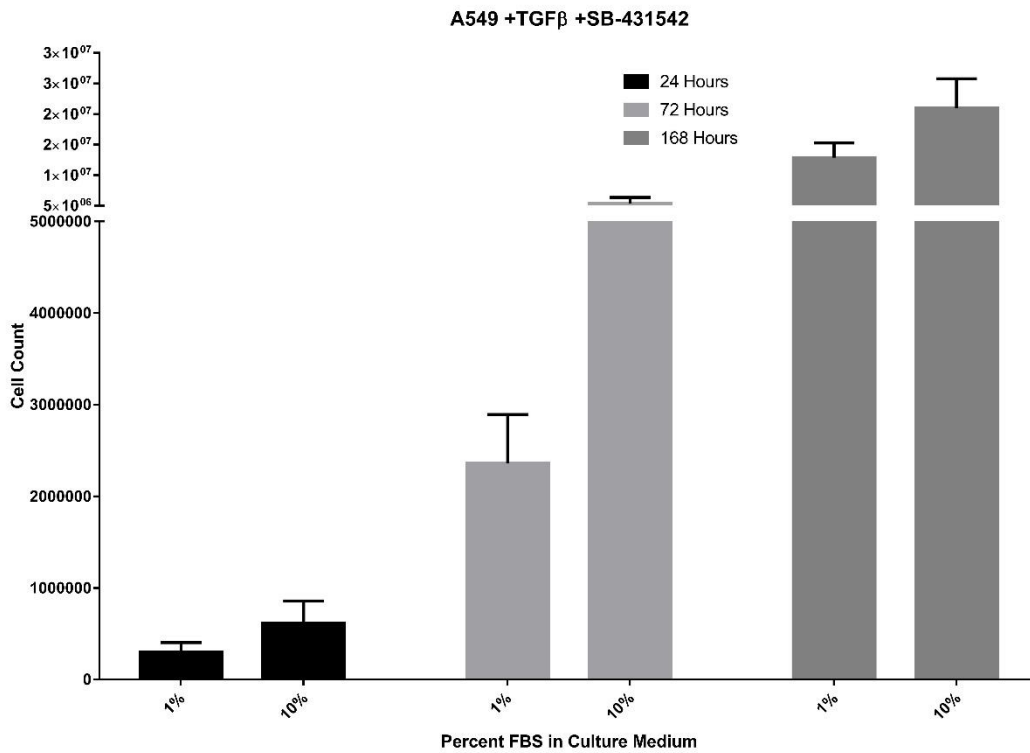
**C**



CHAPTER 2

**Figure 2.12 (continued): A549 cell counts following corresponding treatments and time points comparing growth in 1% and 10% serum media. (A) Untreated (B) +5ng/ml TGF $\beta$  (C) +3 $\mu$ M SB-431542 (D) +5ng/ml TGF $\beta$  +3 $\mu$ M SB-431542. Cells were plated at  $1 \times 10^4$  cells/well in a 6-well dish 48 hours prior to 0 hour treatment introduction and counted at the appropriate harvest time using a hemocytometer. (n=2)**

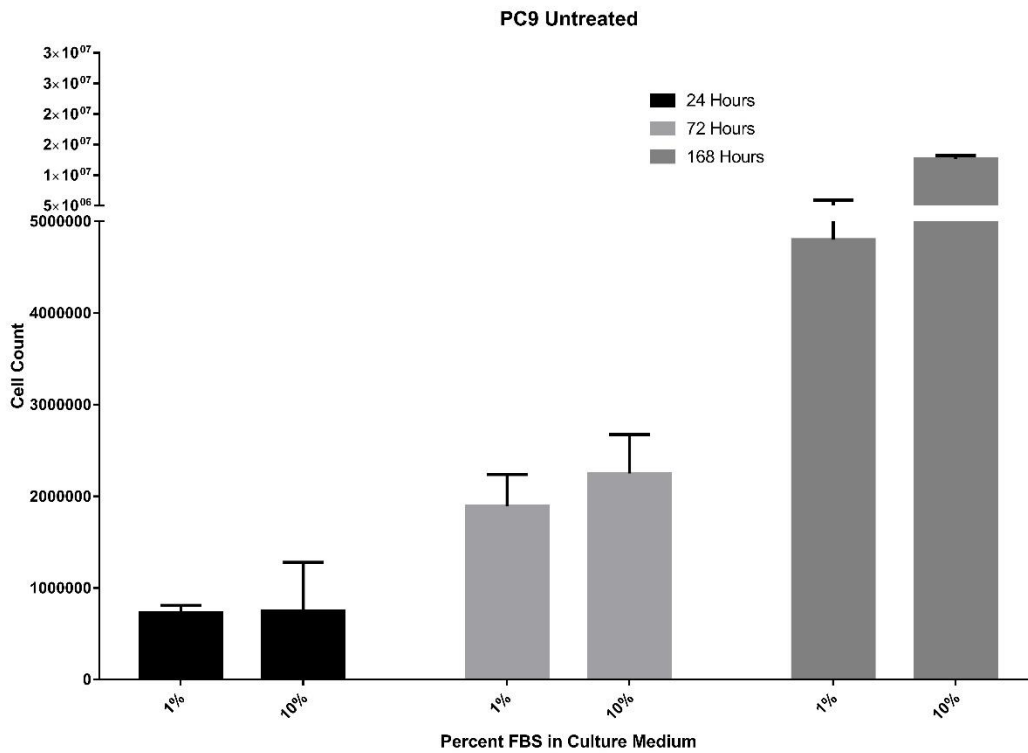
**D**



CHAPTER 2

**Figure 2.13: PC9 cell counts following corresponding treatments and time points comparing growth in 1% and 10% serum media. (A) Untreated (B) +5ng/ml TGF $\beta$  (C) +3 $\mu$ M SB-431542 (D) +5ng/ml TGF $\beta$  +3 $\mu$ M SB-431542. Cells were plated at  $1 \times 10^4$  cells/well in a 6-well dish 48 hours prior to 0 hour treatment introduction and counted at the appropriate harvest time using a hemocytometer. (n=2)**

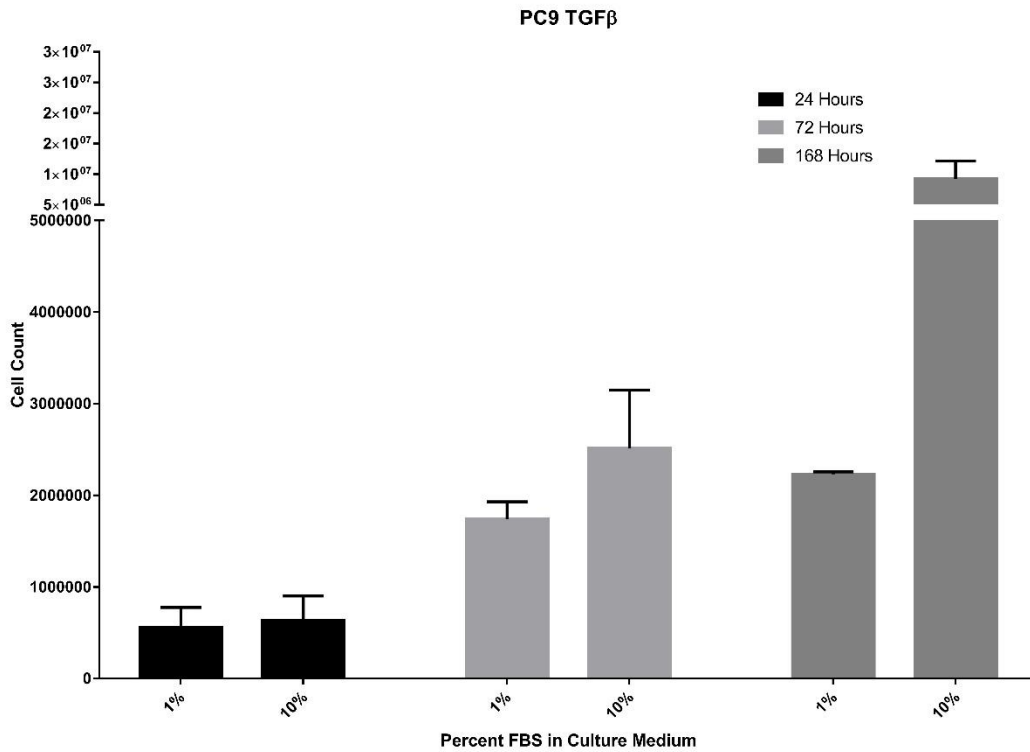
**A**



CHAPTER 2

**Figure 2.13 (continued): PC9 cell counts following corresponding treatments and time points comparing growth in 1% and 10% serum media. (A) Untreated (B) +5ng/ml TGF $\beta$  (C) +3 $\mu$ M SB-431542 (D) +5ng/ml TGF $\beta$  +3 $\mu$ M SB-431542. Cells were plated at  $1 \times 10^4$  cells/well in a 6-well dish 48 hours prior to 0 hour treatment introduction and counted at the appropriate harvest time using a hemocytometer. (n=2)**

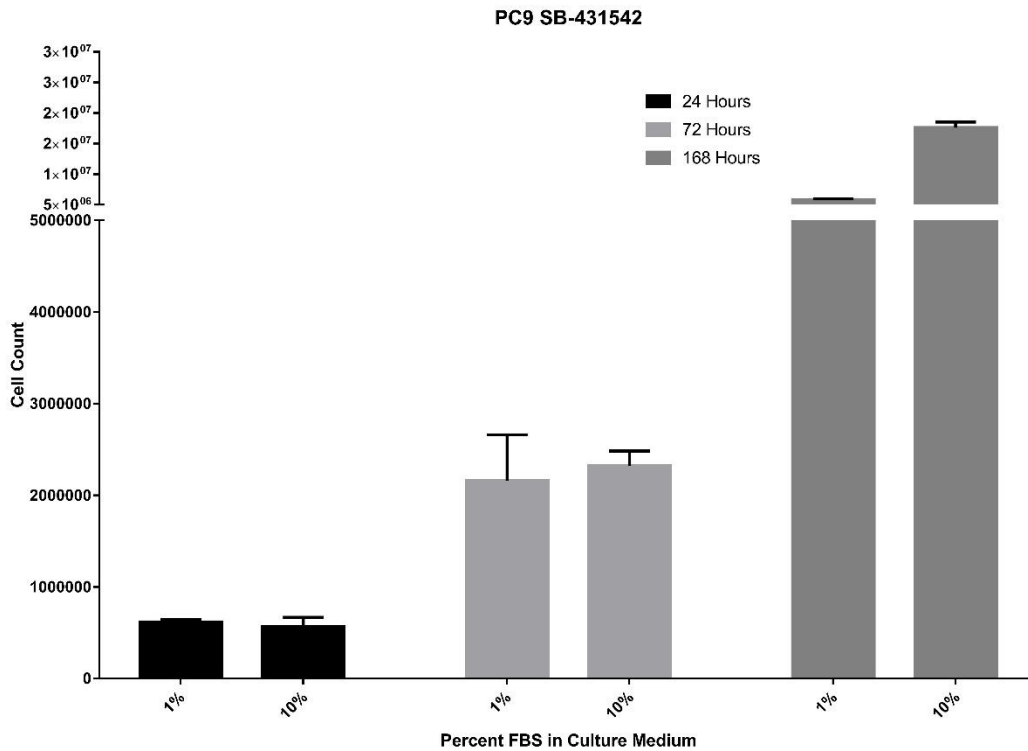
**B**



CHAPTER 2

**Figure 2.13 (continued): PC9 cell counts following corresponding treatments and time points comparing growth in 1% and 10% serum media. (A) Untreated (B) +5ng/ml TGF $\beta$  (C) +3 $\mu$ M SB-431542 (D) +5ng/ml TGF $\beta$  +3 $\mu$ M SB-431542. Cells were plated at  $1 \times 10^4$  cells/well in a 6-well dish 48 hours prior to 0 hour treatment introduction and counted at the appropriate harvest time using a hemocytometer. (n=2)**

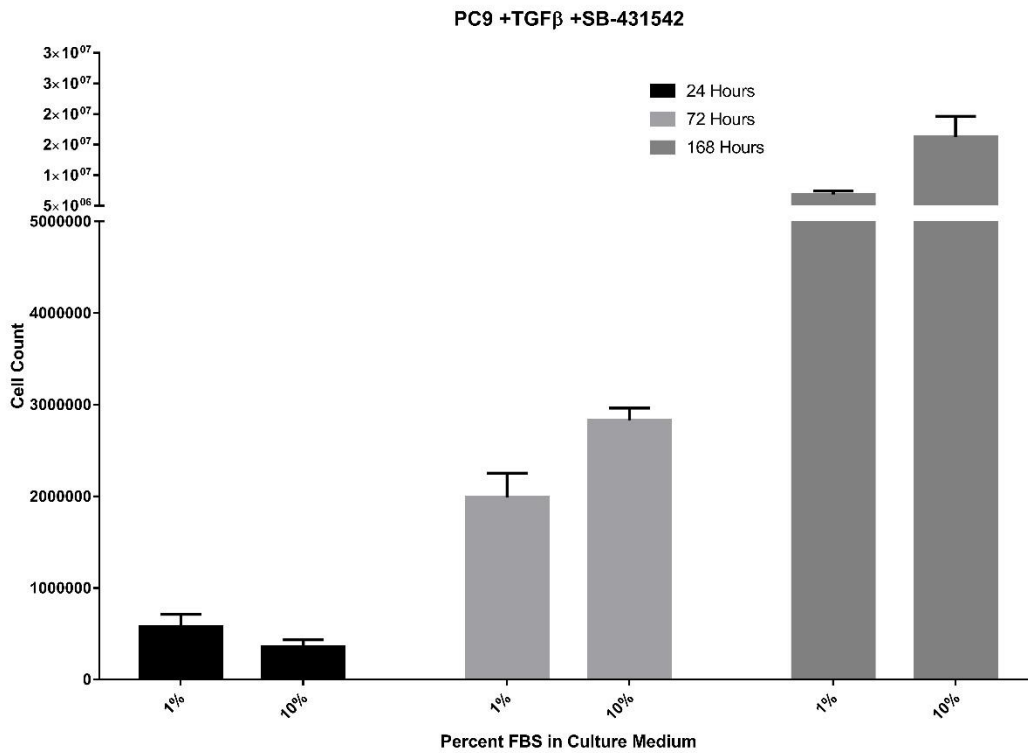
**C**



CHAPTER 2

**Figure 2.13 (continued): PC9 cell counts following corresponding treatments and time points comparing growth in 1% and 10% serum media. (A) Untreated (B) +5ng/ml TGF $\beta$  (C) +3 $\mu$ M SB-431542 (D) +5ng/ml TGF $\beta$  +3 $\mu$ M SB-431542. Cells were plated at  $1 \times 10^4$  cells/well in a 6-well dish 48 hours prior to 0 hour treatment introduction and counted at the appropriate harvest time using a hemocytometer. (n=2)**

**D**



CHAPTER 2

**Figure 2.14: Densitometry of Figure 2.6 western blots. (A)** pERK and tERK in A549 **(B)** pERK and tERK in PC9 **(C)** pAKT and AKT in A549 **(D)** pAKT and AKT in PC9. Blots were quantified using ImageJ and quantification was calculated using the area under the curve measurements for each band using the same sized box sample for each to ensure consistency (n=1).

**A**

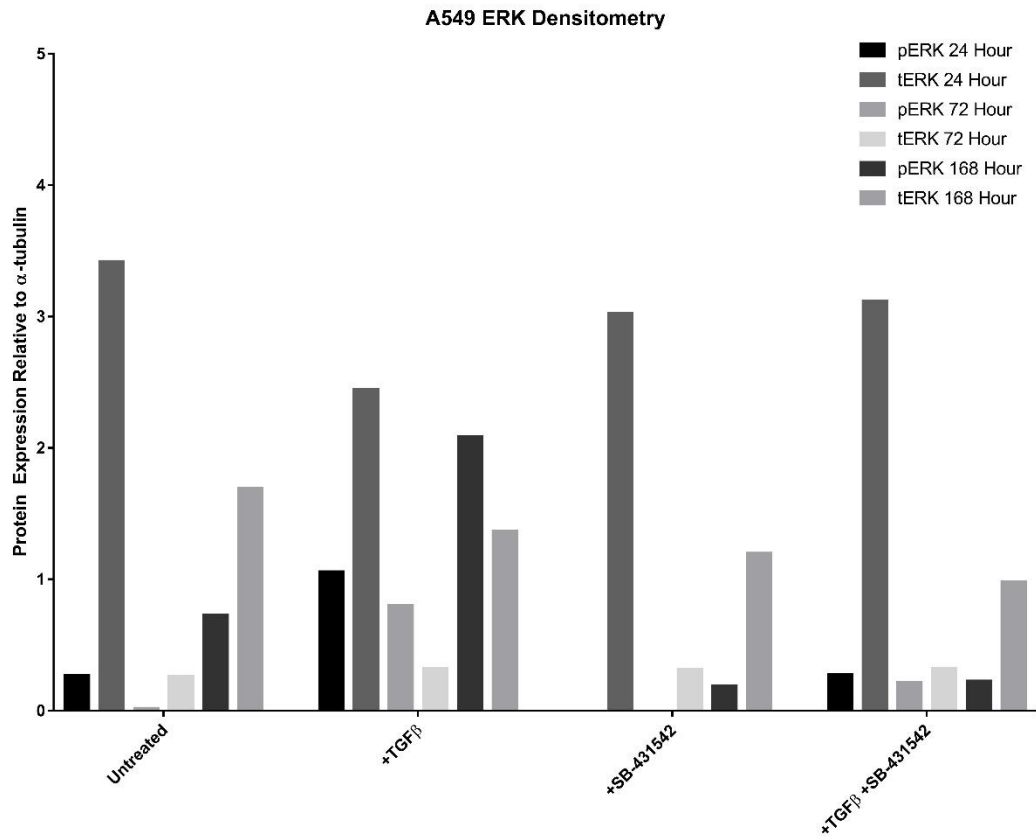


**Figure 2.14 (continued): Densitometry of Figure 2.6 western blots. (A)** pERK and tERK in A549 **(B)** pERK and tERK in PC9 **(C)** pAKT and AKT in A549 **(D)** pAKT and AKT in PC9. Blots were quantified using ImageJ and quantification was calculated using the area under the curve measurements for each band using the same sized box sample for each to ensure consistency (n=1).

**B**

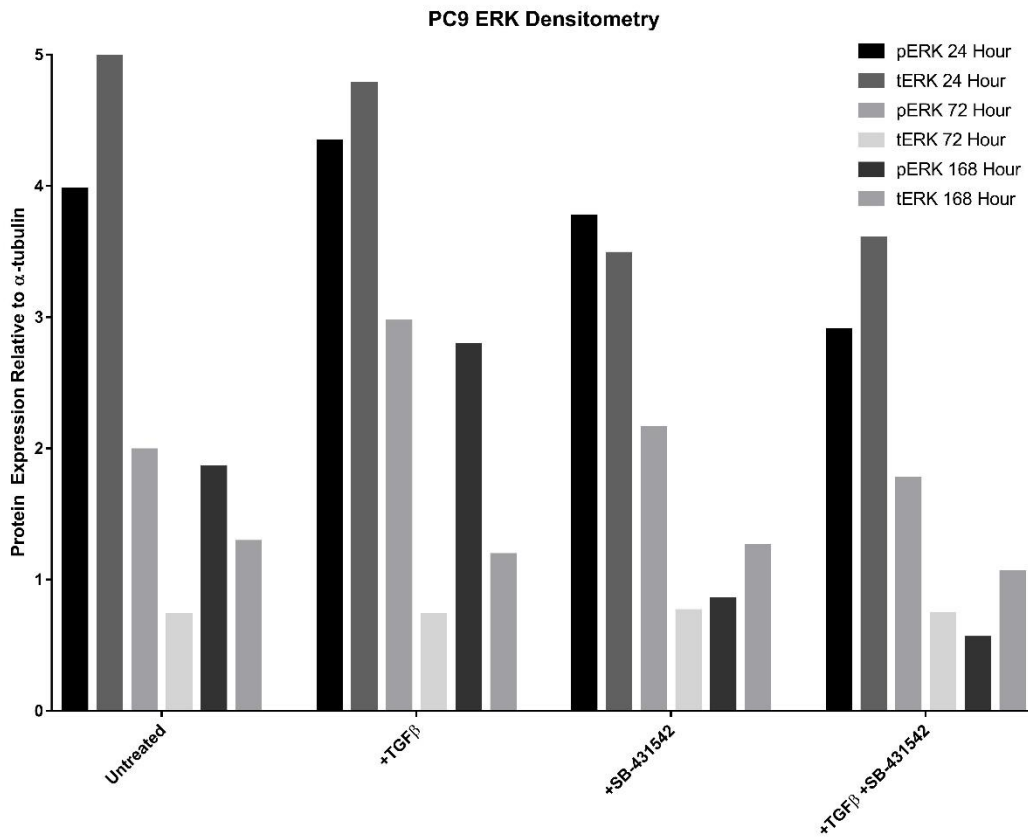


**Figure 2.14 (continued): Densitometry of Figure 2.6 western blots. (A)** pERK and tERK in A549 **(B)** pERK and tERK in PC9 **(C)** pAKT and AKT in A549 **(D)** pAKT and AKT in PC9. Blots were quantified using ImageJ and quantification was calculated using the area under the curve measurements for each band using the same sized box sample for each to ensure consistency (n=1).

**C**

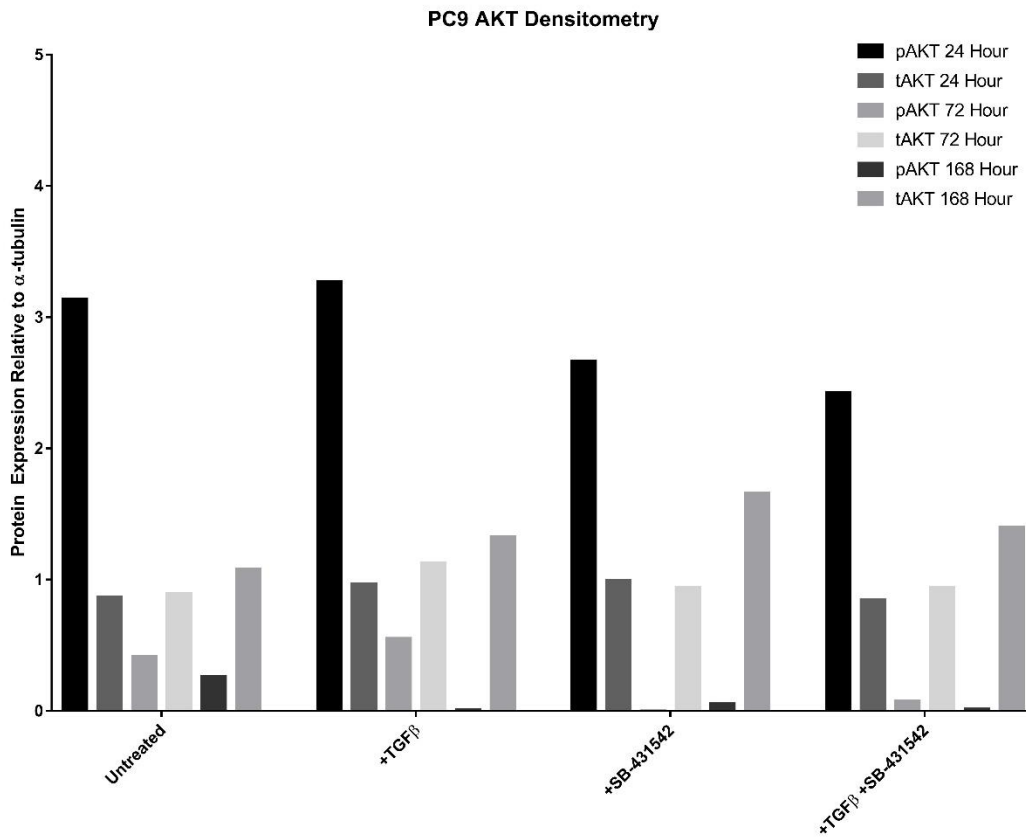


**Figure 2.14 (continued): Densitometry of Figure 2.6 western blots. (A)** pERK and tERK in A549 **(B)** pERK and tERK in PC9 **(C)** pAKT and AKT in A549 **(D)** pAKT and AKT in PC9. Blots were quantified using ImageJ and quantification was calculated using the area under the curve measurements for each band using the same sized box sample for each to ensure consistency (n=1).

**D**

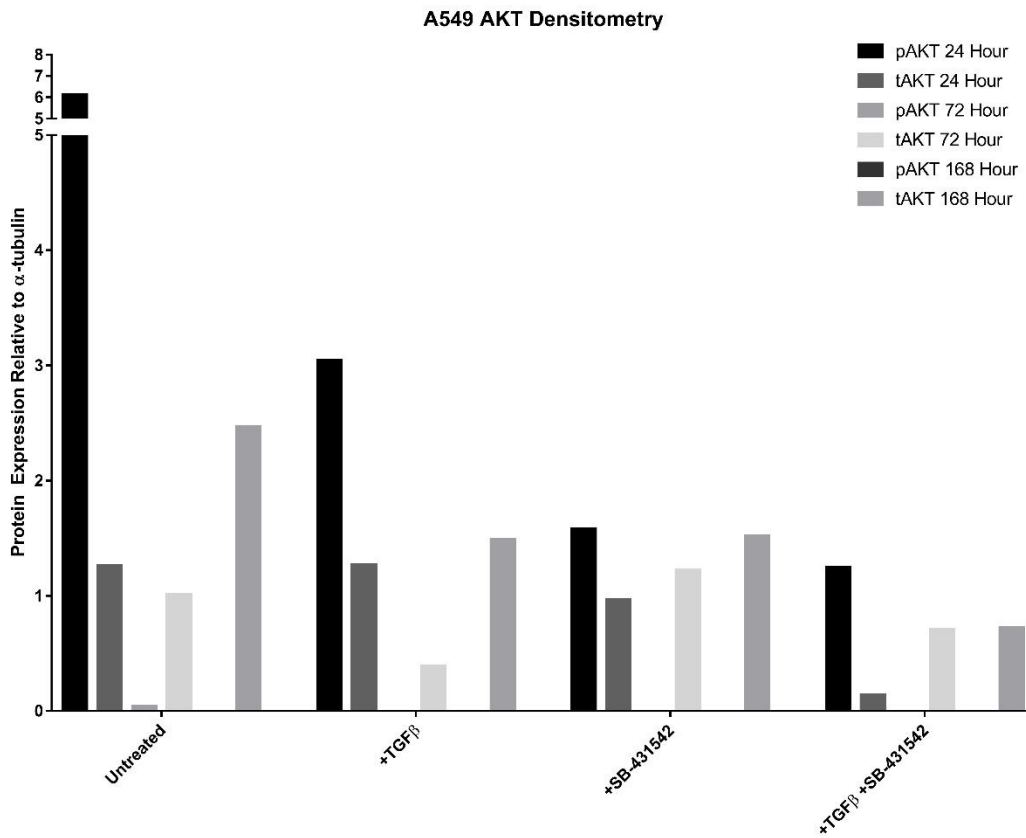
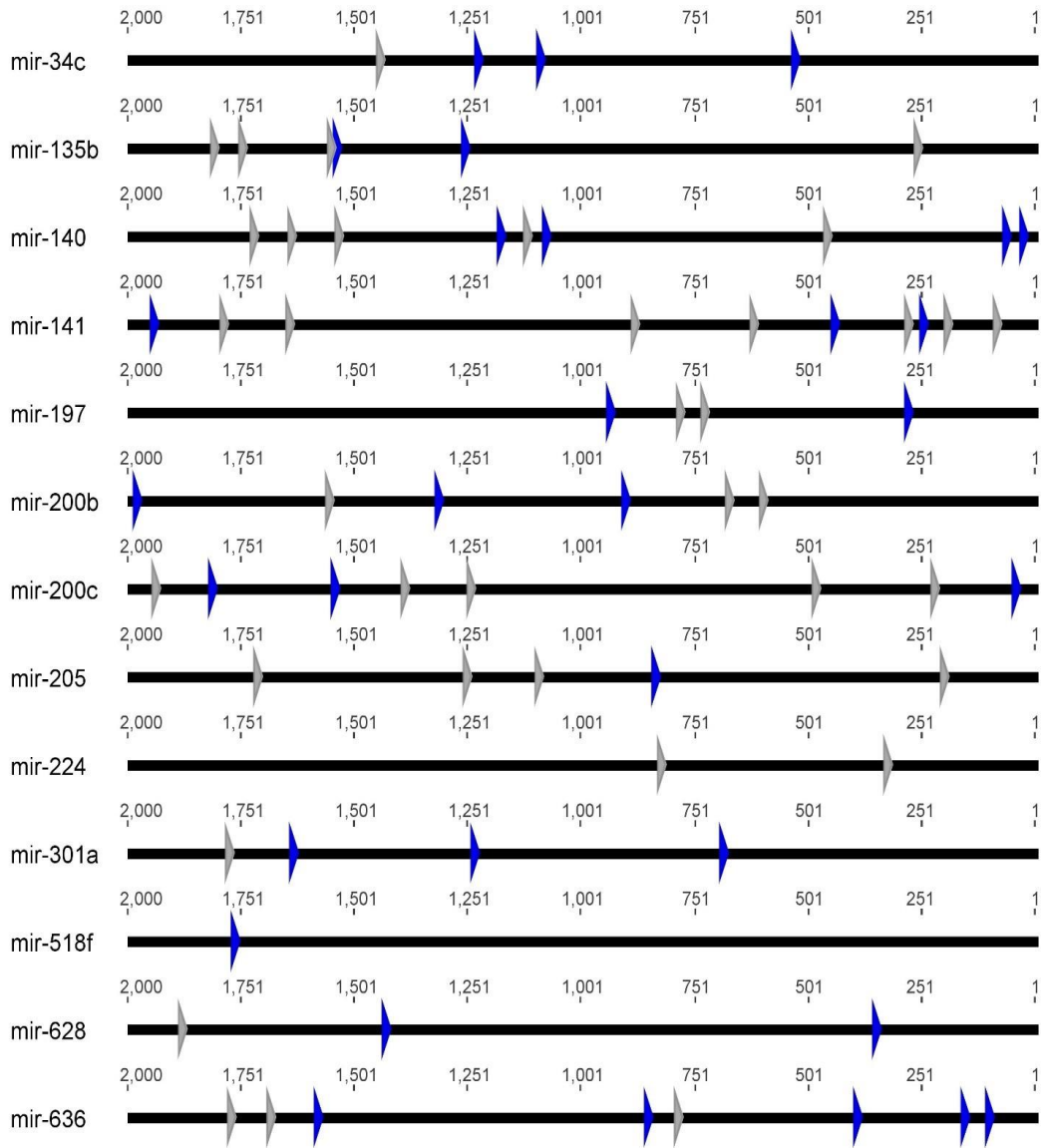


**Figure 2.15: Signature microRNA genes contain both putative SBE elements and putative ELK1 binding sites.** Promoter analysis was conducted using the ChipMAPPER algorithm (348). Twelve out of 13 of the signature microRNA genes contain putative SBE elements as represented by the grey triangle with conservative E-values less than or equal to 25 and a score greater than 3.0. Twelve out of the thirteen signature miRNA also contain putative ELK1 binding sites meeting the same inclusion criteria as represented by the blue triangles.



## CHAPTER 3

### A. OVERVIEW

Erlotinib is a small molecule Epidermal Growth Factor Receptor (EGFR) inhibitor that has been FDA approved for clinical use since 2004 (144). In October 2016, it was specifically redesignated by the FDA for the treatment of locally advanced or metastatic Non-Small Cell Lung Cancer (NSCLC) harboring EGFR exon 19 deletions or exon 21 L858R substitution mutations (143). However, utilizing EGFR mutation statuses as the sole determinant of erlotinib treatment remains limiting because EGFR somatic mutations alone may not encompass all NSCLC that would respond to erlotinib. Further, the majority of responders do eventually develop resistance to erlotinib therapy (365).

To encompass responders not captured by these EGFR mutations, prior work in the Black laboratory showed that estimating response to EGFR<sup>T</sup> can likely be improved by using multivariate gene expression patterns demonstrated in NSCLC cells and in a retrospective analysis of tumors (327, 328). From this work, a 13-gene miRNA signature predictive of response to the EGFR<sup>T</sup>, erlotinib, was identified (327). Bioinformatic analysis of the 13-gene miRNA signature revealed a functional convergence on the TGF $\beta$  signaling pathway, suggesting a relationship between the TGF $\beta$  and EGFR signaling pathways (327). The 13-gene miRNA signature of response was able to stratify cells and tumor samples into erlotinib-sensitive and -resistant groups and it discriminated primary tumors from metastatic lesions (327). Others have shown that NSCLC patient tumors that have undergone the Epithelial to Mesenchymal Transition (EMT) are largely erlotinib-resistant when compared with the epithelial-phenotype tumors (366). TGF $\beta$  is an inducer of EMT and it has also been shown to have paradoxical functions in tumorigenesis, as a tumor suppressor in early stages of the disease and as an oncogenic, pro-metastatic player in later stages (349, 350).

In a previous study comparing the effects of TGF $\beta$  treatment between representative erlotinib-resistant and -sensitive NSCLC cell lines, I showed that erlotinib-resistant, A549, and erlotinib-sensitive, PC9, cells show different activation and

## CHAPTER 3

expression profiles of the canonical TGF $\beta$  effectors, Smads 2, 3, and 4, as well as differential activation of non-canonical TGF $\beta$  signaling pathways (ERK-MAPK and PI3K-AKT) after TGF $\beta$  treatment (367). As expected, TGF $\beta$  treatment induced a mesenchymal phenotype in A549 cells as evidenced by morphological changes and expression of EMT marker proteins (368). In PC9 cells, which maintain a baseline epithelial phenotype, inhibiting TGF $\beta$  with the TGF $\beta$  inhibitor, SB-431542, induced an EMT-intermediate morphological change even though EMT marker protein expression did not change (367). These results suggest that there are relationships between the induction of EMT by TGF $\beta$ , EMT and erlotinib resistance, and the expression of the 13 miRNA genes comprising the signature.

For these reasons, we hypothesize that TGF $\beta$  induces EMT in erlotinib-resistant NSCLC and that inhibiting TGF $\beta$  signaling may sensitize these NSCLC to erlotinib treatment.

### **B. METHODS**

#### **Cell Culture**

NSCLC cell lines are from ATCC (A549) or gifted from the Haura laboratory (Moffitt Cancer Center, FL). All cells were cultured in RPMI 1640 (Life Technologies) supplemented with 10% Fetal Bovine Serum (FBS/serum) (USA Scientific), HEPES, glucose and pyruvate and maintained in a humidified incubator at 37 °C at 5% CO<sub>2</sub> unless otherwise specified. Cells were seeded in 6 well plates and were allowed to grow in 10% serum-containing RPMI 1640 media conditions for 48 hours prior to treatments. Dishes were seeded with 1 x 10<sup>4</sup> cells and were treated with SB-431542 (3  $\mu$ M) (Selleck Chem), LY-2109761 (3  $\mu$ M) (Cayman Chem), and/or TGF $\beta$  (5 ng/ml) (Cell Signalling Technologies) under minimal serum (1% FBS) conditions for time frames specified. Treatment media was replenished at the 72-hour time point in 168-hour culture experiments.

#### **Transwell Migration Assay**

## CHAPTER 3

Cells were pre-treated for 7 days as described above prior to plating for the viability assay. After pretreatment, cells were trypsinized and resuspended in serum-free RPMI 1640 media. The top of the 96-well HTS Transwell permeable plate (Corning) membranes was coated with 600  $\mu$ l of a collagen coating solution (750  $\mu$ l 10X PBS, 14  $\mu$ l culture-grade collagen, 3.2  $\mu$ l 0.1 M NaOH, 6.73 ml dH<sub>2</sub>O) and incubated for 1 hour in the culture incubator at 37 °C. The collagen was aspirated, and the inserts were washed once with 1X PBS. Next, the bottoms of each Transwell were blocked with 600  $\mu$ l of a serum-free RPMI 1640 containing 0.1% BSA, and 100  $\mu$ l of the blocking media was placed into each Transwell insert. Blocking continued in the culture incubator at 37 °C for at least 1 hour up to overnight. Following blocking, blocking medium is aspirated from the top and the bottom wells. Cells ( $1 \times 10^3$ ) were seeded on top of each Transwell in serum free media and allowed to migrate towards a bottom chamber containing RPMI 1640 and 1% serum for 16 hours. At this time, membranes were fixed in 100% methanol and stained with 0.5% crystal violet in 100% methanol.

### **Wound Healing Assay**

Cells were plated in 12-well plates at  $5 \times 10^5$  cells/well to ensure confluence at time of wounding. Cells were incubated in maintenance media (RPMI 1640 containing 10% serum) for 24 hours following plating. After the initial 24-hour incubation, media was changed to RPMI 1640 and 1% serum with respective treatments for 24 additional hours. After 24 hours in treatments, cell monolayers were wounded using a 200  $\mu$ l pipette tip and media was changed to fresh RPMI 1640 and 1% serum with corresponding treatment. Plates were marked to ensure the same point in the wound was analyzed each day. Wound healing was measured over 72 hours and imaged using the Zeiss AxioObserver Microscope and processed using the AxioVision software. Wounds were imaged at 24 hour intervals for 72 hours total. Wound healing measurements are averaged from 3 independent linear measurements across the field imaged per sample, per recording time.

### **Cell Viability Assay**

Cells underwent pretreatment in 1% serum-containing RPMI 1640 with drug and/or cytokine for 7 days as described above to ensure that all EMT-like events occurring in

## CHAPTER 3

response to TGF $\beta$  treatment were fully realized prior to assessment of erlotinib response. After treatment, cells were trypsinized, counted, and plated at  $3 \times 10^3$  cells/well in a 96-well plate in fresh treatments matching those from the 7-day period. After 36 hours adherence time, erlotinib was added in indicated concentrations. Drug treatment persisted for 72 hours. After 72 hours, resazurin was added (100  $\mu$ M final concentration) to each well, the plates were gently rocked for 1 minute and then incubated for 3 hours prior to reading. The plate was read for fluorescence at excitation, 560 nm, and emission, 590 nm, wavelengths using a Spectramax M5 and corresponding Spectramax X5 software (Spectramax).

### **Data Processing and Statistics**

All graphical representations of data were made and analyzed using Prism Version 7.00 (GraphPad). Significance points in viability assay data compare the points specified in each figure legend and in the results section. Significance was determined using unpaired t-tests. Values measured between biological replicates from all viability assays and wound healing assays were subjected to a Dixon's Q test to eliminate outlier values.

For the Transwell migration assay, 'cells migrated' values are the number of cells counted in five non-overlapping views per well, averaged from triplicate technical replicates per individual experiment by three separate viewers. Values determined by each individual were subjected to a Dixon's Q-test outlier analysis prior to acceptance.

For the wound healing assay, 'percent wound remaining' was determined relative to respective 0 hour wound width. Four independent biological replicates were performed, and the four replicates were assessed for outliers using a Dixon's Q-test.

For the viability assay, response to each treatment is normalized to cells from each corresponding treatment that were not subjected to erlotinib. Readings were also normalized to empty wells on each plate containing only media and resazurin. Data is the result of four biological replicate experiments (n=4).

## **C. RESULTS**

### **TGF $\beta$ Treatment Has Opposing Effects on Migration in Erlotinib-Sensitive versus Erlotinib-Resistant NSCLC Cells**

We first wanted to understand the long-term functional changes in erlotinib-resistant, A549 cells, and erlotinib-sensitive, PC9 cells, subjected to long-term TGF $\beta$  treatment, and we assessed their migration ability using a Transwell Assay. TGF $\beta$  pre-treatment induced a significant increase in A549 cells that migrated compared to untreated cells (Figure 3.1). PC9 cells, pre-treated with TGF $\beta$ , demonstrated reduced migratory ability, but this effect was not found to be significant (Figure 3.1). Since TGF $\beta$  treatment induced migration in A549 cells, we next asked how TGF $\beta$  influenced wound healing ability of cells.

### **TGF $\beta$ Inhibition Significantly Impairs Wound Healing Ability in PC9 Cells**

Another measurable characteristic of migratory ability is wound healing and we used this assay to determine the cellular response of A549 and PC9 cells to short-term TGF $\beta$  treatment. For this experiment, we also used the TGF $\beta$  receptor inhibitor, LY-2109761, that targets both type I and II TGF $\beta$  receptors, unlike SB-431542, to determine whether differences observed could be attributed to partial TGF $\beta$  receptor inhibition. TGF $\beta$  treatment did not significantly change the wound healing ability of either cell line. Treatment with LY-2109761 significantly impaired the ability of A549 cells to migrate at the 48-hour time point (Figure 3.2A). PC9 cells treated with LY-2109761, with and without co-treatment with TGF $\beta$ , were significantly impaired in wound healing at the 48- and 72-hour time points (Figure 3.2B).

### **TGF $\beta$ Influences Erlotinib Resistance Differently between A549 and PC9 Cells**

We found that TGF $\beta$  induced an EMT-phenotype and increased chemotactic ability in A549 cells, but not in PC9 cells. Next, we aimed to determine if TGF $\beta$  treatment had an impact on erlotinib-sensitivity in each cell line. A549 cells pre-treated with TGF $\beta$  showed significantly increased erlotinib resistance at lower erlotinib concentrations, but at 10  $\mu$ M and 30  $\mu$ M erlotinib levels, TGF $\beta$  pre-treated A549 cells were significantly more sensitive to erlotinib than untreated A549 cells (Figure 3.3A). No significant impact was observed in

## CHAPTER 3

any combination of either TGF $\beta$  inhibitor with or without TGF $\beta$  ligand in A549 cells when compared to untreated A549 cells (Figure 3.3A). Most notably, PC9 cells that had undergone pre-treatment with TGF $\beta$  showed significant increased sensitivity to erlotinib (Figure 3.3B). Moreover, pre-treatment with either TGF $\beta$  inhibitor with or without TGF $\beta$  ligand significantly reversed the phenotype in PC9 cells (Figure 3.3B).

### D. DISCUSSION

Bioinformatic analysis of a previously published 13-gene miRNA signature led us to explore the contribution of TGF $\beta$  with respect to EMT-progression and its relationship to erlotinib-sensitivity (327). Our previous work showed that TGF $\beta$  likely has opposing roles in relation to EMT-induction and erlotinib-resistance between erlotinib-resistant and -sensitive NSCLC cells. We observed that TGF $\beta$  treatment induced mesenchymal morphologies between 5-6 days of treatment (367), so we chose to pre-treat cells for 7 days prior to the Transwell assay. We found that TGF $\beta$  pre-treatment in A549 cells significantly increased cell migration by Transwell assay. TGF $\beta$  pre-treatment in PC9 cells modestly decreased mobility, but this effect was not found to be significant. Changes in PC9 cell migration after SB-431542 pre-treatment were not observed (Figure 3.1). We also examined treatment with the TGF $\beta$  receptor type 1/2 inhibitor, LY-2109761, as a comparison to SB-431542 by wound healing (369). We found that LY-2109761 pre-treatment also induces a morphological change in PC9 cells consistent with the EMT-intermediate phenotype known as metastable (353) (Data not shown). However, we observed that LY-2109761 treatment, both alone and in conjunction with TGF $\beta$ , resulted in a significantly suppressed wound healing capability in PC9 cells which is inconsistent with an induction of EMT in PC9.

It has been noted by many groups that NSCLC cells sensitive to erlotinib usually to have an epithelial phenotype and NSCLC cells resistant to erlotinib often have a mesenchymal phenotype (366). We have shown that TGF $\beta$  treatment induces EMT-progression in erlotinib-resistant A549 cells and does not in erlotinib-sensitive PC9 cells (367). For this reason, we endeavored to understand whether modulating TGF $\beta$  activity contributed to changes in erlotinib sensitivity in the two cell lines. Most interestingly, PC9

## CHAPTER 3

cells pre-treated with SB-431542 or LY-2109761, with and without TGF $\beta$  treatment, showed significantly decreased erlotinib sensitivity. While these cells did not undergo an EMT-reprogramming as defined by EMT marker-protein expression, increased wound healing and increased migratory capabilities, our observation that the metastable morphology corresponds with significantly decreased erlotinib-sensitivity in PC9 cells is consistent with the observation that stable EMT intermediate phenotypes tend to be more drug resistant (353, 370). Importantly, we did not examine whether the phenotypes induced by TGF $\beta$  inhibitors correlated with changes in expression of EGFR or the rate of EGFR receptor turnover. We have demonstrated that extended treatment did result in a decrease of constitutively active ERK1/2 and AKT signaling (Figure 3.6). However, Supplementary Figure I-7 (Appendix I) demonstrates that the decreases in ERK and AKT signals in PC9 cells do not correlate with a cytostatic response by PC9 cells to TGF $\beta$ -inhibition.

Here, I have shown that TGF $\beta$  treatment influences erlotinib resistance in A549 cells but TGF $\beta$  inhibitors in combination with erlotinib do not sensitize A549 cells to treatment. The novel observation of this work is that TGF $\beta$ -inhibition significantly decreased erlotinib-sensitivity in PC9 cells, whereas TGF $\beta$  ligand induced more cell death in conjunction with erlotinib than erlotinib did alone in PC9 cells. This indicates that TGF $\beta$  likely plays a role in the maintenance of erlotinib-sensitivity in PC9 cells. Importantly, this mirrors the observations of unsuccessful TGF $\beta$  inhibitor drug trials that cite side effects that are likely due to pro- and anti-tumorigenic activities of TGF $\beta$  signaling (179, 219). Accurately pinpointing which half of the TGF $\beta$  paradox is occurring and where is an ongoing effort that has not been well established at this point in time (352, 371). This work should be expanded into other NSCLC cell lines across the erlotinib-sensitivity spectrum to reveal if these observations are specific to erlotinib-sensitivity status or linked to other factors (e.g., KRAS mutation status).

### **E. CONCLUSIONS**

While the relationship between the TGF $\beta$  and EGFR signaling networks suggests that TGF $\beta$  represents a logical secondary target for the prevention of EMT and subsequent

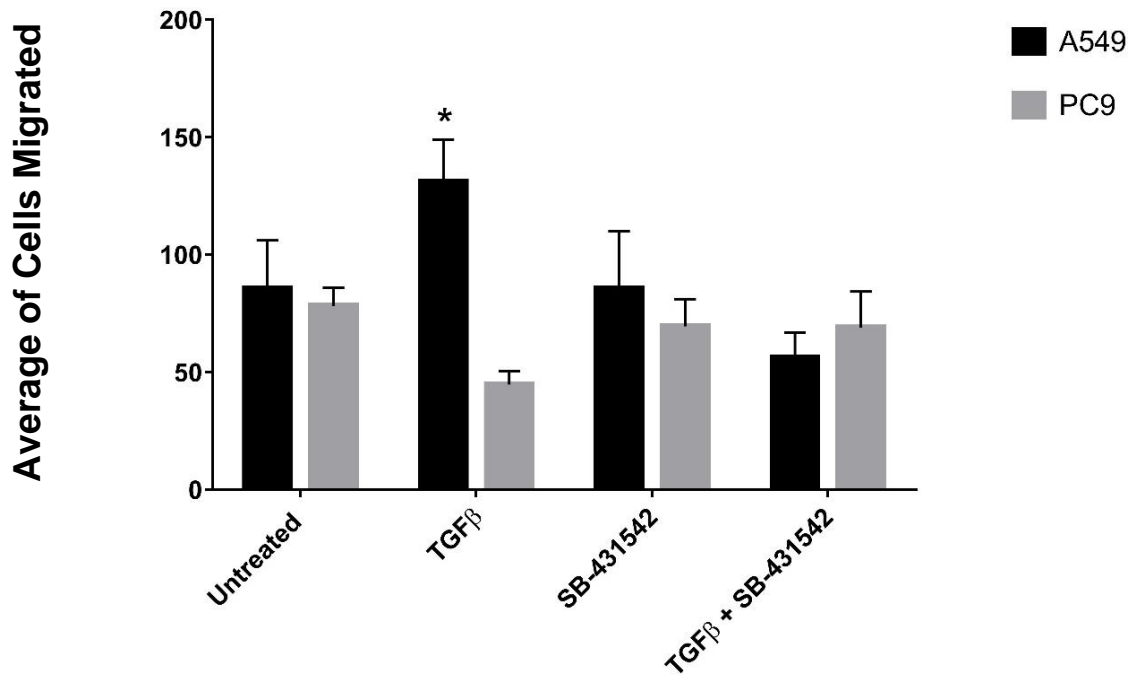
## CHAPTER 3

EMT-driven EGFR<sup>T</sup> resistance, the limitation of targeting TGF $\beta$  in unselected tumor populations is evidenced by the PC9 cell model. Until a diagnostic test capable of dissecting the TGF $\beta$  paradox exists, targeting TGF $\beta$  will remain an enigmatic and implausible target in NSCLC and other tumor types. Further study to dissect the mechanism of how TGF $\beta$ -inhibition significantly increases erlotinib resistance in PC9 cells could have important implications for elucidating and diagnosing the arms of the TGF $\beta$  paradox as well as the future of targeting TGF $\beta$  in lung cancers.

Copyright © Madeline Krentz Gober, 2017

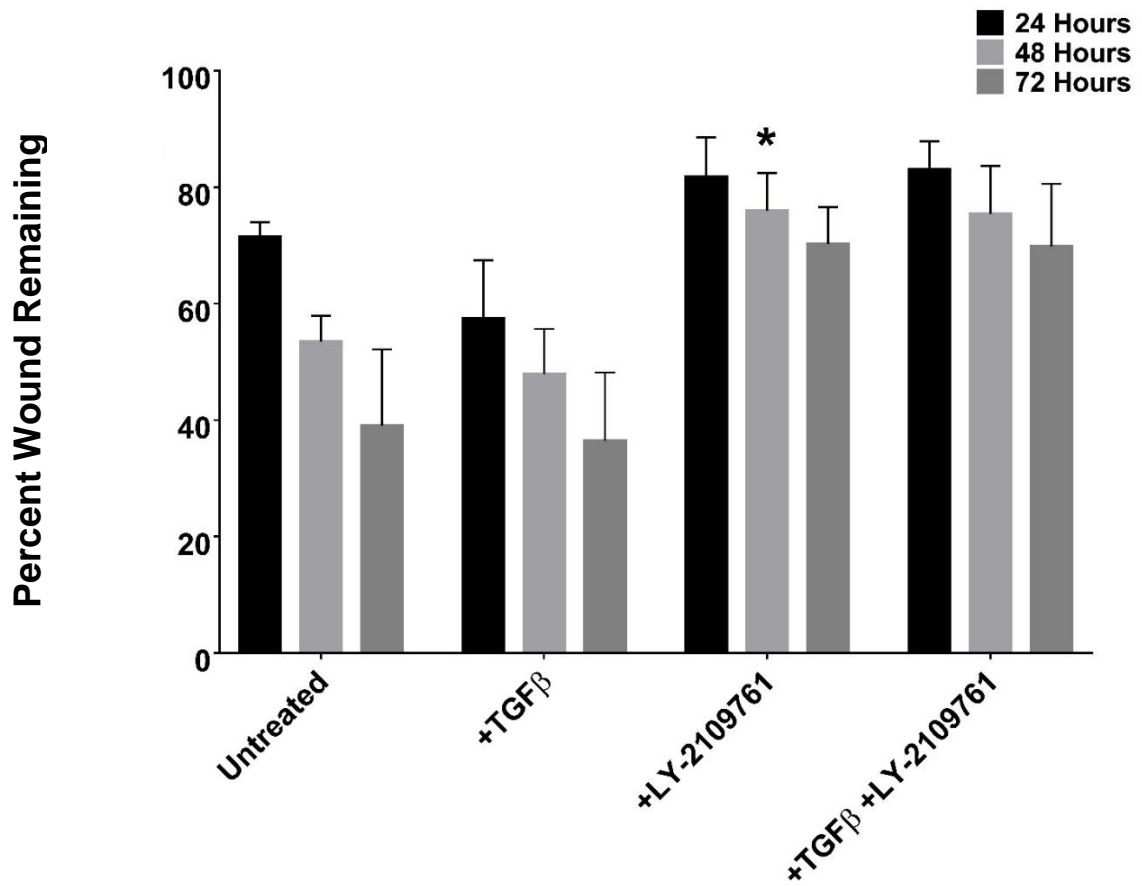
**Figure 3.1: TGF $\beta$  treatment influences the migratory ability of A549 and PC9 cells.**

Cells were plated as described in cell culture methods with the treatments specified over a course of 7 days. Values graphed are the total number of migrated cells counted between five independent views of each well by three independent readers. Outliers between biological replicates, technical replicates, and individual readers were identified and excluded using a Dixon's Q-test. Significance was determined by an unpaired t-test comparing each experimental treatment to its respective untreated values (n = 3). \* indicates p-value is  $0.05 \geq p$ .



**Figure 3.2: LY-2109761 alters wound healing capabilities of A549 and PC9 cells. (A)**

A549 and **(B)** PC9 cells were plated and treated as described in the methods. Percent wound remaining is calculated for each biological replicate compared to the respective 0 hour wound size. Biological replicates were assessed for outliers using a Dixon's Q-test (n=4). \* indicates p-value is  $0.05 \geq p > 0.0001$ , † indicates that p-value is  $\leq 0.0001$ .

**A**

**Figure 3.2 (continued): LY-2109761 alters wound healing capabilities of A549 and PC9 cells. (A)** A549 and **(B)** PC9 cells were plated and treated as described in the methods. Percent wound remaining is calculated for each biological replicate compared to the respective 0 hour wound size. Biological replicates were assessed for outliers using a Dixon's Q-test (n=4). \* indicates p-value is  $0.05 \geq p > 0.0001$ , † indicates that p-value is  $\leq 0.0001$ .

**B**

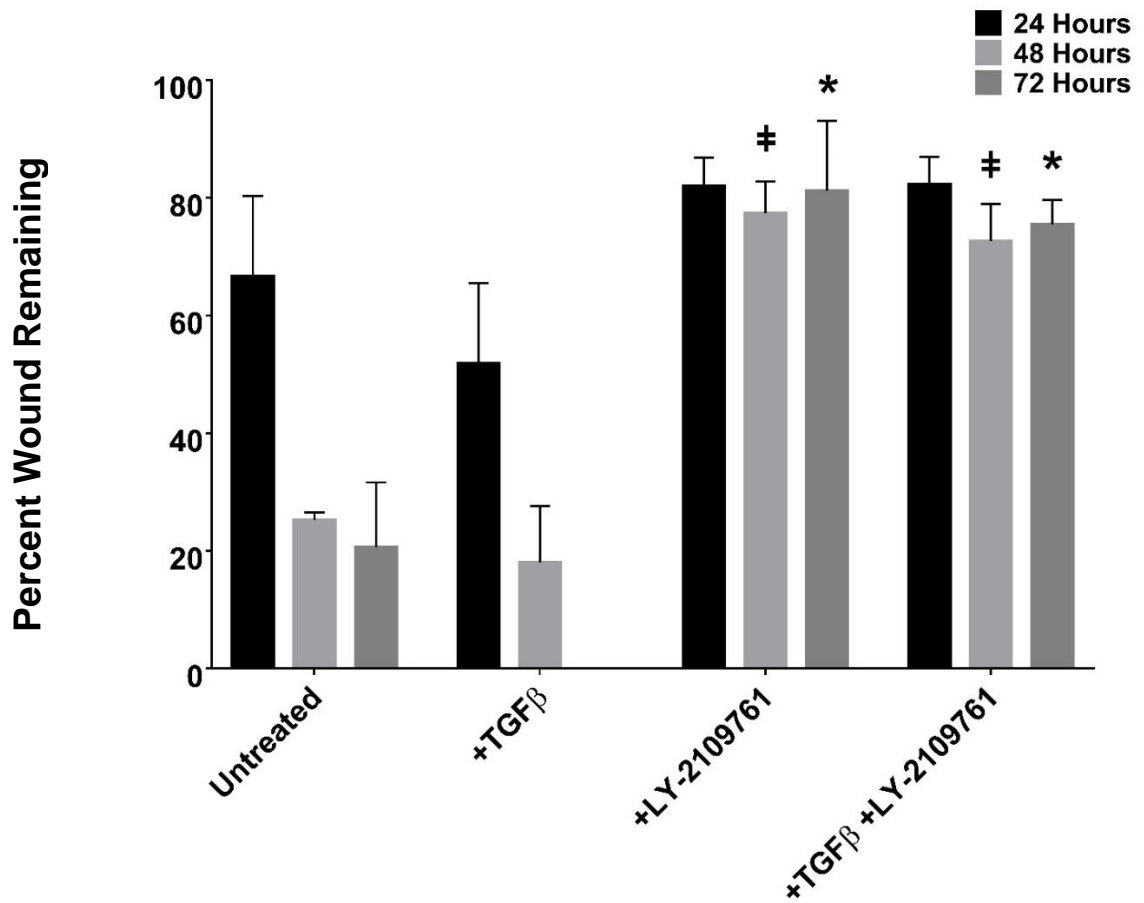


**Figure 3.3: TGF $\beta$  treatment alters erlotinib response in A549 and PC9 cells. (A)** A549 and **(B)** PC9 cells were treated for 7 days prior to initiation of the proliferation assay and treated as described. \* indicates p-value is  $0.05 \geq p > 0.0001$ , † indicates that p-value is  $\leq 0.0001$ . (n=3)

**A**

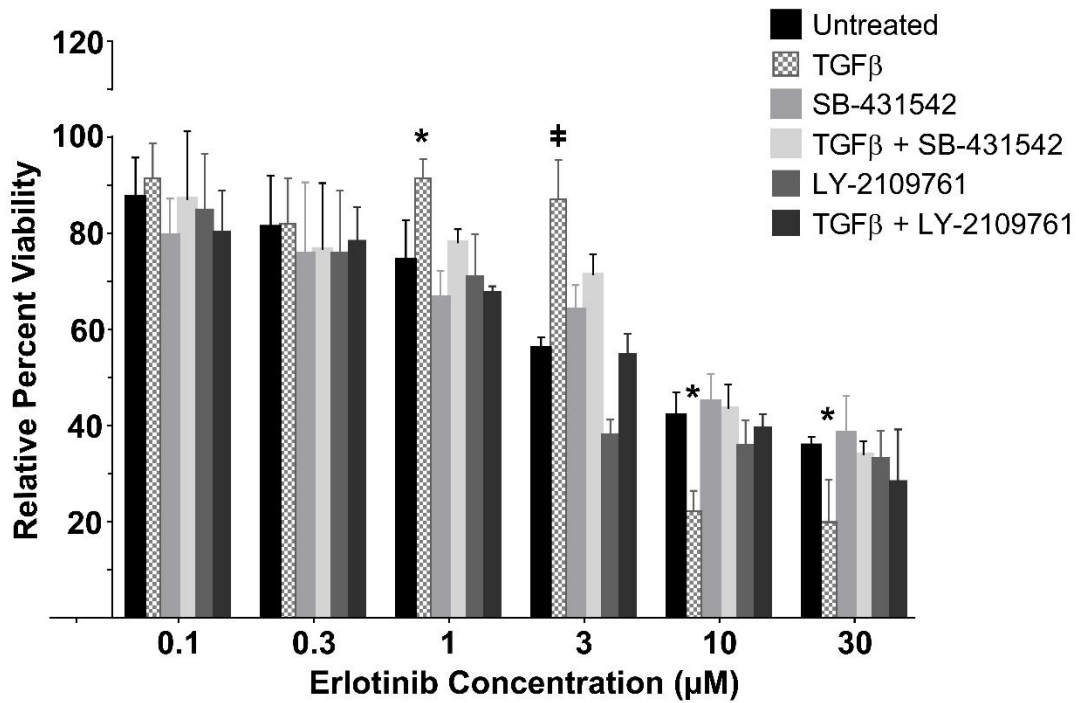
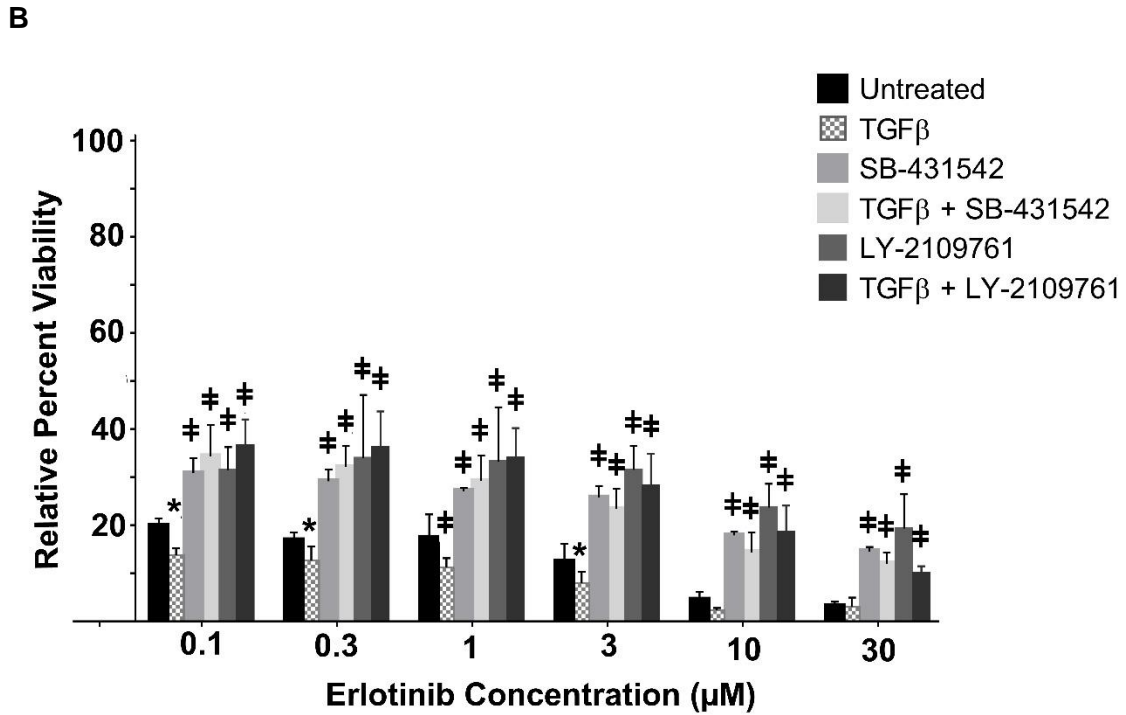


**Figure 3.3 (Continued): TGF $\beta$  treatment alters erlotinib response in A549 and PC9 cells. (A) A549 and (B) PC9 cells were treated for 7 days prior to initiation of the proliferation assay and treated as described. \* indicates p-value is  $0.05 \geq p > 0.0001$ , # indicates that p-value is  $\leq 0.0001$ . (n=3)**



## CHAPTER 4

## A. OVERVIEW

Inhibitors of the epidermal growth factor receptor (EGFR) were introduced as a targeted therapy because some non-small cell lung cancers (NSCLC) are dependent on the EGFR oncogene for growth and proliferation (3). Further, it was observed that cells and tumors with KRAS activating mutations were inherently resistant to treatment with these inhibitors (EGFRI) (67). KRAS activation mutations are the most common mutation in lung adenocarcinomas and are observed in 25-40% of cases (19, 22). Methods for targeting KRAS that have been investigated include farnesyl transferase inhibitors that target the necessary association of KRAS with the cell membrane, but resistance mechanisms involving other transferases occur (372, 373). Antisense oligonucleotides, including engineered miRNA, have also been explored as a method for targeting mutant KRAS without disrupting the expression of non-mutant KRAS and some have been successful in pre-clinical testing (374, 375). The high prevalence of patients with this inherent EGFRI resistance mechanism has made targeting mutant KRAS a priority, but so far, significant clinical benefits have not been observed (375). To overcome the limitation of our inability to successfully target mutant KRAS directly at this time is to target the multiple pathways that KRAS influences downstream (376).

In early EGFRI research on gefitinib and erlotinib, several groups found that many patients who were initially sensitive to first-generation EGFRI became resistant because tumor cells emerge after therapy with secondary mutations in the EGFR gene (e.g., T790M) and mutations in other molecules (e.g., MET) from compensating signaling cascades (377). Regardless, inherent and acquired resistance leaves many patients without treatment options (23). Second- and third-generation EGFRI have been developed to subvert some resistance mechanisms that can provide new therapeutic options for some patients, but next generation inhibitors have already been met with new resistance mechanisms (147). We believe that bioinformatics interrogation of existing gene expression data may reveal alternative therapeutic strategies to overcome both inherent (e.g., KRAS) and acquired EGFRI resistance (e.g., EGFR T790M) (378).

## CHAPTER 4

This laboratory previously developed two gene expression signatures of response to the EGFR, erlotinib, with the hypothesis that patients without EGFR activating mutations may also respond to EGFR, and those patients might be identified by particular gene expression phenotypes (327). Genes from the second EGFR response signature, comprised of miRNA genes, not only predicted response to erlotinib but also intersected the TGF $\beta$  signaling cascade (327). These data suggested that response to EGFR may be influenced by activation of TGF $\beta$  receptors, and inhibition of this signaling pathway could sensitize EGFR-resistant tumor cells to erlotinib (327). However, other groups have tested this hypothesis in clinical practice and have been largely unsuccessful in targeting TGF $\beta$ , likely due to the competing pro- and anti- tumorigenic activities of the TGF $\beta$  axis (179, 219). Despite these shortcomings, efforts to target aberrant TGF $\beta$  signaling are ongoing (379).

Further inspection of the interactions between the mRNA and miRNA signatures of erlotinib response revealed enzymatic activities that integrated both the EGFR and TGF $\beta$  signaling cascades. Casein kinase 2 (CK2) emerged as a potential target. CK2 is a multi-subunit kinase that can contribute to tumorigenesis when subunit expression is altered. CK2 exists mainly as a tetrameric holoenzyme consisting of any combination of two  $\alpha$  or  $\alpha'$  subunits and two  $\beta$  subunits, but it has been suggested that the  $\alpha$  and  $\alpha'$  subunits have monomeric kinase activity as well (243, 244). Interestingly, no oncogenic mutations have been found in CK2 kinase subunits, but deregulation of subunit expression levels might contribute to the oncogenic process (252). Moreover, it has been shown to be an upstream regulator of AKT/PI3K/mTOR, NF $\kappa$ B, and JAK/STAT signaling cascades irrespective of the receptor tyrosine kinases shown to activate them (380). As stated earlier, EGFR resistance is known to be caused by alterations in parallel signaling pathways, including the PI3K/AKT/mTOR and JAK/STAT (145). Therefore, we postulated that inhibition of CK2 might represent an alternative target for the treatment of NSCLC that are resistant to EGFR. This strategy may provide some NSCLC patients an additional opportunity for therapeutic intervention.

### **B. METHODS**

#### **Cell Culture and Western Blotting**

## CHAPTER 4

A549, H460, and H1650 (NSCLC) cell lines were purchased from ATCC. PC9 cells were a gift from the Haura lab (Moffitt Cancer Center, FL). Cells were cultured in RPMI 1640 (Life Technologies) supplemented with 10% fetal bovine serum (FBS) (USA Scientific), HEPES, glucose and pyruvate and maintained in a humidified incubator at 37°C at 5% CO<sub>2</sub> unless otherwise specified. For western experiments, 1 x 10<sup>4</sup> cells were plated into a 12-well dish and allowed to adhere in RPMI 1640 containing 10% FBS for 48 hours. Following the adherence period, cells were treated with the drug concentrations of CX-4945 (Cayman Chem) or AZD6244 (Astra Zeneca) in RPMI 1640 containing 1% FBS for the treatment durations indicated. Both adherent and non-adherent cells from each sample were harvested for total protein. Equal volumes of cell total cell extracts were loaded. Cleaved PARP and  $\alpha$ -tubulin antibodies were purchased from Cell Signaling Technologies.

### **Generation of miRNA and mRNA Expression Datasets**

mRNA and miRNA expression levels were measured in growing non-small cell lung cancer (NSCLC) cell lines using Affymetrix U133 2.0 microarrays (GSE31625) and Taqman cards from Applied Biosystems (ABI) (previously published data) (327, 328). We evaluated interactions among the 1495 mRNA genes and 23 miRNA that are significantly deregulated in erlotinib-sensitive compared with erlotinib-resistant NSCLC cells (327, 328).

### **Feasible Solutions (FS) Statistical Methodology with Work Flow and Protein-Protein Interaction Network Analysis**

The following analysis was performed by Dr. Arnold Stromberg and Josh Lambert (Department of Statistics, University of Kentucky):

Feasible Solutions (FS) was used to identify mathematical interactions in the expression data. We included mRNA that demonstrated higher expression (~800 probeIDs) in the erlotinib-resistant cell lines, and we enumerated the possible solutions, or interacting miRNA, that resulted, regardless of direction of expression relative to the mRNA. The algorithm works as follows:

## CHAPTER 4

Consider fixing  $p+$  explanatory variables in a preliminary model. Denote these variables  $X_{p+}$ . Let  $m(Y;X_{p+})$  be an objective function that can be a measure of model quality i.e.,  $R^2$ ; AIC; BIC; etc. We wish to find the  $k$  additional variables denoted  $X_k$  to add to the model that optimizes the objective function  $m(Y;X_{p+};X_k)$ . The FS algorithm attempts to solve this problem in the following way:

1. Choose  $X_k$  randomly and compute the objective function  $m$ .
2. Consider exchanging one of the  $k$  selected variables from the current model.
3. Make the exchange that improves the objective function  $m$  the most.
4. Keep making exchanges until the objective function does not improve. These variables  $X_{p+};X_k$  are called a feasible solution.
5. Return to (1) to find another feasible solution.

We chose the 100 probeIDs with the lowest  $\text{Prob}>F$  (Supplementary Table II-1, Appendix II) for further biological evaluation by STRING analysis that was performed by Dr. Robert Flight (Markey Cancer Center, University of Kentucky).

Using the miRNA:mRNA interactions described by FS modeling, the Affymetrix probesets were converted to Ensembl IDs. STRING database v 10.0 (FS) (381) files specific for human proteins were downloaded for further processing. The Bioconductor v3.0 package (382) for Affymetrix(R) HGU133-plus2 chips (hgu133plus2.db v3.0.0) was used to translate Affymetrix (R) probeset identifiers to gene identifiers (symbols, gene names, Entrez IDs and ENSEMBL Proteins) in R v3.3.2 (2016). From ENSEMBL protein IDs, the species ID 9606 was added to provide STRING protein IDs. The full set of STRING protein-protein interactions (PPI) were filtered to those with a combined score greater than 400, as well as individual scores greater than 400 in any one of the "experimental", "database", and "co-expression" evidences. From this subset of PPIs, the interactions with the original set of genes and their interactors (those genes within one edge or interaction) were extracted from the PPI database (Full list of initial genes extracted in Supplementary Table II-2, Appendix II). We were interested in interactions  $G1-X-G2$ , where  $G1$  and  $G2$  are from our list of proteins,  $X$  can be any protein that connects  $G1$  to  $G2$  (Full list of genes comprising the expanded network in Supplementary Table II-3, Appendix II). For each PPI, only a record that there was an interaction between

## CHAPTER 4

the two proteins was kept with no information on the number of evidences or the score of the interaction. STRING protein IDs were translated to gene IDs using the human database (org.Hs.eg.db v3.0.0) with Ensembl Protein (ENSEMBLPROT) as the query key (STRING protein identifiers are a combination of species ID and Ensembl protein ID). Cytoscape (383) and BioFabric (384) networks were constructed from these data.

Within the induced network, communities of genes with shared and related functions (Supplementary Table II-7, Appendix II) were identified using the cluster\_walktrap function in igraph 1.0.1 (385, 386).

### **Cell Viability Assay**

Cells were plated at  $3 \times 10^3$  cells/well in a 96-well plate in fresh treatments and allowed to adhere in RPMI 1640 containing 10% FBS for 36 hours. After 36 hours, CX-4945 (Apex Bio) and AZD6244 (Astra Zeneca) was added in the final concentrations indicated in RPMI 1640 containing 1% FBS. Drug treatment persisted for 72 hours. After 72 hours, resazurin was added (100  $\mu$ M final concentration) to each well, the plates were gently rocked for 1 minute and then incubated for 3 hours prior to reading. Each plate was read for fluorescence at excitation, 560 nm, and emission, 590 nm, wavelengths using a Spectramax M5 and corresponding Spectramax X5 software (Spectramax). Response to each treatment is normalized to untreated cells from each corresponding treatment and normalized to empty wells on each plate containing only media and resazurin. Three biological replicates were performed and were assessed for outliers using a Dixon's Q-test. Data were analyzed using Prism Version 7.00 (GraphPad).

### **Availability of Data**

All code for network generation and enrichment analysis and Supplemental files are available for download from figshare at: <https://figshare.com/s/7e50e9ab2a66b5041451>.

## **C. RESULTS**

## **CK2 Connects the miRNA and mRNA Signatures of EGFR Sensitivity**

We hypothesized that mRNA and microRNA gene expression data from NSCLC cell lines could be used to identify novel targets for therapy in lung cancer patients resistant to EGFR. The Black laboratory previously identified two independent gene expression signatures of response to EGFR using a panel of NSCLC cell lines demonstrating differential response to EGFR inhibition as measured by a cell death assay (327). The signatures were culled from a larger set of differentially-expressed mRNA and miRNA. Using the larger lists of genes (1495 mRNA and 23 miRNA), we sought to identify new protein targets for therapy using statistically significant interacting pairs of mRNA and miRNA discovered by the feasible solutions algorithm (FS) (Supplementary Table II-1, Appendix II). FS modeling first evaluates expression levels of a random combination of mRNA and miRNA pairs then considers swap-pairings of other miRNA to improve model fit and arrive at significant pairings. Each pairing then becomes a feasible solution. In this case, the model sought mRNA-miRNA pairs that have the property of high mRNA expression in the erlotinib-resistant cell lines (~800 probe IDs) in order to find targets that may have therapeutic value in erlotinib-resistant tumors. Given this outcome, we hypothesized that identifying new druggable targets for erlotinib-resistant NSCLC may depend on interactions with the EGFR signaling network. To investigate this hypothesis, we chose to use our FS gene list to find other proteins that physically interact with the candidate(s) and EGFR.

The 100 probes with the lowest probability (low Prob>F, Supplementary Table II-1, Appendix II) were identified by FS. These 100 probes translated into 85 Ensembl IDs that had matches in the STRING v10 network (387). We also included EGFR as a node to triangulate the network specifically around EGFR resistance. We carried out the network expansion analysis considering the scenario G1-X-G2 wherein G1 and G2 were proteins from the original list of 85 Ensembl IDs while X could be anything. Only 81 of the 85 proteins remained in this “induced network” (Supplementary Table II-3, Appendix II). However, another 304 nodes were found (for a total of 385 proteins in the network) that fit in the G1-X-G2 network (Supplementary Table II-3, Appendix II).

## CHAPTER 4

From these induced nodes, CK2 was chosen for further study for three reasons: 1) It has been shown to regulate many of the signaling pathways represented in the network, 2) it has been shown to be within 2 edges of 366 out of 385 of the identified nodes in the network (Supplementary Table II-5, Appendix II), and 3) it has enzymatic activity with an available pharmacological inhibitor (Table 4.1). The aim of this study was to understand whether CK2 inhibition reduced cell viability in EGFR1 resistant NSCLC cells. We chose to examine the impact of CK2 inhibition on EGFR1 resistant NSCLC cells with a variety of driver mutations (Figure 4.2B).

### **CK2 Inhibition Induces Greatest Cell Death in KRAS Active NSCLC**

To determine if CK2 activity is a novel target in EGFR1-resistant NSCLC with KRAS-activation mutations, we performed a viability assay to determine whether treatment with the CK2 small molecule inhibitor, CX-4945, decreased viability of KRAS-active NSCLC cells. In A549 and H460 cells, we observed a ~50% decrease in cell viability in CX-4945 treated cells compared to untreated cells (Figure 4.2). Considering CK2 inhibition alone was not sufficient to decrease cell viability completely, we next aimed to identify and test a secondary target within or related to the expanded network.

### **CK2 and the Members of the EGFR-MAPK-ERK Signaling Cascade Appear to Function Exclusively of one Another**

Of the 366 members of the induced network shown to be within two edges of CK2 $\alpha$  and CK2 $\alpha'$  (CSNK2A1/CSNK2A2), we isolated the network members that are within one edge of CK2 $\alpha$ /CK2 $\alpha'$  (Supplementary Table II-4, Appendix II). Unexpectedly, Supplementary Table II-4 (Appendix II) specifically demonstrates that CK2 $\alpha$  and CK2 $\alpha'$  do not directly interact with any of the members of the EGFR-RAS-RAF-MEK-ERK signaling cascade. All of the members of that signaling cascade identified by FS (HRAS, KRAS, NRAS, MAPK1, RAF1) were found to be at least two edges away from CK2 $\alpha$ /CK2 $\alpha'$  (Supplementary Table II-5, Appendix II). Because CK2 inhibition alone did not reduce cell viability completely in any cell line, we next explored whether downstream members of the

## CHAPTER 4

MAPK-ERK pathway could be logically co-targeted with CK2 in EGFR resistant NSCLC cells.

### **Combinatorial Targeting of CK2 and MEK Induces Apoptosis in KRAS Active NSCLC Cells**

We focused our selection of a secondary target on the goal of inhibiting the EGFR-MAPK-ERK pathway without targeting the EGFR receptor. CX-4945 resistance has been demonstrated in head and neck cancers and was shown to be overcome by MEK inhibition (388). Importantly, MEK was not a member of the induced network and none of the other EGFR-MAPK-ERK pathway members identified exist within one edge of CK2 $\alpha$ /CK2 $\alpha'$  (Supplementary Tables II-3 and II-4, Appendix II). Moreover, CK2 $\alpha$ /CK2 $\alpha'$  were determined to be members of community #19 whereas EGFR was identified in community #4 and other ERBB receptor family members and KRAS were identified in community #2 (Supplementary Table II-7, Appendix II). This suggests that while connected in the overall network, the MAPK-ERK cascade and CK2 likely function independently of one another.

To examine the impact of CK2 inhibition (CX-4945) in combination with MEK inhibition (AZD6244), we observed the induction of apoptosis in NSCLC cells by western blot (Figure 4.3). Both of the KRAS active cell lines examined demonstrated elevated levels of cleaved PARP at the higher concentrations of CX-4945. Levels of cleaved PARP also appear to increase between the 24- and 48-hour time points in both cell lines.

We screened A549 and H460 cells to determine if the responses to the combination of CX-4945 and AZD6244 represented a synergistic, additive, or antagonistic using a resazurin-based viability assay as was used for the single agent CX-4945 viability assays (Figure 4.4). The strongest synergism between the CX-4945 inhibitor and the AZD6244 inhibitor occurred when AZD6244 was present at 10 $\mu$ M and 3 $\mu$ M and concentrations of CX-4945 were between 0.1-30 $\mu$ M in both KRAS active cell lines (Figure 4.4).

### D. DISCUSSION

There is an urgent need to develop strategies for treating lung tumors harboring KRAS activation or other EGFR-resistance mutations. Not only are inherent EGFR-resistance mutations common, but secondary mutations that cause EGFR-resistance to develop are also prevalent and novel drug targets and treatment strategies are paramount for all lung cancer patients. Our goal was to use a combination of statistical and computational methods that integrated existing gene expression signatures linked by disease and drug response phenotypes. From this, we aimed to use interacting pairs of mRNA:miRNA to identify a network of relevant protein-protein interactions (389). In collaboration with Dr. Flight and the Stromberg group, we used the FS algorithm to identify interacting pairs of mRNA and miRNA because of prior work that indicated that pairing these RNA species may lead to an improved understanding of the disease (390). To return pharmacologically actionable targets, we focused on evaluating the protein-coding genes as drug targets, rather than the microRNA partner of the pair. The FS data was empirically reduced to the top 100 statistically-significant pairs of which the mRNA partner had highest expression in erlotinib-resistant cell lines (Supplementary Table II-1, Appendix II). Using KEGG GENES and Gene Ontology databases, each mRNA gene was paired with a molecular function, and STRING was utilized to determine protein-protein interactions (PPI). Each of these filters was intended to be an *in silico* screen to identify candidate protein-coding genes that are involved in or linked to EGFR signaling in EGFR-resistant NSCLC. Because of our efforts to focus the network identification around EGFR and EGFR resistance, the nodes identified thereby represent putative drug targets for the treatment of EGFR-resistant NSCLC.

The limitation of our initial method of identifying alternative drug targets is that not all pharmacologically actionable proteins influencing EGFR resistance are captured when considering only those deregulated genes directly connected to EGFR. For this reason, we chose to expand the network of deregulation in search of plausible nodes controlling EGFR resistance. We specifically chose to look for a node linking at least two oncogenic signaling pathways (391).

To identify actionable nodes linking the members of our list of significantly deregulated proteins, we chose to expand our network by only identifying and adding

## CHAPTER 4

proteins known to link two members of the original list. We did this by identifying proteins that met the criteria: G1-X-G2, where G1 and G2 are members of the original list of deregulated genes including EGFR while X is any protein linking the two. What we determined is that by adding this additional level of selection, we identified nearly every EGFR resistance mechanism described in NSCLC thus far (Communities #2 and #4, Supplementary Table II-7, Appendix II) among a number of novel putative targets (Supplementary Table II-7, Appendix II). Of the expanded network, we selected CSNK2A1 and CSNK2A2, which encode the kinase subunits of CK2. We determined that they are within two edges of 366 out of 385 members of the expanded network indicating their value as a well-connected target (Supplementary Table II-3, Appendix II). Not only was CK2 predicted by our *in silico* model to interact with many sources of EGFR resistance, but it has been also described as influencing many other members of the network of deregulated genes between EGFR resistant and sensitive NSCLC, notably including NF- $\kappa$ B and PI3K/AKT (392). The network specifically includes nearly every source of inherent or acquired EGFR resistance described to date (19, 145) and they were largely contained to two communities of common action, neither of which included CK2 (Supplementary Table II-7). Considering the global potential influence of CK2 in the network of dysregulation of EGFR resistance, and that a kinase inhibitor of CK2 has been tested in Phase II trials (323), we next aimed to determine if CK2 inhibition was impactful against NSCLC cells that are resistant to EGFR.

EGFR-resistant, KRAS active NSCLC cells were found to be sensitive to CK2 inhibition, but the maximal response observed was only around 50% cell viability compared to untreated cells (Figure 4.2A). We compared the effect of CX-4945 in KRAS active NSCLC to other cell lines harboring EGFR mutations. We found that PC9 cells, that harbor only an EGFR exon 19 deletion mutation, were resistant to CX-4945. However, H1650 cells that harbor both an exon 19 deletion as well as a PTEN null mutation demonstrated a response curve similar to KRAS active A549 and H460 (Figure 4.2A). Specifically, H1650 cells only have intermediate sensitivity to EGFR despite the EGFR activation mutation because loss of the PTEN tumor suppressor allowing these cells to compensate for EGFR action through deregulated PI3K/AKT signaling. Importantly, CK2 was identified as a possible target for overcoming PTEN null mutations via a chemogenomic study in 2015 (393). It is also interesting to note that both PC9 and H1650 harbor a p53 mutation, and from these data, it would appear that mutant p53 likely does

## CHAPTER 4

not influence CX-4945 efficacy. Interestingly, H460 cells have a PIK3CA E545K mutation resulting in less efficient activation of the p110 $\alpha$  isoform of the PI3K catalytic domain but were still sensitive to upstream CK2 inhibition. We have previously demonstrated that PI3K p110 isoforms are capable of compensation. H460 express high levels of the p110 $\beta$  isoform as well as high levels of PTEN protein expression suggesting that the regulation of this pathway by CK2 is still possible despite the PIK3CA mutation (331). To examine whether these observations were related to expression of CK2 subunits, we profiled each of the NSCLC cell lines tested above for CSNK2A1, CSNK2A2 and CSNK2B mRNA expression (Supplementary Figure II-1, Appendix II). Of the NSCLC cell lines we profiled, KRAS active cells demonstrated the lowest expression of CSNK2B compared to normal cells. This suggests that constitutively active KRAS signaling may play a role in repressing CK2 $\beta$  expression.

We next aimed to identify a second expanded network member or member of a network pathway as a plausible secondary target to be paired with CK2 inhibition because none of the cell lines tested were exquisitely sensitive to CK2 inhibition. Importantly, the KRAS active NSCLC tested were the most sensitive to CK2 inhibition. The KRAS activation mutation drives MAPK-ERK signaling regardless of EGFR activation or inhibition, and we observed in the expanded network that not all of the MAPK-ERK signaling cascade were represented and none were directly connected to CK2. For this reason, we hypothesized that CK2 and MEK inhibition would be sufficient to overcome compensatory signaling by the induced network identified in KRAS active NSCLC. This hypothesis was also founded with the knowledge that MEK inhibition has been used to overcome CX-4945 resistance in head and neck cancers (388). Our lab and others have similarly demonstrated that inhibition of MEK concurrently with EGFR sensitizes NSCLC with EGFR T790M mutations to treatment (329, 394). Initial exploration of AZD6244 and CX-4945 co-treatment on NSCLC cells revealed that the apoptotic marker, cleaved PARP, was expressed in KRAS active NSCLC cells. Moreover, increased cleaved PARP relative to  $\alpha$ -tubulin were observed at 48 hours when compared with 24 hours. We screened KRAS active A549 and H460 for synergistic drug interactions between CX-4945 and AZD6244 and found that the strongest synergism between the two drugs occurred when AZD6244 was present at 10 $\mu$ M and 3 $\mu$ M and concentrations of CX-4945 were between 0.1-30 $\mu$ M in both KRAS active cell lines (Figure 4.4). These data demonstrate that this combination of CK2 and MEK inhibition may represent a novel approach for the treatment of EGFR-

## CHAPTER 4

resistant, KRAS-active NSCLC. We plan to expand on this observation by performing a battery of viability assays against a range of NSCLC cells to determine if these observations reign true for other cell lines with varying responses to EGFRi therapies.

A combination of MEK and CK2 inhibition encompasses many of the signaling pathways by which non-EGFR-receptor EGFRi resistance develops and should continue to be explored as an avenue for the treatment of inherently resistant NSCLC (e.g., KRAS). It should also be explored as an avenue for overcoming acquired EGFRi-resistance (e.g., EGFR T790M) as well. This strategy of bypassing EGFR and KRAS as therapeutic targets may represent a novel therapeutic approach for treating a variety of NSCLC tumors.

### **E. CONCLUSIONS**

Many cancers are quickly becoming chronic diseases and will require new therapies for patient care and management of emerging resistant diseases. We have demonstrated that gene expression signatures descriptive of a specific tumor phenotype can be used to identify potential targets for new therapeutics or co-therapeutic methodologies. Using the FS algorithm and STRING, we unveiled a network of proteins found to be deregulated between EGFRi resistant and sensitive NSCLC. From this network, we identified and tested CK2 $\alpha$ /CK2 $\alpha'$  as a therapeutic target for the treatment of EGFRi resistant NSCLC, but CK2 inhibition alone did not substantially decrease cell viability. The expanded network suggests that EGFR-MAPK-ERK signaling and CK2 activity exist somewhat exclusively which prompted us to examine the impact of combinatorial CK2 and MEK inhibition. Initial CK2+MEK inhibition experiments revealed that the combination of the two drugs is lethal in KRAS active NSCLC cells and was synergistic when AZD6244 was present at 10 $\mu$ M and 3 $\mu$ M with all concentrations of CX-4945 in both KRAS active cell lines. We believe that the combination of MEK and CK2 inhibition has important implications for the treatment of KRAS active NSCLC and has potential as an alternative to those who acquire EGFRi-resistance during treatment. We also seek to improve this novel pipeline for drug discovery by automating a process that utilizes gene expression signature as inputs and objectively leverages bioinformatics filtering of prospective targets to minimize wet lab validation. We must also consider multiple computational and statistical methods to

## CHAPTER 4

identify gene-gene interactions and associated validation schemes that appropriately manage high-density data from comparatively few biological observations.

Copyright © Madeline Krentz Gober, 2017

**Figure 4.1: The G1-X-G2 expanded network links nearly every EGFR1 resistance described to date.** The network of protein protein interactions was simplified to a collection of “communities” with collective activities using the cluster\_walktrap function in igraph. Putative community activities were determined by manual data mining and literature search. **(A)** Complete network of communities. **(B)** Magnification of central communities with putative actions and known EGFR1 resistance mechanisms highlighted.

**A**

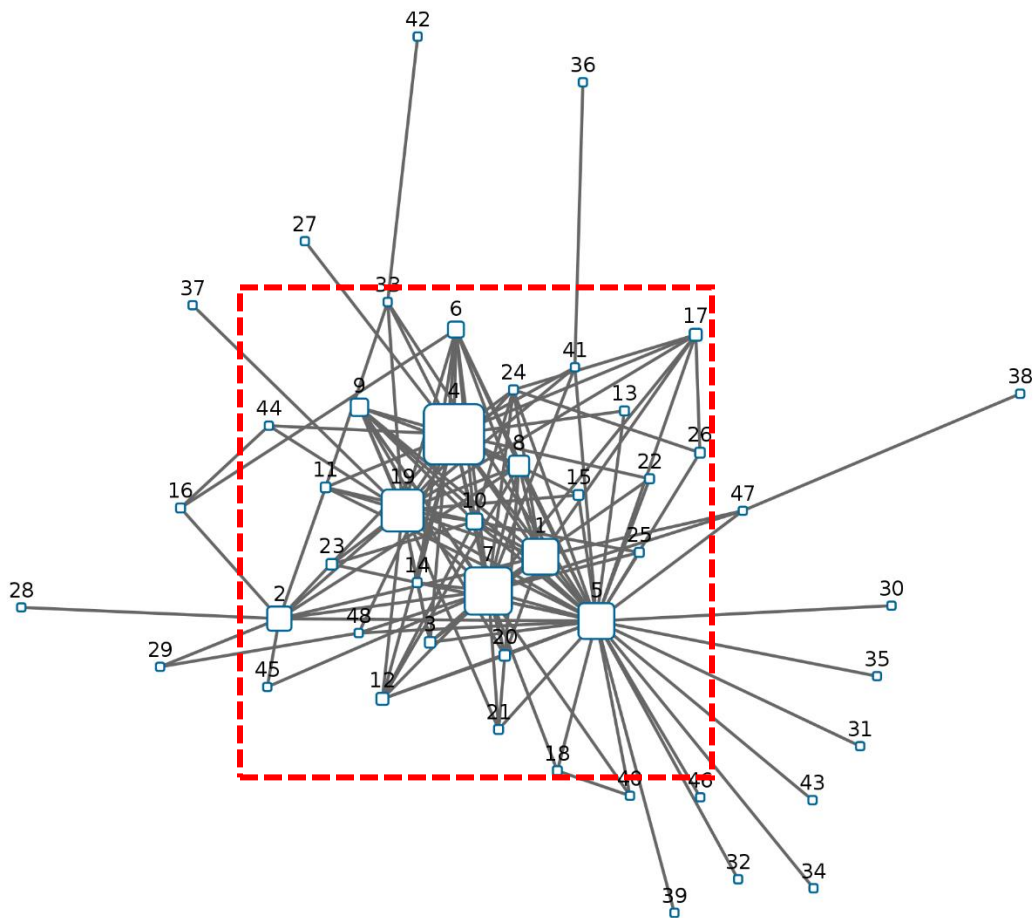
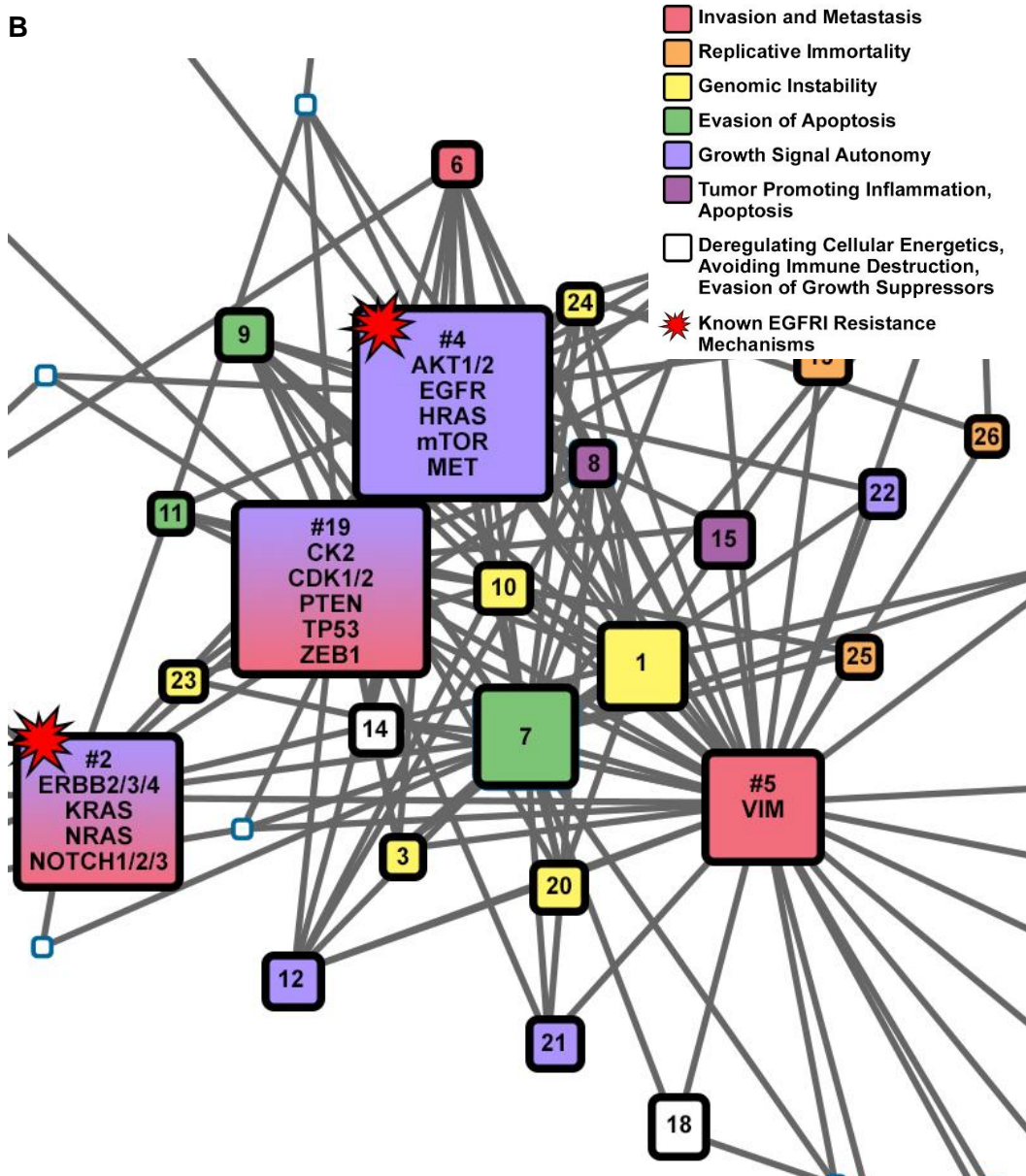


**Figure 4.1 (continued): The G1-X-G2 expanded network links nearly every EGFR1 resistance described to date.** The network of protein protein interactions was simplified to a collection of “communities” with collective activities using the cluster\_walktrap function in igraph. Putative community activities were determined by manual data mining and literature search. **(A)** Complete network of communities. **(B)** Magnification of central communities with putative actions and known EGFR1 resistance mechanisms highlighted.



## CHAPTER 4

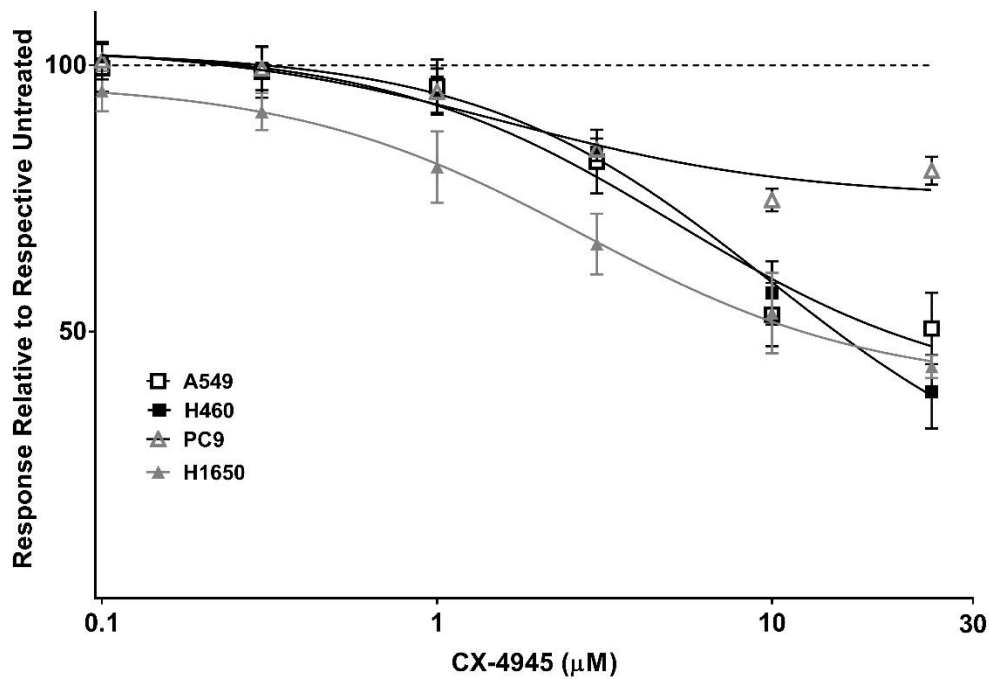
**Table 4.1: G1-X-G2 Analysis-Induced EGFR1 Resistance Network Members that interact with CK2 $\alpha$  or CK2 $\alpha'$  within one edge and are pharmacologically actionable.**

Table members are from the complete network of 385 proteins that interact with CK2 $\alpha$  or CK2 $\alpha'$  within one edge (Supplementary Table II-4, Appendix II). Abridged table members below represent those for which both pharmacological inhibitors exist and have at least entered Phase I clinical trials.

<b>SYMBOL</b>	<b>GENE NAME</b>	<b>TYPE</b>
AKT1	v-akt murine thymoma viral oncogene homolog 1	Induced
CDK1	cyclin-dependent kinase 1	Induced
CSNK2A1	casein kinase 2, alpha 1 polypeptide	Induced
CSNK2A2	casein kinase 2, alpha prime polypeptide	Induced
CTNNB1	catenin (cadherin-associated protein), beta 1, 88kDa	Induced
HDAC1	histone deacetylase 1	Induced
HSP90AA1	heat shock protein 90kDa alpha (cytosolic), class A member 1	Induced
HSP90AB1	heat shock protein 90kDa alpha (cytosolic), class B member 1	Induced
HSP90B1	heat shock protein 90kDa beta (Grp94), member 1	Induced
PSMA3	proteasome subunit alpha 3	Induced
PSMA4	proteasome subunit alpha 4	Induced
PTEN	phosphatase and tensin homolog	Input
SIRT1	sirtuin 1	Induced
SRC	SRC proto-oncogene, non-receptor tyrosine kinase	Induced

**Figure 4.2: NSCLC cells resistant to EGFR1 are most sensitive to CK2 inhibition. (A)**

Viability assays were performed on KRAS active, EGFR1 resistant NSCLC (A549 and H460 cells) treated with CX-4945. Shown in comparison with intermediate-EGFR1 sensitivity, H1650 cells (EGFR exon 19 deletion and PTEN null), and EGFR1-sensitive, PC9 cells (EGFR exon 19 deletion). Values are log-transformed. (n=3) **(B)** A table demonstrating the EGFR1 resistance, mutational statuses, and response to 10 $\mu$ M CX-4945 for each of the NSCLC analyzed.

**A**

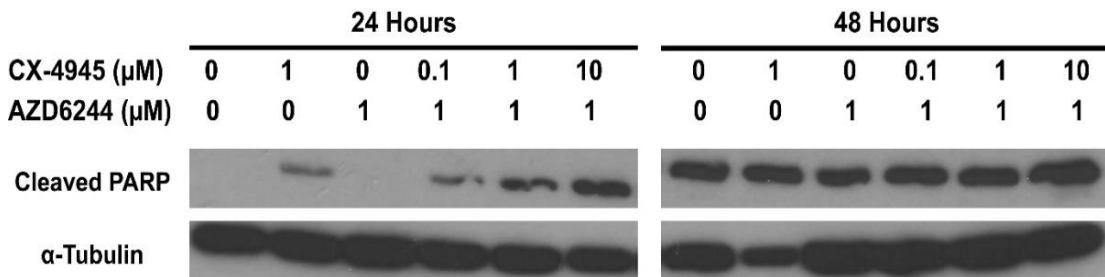
**Figure 4.2 (continued): NSCLC cells resistant to EGFR are most sensitive to CK2 inhibition. (A)** Viability assays were performed on KRAS active, EGFR resistant NSCLC (A549 and H460 cells) treated with CX-4945. Shown in comparison with intermediate-EGFR sensitivity, H1650 cells (EGFR exon 19 deletion and PTEN null), and EGFR-sensitive, PC9 cells (EGFR exon 19 deletion). Values are log-transformed. (n=3) **(B)** A table demonstrating the EGFR resistance, mutational statuses, and response to 10 $\mu$ M CX-4945 for each of the NSCLC analyzed.

**B**

CELL LINE	EGFR Resistance Status	EGFR Mutation Status	KRAS Mutation Status	PI3K/AKT Mutations Status	Percent Viability at 10 $\mu$ M CX-4945
A549	Resistant	WT	G12S (Active)	WT	53.2405
H460	Resistant	WT	Q61H (Active)	PIK3CA E545K (Null)	57.2708
H1650	Intermediate	Exon 19 Deletion (Activating)	WT	PTEN Null (Activating)	53.4981
PC9	Sensitive	Exon 19 Deletion (Activating)	WT	WT	74.7392

**Figure 4.3: Co-treatment with CX-4945 and MEK inhibitor, AZD6244, induces cell death in KRAS active NSCLC.** Cells handled and treated as described in the methods. Both adherent and non-adherent components of each well were harvested for total protein. Each well represents 1/3 of the total volume of protein harvested from each sample assessed for cleaved PARP and  $\alpha$ -tubulin. Response to drug combinations were observed by western blot using the apoptotic marker, cleaved PARP at 24 and 48 hours. **(A)** A549 cells **(B)** H460 cells.

**A**



**B**

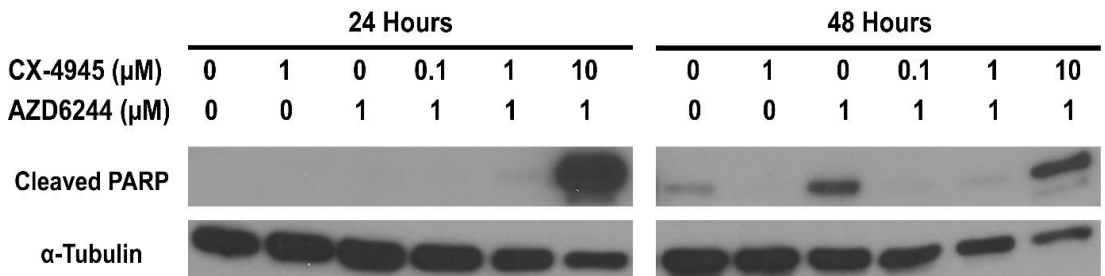


**Figure 4.4: Screening for synergistic interactions between the CK2 inhibitor, CX-4945, and the MEK inhibitor, AZD6244.** Cells were assessed by resazurin viability assay to identify possible synergistic, additive or antagonistic responses of CX-4945 in combination with AZD6244 using combination index (CI) values. CI values were then used to generate the heat map for each cell line. **(A)** A549 cells **(B)** H460 cells.

CI Values	
≤0.5	Synergism
0.51-0.99	Slight Synergism
1-1.49	Additive
1.5-1.99	Slight Antagonism
≥2.0	Antagonism

A

		AZD6244 (μM)					
		30	10	3	1	0.3	0.1
CX-4945 (μM)	30	1.02049	0.71992	0.59235	0.55049	0.61981	0.73616
	10	0.95206	0.55608	0.5078	0.98279	0.98735	0.73973
	3	0.79595	0.42711	0.72412	1.63317	6.43996	3.39567
	1	1.14371	0.67159	0.89036	2.10645	15.3454	1.78956
	0.3	1.258	0.71075	0.65023	1.00434	12.1634	0.36242
	0.1	1.51505	0.85743	0.72815	0.59457	115.893	0.29457

B

		AZD6244 (μM)					
		30	10	3	1	0.3	0.1
CX-4945 (μM)	30	0.23853	0.15484	0.24985	0.35815	0.1522	0.23068
	10	0.6804	0.78631	0.59991	2.73233	0.7952	0.74581
	3	1.79495	0.59703	0.41602	1.09675	4.1732	0.44567
	1	5.32872	0.68241	0.52064	1.04351	0.78227	0.97133
	0.3	10.7842	0.57414	0.45335	10.8271	7.33228	0.40307
	0.1	0.67055	0.56424	0.26205	25.8473	37.7681	0.13553

**CHAPTER 5****A. OVERVIEW**

EGFR is not the only driver mutations found in NSCLC which is why not all tumors are responsive to EGFR treatments (19). Moreover, many patients that receive EGFR therapies eventually develop resistance which underscores the need for alternative therapeutic options to overcome these limitations of EGFR. Our 13-gene miRNA signature of EGFR response initially indicated that the TGF $\beta$  signaling cascade may be a putative secondary target for the treatment of drug-resistant NSCLC (327). In Chapter 3, we demonstrated that TGF $\beta$  inhibitors had value in impeding cell mobility as well as increased erlotinib resistance in A549 cells. However, we also determined that the inhibition of TGF $\beta$  induced a significant increase in erlotinib resistance in PC9 cells that are otherwise exquisitely sensitive to erlotinib treatment. Our work examining the value of TGF $\beta$  as a target confirmed observations that targeting TGF $\beta$  may be detrimental in unselected tumor populations (Chapter 3) (179, 213).

Further analysis of our gene expression data using Feasible Solutions mathematical model to find putative mRNA-miRNA gene interactions (Chapter 4) identified CK2 as an alternative target for the treatment of EGFR-resistant NSCLC. Initial examination of CK2 as a therapeutic target demonstrated that it may have value as a treatment option for NSCLC harboring KRAS activation mutations or PTEN null mutations (Chapter 4). Maximal cell viability decreases were only observed at approximately 50% cell viability suggesting that CK2 inhibition would likely be most successful as part of a combination therapy. Interestingly, the inhibition of CK2 has been shown to impede the induction of EMT by TGF $\beta$  (239). CK2 inhibition showed promise in treating A549 cells, but had no effect in PC9 cells (Chapter 4). Given these results combined with the observed relationship between the induction of EMT by TGF $\beta$  and CK2, we hypothesize that inhibition of CK2 can block TGF $\beta$ -induction of EMT and reduce erlotinib resistance in A549 cells. In this context, CK2 inhibition could augment EGFR by blocking the induction of EMT and EGFR-resistance thereby eliminating the need for TGF $\beta$  inhibition all together.

### **B. METHODS**

#### **Cell Culture**

The NSCLC cell lines used were A549, purchased from ATCC, and PC9, gifted from the Haura lab (Moffitt Cancer Center, FL). All cells were cultured in RPMI 1640 (Life Technologies) supplemented with 10% FBS (USA Scientific), HEPES, glucose and pyruvate and maintained in a humidified incubator at 37 °C at 5% CO<sub>2</sub> unless otherwise specified. Cells were seeded in 6-well plates and were allowed to grow under RPMI 1640 containing 10% serum media conditions for 48 hours prior to treatments. Cells were plated at  $1 \times 10^4$  cells and were treated with SB-431542 (3  $\mu$ M) (Selleck Chem), LY-2109761 (3  $\mu$ M) (Cayman Chem), CX-4945 (1  $\mu$ M) (Apex Bio) and/or TGF $\beta$  (5 ng/ml) (Cell Signalling) under minimal serum (1%) conditions for time frames specified. Treatment media was replenished at the 72-hour time point in 168-hour culture experiments.

#### **Cell Viability Assay**

Cells underwent pretreatment in 1% serum-containing RPMI 1640 with drug and/or cytokine for 7 days following the plating and treatment conditions described above. After treatment, cells were trypsinized, counted, and plated at  $3 \times 10^3$  cells/well in a 96-well plate in fresh treatments matching those from the 7-day period. After 36 hours adherence time, erlotinib was added in indicated concentrations. Drug treatment persisted for 72 hours. After 72 hours, resazurin was added (100  $\mu$ M final concentration) to each well, the plates were gently rocked for 1 minute and then incubated for 3 hours prior to reading. The plate was read for fluorescence at excitation, 560 nm, and emission, 590 nm, wavelengths using a Spectramax M5 and corresponding Spectramax X5 software (Spectramax).

#### **Data Processing and Statistics**

Values measured between biological replicates from all viability assays and wound healing assays were subjected to a Dixon's Q test to eliminate outlier values. For viability assays, response to each treatment is normalized to cells from each corresponding

## CHAPTER 5

treatment that were not subjected to erlotinib. Readings were also normalized to empty wells on each plate containing only media and resazurin. Individual experiments were done in triplicate and were assessed for outliers using a Dixon's Q-test (n=4). All graphical representations of data were made and analyzed using Prism Version 7.00 (GraphPad). Significance points in viability assay data compare the points specified in each figure legend and in the results section. Significance was determined using unpaired t-tests.

### C. RESULTS

#### **CX-4945 increases erlotinib-sensitivity in PC9 but not in A549 cells**

In Chapter 3, we demonstrated that while TGF $\beta$  ligand treatment increases erlotinib sensitivity in PC9 cells, it significantly decreased A549 erlotinib-sensitivity in a dose-dependent manner (Figure 3.3). Also, TGF $\beta$  receptor inhibition (with SB-431542 or LY-2109761) reversed the erlotinib phenotype in TGF $\beta$  ligand-treated A549 cells, and the presence of either TGF $\beta$  receptor inhibitor significantly decreased erlotinib sensitivity in PC9 cells (Figure 3.3). For this reason, we endeavored to determine whether co-inhibition of another linked target, CK2, could sensitize erlotinib-resistant A549 cells to treatment. CK2 and TGF $\beta$  activate common growth, proliferation and survival pathways. For these reasons, we sought to elucidate whether CK2 inhibition could prevent the changes on erlotinib-sensitivity in A549 and PC9 cells induced by TGF $\beta$  ligand or TGF $\beta$  inhibitors respectively.

Pre-treatment of A549 cells with a combination of CX-4945 and TGF $\beta$  ligand (Figure 5.1A) prevented the increased erlotinib-resistance phenotype observed in A549 cells that had been pre-treated with TGF $\beta$  ligand alone (Chapter 3, Figure 3.3A). Conversely, SB-431542 pre-treatment in combination with CX-4945 decreased erlotinib-resistance in A549 cells at lower erlotinib concentrations (0.1-3  $\mu$ M) compared with cells pre-treated with CX-4945 alone (Figure 5.1A).

## CHAPTER 5

In PC9 cells, pre-treatment with CX-4945 alone and in combination with TGF $\beta$  ligand increased erlotinib sensitivity when compared to the matched CX-4945 naïve cells in Chapter 3, Figure 3.3B (Figure 5.1B). Importantly, this experiment showed that the pre-treatment of PC9 cells with CX-4945 did not eliminate the decrease in erlotinib-sensitivity resulting from exposure to either of the TGF $\beta$  inhibitors (SB-431542 or LY-2109761) with or without TGF $\beta$  ligand (Figure 5.1B).

### D. DISCUSSION

In Chapter 3, we showed that TGF $\beta$  ligand can contribute to erlotinib resistance in A549 cells because TGF $\beta$  inhibitors reversed this phenotype. Conversely, TGF $\beta$ -inhibition significantly reduced erlotinib sensitivity in PC9 cells, whereas TGF $\beta$  ligand induced more cell death in conjunction with erlotinib than erlotinib did alone (Figure 3.3B, Chapter 3). Identifying which arm of the TGF $\beta$  paradox signaling is active remains elusive, but CK2 inhibition has been shown to reverse TGF $\beta$ -driven EMT offering a possible alternative (239). For this reason, we endeavored to determine if CK2 inhibition using CX-4945 (Silmitasertib) could similarly prevent the increase in erlotinib resistance.

We found that CX-4945 impedes the increase in erlotinib resistance induced by TGF $\beta$  ligand in A549 cells (Figure 3.3A), but it does not sensitize A549 cells to erlotinib. This suggests that the combination of EGFR1 and CK2 inhibition is not a sufficient treatment option for KRAS active NSCLC like A549. Importantly, the significant decrease in erlotinib-sensitivity induced by TGF $\beta$ -inhibition in PC9 cells was not blocked by co-inhibition with CX-4945. CX-4945 treatment did increase erlotinib sensitivity significantly in PC9 cells both treated and untreated with TGF $\beta$  ligand when compared to matched PC9 (Supplemental Figure III-1, Appendix III).

### E. CONCLUSIONS

EGFR1 and CX-4945 efficacy appear to be linked by a co-dependent relationship between PI3K/AKT and MAPK-ERK signaling (238, 395, 396). The decrease in erlotinib

## CHAPTER 5

sensitivity in PC9 cells induced by TGF $\beta$  inhibitors was not prevented by co-incubation with the CK2 inhibitor, CX-4945. This reinforces that TGF $\beta$ -inhibitors continue to have limited to no value in this context since the off-target effects of TGF $\beta$ -inhibition are still evident in PC9 cells. While the interactions among signaling networks certainly impacts the influence of TGF $\beta$  on EGFR1 resistance, the limitation of targeting TGF $\beta$  in unselected tumor populations is not mitigated by the inclusion of CK2 inhibitors.

Copyright © Madeline Krentz Gober, 2017

**Figure 5.1: TGF $\beta$  treatment in combination with CX-4945 alters erlotinib response in A549 and PC9 cells. (A) A549 and (B) PC9 cells. Cells were treated with TGF $\beta$  in combination with CX-4945 with or without SB-431542 or LY-2109761 at the same time as the samples used in figure 3.3. Values are normalized to corresponding cells untreated by erlotinib. \* indicates p-value is  $0.05 \geq p > 0.0001$ , † indicates that p-value is  $\leq 0.0001$ . (n = 3)**

A

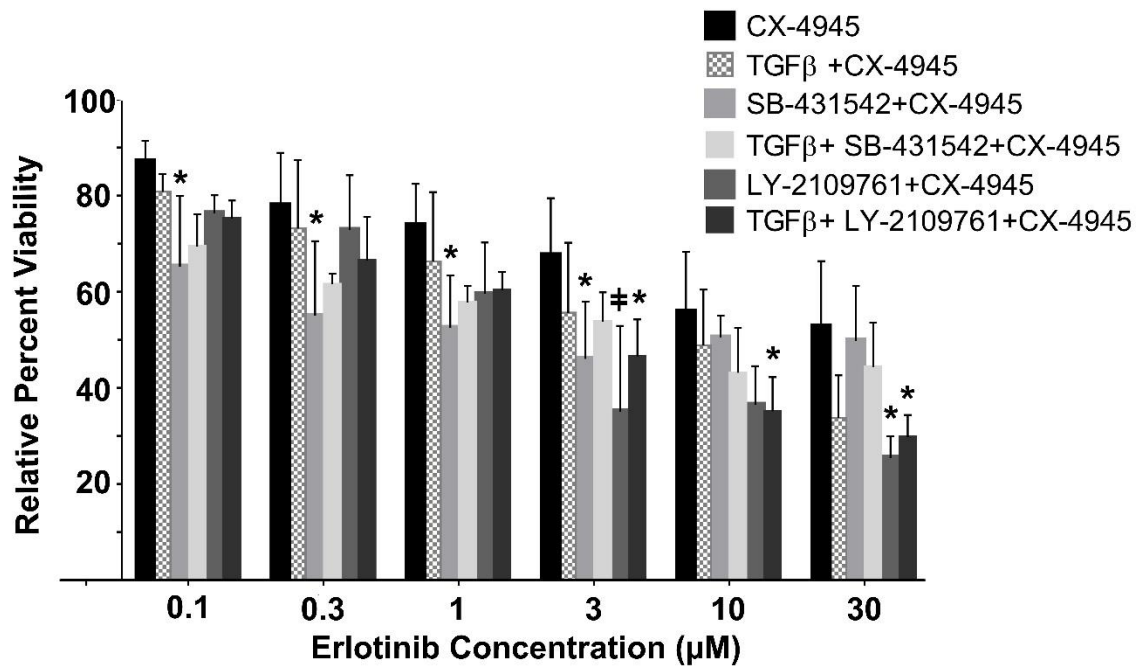
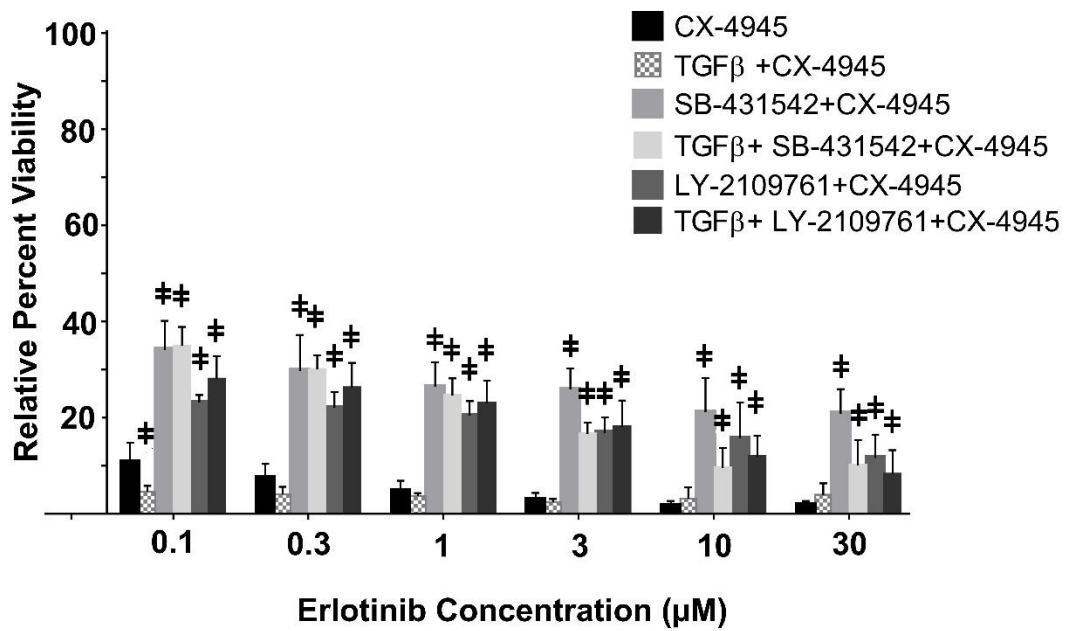


**Figure 5.1 (Continued): TGF $\beta$  treatment in combination with CX-4945 alters erlotinib response in A549 and PC9 cells. (A) A549 and (B) PC9 cells. Cells were treated with TGF $\beta$  in combination with CX-4945 with or without SB-431542 or LY-2109761 at the same time as the samples used in figure 3.3. Values are normalized to corresponding cells untreated by erlotinib. \* indicates p-value is  $0.05 \geq p > 0.0001$ , # indicates that p-value is  $\leq 0.0001$ . (n = 3)**

**B**



## CHAPTER 6

## A. SUMMARY OF RESULTS

My goal for this body of work was to utilize genomic data to identify and test putative targets for the treatment of drug-resistant lung cancers. Using the previous data generated by the lab to produce two gene signatures of EGFR1 response, I hypothesized that:

- 1) The 13 miRNA genes comprising the second expression signature of response to EGFR1 are transcriptionally regulated by TGF $\beta$  signaling.
- 2) TGF $\beta$  drives EMT and enforces EGFR1 resistance in EGFR1-resistant NSCLC.
- 3) The cell line RNA expression data used to generate the miRNA and mRNA signatures can be analyzed using novel mathematical and computational models to uncover interactions among these RNA. These nodes of cellular regulation, captured by utilizing both lists of deregulated genes, may identify novel targets to combat EGFR1-resistance in NSCLC.

In Chapter 2, I explored my first hypothesis **that the miRNA comprising the signature of response were being transcriptionally regulated by canonical TGF $\beta$  signaling via the Smads**. It has been demonstrated that TGF $\beta$  has the ability to promote or repress the expression of genes in a contextually-specific manner (351, 352). More importantly, twelve out of the thirteen miRNA genes contained putative Smad binding elements (SBEs) in their promoter regions (Figure 2.7) (347, 348). Considering that miRNA frequently act upon the pathways that regulate their expression, I aimed to determine if the differences in signature miRNA expression between EGFR1-resistant and EGFR1-sensitive NSCLC cells were regulated by TGF $\beta$  (327, 397). I demonstrated that over a 7-day course of TGF $\beta$  treatment, activation of the canonical TGF $\beta$  signaling pathway via the R-smads, Smad 2, Smad 3 and Smad 4, occurs differently between the model EGFR1-resistant and EGFR1-sensitive cell lines. Moreover, extended TGF $\beta$  treatment induced downregulation of total Smad 2, Smad 3, and Smad 4 by long-term TGF $\beta$  treatment in the EGFR1-sensitive cell line. TGF $\beta$  induced morphological and protein

## CHAPTER 6

expression changes in the EGFR1-resistance model consistent with EMT, but this effect was not observed in the EGFR1-sensitive model. In the EGFR1-sensitivity model, the inhibition of TGF $\beta$  induced a morphology consistent with an EMT intermediate phenotype known as metastable (353). These data confirm that TGF $\beta$  possesses differential activity that may be responsible for the expression of the miRNA differentiating EGFR1-resistant from EGFR1-sensitive cells. Because of this, I next explored the direct contribution of TGF $\beta$  on the expression of three candidate miRNA from opposing sides of the response signature, miR-140, miR-141, and miR-200c.

Using chromatin immunoprecipitation, I determined that Smad 4 bound to the shared promoter of miR-141 and miR-200c in EGFR1-sensitive cell lines in response to TGF $\beta$  stimulation. Because there was no binding to the promoter of miR-140, I suspected that differential regulation was occurring in line with the initial hypothesis. Because of this, I next aimed to observe if TGF $\beta$  induced differential endogenous expression changes of the three candidate miRNA. Using a 5-way ANOVA and two models of EGFR1-resistant cells and two EGFR1-sensitive cell lines, I aimed to elucidate the source of the endogenous expression changes considering five factors: 1) miRNA expression, 2) time of treatment, 3) TGF $\beta$  treatment, 4) SB-431542 treatment, 5) cell line. I considered the additional H460 and H1650 cell lines as a metric of determining if the changes observed correlated with EGFR1-sensitivity status of cells or if miRNA expression changes were a cell line specific phenomena. I determined that the most impactful variable governing the expression of the signature miRNA levels was the time of treatment. I interpreted this to be a response to the loss of cell cycle progression and aimed to elucidate whether the percentage of cells in the G<sub>0</sub>G<sub>1</sub> phase of the cell cycle correlated with the changes in miRNA endogenous expression levels. I determined that regardless of treatment conditions, all cell lines accumulated in the G<sub>0</sub>G<sub>1</sub> phase of the cell cycle as a function of time in culture.

Analysis of the qRT-PCR data and the cell cycle experiment led us to explore whether the signature miRNA promoters contained putative cell-cycle responsive elements. I determined that twelve of thirteen signature miRNA contained promoter elements that may be cell-cycle responsive (Supplementary Figure I-9, Appendix I). I then asked whether TGF $\beta$  stimulation activated growth and proliferation pathways, MAPK-ERK and PI3K/AKT, and correlated with endogenous miRNA expression level changes. I determined that TGF $\beta$  activation of these pathways was different between the cell models

## CHAPTER 6

but did not correlate with the endogenous miRNA expression changes observed. I concluded that the signature miRNA are likely responsive to elements associated with cell cycle progression. I also concluded that while the activity of TGF $\beta$  in the EGFR1-resistance model is consistent with the ability of TGF $\beta$  to drive EMT, an opposing phenotype was found in the EGFR1-sensitive cell line.

Future directions of this work will explore the influence of the cell cycle on the expression of the signature miRNA. To start, we will use the ChIP method for determining transcription factor association with a promoter to determine if ELK1 is bound to the sites in each of the promoters. We will triangulate this back to the changes in miRNA expression at each time point as well as the percentage of cells exiting the cell cycle at this time point. If ELK1 is not found to be bound to the promoters of the signature miRNA, other cell cycle responsive transcription factors will also be examined by western blot at each time point in order to isolate another cell cycle responsive candidate to interrogate.

In Chapter 3, **I tested my second hypothesis that TGF $\beta$  signaling enforces EGFR1-resistance correlating with its ability to activate EMT.** I explored the contribution of the differential TGF $\beta$  activity observed to cellular migration, wound healing and response to a candidate EGFR1, erlotinib. I determined that TGF $\beta$  induced migration in the EGFR1-resistance model and the phenotype was reversed with the TGF $\beta$  inhibitor. I also determined by wound healing assay that TGF $\beta$  inhibition prevented wound healing in both the EGFR1-resistance and EGFR1-sensitive models. This demonstrated that the TGF $\beta$ -induced, EMT phenotype in the EGFR1-resistant cells was prevented by TGF $\beta$ -inhibition. It also demonstrated that the EMT-like intermediate observed in the EGFR1-sensitive model did not correlate with the induction of other EMT-characteristics such as migratory ability. Finally, to determine if TGF $\beta$  represented a clinically-relevant secondary target in relation to resistance to EGFR1, I determined whether extended TGF $\beta$  treatments altered sensitivity to EGFR1. In the EGFR1-resistance cell model, I determined that long-term TGF $\beta$  treatment significantly increased cell viability in response to erlotinib. This increase in erlotinib resistance by TGF $\beta$  in EGFR1-resistant cells was not observed in cells co-treated with a TGF $\beta$  inhibitor. This suggests that while TGF $\beta$  inhibitors may reduce TGF $\beta$ -driven EMT events and erlotinib resistance, it is not a secondary target that will sensitize EGFR1-resistant cells to EGFR1 treatment.

## CHAPTER 6

I also examined the role of TGF $\beta$  signaling on EGFR sensitivity in known EGFR-sensitive cell line model. Interestingly, extended TGF $\beta$  pre-treatment in the EGFR-sensitive model cell significantly decreased erlotinib sensitivity in these cells. This effect may be due to the ability of TGF $\beta$  to impair cell proliferation in this cell line model (179, 371). Because these were cells treated with TGF $\beta$  in minimal serum (1% FBS) media conditions, the reduced proliferation may be due to a cross talk between TGF $\beta$  and EGFR signaling in response to nutrient availability. These observations are consistent with the anti-tumorigenic-arm of the “TGF $\beta$  paradox” theory (371). Most importantly, all instances of TGF $\beta$ -inhibition in the EGFR-sensitive cell model resulted in a significant increase in erlotinib resistance. However, I confirmed by measuring the migration and wound healing capabilities indicative of EMT induction that TGF $\beta$ -inhibition was not inducing EMT in the EGFR-sensitive cell line. Remarkably, the change in erlotinib-sensitivity aligns with the observations from Figure 2.6 where TGF $\beta$  inhibition resulted in a reduction of pERK1/2 and pAKT signaling in these cells. I did not examine whether the phenotype was related to an increase in internalization and ubiquitination of active EGFR or the result of downstream signal ablation (e.g., RAS downregulation). From the data herein, I cannot confirm a mechanism for how TGF $\beta$  inhibition reduces erlotinib sensitivity in cells that are otherwise exquisitely sensitive to EGFR treatment. To determine a mechanism, I would propose measuring the impact of TGF $\beta$  modulation on the expression of EGFR mRNA and protein levels. A study on the internalization and degradation rates of EGFR would also be informative in determining the source of the decreasing pERK1/2 and pAKT levels in response to TGF $\beta$  inhibition. Nevertheless, this observation reinforces that anti-TGF $\beta$  therapies will likely continue to be unsuccessful clinically in unselected patient populations, as has been observed (179, 219).

Future directions of this work will be to identify alternative targets besides TGF $\beta$  for the treatment of drug-resistant NSCLC. To identify targets for the treatment of drug-resistant NSCLC, I employed mathematical and protein-protein interaction modeling algorithms. This effort to identify alternative targets for EGFR-resistant NSCLC is described in Chapter 4.

In Chapter 4, **I tested my hypothesis that combining the mRNA and miRNA data would identify nodes of cellular deregulation captured by both lists of deregulated genes. This may identify alternative targets for combatting EGFR**

**resistance in NSCLC.** I sought to identify other, pharmacologically actionable signaling nodes that may be targeted to overcome EGFR1 resistance in NSCLC. We used the Feasible Solutions (FS) algorithm to systematically test for possible direct interactions between the 1495 mRNA and 23 miRNA found to be deregulated in EGFR1 resistant NSCLC cells. We took the mRNA member of each of the 100 most statistically-significant interacting mRNA:miRNA pairs as determined by FS and annotated them to 85 separate Ensembl IDs that had protein matches in STRING v10 (387). The 85 proteins were inducted in the STRING network to search for interactions with EGFR. We found that 81 proteins were within two edges of EGFR in the initial STRING network. Of the 81 proteins, many have been studied and/or implicated in EGFR1 resistance. We chose to expand the network of genes considering the scenario “G1-X-G2” where G1 and G2 are any member of the original 85 Ensembl IDs imported into STRING and X is any induced node that connects them. From this, the network grew to 304 induced nodes, for a total of 385 nodes in the expanded deregulated network.

The resulting network identified nearly every EGFR1 resistance or compensatory signaling mechanism currently known, including: AKT/PI3K/mTOR (398), ataxia telangiectasia mutated (ATM) kinase (399), Aurora kinase (400), other ErbB family receptors (Her2, ErbB3 and ErbB4)(401), all three RAS isoforms (HRAS, KRAS and NRAS) (402), insulin-like growth factor receptor (IGFR) (403), MET receptor tyrosine kinase (39), and members of NF $\kappa$ B, Notch, and TNF $\alpha$  signaling (109, 404, 405). The list also includes a number of cellular functions related to EGFR signaling regulation mechanisms including internalization (e.g., calmodulin1/2), ubiquitination (e.g., E3 protein ligases), and proteosomal degradation (e.g., proteasome subunits). Moreover, when divided into “communities” of node cellular functionality (Supplementary Table II-5, Appendix II), nearly every of the hallmarks of cancer were represented in the deregulated network suggesting that this network encompasses many of the mechanisms employed by EGFR1 resistant NSCLC cells to maintain proliferation.

Of the list of proteins comprising the network of deregulation we, I selected CK2 $\alpha$ /CK2 $\alpha'$  (the catalytic subunits of CK2 encoded by genes CSNK2A1 and CSNK2A2) to further pursue for three reasons: 1) the complete holoenzyme has been shown to interact with/regulate many of the members and pathways represented in the network, 2)

## CHAPTER 6

it was shown to be within two edges of most of the induced nodes in the network, and 3) it possesses enzymatic activity that can be inhibited by a pharmacological agent.

I assessed pharmacological inhibition of CK2 using the CK2 inhibitor, CX-4945, on NSCLC cells that are resistant to EGFR. I determined that NSCLC harboring KRAS activation and PTEN null mutations, both inherently resistant to EGFR, were most sensitive to CK2 inhibition. However, the maximal response observed in these cells was approximately 50% cell viability, suggesting that CX-4945 may be most successful as a combination therapy. Further, cells harboring EGFR activation mutations were resistant to CX-4945 treatment suggesting that a coupling of EGFR and CX-4945 would likely have no added therapeutic value.

My goal was to identify an alternate target or a combination of targets to overcome EGFR resistance in NSCLC. Considering that the majority of EGFR resistance occurs as either mutations to EGFR (e.g., EGFR T790M) or downstream (e.g., KRAS), I aimed to identify a secondary drug target downstream of these resistance mechanisms. When we reduced the network to include only proteins within one edge of CK2 $\alpha$ /CK2 $\alpha'$ , no member of the EGFR-RAS-RAF-MEK-ERK signaling cascade was represented. This suggests that while EGFR-MAPK-ERK and CK2 signaling may interact, they do not do so directly (Table 4.2). Because of this, I chose to evaluate the value of coupling CK2 and MEK inhibition. Initial experiments examining the impact of co-treatment of CX-4945 and the MEK inhibitor, AZD6244, revealed that the drug combination resulted in increasing levels of the apoptotic marker, cleaved PARP, across increasing drug concentrations and across time points (Figure 4.3). Future experiments will determine if this effect is also observed in cell viability assays, and if so, whether the effect is additive or synergistic.

Finally, I explored whether CK2 inhibition could act as a surrogate for inhibition of TGF $\beta$  in KRAS active NSCLC. I previously demonstrated that TGF $\beta$  inhibition prevented increased EGFR resistance in A549 cells and TGF $\beta$  inhibition induced EGFR resistance in PC9 cells. This illustrates that in unselected populations, TGF $\beta$  inhibition is not clinically meaningful. I found that the combination of treatments did not increase cell death overall in A549 cells. I observed that CK2 inhibition can act as a surrogate for TGF $\beta$  inhibition blocking the increased erlotinib resistance brought on by TGF $\beta$ . Unfortunately, CK2 inhibition did not prevent the induction of EGFR resistance by TGF $\beta$  inhibitors in PC9.

## CHAPTER 6

These results suggest that TGF $\beta$  inhibition will still be a clinically-irrelevant treatment option until we have a methodology for selecting patients considering the status of TGF $\beta$  with regards to the “TGF $\beta$  paradox”.

Intriguingly, I observed that the combination of CX-4945 and EGFRi decreased cell viability in PC9 cells at low doses of EGFRi although this effect was not found to be significant. These data suggest that the combination of therapies may be ideal in EGFRi-sensitive tumors to prevent acquired mutations. CX-4945 treatment has already been shown specifically to prevent the development of EGFR T790M acquired-EGFRi-resistance mutations in PC9 (238).

### **B. EXPERIMENTAL LIMITATIONS**

The work described herein is the result of a combination of pharmacogenomic, systems biology, and pharmacologic methods to identify treatment alternatives for drug-resistant NSCLC using gene expression data. This combinatorial analysis allows us to test broad inferences about the biology that underpins the phenotype of EGFRi resistance in NSCLC. From the data analyzed, I formed hypotheses regarding the role of the deregulated proteins identified in EGFRi sensitivity and/or resistance. Finally, I tested my hypotheses using cell line models of NSCLC with pharmacological agents that interrupt the pathways of interest. While this method allows us to gain a valuable understanding of the biology of EGFRi resistance and streamline the putative target discovery pipeline, it does have a number of limitations.

#### **Genomic Modeling of the Deregulation of EGFRi-Resistant NSCLC**

The strength in this methodology is that the *in silico* models can identify large networks of deregulated genes and proteins. Bioinformatic tools can also identify the nodes that connect them. The difficulty in developing and employing these methodologies is that many data points are generated and must be annotated in order to find meaningful putative targets. In revisiting Supplementary Table II-2 (Appendix II), one will find that there are many known oncogenic kinases and deregulated signaling pathways known to

## CHAPTER 6

drive tumorigenesis. There are also many network members that are less characterized that must be sorted through. The expanded network of 385 proteins also includes members known to be pharmacologically non-targetable to date (e.g., KRAS).

Another limitation to the specific genomic analyses that we performed is that we specifically used expression data derived from NSCLC cells with known EGFR1 sensitivity and known mutational statuses influencing EGFR1 sensitivity in each of the lines. For the first of these profiling endeavors (the deregulated mRNA), the favorable alternative would have been to use human tumors with known EGFR1 clinical outcomes. Unfortunately, samples with known EGFR1 outcomes were not available at the time of the mRNA signature development (328). By the time we profiled the miRNA genes in the same cells, clinical samples were growing increasingly available. However, the ideal choice was to profile for miRNA expression in the same cell lines profiled for mRNA deregulation so the data sets could be compared. Specifically, this also allowed us to revisit the miRNA data and mRNA together with the goal of identifying nodes of deregulation shared between the two probesets as we've done here. This allowed us to identify a network of putative drug targets with more evidence than the original two analyses because it encompasses two "omic" levels of deregulation between EGFR1-resistant and -sensitive NSCLC.

### **Biological and Pharmacological Testing of the Hypotheses Identified *in silico***

A prominent limitation of the work herein is the use of only cell line models for examining *in silico* generated hypotheses for the sake of determining novel avenues for the clinical treatment of lung tumors. The value of cell culture models lies in their ability to be a method for testing hypotheses in a well-controlled environment, but this is also the downside of the model. Cell line testing is an important stage in the development of an *in silico* hypothesis to a clinical treatment model because it allows us to rapidly test the value of novel targets both alone and in combinatorial analyses in a model that is significantly less expensive than *in vivo* models.

### **C. CONTRIBUTION TO THE FIELD**

## CHAPTER 6

Bioinformatic analysis of the 13-miRNA gene signature that predicts erlotinib sensitivity in NSCLC cells and tumor samples identified TGF $\beta$  signaling as a pathway of convergence of the miRNA genes. For this reason, I asked whether TGF $\beta$  played a role in the expression regulation of three of the candidate miRNA. We determined that TGF $\beta$  did not directly impact the expression of the miRNA, but cell cycle position may be important. Further study to characterize the remaining miRNA and to directly test the promoter elements for the transcriptional regulation of the signature miRNA is necessary to validate this hypothesis. However, a deeper understanding of if and how the cell cycle contributes to the expression of the signature miRNA could be useful for retraining the 13-miRNA gene signature to not only indicate putative erlotinib response, but to indicate reliance on rapid cell cycle passage for viability. This additional piece of information could have value in determining which tumors are likely to respond to cell cycle targeting agents.

This study was the first to characterize that TGF $\beta$  inhibition in PC9 cells leads to a significant loss of erlotinib sensitivity. TGF $\beta$  also decreased proliferation in these cells in low serum conditions indicating that it may play a role in attenuating mutant EGFR signaling. TGF $\beta$  inhibitors have entered clinical trials numerous times and are chronically unsuccessful due to side effects on TGF $\beta$  signaling in normal cells (179, 219).

This is a combinatorial analysis of two “omic”-level studies of deregulated mRNA and miRNA species adds value to the targets identified as they are represented in both the mRNA and miRNA transcriptomes. This methodology for identifying networks of deregulation between phenotypes is valuable for dissecting the differences between many cellular phenotypes. We believe this paired analysis of functionally-related “omic”-level data (such as miRNA that act on mRNA) is ideal for identifying the network of genes most pertinent to a closed phenotype (e.g., EGFRi-resistance). This study is also proof-of-concept that mining existing gene expression data has merit for identifying and addressing new hypotheses surrounding specific phenotypes (e.g., EGFRi-resistance versus -sensitivity).

This study is the first to specifically identify the network of deregulated signaling surrounding CK2 as it relates to EGFRi-resistance. CK2 is both a member of this network and is connected to most of its members. A relationship between EGFR and CK2 signaling activity has been described in the sense of co-targetability and common influence.

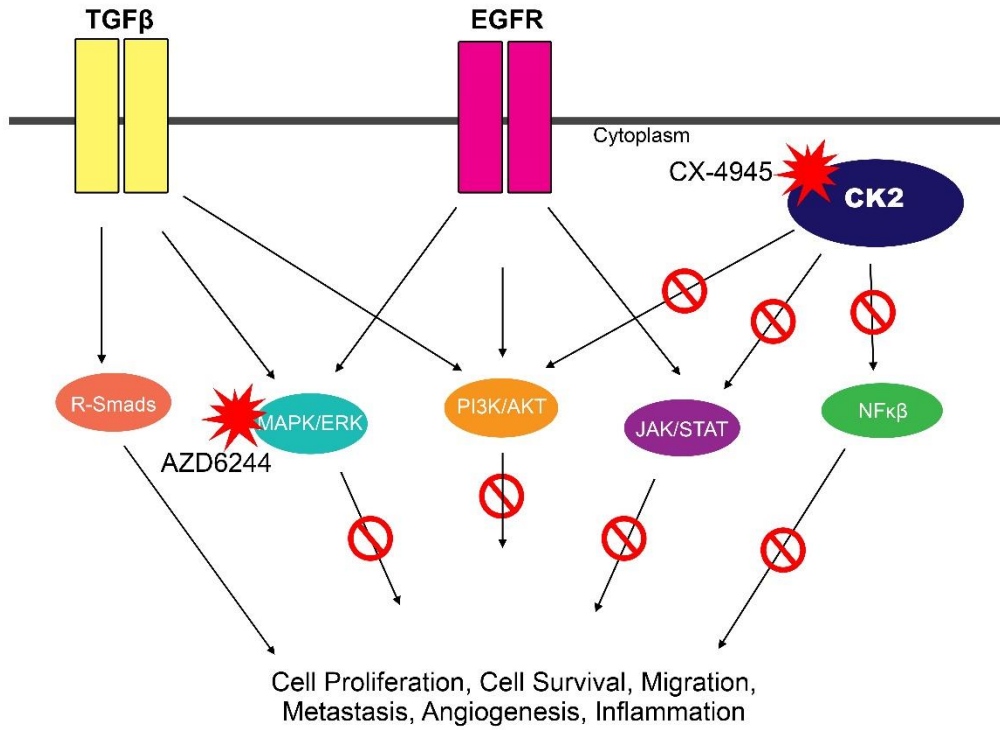


**Figure 6.1: The Impact of Co-Targeting MEK and CK2 on Cancer Signaling Pathways.**

## CHAPTER 6

However, our analysis is the first to model that they likely act independently of one another with common downstream signaling nodes in pathways other than MAPK-ERK. I showed that EGFR1 resistant cells harboring a KRAS activation mutation were most sensitive to CK2 inhibition suggesting that it could be a viable option for KRAS active lung tumors that comprise approximately 20% of the lung cancer population (168). I demonstrated that CK2 inhibition in conjunction with EGFR1 was not sufficient to sensitize KRAS active cells to EGFR1. This indicates that inhibition downstream of active KRAS is likely necessary to attenuate signaling. My initial examination of the CK2 and MEK co-inhibition is the first study to demonstrate that this combination likely has value in treating EGFR1 resistant NSCLC harboring a KRAS activation mutation.

### **D. CONCLUSIONS**

I conclude that an analysis considering multiple gene expression species that physically interact and regulate one another (e.g., mRNA and miRNA) are ideal for identifying a concise network of proteins that define a phenotype of choice. The network identified using this methodology performed best for us using the G1-X-G2 scheme to capture other the contributing members of a network. This novel approach for identifying possible therapeutic targets requires further validation in cell culture as well as in another data set to determine the sensitivity and specificity of the approach. I identified CK2 as a putative target due to its expansive relationships with the other network members, specifically those known to contribute mechanistically to the generation of EGFR1-resistance. Examination of its activity suggests that CK2 inhibition shows promise for treating EGFR1-resistant NSCLC, specifically those harboring KRAS active mutations. We also conclude that inhibition of CK2 concurrently with MEK inhibition has the potential to maximize targeted therapy benefit for the treatment of KRAS active, EGFR1-resistant NSCLC tumors.

**APPENDIX I: SUPPLEMENTARY FIGURES FOR CHAPTER 2**

*Supplementary Table I-1: Output of 5-way ANOVA analysis. (Data pairs with Supplementary figures I-4 and I-5) (A) Variable names used in analysis. (B) Five-way ANOVA Overall F-test of the endogenous miRNA data. (C) Tests of the effects within the five-way ANOVA.*

**A**

Class Level Information		
Class	Levels	Values
Time	3	168 Hour 24 Hour 72 Hour
Expr	3	miR-140 miR-141 miR200
status	4	A549 H1650 H460 PC9
TGF	2	N Y
SB	2	N Y

**B**

Source	DF	Sum of Squares	Mean Square	F Value	Pr > F
Model	143	8088.984432	56.566325	57.40	<.0001
Error	288	283.797472	0.985408		
Corrected Total	431	8372.781904			

APPENDIX I

**Supplementary Table I-1 (Continued): Output of 5-way ANOVA analysis. (Data pairs with Supplementary figures I-4 and I-5)**

**C**

Source	DF	Type III SS	Mean Square	F Value	Pr > F
Time	2	79.952136	39.976068	40.57	<.0001
Expr	2	1885.221769	942.610885	956.57	<.0001
Time*expr	4	54.519027	13.629757	13.83	<.0001
TGF	1	10.424204	10.424204	10.58	0.0013
Time*TGF	2	1.076126	0.538063	0.55	0.5798
expr*TGF	2	1.079149	0.539574	0.55	0.5790
Time*expr*TGF	4	0.646410	0.161602	0.16	0.9565
SB	1	1.546384	1.546384	1.57	0.2113
Time*SB	2	0.471393	0.235697	0.24	0.7874
expr*SB	2	1.520563	0.760281	0.77	0.4633
Time*expr*SB	4	0.324106	0.081027	0.08	0.9878
TGF*SB	1	0.134397	0.134397	0.14	0.7122
Time*TGF*SB	2	0.541967	0.270983	0.27	0.7598
expr*TGF*SB	2	1.295853	0.647926	0.66	0.5189
Time*expr*TGF*SB	4	0.965323	0.241331	0.24	0.9126
Status	3	3240.479541	1080.159847	1096.16	<.0001
Time*status	6	364.036762	60.672794	61.57	<.0001
expr*status	6	2266.034942	377.672490	383.27	<.0001
Time*expr*status	12	127.856402	10.654700	10.81	<.0001

APPENDIX I

**Supplementary Table I-1 (Continued): Output of 5-way ANOVA analysis. (Data pairs with Supplementary figures I-4 and I-5)**

Source	DF	Type III SS	Mean Square	F Value	Pr > F
status*TGF	3	2.810260	0.936753	0.95	0.4165
Time*status*TGF	6	4.252351	0.708725	0.72	0.6344
expr*status*TGF	6	2.875868	0.479311	0.49	0.8183
Time*expr*status*TGF	12	2.785062	0.232089	0.24	0.9964
status*SB	3	12.852156	4.284052	4.35	0.0051
Time*status*SB	6	0.954675	0.159113	0.16	0.9866
expr*status*SB	6	6.327867	1.054644	1.07	0.3804
Time*expr*status*SB	12	3.120940	0.260078	0.26	0.9939
status*TGF*SB	3	6.390615	2.130205	2.16	0.0927
Time*status*TGF*SB	6	2.107473	0.351246	0.36	0.9058
expr*status*TGF*SB	6	4.105405	0.684234	0.69	0.6544
Tim*expr*stat*TGF*SB	12	2.275306	0.189609	0.19	0.9987

APPENDIX I

**Supplementary File I-1: Experimental Ct Averages. (A)A549, (B) H460, (C) H1650, (D) PC9.**

**(A) A549**

		Untreated			+TGFβ		
miR-140	24 Hour	12.33757	11.43739	11.60239	12.39578	12.97549	12.15190
	72 Hour	9.787602	10.08148	10.61999	9.900755	10.42333	11.50879
	168 Hour	9.758026	10.54176	11.49169	10.53289	11.00631	11.92199
miR-141	24 Hour	17.06016	15.32151	19.90596	17.07662	17.98000	20.07600
	72 Hour	15.54128	13.97606	14.51325	15.44358	15.80907	16.95060
	168 Hour	14.27188	12.21063	11.12456	15.88630	13.84227	15.35418
miR-200c	24 Hour	14.10283	14.30923	14.84075	14.54479	14.74094	15.67361
	72 Hour	13.32989	12.92316	14.99424	13.60149	13.89697	15.47936
	168 Hour	12.67405	13.07983	14.84481	13.63927	14.52270	16.56609
		<b>+SB-431542</b>			<b>+TGFβ + SB-431542</b>		
miR-140	24 Hour	11.89172	12.01508	11.48558	12.45281	11.61382	12.25275
	72 Hour	9.535458	10.08252	10.83031	9.738522	10.67040	11.51334
	168 Hour	8.811357	9.751716	10.45633	10.03573	10.56819	11.34701
miR-141	24 Hour	12.00429	16.11283	19.87011	14.06351	15.08848	19.66269
	72 Hour	14.33568	16.13022	13.74338	14.67358	11.94453	12.31492
	168 Hour	13.87545	11.08248	12.75059	14.71158	10.58473	13.92210
miR-200c	24 Hour	14.04283	14.31766	14.49006	14.54913	14.46255	15.62704
	72 Hour	13.09006	12.68363	15.03674	12.67218	12.74576	15.55015
	168 Hour	12.99181	13.09153	14.56104	12.99181	12.78577	15.02792

APPENDIX I

**Supplementary File I-1 (Continued): Experimental Ct Averages. (A)A549, (B) H460, (C) H1650, (D) PC9.**

**(B) H460**

		Untreated			+TGFβ		
miR-140	24 Hour	17.14272	17.91426	18.13599	17.05264	17.90481	17.99017
	72 Hour	17.21708	17.84024	17.46496	17.12854	16.66626	18.02826
	168 Hour	16.66319	17.54043	16.98263	16.64818	17.56977	17.08109
miR-141	24 Hour	17.08539	17.28380	17.33617	17.18618	17.62590	17.00420
	72 Hour	16.61845	17.04087	15.97914	17.28608	16.24639	16.81126
	168 Hour	16.26302	16.34669	15.99137	16.66824	17.00029	16.70879
miR-200c	24 Hour	10.67178	11.04102	11.36006	10.62387	11.23187	11.26765
	72 Hour	10.96402	11.11371	10.36812	11.05747	10.45827	11.33282
	168 Hour	10.77904	13.99327	10.41068	11.04071	11.77847	11.16143
		<b>+SB-431542</b>			<b>+TGFβ + SB-431542</b>		
miR-140	24 Hour	17.39966	18.23286	18.15083	17.61480	18.01347	18.38200
	72 Hour	16.91612	18.07499	17.15804	17.68611	18.51481	18.12220
	168 Hour	16.93595	17.08220	16.81208	16.85756	17.29420	17.47745
miR-141	24 Hour	17.10256	17.40165	17.29394	17.65773	17.38723	16.82007
	72 Hour	16.67177	17.03223	16.15025	17.48135	17.73611	16.58182
	168 Hour	16.83432	16.60688	16.06160	16.52186	16.67512	16.34198
miR-200c	24 Hour	10.75649	11.10807	11.17131	10.87258	11.09417	11.12668
	72 Hour	10.32638	11.28246	10.31851	11.51607	12.77857	11.01471
	168 Hour	13.58082	10.98377	10.31083	11.05021	11.20028	13.88309

APPENDIX I

**Supplementary File I-1 (Continued): Experimental Ct Averages. (A)A549, (B) H460, (C) H1650, (D) PC9.**

**(C) H1650**

		Untreated			+TGFβ		
miR-140	24 Hour	12.24568	12.01147	12.93231	12.28511	12.96206	12.49449
	72 Hour	12.17126	12.94157	12.64218	12.49287	13.47596	13.12842
	168 Hour	17.22546	17.23288	17.92211	17.46275	17.47145	17.98014
miR-141	24 Hour	7.839454	7.535492	7.558471	8.04034	7.626134	6.945391
	72 Hour	7.115704	6.608805	7.225541	7.719368	7.437265	7.523124
	168 Hour	11.69064	11.75101	11.83241	11.88982	11.90958	11.97695
miR-200c	24 Hour	4.654358	4.169437	5.087824	4.834063	5.230578	4.853105
	72 Hour	4.231399	4.793982	4.516056	4.626641	5.374649	5.112733
	168 Hour	5.979657	6.024038	6.170614	5.993081	6.253736	6.156914
		<b>+SB-431542</b>			<b>+TGFβ + SB-431542</b>		
miR-140	24 Hour	12.02541	13.26263	12.93686	12.56955	13.30433	12.94468
	72 Hour	12.13073	13.18402	12.97675	12.74410	13.90631	11.57144
	168 Hour	17.24517	17.57818	17.67087	17.44893	17.80485	17.78832
miR-141	24 Hour	7.658577	8.035284	7.288847	7.757186	8.216744	6.859854
	72 Hour	7.295649	7.448415	7.114004	7.415254	8.310852	6.352814
	168 Hour	11.48486	11.61927	11.82947	11.41379	11.91031	11.76493
miR-200c	24 Hour	4.553339	5.694854	5.120974	5.110865	5.906208	4.517555
	72 Hour	4.311621	4.661685	4.998656	4.919242	7.163925	3.526715
	168 Hour	5.897517	6.226531	6.095646	6.014628	6.505982	6.126934

APPENDIX I

**Supplementary File I-1 (Continued): Experimental Ct Averages. (A)A549, (B) H460, (C) H1650, (D) PC9.**

**(D) PC9**

		Untreated			+TGFβ		
miR-140	24 Hour	14.94061	13.26866	14.54584	14.57736	11.73476	13.76189
	72 Hour	12.83986	13.43117	13.88492	12.71534	13.55068	14.44901
	168 Hour	13.50625	13.77642	14.75037	13.84855	14.09694	14.88830
miR-141	24 Hour	7.121312	10.00169	9.931498	7.876611	8.188897	10.06823
	72 Hour	6.306454	3.402984	3.121106	6.319069	4.80151	5.335824
	168 Hour	5.817623	3.519702	5.124096	5.819985	4.690588	5.166902
miR-200c	24 Hour	5.756327	6.305108	6.344949	5.612942	5.945666	6.384396
	72 Hour	4.948423	4.166431	6.540284	4.255959	3.853093	7.538871
	168 Hour	4.483598	4.663599	6.590467	4.483084	4.430461	6.680311
		<b>+SB-431542</b>			<b>+TGFβ + SB-431542</b>		
miR-140	24 Hour	14.78079	13.46474	13.18096	14.64627	13.47323	13.75304
	72 Hour	12.70899	13.05903	13.79732	12.37238	13.11935	13.77495
	168 Hour	13.05962	14.00124	14.74730	13.65988	13.76325	14.75263
miR-141	24 Hour	8.433583	10.00693	8.825805	8.76599	10.44693	10.97337
	72 Hour	6.583571	3.124386	2.23386	6.249595	4.266571	6.207948
	168 Hour	6.500151	1.581450	5.662973	6.34292	3.582123	6.186862
miR-200c	24 Hour	6.06497	5.257848	5.868316	5.77605	6.038063	5.926589
	72 Hour	4.760397	3.741873	6.390911	4.907626	4.191823	6.659156
	168 Hour	4.517351	4.478639	6.310415	4.340795	4.377823	6.354835

## APPENDIX II: SUPPLEMENTARY FIGURES FOR CHAPTER 4

**Supplementary Table II-1: Interacting mRNA:miRNA genes (100) from the Feasible Solutions (FS) analysis.** The 100 probe IDs with the lowest probability (low Prob>F) as determined by the FS analysis. To identify targets that may have value in EGFR1 resistant tumors, the model sought mRNA with high expression in EGFR1-resistant NSCLC cells.

Probe ID	Interacting miRNA		Prob > F
213302_at	hsa.miR.135b	hsa.miR.616.4395525	2.14712E-05
204497_at	hsa.miR.210	hsa.miR.616.4395525	2.49071E-05
201002_s_at	hsa.miR.135b	hsa.miR.616.4395525	3.56988E-05
210139_s_at	hsa.miR.197.	hsa.miR.616.4395525	5.82491E-05
214830_at	hsa.miR.410	hsa.miR.616.4395525	8.11249E-05
208241_at	hsa.miR.135b	hsa.miR.616.4395525	8.31544E-05
218467_at	hsa.miR.200b	hsa.miR.628.5p.4395544	0.000132681
218970_s_at	hsa.miR.200b	hsa.miR.616.4395525	0.000168687
211505_s_at	hsa.miR.200b	hsa.miR.628.5p.4395544	0.000169371
203482_at	hsa.miR.200b	hsa.miR.616.4395525	0.000169684
212764_at	hsa.miR.518b	hsa.miR.125a.3p.4395310	0.000211397
58780_s_at	hsa.miR.873	hsa.miR.628.5p.4395544	0.000233999
208919_s_at	hsa.miR.30c	hsa.miR.616.4395525	0.000251931
201379_s_at	hsa.miR.141	hsa.miR.616.4395525	0.000320846
213262_at	hsa.miR.873	hsa.miR.636.4395199	0.000364971
210910_s_at	hsa.miR.205	hsa.miR.873.4395467	0.000398141
201778_s_at	hsa.miR.873	hsa.miR.616.4395525	0.000410072
37117_at	hsa.miR.197	hsa.miR.518f.4395499	0.000434778
219002_at	hsa.miR.873.43 95467	hsa.miR.636.4395199	0.000449861
219020_at	hsa.miR.758.43 95180	hsa.miR.616.4395525	0.000511882
204115_at	hsa.miR.873.43 95467	hsa.miR.636.4395199	0.000574862
213058_at	hsa.miR.873.43 95467	hsa.miR.30c.4373060	0.000638761
219395_at	hsa.miR.125a.5 p.4395309	hsa.miR.616.4395525	0.000662677
213798_s_at	hsa.miR.636.43 95199	hsa.miR.628.5p.4395544	0.000670364

APPENDIX II

**Supplementary Table II-1 (continued): Interacting mRNA:miRNA genes (100) from the Feasible Solutions (FS) analysis.**

<b>Probe ID</b>	<b>Interacting miRNA</b>		<b>Prob &gt; F</b>
219388_at	hsa.miR.200c.4 395411	hsa.miR.363.4378090	0.000675789
201565_s_at	hsa.miR.200c.4 395411	hsa.miR.363.4378090	0.000684861
209222_s_at	hsa.miR.200c.4 395411	hsa.miR.363.4378090	0.000752997
204243_at	hsa.miR.200b.4 395362	hsa.miR.410.4378093	0.000754944
219785_s_at	hsa.miR.135b.4 395372	hsa.miR.616.4395525	0.000762204
217744_s_at	hsa.miR.125a.5 p.4395309	hsa.miR.616.4395525	0.000856678
209225_x_at	hsa.miR.363.43 78090	hsa.miR.628.5p.4395544	0.000926545
219547_at	hsa.miR.200b.4 395362	hsa.miR.224.4395210	0.000932786
221704_s_at	hsa.miR.135b.4 395372	hsa.miR.873.4395467	0.001141837
205807_s_at	hsa.miR.224.43 95210	hsa.miR.628.5p.4395544	0.001186811
203551_s_at	hsa.miR.135b.4 395372	hsa.miR.616.4395525	0.001191469
201380_at	hsa.miR.873.43 95467	hsa.miR.616.4395525	0.001287701
218264_at	hsa.miR.628.5p .4395544	hsa.miR.616.4395525	0.001328277
207320_x_at	hsa.miR.410.43 78093	hsa.miR.628.5p.4395544	0.001400914
218720_x_at	hsa.miR.200b.4 395362	hsa.miR.197.4373102	0.001477025
207000_s_at	hsa.miR.200b.4 395362	hsa.miR.616.4395525	0.001484342
201608_s_at	hsa.miR.873.43 95467	hsa.miR.628.5p.4395544	0.001502097
201566_x_at	hsa.miR.200b.4 395362	hsa.miR.616.4395525	0.001534329
201589_at	hsa.miR.125a.5 p.4395309	hsa.miR.363.4378090	0.001595775

APPENDIX II

**Supplementary Table II-1 (continued): Interacting mRNA:miRNA genes (100) from the Feasible Solutions (FS) analysis.**

<b>Probe ID</b>	<b>Interacting miRNA</b>		<b>Prob &gt; F</b>
55065_at	hsa.miR.518f.4 395499	hsa.miR.616.4395525	0.001647671
200929_at	hsa.miR.636.43 95199	hsa.miR.628.5p.4395544	0.001668389
218365_s_at	hsa.miR.197.43 73102	hsa.miR.518b.4373246	0.001691602
213434_at	hsa.miR.628.5p .4395544	hsa.miR.758.4395180	0.001763671
210662_at	hsa.miR.873.43 95467	hsa.miR.616.4395525	0.001784274
201594_s_at	hsa.miR.205.43 73093	hsa.miR.363.4378090	0.001825064
208747_s_at	hsa.miR.210.43 73089	hsa.miR.363.4378090	0.001914552
211240_x_at	hsa.miR.363.43 78090	hsa.miR.616.4395525	0.002018453
203650_at	hsa.miR.873.43 95467	hsa.miR.636.4395199	0.002040117
210114_at	hsa.miR.873.43 95467	hsa.miR.616.4395525	0.0020832
205847_at	hsa.miR.125a.5 p.4395309	hsa.miR.616.4395525	0.002085028
215146_s_at	hsa.miR.873.43 95467	hsa.miR.636.4395199	0.002090153
219121_s_at	hsa.miR.363.43 78090	hsa.miR.616.4395525	0.002093259
216095_x_at	hsa.miR.30c.43 73060	hsa.miR.628.5p.4395544	0.002122563
219733_s_at	hsa.miR.221.43 73077	hsa.miR.616.4395525	0.002188182
200640_at	hsa.miR.205.43 73093	hsa.miR.628.5p.4395544	0.002204398
203884_s_at	hsa.miR.200b.4 395362	hsa.miR.636.4395199	0.002214892
201426_s_at	hsa.miR.125a.5 p.4395309	hsa.miR.616.4395525	0.00231613
218451_at	hsa.miR.141.43 73137	hsa.miR.139.5p.4395400	0.00236974

APPENDIX II

**Supplementary Table II-1 (continued): Interacting mRNA:miRNA genes (100) from the Feasible Solutions (FS) analysis.**

<b>Probe ID</b>	<b>Interacting miRNA</b>		<b>Prob &gt; F</b>
205980_s_at	hsa.miR.197.43 73102	hsa.miR.410.4378093	0.002425474
201839_s_at	hsa.miR.200b.4 395362	hsa.miR.628.5p.4395544	0.002481076
203287_at	hsa.miR.205.43 73093	hsa.miR.758.4395180	0.002584299
216641_s_at	hsa.miR.200c.4 395411	hsa.miR.363.4378090	0.002615599
213220_at	hsa.miR.200c.4 395411	hsa.miR.200b.4395362	0.002645648
217388_s_at	hsa.miR.200c.4 395411	hsa.miR.628.5p.4395544	0.002692429
208862_s_at	hsa.miR.873.43 95467	hsa.miR.616.4395525	0.002761436
208634_s_at	hsa.miR.200c.4 395411	hsa.miR.363.4378090	0.002775792
221646_s_at	hsa.miR.197.43 73102	hsa.miR.616.4395525	0.002913831
218526_s_at	hsa.miR.224.43 95210	hsa.miR.616.4395525	0.0029388
214136_at	hsa.miR.873.43 95467	hsa.miR.636.4395199	0.002991045
206343_s_at	hsa.miR.200b.4 395362	hsa.miR.197.4373102	0.002996291
202286_s_at	hsa.miR.224.43 95210	hsa.miR.628.5p.4395544	0.003004819
208319_s_at	hsa.miR.873.43 95467	hsa.miR.636.4395199	0.003172694
205667_at	hsa.miR.873.43 95467	hsa.miR.616.4395525	0.003211669
203883_s_at	hsa.miR.200b.4 395362	hsa.miR.30c.4373060	0.003239375
206907_at	hsa.miR.200c.4 395411	hsa.miR.616.4395525	0.003303832
207011_s_at	hsa.miR.200b.4 395362	hsa.miR.628.5p.4395544	0.003310737
214876_s_at	hsa.miR.200c.4 395411	hsa.miR.616.4395525	0.003649619

## APPENDIX II

**Supplementary Table II-1 (continued): Interacting mRNA:miRNA genes (100) from the Feasible Solutions (FS) analysis.**

Probe ID	Interacting miRNA		Prob > F
209110_s_at	hsa.miR.873.43 95467	hsa.miR.616.4395525	0.003676755
208009_s_at	hsa.miR.139.5p .4395400	hsa.miR.758.4395180	0.003697195
200982_s_at	hsa.miR.873.43 95467	hsa.miR.636.4395199	0.003710188
202087_s_at	hsa.miR.200b.4 395362	hsa.miR.758.4395180	0.003774459
204416_x_at	hsa.miR.410.43 78093	hsa.miR.628.5p.4395544	0.003811245
221825_at	hsa.miR.135b.4 395372	hsa.miR.139.5p.4395400	0.003949163
206015_s_at	hsa.miR.200c.4 395411	hsa.miR.363.4378090	0.00401435
209666_s_at	hsa.miR.197.43 73102	hsa.miR.518b.4373246	0.004126397
55872_at	hsa.miR.135b.4 395372	hsa.miR.628.5p.4395544	0.004136091
217717_s_at	hsa.miR.205.43 73093	hsa.miR.224.4395210	0.004187272
219157_at	hsa.miR.363.43 78090	hsa.miR.616.4395525	0.004209738
218823_s_at	hsa.miR.200b.4 395362	hsa.miR.410.4378093	0.004274431
205263_at	hsa.miR.200b.4 395362	hsa.miR.335.4373045	0.004329786
209188_x_at	hsa.miR.210.43 73089	hsa.miR.363.4378090	0.004396567
219338_s_at	hsa.miR.141.43 73137	hsa.miR.224.4395210	0.004645033
201131_s_at	hsa.miR.221.43 73077	hsa.miR.616.4395525	0.004743977
214724_at	hsa.miR.125a.3 p.4395310	hsa.miR.518f.4395499	0.004792734
203011_at	hsa.miR.125a.3 p.4395310	hsa.miR.518f.4395499	0.004849912
204148_s_at	hsa.miR.197.43 73102	hsa.miR.616.4395525	0.004863654

## APPENDIX II

**Supplementary Table II-2: Initial FS candidates that interact with EGFR.** Table members represent the 85 independent Ensembl IDs identified by the FS analysis.

SOURCE	GENE NAME
ARHGEF9	Cdc42 guanine nucleotide exchange factor (406) 9
DHRS4:DH RS4L2:DHR S4L1	dehydrogenase/reductase (SDR family) member 4, dehydrogenase/reductase (SDR family) member 4 like 2, dehydrogenase/reductase (SDR family) member 4 like 1
FANCF	Fanconi anemia, complementation group F
FBXO31	F-box protein 31
GNG11	guanine nucleotide binding protein (G protein), gamma 11
NRG1	neuregulin 1
NUBP2	nucleotide binding protein 2
PMP22	peripheral myelin protein 22
RAB11FIP2	RAB11 family interacting protein 2 (class I)
RNMTL1	RNA methyltransferase like 1
S100A3	S100 calcium binding protein A3
TFE3	transcription factor binding to IGHM enhancer 3
TNFSF9	tumor necrosis factor (ligand) superfamily, member 9
ACTA2	actin, alpha 2, smooth muscle, aorta
ADCY9	adenylate cyclase 9
ALDH1B1	aldehyde dehydrogenase 1 family, member B1
ANGEL2	angel homolog 2 (Drosophila)
ANXA6	annexin A6
ARHGEF40	Rho guanine nucleotide exchange factor (406) 40
ATP5G1	ATP synthase, H <sup>+</sup> transporting, mitochondrial Fo complex, subunit C1 (subunit 9)
BCCIP	BRCA2 and CDKN1A interacting protein
BRCC3	BRCA1/BRCA2-containing complex, subunit 3
C1QBP	complement component 1, q subcomponent binding protein
CAMK1	calcium/calmodulin-dependent protein kinase I

APPENDIX II

**Supplementary Table II-2 (continued): Initial FS candidates that interact with EGFR.**

Table members represent the 85 independent Ensembl IDs identified by the FS analysis.

<b>SOURCE</b>	<b>GENE NAME</b>
COX15	cytochrome c oxidase assembly homolog 15 (yeast)
CRTAP	cartilage associated protein
CTSL	cathepsin L
CUTC	cutC copper transporter
DARS2	aspartyl-tRNA synthetase 2, mitochondrial
DIP2C	disco-interacting protein 2 homolog C
DIXDC1	DIX domain containing 1
DOCK10	dedicator of cytokinesis 10
DPYSL3	dihydropyrimidinase-like 3
EGFR	epidermal growth factor receptor
EIF3A	eukaryotic translation initiation factor 3, subunit A
FASTKD1	FAST kinase domains 1
FBXL15	F-box and leucine-rich repeat protein 15
GLRX	glutaredoxin (thioltransferase)
HS1BP3	HCLS1 binding protein 3
HSPA12A	heat shock 70kDa protein 12A
ID2	inhibitor of DNA binding 2, dominant negative helix-loop-helix protein
IMPA1	inositol(myo)-1(or 4)-monophosphatase 1
INVS	Inversin
KCTD9	potassium channel tetramerization domain containing 9
KYNU	Kynureninase
LIG3	ligase III, DNA, ATP-dependent
MID1IP1	MID1 interacting protein 1
MTMR9	myotubularin related protein 9

APPENDIX II

**Supplementary Table II-2 (continued): Initial FS candidates that interact with EGFR.**

Table members represent the 85 independent Ensembl IDs identified by the FS analysis.

<b>SOURCE</b>	<b>GENE NAME</b>
PFAS	phosphoribosylformylglycinamide synthase
POMZP3	POM121 and ZP3 fusion
PPP3CC	protein phosphatase 3, catalytic subunit, gamma isozyme
PROCR	protein C receptor, endothelial
PWP1	PWP1 homolog, endonuclein
RANGRF	RAN guanine nucleotide release factor
RBM3	RNA binding motif (RNP1, RRM) protein 3
SACS	sacsin molecular chaperone
SMC1A	structural maintenance of chromosomes 1A
STX2	syntaxin 2
TNPO1	transportin 1
TTC28	tetratricopeptide repeat domain 28
TUBGCP2	tubulin, gamma complex associated protein 2
UIMC1	ubiquitin interaction motif containing 1
USP9X	ubiquitin specific peptidase 9, X-linked
VIM	Vimentin
VPS33B	vacuolar protein sorting 33 homolog B (yeast)
WRN	Werner syndrome, RecQ helicase-like
ZC3H14	zinc finger CCCH-type containing 14
ZEB1	zinc finger E-box binding homeobox 1
CHUK	conserved helix-loop-helix ubiquitous kinase
PBK	PDZ binding kinase
PTEN	phosphatase and tensin homolog

APPENDIX II

**Supplementary Table II-3: G1-X-G2 Analysis-Induced EGFR1 Resistance Network Members.** Table members were generated using the 85 independent Ensembl IDs identified by the FS analysis. Table members generated by the STRING analysis considering the scenario G1-X-G2 where G1 and G2 are from the original list of 85 Ensembl IDs of mRNA found to be upregulated in EGFR1 resistant NSCLC cells and X is any other node that connects them.

<b>SYMBOL</b>	<b>GENE NAME</b>	<b>TYPE</b>
ACACB	acetyl-CoA carboxylase beta	Induced
ACTA1	actin, alpha 1, skeletal muscle	Induced
ACTA2	actin, alpha 2, smooth muscle, aorta	Input
ADCY9	adenylate cyclase 9	Input
ADSS	adenylosuccinate synthase	Induced
AKT1	v-akt murine thymoma viral oncogene homolog 1	Induced
AKT2	v-akt murine thymoma viral oncogene homolog 2	Induced
ALDH1B1	aldehyde dehydrogenase 1 family, member B1	Input
ANGEL2	angel homolog 2 (Drosophila)	Input
ANXA6	annexin A6	Input
AP2A1	adaptor-related protein complex 2, alpha 1 subunit	Induced
APC	adenomatous polyposis coli	Induced
AR	androgen receptor	Induced
ARHGEF 40	Rho guanine nucleotide exchange factor (406) 40	Input
ARHGEF 9	Cdc42 guanine nucleotide exchange factor (406) 9	Input
ARRB2	arrestin, beta 2	Induced
ATM	ATM serine/threonine kinase	Induced
ATP5C1	ATP synthase, H <sup>+</sup> transporting, mitochondrial F1 complex, gamma polypeptide 1	Induced
ATP5G1	ATP synthase, H <sup>+</sup> transporting, mitochondrial Fo complex, subunit C1 (subunit 9)	Input
AURKA	aurora kinase A	Induced
BABAM1	BRISC and BRCA1 A complex member 1	Induced

**Supplementary Table II-3 (continued): G1-X-G2 Analysis-Induced EGFR1 Resistance Network Members.**

<b>SYMBOL</b>	<b>GENE NAME</b>	<b>TYPE</b>
BARD1	BRCA1 associated RING domain 1	Induced
BCCIP	BRCA2 and CDKN1A interacting protein	Input
BCL2	B-cell CLL/lymphoma 2	Induced
BIRC2	baculoviral IAP repeat containing 2	Induced
BIRC3	baculoviral IAP repeat containing 3	Induced
BLM	Bloom syndrome, RecQ helicase-like	Induced
BRCA1	breast cancer 1, early onset	Induced
BRCC3	BRCA1/BRCA2-containing complex, subunit 3	Input
BRE	brain and reproductive organ-expressed (TNFRSF1A modulator)	Induced
BTRC	beta-transducin repeat containing E3 ubiquitin protein ligase	Induced
C1QBP	complement component 1, q subcomponent binding protein	Input
CAD	carbamoyl-phosphate synthetase 2, aspartate transcarbamylase, and dihydroorotase	Induced
CALM1 CALM2	calmodulin 1 (phosphorylase kinase, delta), calmodulin 2 (phosphorylase kinase, delta)	Induced
CALM2	calmodulin 2 (phosphorylase kinase, delta)	Induced
CAMK1	calcium/calmodulin-dependent protein kinase I	Input
CAPZA1	capping protein (actin filament) muscle Z-line, alpha 1	Induced
CAPZB	capping protein (actin filament) muscle Z-line, beta	Induced
CASP8	caspase 8, apoptosis-related cysteine peptidase	Induced
CAV1	caveolin 1, caveolae protein, 22kDa	Induced
CBL	Cbl proto-oncogene, E3 ubiquitin protein ligase	Induced
CCND1	cyclin D1	Induced
CCT4	chaperonin containing TCP1, subunit 4 (delta)	Induced
CD2AP	CD2-associated protein	Induced

**Supplementary Table II-3 (continued): G1-X-G2 Analysis-Induced EGFR1 Resistance Network Members.**

<b>SYMBOL</b>	<b>GENE NAME</b>	<b>TYPE</b>
CDC37	cell division cycle 37	Induced
CDH1	cadherin 1, type 1	Induced
CDK1	cyclin-dependent kinase 1	Induced
CDK2	cyclin-dependent kinase 2	Induced
CDKN1A	cyclin-dependent kinase inhibitor 1A (p21, Cip1)	Induced
CDKN1B	cyclin-dependent kinase inhibitor 1B (p27, Kip1)	Induced
CFL1	cofilin 1 (non-muscle)	Induced
CHAF1A	chromatin assembly factor 1, subunit A (p150)	Induced
CHORDC1	cysteine and histidine-rich domain (CHORD) containing 1	Induced
CHUK	conserved helix-loop-helix ubiquitous kinase	Input
CKAP5	cytoskeleton associated protein 5	Induced
CNOT4	CCR4-NOT transcription complex, subunit 4	Induced
COPS5	COP9 signalosome subunit 5	Induced
COX15	cytochrome c oxidase assembly homolog 15 (yeast)	Input
CREBBP	CREB binding protein	Induced
CRTAP	cartilage associated protein	Input
CSE1L	CSE1 chromosome segregation 1-like (yeast)	Induced
CSNK2A1	casein kinase 2, alpha 1 polypeptide	Induced
CSNK2A2	casein kinase 2, alpha prime polypeptide	Induced
CTNNB1	catenin (cadherin-associated protein), beta 1, 88kDa	Induced
CTSL	cathepsin L	Input
CUL1	cullin 1	Induced

**Supplementary Table II-3 (continued): G1-X-G2 Analysis-Induced EGFR1 Resistance Network Members.**

<b>SYMBOL</b>	<b>GENE NAME</b>	<b>TYPE</b>
CUTC	cutC copper transporter	Input
DARS2	aspartyl-tRNA synthetase 2, mitochondrial	Input
DAZAP1	DAZ associated protein 1	Induced
DCP2	decapping mRNA 2	Induced
DHRS4 DHRS4L2 DHRS4L1	dehydrogenase/reductase (SDR family) member 4, dehydrogenase/reductase (SDR family) member 4 like 2, dehydrogenase/reductase (SDR family) member 4 like 1	Input
DIP2C	disco-interacting protein 2 homolog C	Input
DIXDC1	DIX domain containing 1	Input
DKC1	dyskeratosis congenita 1, dyskerin	Induced
DLG1	discs, large homolog 1 (Drosophila)	Induced
DOCK10	dedicator of cytokinesis 10	Input
DPYSL3	dihydropyrimidinase-like 3	Input
DVL2	dishevelled segment polarity protein 2	Induced
EEF1A1	eukaryotic translation elongation factor 1 alpha 1	Induced
EGF	epidermal growth factor	Induced
EGFR	epidermal growth factor receptor	Input
EIF2AK2	eukaryotic translation initiation factor 2-alpha kinase 2	Induced
EIF3A	eukaryotic translation initiation factor 3, subunit A	Input
EIF4A3	eukaryotic translation initiation factor 4A3	Induced
ELAVL1	ELAV like RNA binding protein 1	Induced
EP300	E1A binding protein p300	Induced
EPN1	epsin 1	Induced
EPS15	epidermal growth factor receptor pathway substrate 15	Induced

**Supplementary Table II-3 (continued): G1-X-G2 Analysis-Induced EGFR1 Resistance Network Members.**

<b>SYMBOL</b>	<b>GENE NAME</b>	<b>TYPE</b>
ERBB2	erb-b2 receptor tyrosine kinase 2	Induced
ERBB3	erb-b2 receptor tyrosine kinase 3	Induced
ERBB4	erb-b2 receptor tyrosine kinase 4	Induced
ERP44	endoplasmic reticulum protein 44	Induced
ESR1	estrogen receptor 1	Induced
EXOSC10	exosome component 10	Induced
FAM175A	family with sequence similarity 175, member A	Induced
FAM175B	family with sequence similarity 175, member B	Induced
FANCA	Fanconi anemia, complementation group A	Induced
FANCF	Fanconi anemia, complementation group F	Input
FANCG	Fanconi anemia, complementation group G	Induced
FANCM	Fanconi anemia, complementation group M	Induced
FASTKD1	FAST kinase domains 1	Input
FBXL15	F-box and leucine-rich repeat protein 15	Input
FBXO31	F-box protein 31	Input
FBXW7	F-box and WD repeat domain containing 7, E3 ubiquitin protein ligase	Induced
GAB1	GRB2-associated binding protein 1	Induced
GAPDH	glyceraldehyde-3-phosphate dehydrogenase	Induced
GDA	guanine deaminase	Induced
GLRX	glutaredoxin (thioltransferase)	Input
GNG11	guanine nucleotide binding protein (G protein), gamma 11	Input
GNS	glucosamine (N-acetyl)-6-sulfatase	Induced

**Supplementary Table II-3 (continued): G1-X-G2 Analysis-Induced EGFR1 Resistance Network Members.**

<b>SYMBOL</b>	<b>GENE NAME</b>	<b>TYPE</b>
GPHN	Gephyrin	Induced
GRSF1	G-rich RNA sequence binding factor 1	Induced
H2AFV	H2A histone family, member V	Induced
H2AFX	H2A histone family, member X	Induced
HDAC1	histone deacetylase 1	Induced
HECW2	HECT, C2 and WW domain containing E3 ubiquitin protein ligase 2	Induced
HES1	hes family bHLH transcription factor 1	Induced
HGS	hepatocyte growth factor-regulated tyrosine kinase substrate	Induced
HIST3H3	histone cluster 3, H3	Induced
HNRNPA1	heterogeneous nuclear ribonucleoprotein A1	Induced
HNRNPF	heterogeneous nuclear ribonucleoprotein F	Induced
HRAS	Harvey rat sarcoma viral oncogene homolog	Induced
HS1BP3	HCLS1 binding protein 3	Input
HSP90A A1	heat shock protein 90kDa alpha (cytosolic), class A member 1	Induced
HSP90A B1	heat shock protein 90kDa alpha (cytosolic), class B member 1	Induced
HSP90B 1	heat shock protein 90kDa beta (Grp94), member 1	Induced
HSPA12 A	heat shock 70kDa protein 12A	Input
HSPA4	heat shock 70kDa protein 4	Induced
HSPA5	heat shock 70kDa protein 5 (glucose-regulated protein, 78kDa)	Induced
HSPA9	heat shock 70kDa protein 9 (mortalin)	Induced
HSPB1	heat shock 27kDa protein 1	Induced
HTT	Huntingtin	Induced

**Supplementary Table II-3 (continued): G1-X-G2 Analysis-Induced EGFR1 Resistance Network Members.**

<b>SYMBOL</b>	<b>GENE NAME</b>	<b>TYPE</b>
HUWE1	HECT, UBA and WWE domain containing 1, E3 ubiquitin protein ligase	Induced
ID2	inhibitor of DNA binding 2, dominant negative helix-loop-helix protein	Input
IGBP1	immunoglobulin (CD79A) binding protein 1	Induced
IGF1R	insulin-like growth factor 1 receptor	Induced
IGFBP3	insulin-like growth factor binding protein 3	Induced
IKBKAP	inhibitor of kappa light polypeptide gene enhancer in B-cells, kinase complex-associated protein	Induced
IMPA1	inositol(myo)-1(or 4)-monophosphatase 1	Input
INVS	Inversin	Input
IQGAP1	IQ motif containing GTPase activating protein 1	Induced
IRS1	insulin receptor substrate 1	Induced
IRS2	insulin receptor substrate 2	Induced
IRS4	insulin receptor substrate 4	Induced
ITCH	itchy E3 ubiquitin protein ligase	Induced
KCTD9	potassium channel tetramerization domain containing 9	Input
KEAP1	kelch-like ECH-associated protein 1	Induced
KNG1	kininogen 1	Induced
KRAS	Kirsten rat sarcoma viral oncogene homolog	Induced
KYNU	Kynureninase	Input
LAMTOR3	late endosomal/lysosomal adaptor, MAPK and MTOR activator 3	Induced
LDHA	lactate dehydrogenase A	Induced
LDHAL6B	lactate dehydrogenase A-like 6B	Induced
LIG3	ligase III, DNA, ATP-dependent	Input

**Supplementary Table II-3 (continued): G1-X-G2 Analysis-Induced EGFR1 Resistance Network Members.**

<b>SYMBOL</b>	<b>GENE NAME</b>	<b>TYPE</b>
LIN7C	lin-7 homolog C (C. elegans)	Induced
LRRK2	leucine-rich repeat kinase 2	Induced
MAD2L1	MAD2 mitotic arrest deficient-like 1 (yeast)	Induced
MAGOH	mago homolog, exon junction complex core component	Induced
MAP1LC3A	microtubule-associated protein 1 light chain 3 alpha	Induced
MAP3K1	mitogen-activated protein kinase kinase kinase 1, E3 ubiquitin protein ligase	Induced
MAP3K3	mitogen-activated protein kinase kinase kinase 3	Induced
MAP3K5	mitogen-activated protein kinase kinase kinase 5	Induced
MAP4K4	mitogen-activated protein kinase kinase kinase kinase 4	Induced
MAPK1	mitogen-activated protein kinase 1	Induced
MAPT	microtubule-associated protein tau	Induced
MARK2	MAP/microtubule affinity-regulating kinase 2	Induced
MAVS	mitochondrial antiviral signaling protein	Induced
MDC1	mediator of DNA-damage checkpoint 1	Induced
MET	MET proto-oncogene, receptor tyrosine kinase	Induced
MID1IP1	MID1 interacting protein 1	Input
MINOS1	mitochondrial inner membrane organizing system 1	Induced
MLH3	mutL homolog 3	Induced
MRPS7	mitochondrial ribosomal protein S7	Induced
MSH2	mutS homolog 2	Induced
MSI1	musashi RNA-binding protein 1	Induced
MSI2	musashi RNA-binding protein 2	Induced

**Supplementary Table II-3 (continued): G1-X-G2 Analysis-Induced EGFR1 Resistance Network Members.**

<b>SYMBOL</b>	<b>GENE NAME</b>	<b>TYPE</b>
MTMR9	myotubularin related protein 9	Input
MTOR	mechanistic target of rapamycin (serine/threonine kinase)	Induced
MVP	major vault protein	Induced
MYH11	myosin, heavy chain 11, smooth muscle	Induced
MYH9	myosin, heavy chain 9, non-muscle	Induced
NAGK	N-acetylglucosamine kinase	Induced
NCOA3	nuclear receptor coactivator 3	Induced
NDFIP1	Nedd4 family interacting protein 1	Induced
NDFIP2	Nedd4 family interacting protein 2	Induced
NEDD4	neural precursor cell expressed, developmentally down-regulated 4, E3 ubiquitin protein ligase	Induced
NEDD8	neural precursor cell expressed, developmentally down-regulated 8	Induced
NMI	N-myc (and STAT) interactor	Induced
NOTCH1	notch 1	Induced
NOTCH2	notch 2	Induced
NOTCH3	notch 3	Induced
NR3C1	nuclear receptor subfamily 3, group C, member 1 (glucocorticoid receptor)	Induced
NRAS	neuroblastoma RAS viral (v-ras) oncogene homolog	Induced
NRG1	neuregulin 1	Input
NSF	N-ethylmaleimide-sensitive factor	Induced
NSMCE2	NSE2/MMS21 homolog, SMC5-SMC6 complex SUMO ligase	Induced
NUBP2	nucleotide binding protein 2	Input
NUDT21	nudix (nucleoside diphosphate linked moiety X)-type motif 21	Induced

APPENDIX II

**Supplementary Table II-3 (continued): G1-X-G2 Analysis-Induced EGFR1 Resistance Network Members.**

<b>SYMBOL</b>	<b>GENE NAME</b>	<b>TYPE</b>
NUP153	nucleoporin 153kDa	Induced
NXF1	nuclear RNA export factor 1	Induced
OAS3	2'-5'-oligoadenylate synthetase 3, 100kDa	Induced
PABPC4	poly(A) binding protein, cytoplasmic 4 (inducible form)	Induced
PARP1	poly (ADP-ribose) polymerase 1	Induced
PBK	PDZ binding kinase	Input
PCNA	proliferating cell nuclear antigen	Induced
PDGFRB	platelet-derived growth factor receptor, beta polypeptide	Induced
PEX19	peroxisomal biogenesis factor 19	Induced
PEX5	peroxisomal biogenesis factor 5	Induced
PFAS	phosphoribosylformylglycinamide synthase	Input
PIK3C2A	phosphatidylinositol-4-phosphate 3-kinase, catalytic subunit type 2 alpha	Induced
PIP5K1A	phosphatidylinositol-4-phosphate 5-kinase, type I, alpha	Induced
PLK1	polo-like kinase 1	Induced
PLK2	polo-like kinase 2	Induced
PLK3	polo-like kinase 3	Induced
PLK4	polo-like kinase 4	Induced
PLK5	polo-like kinase 5	Induced
PML	promyelocytic leukemia	Induced
PMP22	peripheral myelin protein 22	Input
POLB	polymerase (DNA directed), beta	Induced
POLR1C	polymerase (RNA) I polypeptide C, 30kDa	Induced

**Supplementary Table II-3 (continued): G1-X-G2 Analysis-Induced EGFR1 Resistance Network Members.**

<b>SYMBOL</b>	<b>GENE NAME</b>	<b>TYPE</b>
POMZP3	POM121 and ZP3 fusion	Input
PPP2CA	protein phosphatase 2, catalytic subunit, alpha isozyme	Induced
PPP3CA	protein phosphatase 3, catalytic subunit, alpha isozyme	Induced
PPP3CC	protein phosphatase 3, catalytic subunit, gamma isozyme	Input
PRDX1	peroxiredoxin 1	Induced
PRKACA	protein kinase, cAMP-dependent, catalytic, alpha	Induced
PRKCA	protein kinase C, alpha	Induced
PRKCB	protein kinase C, beta	Induced
PRKCD	protein kinase C, delta	Induced
PRKCZ	protein kinase C, zeta	Induced
PRKD1	protein kinase D1	Induced
PRKDC	protein kinase, DNA-activated, catalytic polypeptide	Induced
PROCR	protein C receptor, endothelial	Input
PSMA2	proteasome subunit alpha 2	Induced
PSMA3	proteasome subunit alpha 3	Induced
PSMA4	proteasome subunit alpha 4	Induced
PSMA7	proteasome subunit alpha 7	Induced
PSMA8	proteasome subunit alpha 8	Induced
PSMB1	proteasome subunit beta 1	Induced
PSMB2	proteasome subunit beta 2	Induced
PSMB4	proteasome subunit beta 4	Induced
PSMD4	proteasome 26S subunit, non-ATPase 4	Induced

**Supplementary Table II-3 (continued): G1-X-G2 Analysis-Induced EGFR1 Resistance Network Members.**

<b>SYMBOL</b>	<b>GENE NAME</b>	<b>TYPE</b>
PSMD6	proteasome 26S subunit, non-ATPase 6	Induced
PTEN	phosphatase and tensin homolog	Input
PTK2	protein tyrosine kinase 2	Induced
PTMA	prothymosin, alpha, prothymosin alpha-like	Induced
PTPN1	protein tyrosine phosphatase, non-receptor type 1	Induced
PTPN11	protein tyrosine phosphatase, non-receptor type 11	Induced
PWP1	PWP1 homolog, endonuclein	Input
RAB11A	RAB11A, member RAS oncogene family	Induced
RAB11B	RAB11B, member RAS oncogene family	Induced
RAB11FIP2	RAB11 family interacting protein 2 (class I)	Input
RAB7A	RAB7A, member RAS oncogene family	Induced
RAC3	ras-related C3 botulinum toxin substrate 3 (rho family, small GTP binding protein Rac3)	Induced
RAD23B	RAD23 homolog B, nucleotide excision repair protein	Induced
RAD51	RAD51 recombinase	Induced
RAF1	Raf-1 proto-oncogene, serine/threonine kinase	Induced
RAN	RAN, member RAS oncogene family	Induced
RANGRF	RAN guanine nucleotide release factor	Input
RASA1	RAS p21 protein activator (GTPase activating protein) 1	Induced
RBM3	RNA binding motif (RNP1, RRM) protein 3	Input
RBX1	ring-box 1, E3 ubiquitin protein ligase	Induced
RIPK1	receptor (TNFRSF)-interacting serine-threonine kinase 1	Induced
RNMTL1	RNA methyltransferase like 1	Input

**Supplementary Table II-3 (continued): G1-X-G2 Analysis-Induced EGFR1 Resistance Network Members.**

<b>SYMBOL</b>	<b>GENE NAME</b>	<b>TYPE</b>
RPL17	ribosomal protein L17	Induced
RPL5	ribosomal protein L5	Induced
RPS20	ribosomal protein S20	Induced
RPS23	ribosomal protein S23	Induced
RPS27A	ribosomal protein S27a	Induced
RPS7	ribosomal protein S7	Induced
RPTOR	regulatory associated protein of MTOR, complex 1	Induced
RQCD1	RCD1 required for cell differentiation1 homolog (S. pombe)	Induced
RUVBL1	RuvB-like AAA ATPase 1	Induced
S100A1	S100 calcium binding protein A1	Induced
S100A3	S100 calcium binding protein A3	Input
S100B	S100 calcium binding protein B	Induced
SACS	sacsin molecular chaperone	Input
SEC23A	Sec23 homolog A, COPII coat complex component	Induced
SGTA	small glutamine-rich tetratricopeptide repeat (407)-containing, alpha	Induced
SHARPIN	SHANK-associated RH domain interactor	Induced
SIN3A	SIN3 transcription regulator family member A	Induced
SIRT1	sirtuin 1	Induced
SKP1	S-phase kinase-associated protein 1	Induced
SLC25A3	solute carrier family 25 (mitochondrial carrier; phosphate carrier), member 3	Induced
SLC9A3R1	solute carrier family 9, subfamily A (NHE3, cation proton antiporter 3), member 3 regulator 1	Induced
SMAD1	SMAD family member 1	Induced

**Supplementary Table II-3 (continued): G1-X-G2 Analysis-Induced EGFR1 Resistance Network Members.**

<b>SYMBOL</b>	<b>GENE NAME</b>	<b>TYPE</b>
SMAD 2	SMAD family member 2	Induced
SMAD 3	SMAD family member 3	Induced
SMAD 4	SMAD family member 4	Induced
SMC1A	structural maintenance of chromosomes 1A	Input
SMS	spermine synthase	Induced
SMURF1	SMAD specific E3 ubiquitin protein ligase 1	Induced
SNCA	synuclein, alpha (non A4 component of amyloid precursor)	Induced
SNRPA	small nuclear ribonucleoprotein polypeptide A	Induced
SPTAN1	spectrin, alpha, non-erythrocytic 1	Induced
SRC	SRC proto-oncogene, non-receptor tyrosine kinase	Induced
SSU72	SSU72 homolog, RNA polymerase II CTD phosphatase	Induced
STAT5A	signal transducer and activator of transcription 5A	Induced
STUB1	STIP1 homology and U-box containing protein 1, E3 ubiquitin protein ligase	Induced
STX2	syntaxin 2	Input
SUMO1	small ubiquitin-like modifier 1	Induced
SUMO2	small ubiquitin-like modifier 2	Induced
SUMO3	small ubiquitin-like modifier 3	Induced
TCP1	t-complex 1	Induced
TERT	telomerase reverse transcriptase	Induced
TFE3	transcription factor binding to IGHM enhancer 3	Input
TJP1	tight junction protein 1	Induced
TLR4	toll-like receptor 4	Induced

**Supplementary Table II-3 (continued): G1-X-G2 Analysis-Induced EGFR1 Resistance Network Members.**

<b>SYMBOL</b>	<b>GENE NAME</b>	<b>TYPE</b>
TNFRSF1A	tumor necrosis factor receptor superfamily, member 1A	Induced
TNFSF9	tumor necrosis factor (ligand) superfamily, member 9	Input
TNPO1	transportin 1	Input
TOM1L1	target of myb1 like 1 membrane trafficking protein	Induced
TOMM40	translocase of outer mitochondrial membrane 40 homolog (yeast)	Induced
TOP2A	topoisomerase (DNA) II alpha	Induced
TOP2B	topoisomerase (DNA) II beta	Induced
TOP3B	topoisomerase (DNA) III beta	Induced
TP53	tumor protein p53	Induced
TP53BP1	tumor protein p53 binding protein 1	Induced
TPR	translocated promoter region, nuclear basket protein	Induced
TRAF1	TNF receptor-associated factor 1	Induced
TRAF2	TNF receptor-associated factor 2	Induced
TTC28	tetratricopeptide repeat domain 28	Input
TUBA1A	tubulin, alpha 1a	Induced
TUBA4A	tubulin, alpha 4a	Induced
TUBGCP2	tubulin, gamma complex associated protein 2	Input
TUBGCP4	tubulin, gamma complex associated protein 4	Induced
TXN	Thioredoxin	Induced
UBA52	ubiquitin A-52 residue ribosomal protein fusion product 1	Induced
UBB	ubiquitin B	Induced
UBC	ubiquitin C	Induced

**Supplementary Table II-3 (continued): G1-X-G2 Analysis-Induced EGFR1 Resistance Network Members.**

<b>SYMBOL</b>	<b>GENE NAME</b>	<b>TYPE</b>
UBE2D1	ubiquitin-conjugating enzyme E2D 1	Induced
UBE2D2	ubiquitin-conjugating enzyme E2D 2	Induced
UBE2I	ubiquitin-conjugating enzyme E2I	Induced
UBE2L3	ubiquitin-conjugating enzyme E2L 3	Induced
UBE2N	ubiquitin-conjugating enzyme E2N	Induced
UBE2V2	ubiquitin-conjugating enzyme E2 variant 2	Induced
UBL4A	ubiquitin-like 4A	Induced
UBQLN1	ubiquilin 1	Induced
UBQLN2	ubiquilin 2	Induced
UBQLN4	ubiquilin 4	Induced
UBQLNL	ubiquilin-like	Induced
UBR4	ubiquitin protein ligase E3 component n-recognin 4	Induced
UBR7	ubiquitin protein ligase E3 component n-recognin 7 (putative)	Induced
UBXN7	UBX domain protein 7	Induced
UCHL3	ubiquitin carboxyl-terminal esterase L3 (ubiquitin thiolesterase)	Induced
UIMC1	ubiquitin interaction motif containing 1	Input
USP10	ubiquitin specific peptidase 10	Induced
USP14	ubiquitin specific peptidase 14 (tRNA-guanine transglycosylase)	Induced
USP34	ubiquitin specific peptidase 34	Induced
USP39	ubiquitin specific peptidase 39	Induced
USP7	ubiquitin specific peptidase 7 (herpes virus-associated)	Induced
USP8	ubiquitin specific peptidase 8	Induced

**Supplementary Table II-3 (continued): G1-X-G2 Analysis-Induced EGFR1 Resistance Network Members.**

<b>SYMBOL</b>	<b>GENE NAME</b>	<b>TYPE</b>
USP9X	ubiquitin specific peptidase 9, X-linked	Input
UVRAG	UV radiation resistance associated	Induced
VIM	Vimentin	Input
VPS16	vacuolar protein sorting 16 homolog (S. cerevisiae)	Induced
VPS33B	vacuolar protein sorting 33 homolog B (yeast)	Input
WASL	Wiskott-Aldrich syndrome-like	Induced
WDHD1	WD repeat and HMG-box DNA binding protein 1	Induced
WDR48	WD repeat domain 48	Induced
WRN	Werner syndrome, RecQ helicase-like	Input
WWP1	WW domain containing E3 ubiquitin protein ligase 1	Induced
WWP2	WW domain containing E3 ubiquitin protein ligase 2	Induced
XIAP	X-linked inhibitor of apoptosis, E3 ubiquitin protein ligase	Induced
XRCC5	X-ray repair complementing defective repair in Chinese hamster cells 5 (double-strand-break rejoining)	Induced
XRCC6	X-ray repair complementing defective repair in Chinese hamster cells 6	Induced
YAP1	Yes-associated protein 1	Induced
YBX1	Y box binding protein 1	Induced
YEATS4	YEATS domain containing 4	Induced
YKT6	YKT6 v-SNARE homolog (S. cerevisiae)	Induced
YWHAB	tyrosine 3-monooxygenase/tryptophan 5-monooxygenase activation protein, beta	Induced
YWHAE	tyrosine 3-monooxygenase/tryptophan 5-monooxygenase activation protein, epsilon	Induced
YWHAH	tyrosine 3-monooxygenase/tryptophan 5-monooxygenase activation protein, eta	Induced

APPENDIX II

**Supplementary Table II-3 (continued): G1-X-G2 Analysis-Induced EGFR1 Resistance Network Members.**

<b>SYMBOL</b>	<b>GENE NAME</b>	<b>TYPE</b>
YWHAZ	tyrosine 3-monooxygenase/tryptophan 5-monooxygenase activation protein, zeta	Induced
ZC3H14	zinc finger CCCH-type containing 14	Input
ZEB1	zinc finger E-box binding homeobox 1	Input
ZYX	Zyxin	Induced

APPENDIX II

**Supplementary Table II-4: G1-X-G2 Analysis-Induced EGFR1 Resistance Network Members that interact with CK2 $\alpha$  or CK2 $\alpha'$  within one edge.** Table members were generated using the 85 independent Ensembl IDs identified by the FS analysis. Table members generated by the STRING analysis considering the scenario G1-X-G2 where G1 and G2 are from the original list of 85 Ensembl IDs of mRNA found to be upregulated in EGFR1 resistant NSCLC cells and X is any other node that connects them. Table members are from the complete network of 385 proteins that interact with CK2 $\alpha$  or CK2 $\alpha'$  within one edge.

SYMBOL	GENE NAME	TYPE
AKT1	v-akt murine thymoma viral oncogene homolog 1	Induced
APC	adenomatous polyposis coli	Induced
ARRB2	arrestin, beta 2	Induced
BRCA1	breast cancer 1, early onset	Induced
CALM1:CALM2	calmodulin 1 (phosphorylase kinase, delta), calmodulin 2 (phosphorylase kinase, delta)	Induced
CAV1	caveolin 1, caveolae protein, 22kDa	Induced
CDC37	cell division cycle 37	Induced
CDH1	cadherin 1, type 1	Induced
CDK1	cyclin-dependent kinase 1	Induced
CDKN1A	cyclin-dependent kinase inhibitor 1A (p21, Cip1)	Induced
CHUK	conserved helix-loop-helix ubiquitous kinase	Input
CREBBP	CREB binding protein	Induced
CSNK2A1	casein kinase 2, alpha 1 polypeptide	Induced
CSNK2A2	casein kinase 2, alpha prime polypeptide	Induced
CTNNB1	catenin (cadherin-associated protein), beta 1, 88kDa	Induced
DVL2	dishevelled segment polarity protein 2	Induced
H2AFX	H2A histone family, member X	Induced
HDAC1	histone deacetylase 1	Induced
HSP90AA1	heat shock protein 90kDa alpha (cytosolic), class A member 1	Induced

**Supplementary Table II-4 (continued): G1-X-G2 Analysis-Induced EGFR1 Resistance Network Members that interact with CK2 $\alpha$  or CK2 $\alpha'$  within one edge.** Table members were generated using the 85 independent Ensembl IDs identified by the FS analysis. Table members generated by the STRING analysis considering the scenario G1-X-G2 where G1 and G2 are from the original list of 85 Ensembl IDs of mRNA found to be upregulated in EGFR1 resistant NSCLC cells and X is any other node that connects them. Table members are from the complete network of 385 proteins that interact with CK2 $\alpha$  or CK2 $\alpha'$  within one edge.

<b>SYMBOL</b>	<b>GENE NAME</b>	<b>TYPE</b>
HSP90AB1	heat shock protein 90kDa alpha (cytosolic), class B member 1	Induced
HSP90B1	heat shock protein 90kDa beta (Grp94), member 1	Induced
HSPA4	heat shock 70kDa protein 4	Induced
IGFBP3	insulin-like growth factor binding protein 3	Induced
IRS1	insulin receptor substrate 1	Induced
ITCH	itchy E3 ubiquitin protein ligase	Induced
MAP1LC3A	microtubule-associated protein 1 light chain 3 alpha	Induced
MAPT	microtubule-associated protein tau	Induced
MYH9	myosin, heavy chain 9, non-muscle	Induced
PBK	PDZ binding kinase	Input
PML	promyelocytic leukemia	Induced
PRKDC	protein kinase, DNA-activated, catalytic polypeptide	Induced
PSMA3	proteasome subunit alpha 3	Induced
PSMA4	proteasome subunit alpha 4	Induced
PTEN	phosphatase and tensin homolog	Input
PTPN1	protein tyrosine phosphatase, non-receptor type 1	Induced
RPL5	ribosomal protein L5	Induced
SIN3A	SIN3 transcription regulator family member A	Induced
SIRT1	sirtuin 1	Induced
SNCA	synuclein, alpha (non A4 component of amyloid precursor)	Induced

**Supplementary Table II-4 (continued): G1-X-G2 Analysis-Induced EGFR1 Resistance Network Members that interact with CK2 $\alpha$  or CK2 $\alpha'$  within one edge.** Table members were generated using the 85 independent Ensembl IDs identified by the FS analysis. Table members generated by the STRING analysis considering the scenario G1-X-G2 where G1 and G2 are from the original list of 85 Ensembl IDs of mRNA found to be upregulated in EGFR1 resistant NSCLC cells and X is any other node that connects them. Table members are from the complete network of 385 proteins that interact with CK2 $\alpha$  or CK2 $\alpha'$  within one edge.

<b>SYMBOL</b>	<b>GENE NAME</b>	<b>TYPE</b>
SRC	SRC proto-oncogene, non-receptor tyrosine kinase	Induced
TOP2A	topoisomerase (DNA) II alpha	Induced
TOP2B	topoisomerase (DNA) II beta	Induced
TP53	tumor protein p53	Induced
UBC	ubiquitin C	Induced
WDR48	WD repeat domain 48	Induced
XRCC5	X-ray repair complementing defective repair in Chinese hamster cells 5 (double-strand-break rejoining)	Induced
XRCC6	X-ray repair complementing defective repair in Chinese hamster cells 6	Induced

**Supplementary Table II-5: G1-X-G2 Analysis-Induced EGFR1 Resistance Network Members that interact with CK2 $\alpha$  or CK2 $\alpha'$  within one or two edges.** Table members were generated using the 85 independent Ensembl IDs identified by the FS analysis. Table members generated by the STRING analysis considering the scenario G1-X-G2 where G1 and G2 are from the original list of 85 Ensembl IDs of mRNA found to be upregulated in EGFR1 resistant NSCLC cells and X is any other node that connects them. Table members are from the complete network of 385 proteins that interact with CK2 $\alpha$  or CK2 $\alpha'$  within one or two edges.

<b>SYMBOL</b>	<b>GENE NAME</b>	<b>TYPE</b>
ACACB	acetyl-CoA carboxylase beta	Induced
ACTA1	actin, alpha 1, skeletal muscle	Induced
ACTA2	actin, alpha 2, smooth muscle, aorta	Input
ADCY9	adenylate cyclase 9	Input
ADSS	adenylosuccinate synthase	Induced
AKT1	v-akt murine thymoma viral oncogene homolog 1	Induced
AKT2	v-akt murine thymoma viral oncogene homolog 2	Induced
ALDH1B1	aldehyde dehydrogenase 1 family, member B1	Input
ANGEL2	angel homolog 2 (Drosophila)	Input
ANXA6	annexin A6	Input
AP2A1	adaptor-related protein complex 2, alpha 1 subunit	Induced
APC	adenomatous polyposis coli	Induced
AR	androgen receptor	Induced
ARHGEF40	Rho guanine nucleotide exchange factor (406) 40	Input
ARRB2	arrestin, beta 2	Induced
ATM	ATM serine/threonine kinase	Induced
ATP5C1	ATP synthase, H <sup>+</sup> transporting, mitochondrial F1 complex, gamma polypeptide 1	Induced
ATP5G1	ATP synthase, H <sup>+</sup> transporting, mitochondrial Fo complex, subunit C1 (subunit 9)	Input
AURKA	aurora kinase A	Induced
BABAM1	BRISC and BRCA1 A complex member 1	Induced

**Supplementary Table II-5 (continued): G1-X-G2 Analysis-Induced EGFR1 Resistance Network Members that interact with CK2 $\alpha$  or CK2 $\alpha'$  within one or two edges.**

<b>SYMBOL</b>	<b>GENE NAME</b>	<b>TYPE</b>
BARD1	BRCA1 associated RING domain 1	Induced
BCCIP	BRCA2 and CDKN1A interacting protein	Input
BCL2	B-cell CLL/lymphoma 2	Induced
BIRC2	baculoviral IAP repeat containing 2	Induced
BIRC3	baculoviral IAP repeat containing 3	Induced
BLM	Bloom syndrome, RecQ helicase-like	Induced
BRCA1	breast cancer 1, early onset	Induced
BRCC3	BRCA1/BRCA2-containing complex, subunit 3	Input
BRE	brain and reproductive organ-expressed (TNFRSF1A modulator)	Induced
BTRC	beta-transducin repeat containing E3 ubiquitin protein ligase	Induced
C1QBP	complement component 1, q subcomponent binding protein	Input
CAD	carbamoyl-phosphate synthetase 2, aspartate transcarbamylase, and dihydroorotase	Induced
CALM1:C ALM2	calmodulin 1 (phosphorylase kinase, delta), calmodulin 2 (phosphorylase kinase, delta)	Induced
CALM2	calmodulin 2 (phosphorylase kinase, delta)	Induced
CAMK1	calcium/calmodulin-dependent protein kinase I	Input
CAPZA1	capping protein (actin filament) muscle Z-line, alpha 1	Induced
CAPZB	capping protein (actin filament) muscle Z-line, beta	Induced
CASP8	caspase 8, apoptosis-related cysteine peptidase	Induced
CAV1	caveolin 1, caveolae protein, 22kDa	Induced
CBL	Cbl proto-oncogene, E3 ubiquitin protein ligase	Induced
CCND1	cyclin D1	Induced

## APPENDIX II

**Supplementary Table II-5 (continued): G1-X-G2 Analysis-Induced EGFR1 Resistance Network Members that interact with CK2 $\alpha$  or CK2 $\alpha'$  within one or two edges.**

<b>SYMBOL</b>	<b>GENE NAME</b>	<b>TYPE</b>
CCT4	chaperonin containing TCP1, subunit 4 (delta)	Induced
CD2AP	CD2-associated protein	Induced
CDC37	cell division cycle 37	Induced
CDH1	cadherin 1, type 1	Induced
CDK1	cyclin-dependent kinase 1	Induced
CDK2	cyclin-dependent kinase 2	Induced
CDKN1A	cyclin-dependent kinase inhibitor 1A (p21, Cip1)	Induced
CDKN1B	cyclin-dependent kinase inhibitor 1B (p27, Kip1)	Induced
CFL1	cofilin 1 (non-muscle)	Induced
CHAF1A	chromatin assembly factor 1, subunit A (p150)	Induced
CHORDC1	cysteine and histidine-rich domain (CHORD) containing 1	Induced
CHUK	conserved helix-loop-helix ubiquitous kinase	Input
CKAP5	cytoskeleton associated protein 5	Induced
CNOT4	CCR4-NOT transcription complex, subunit 4	Induced
COPS5	COP9 signalosome subunit 5	Induced
COX15	cytochrome c oxidase assembly homolog 15 (yeast)	Input
CREBBP	CREB binding protein	Induced
CRTAP	cartilage associated protein	Input
CSE1L	CSE1 chromosome segregation 1-like (yeast)	Induced
CSNK2A1	casein kinase 2, alpha 1 polypeptide	Induced
CSNK2A2	casein kinase 2, alpha prime polypeptide	Induced

## APPENDIX II

**Supplementary Table II-5 (continued): G1-X-G2 Analysis-Induced EGFR1 Resistance Network Members that interact with CK2 $\alpha$  or CK2 $\alpha'$  within one or two edges.**

<b>SYMBOL</b>	<b>GENE NAME</b>	<b>TYPE</b>
CTNNB1	catenin (cadherin-associated protein), beta 1, 88kDa	Induced
CTSL	cathepsin L	Input
CUL1	cullin 1	Induced
CUTC	cutC copper transporter	Input
DARS2	aspartyl-tRNA synthetase 2, mitochondrial	Input
DAZAP1	DAZ associated protein 1	Induced
DCP2	decapping mRNA 2	Induced
DIP2C	disco-interacting protein 2 homolog C	Input
DIXDC1	DIX domain containing 1	Input
DKC1	dyskeratosis congenita 1, dyskerin	Induced
DLG1	discs, large homolog 1 (Drosophila)	Induced
DOCK10	dedicator of cytokinesis 10	Input
DPYSL3	dihydropyrimidinase-like 3	Input
DVL2	dishevelled segment polarity protein 2	Induced
EEF1A1	eukaryotic translation elongation factor 1 alpha 1	Induced
EGFR	epidermal growth factor receptor	Input
EIF2AK2	eukaryotic translation initiation factor 2-alpha kinase 2	Induced
EIF3A	eukaryotic translation initiation factor 3, subunit A	Input
EIF4A3	eukaryotic translation initiation factor 4A3	Induced
ELAVL1	ELAV like RNA binding protein 1	Induced
EP300	E1A binding protein p300	Induced

**Supplementary Table II-5 (continued): G1-X-G2 Analysis-Induced EGFR1 Resistance Network Members that interact with CK2 $\alpha$  or CK2 $\alpha'$  within one or two edges.**

<b>SYMBOL</b>	<b>GENE NAME</b>	<b>TYPE</b>
EPN1	epsin 1	Induced
EPS15	epidermal growth factor receptor pathway substrate 15	Induced
ERBB2	erb-b2 receptor tyrosine kinase 2	Induced
ERBB3	erb-b2 receptor tyrosine kinase 3	Induced
ERBB4	erb-b2 receptor tyrosine kinase 4	Induced
ERP44	endoplasmic reticulum protein 44	Induced
ESR1	estrogen receptor 1	Induced
EXOSC10	exosome component 10	Induced
FAM175A	family with sequence similarity 175, member A	Induced
FAM175B	family with sequence similarity 175, member B	Induced
FANCA	Fanconi anemia, complementation group A	Induced
FANCG	Fanconi anemia, complementation group G	Induced
FANCM	Fanconi anemia, complementation group M	Induced
FASTKD1	FAST kinase domains 1	Input
FBXL15	F-box and leucine-rich repeat protein 15	Input
FBXW7	F-box and WD repeat domain containing 7, E3 ubiquitin protein ligase	Induced
GAPDH	glyceraldehyde-3-phosphate dehydrogenase	Induced
GDA	guanine deaminase	Induced
GLRX	glutaredoxin (thioltransferase)	Input
GNS	glucosamine (N-acetyl)-6-sulfatase	Induced
GPHN	Gephyrin	Induced

APPENDIX II

**Supplementary Table II-5 (continued): G1-X-G2 Analysis-Induced EGFR1 Resistance Network Members that interact with CK2 $\alpha$  or CK2 $\alpha'$  within one or two edges.**

<b>SYMBOL</b>	<b>GENE NAME</b>	<b>TYPE</b>
GRSF1	G-rich RNA sequence binding factor 1	Induced
H2AFV	H2A histone family, member V	Induced
H2AFX	H2A histone family, member X	Induced
HDAC1	histone deacetylase 1	Induced
HECW2	HECT, C2 and WW domain containing E3 ubiquitin protein ligase 2	Induced
HES1	hes family bHLH transcription factor 1	Induced
HGS	hepatocyte growth factor-regulated tyrosine kinase substrate	Induced
HIST3H3	histone cluster 3, H3	Induced
HNRNPA1	heterogeneous nuclear ribonucleoprotein A1	Induced
HNRNPF	heterogeneous nuclear ribonucleoprotein F	Induced
HRAS	Harvey rat sarcoma viral oncogene homolog	Induced
HS1BP3	HCLS1 binding protein 3	Input
HSP90A A1	heat shock protein 90kDa alpha (cytosolic), class A member 1	Induced
HSP90A B1	heat shock protein 90kDa alpha (cytosolic), class B member 1	Induced
HSP90B 1	heat shock protein 90kDa beta (Grp94), member 1	Induced
HSPA12 A	heat shock 70kDa protein 12A	Input
HSPA4	heat shock 70kDa protein 4	Induced
HSPA5	heat shock 70kDa protein 5 (glucose-regulated protein, 78kDa)	Induced
HSPA9	heat shock 70kDa protein 9 (mortalin)	Induced
HSPB1	heat shock 27kDa protein 1	Induced

**Supplementary Table II-5 (continued): G1-X-G2 Analysis-Induced EGFR1 Resistance Network Members that interact with CK2 $\alpha$  or CK2 $\alpha'$  within one or two edges.**

<b>SYMBOL</b>	<b>GENE NAME</b>	<b>TYPE</b>
HTT	Huntingtin	Induced
HUWE1	HECT, UBA and WWE domain containing 1, E3 ubiquitin protein ligase	Induced
ID2	inhibitor of DNA binding 2, dominant negative helix-loop-helix protein	Input
IGBP1	immunoglobulin (CD79A) binding protein 1	Induced
IGF1R	insulin-like growth factor 1 receptor	Induced
IGFBP3	insulin-like growth factor binding protein 3	Induced
IKBKAP	inhibitor of kappa light polypeptide gene enhancer in B-cells, kinase complex-associated protein	Induced
IMPA1	inositol(myo)-1(or 4)-monophosphatase 1	Input
INVS	Inversin	Input
IQGAP1	IQ motif containing GTPase activating protein 1	Induced
IRS1	insulin receptor substrate 1	Induced
IRS2	insulin receptor substrate 2	Induced
IRS4	insulin receptor substrate 4	Induced
ITCH	itchy E3 ubiquitin protein ligase	Induced
KCTD9	potassium channel tetramerization domain containing 9	Input
KEAP1	kelch-like ECH-associated protein 1	Induced
KRAS	Kirsten rat sarcoma viral oncogene homolog	Induced
KYNU	Kynureninase	Input
LAMTOR3	late endosomal/lysosomal adaptor, MAPK and MTOR activator 3	Induced
LDHA	lactate dehydrogenase A	Induced
LIG3	ligase III, DNA, ATP-dependent	Input
LIN7C	lin-7 homolog C (C. elegans)	Induced
LRRK2	leucine-rich repeat kinase 2	Induced

**Supplementary Table II-5 (continued): G1-X-G2 Analysis-Induced EGFR1 Resistance Network Members that interact with CK2 $\alpha$  or CK2 $\alpha'$  within one or two edges.**

<b>SYMBOL</b>	<b>GENE NAME</b>	<b>TYPE</b>
MAD2L1	MAD2 mitotic arrest deficient-like 1 (yeast)	Induced
MAGOH	mago homolog, exon junction complex core component	Induced
MAP1LC3A	microtubule-associated protein 1 light chain 3 alpha	Induced
MAP3K1	mitogen-activated protein kinase kinase kinase 1, E3 ubiquitin protein ligase	Induced
MAP3K3	mitogen-activated protein kinase kinase kinase 3	Induced
MAP3K5	mitogen-activated protein kinase kinase kinase 5	Induced
MAP4K4	mitogen-activated protein kinase kinase kinase kinase 4	Induced
MAPK1	mitogen-activated protein kinase 1	Induced
MAPT	microtubule-associated protein tau	Induced
MARK2	MAP/microtubule affinity-regulating kinase 2	Induced
MAVS	mitochondrial antiviral signaling protein	Induced
MDC1	mediator of DNA-damage checkpoint 1	Induced
MET	MET proto-oncogene, receptor tyrosine kinase	Induced
MID1IP1	MID1 interacting protein 1	Input
MLH3	mutL homolog 3	Induced
MRPS7	mitochondrial ribosomal protein S7	Induced
MSH2	mutS homolog 2	Induced
MSI1	musashi RNA-binding protein 1	Induced
MSI2	musashi RNA-binding protein 2	Induced
MTMR9	myotubularin related protein 9	Input
MTOR	mechanistic target of rapamycin (serine/threonine kinase)	Induced
MVP	major vault protein	Induced
MYH11	myosin, heavy chain 11, smooth muscle	Induced

## APPENDIX II

**Supplementary Table II-5 (continued): G1-X-G2 Analysis-Induced EGFR1 Resistance Network Members that interact with CK2 $\alpha$  or CK2 $\alpha'$  within one or two edges.**

<b>SYMBOL</b>	<b>GENE NAME</b>	<b>TYPE</b>
MYH9	myosin, heavy chain 9, non-muscle	Induced
NAGK	N-acetylglucosamine kinase	Induced
NCOA3	nuclear receptor coactivator 3	Induced
NDFIP1	Nedd4 family interacting protein 1	Induced
NDFIP2	Nedd4 family interacting protein 2	Induced
NEDD4	neural precursor cell expressed, developmentally down-regulated 4, E3 ubiquitin protein ligase	Induced
NEDD8	neural precursor cell expressed, developmentally down-regulated 8	Induced
NMI	N-myc (and STAT) interactor	Induced
NOTCH1	notch 1	Induced
NOTCH2	notch 2	Induced
NOTCH3	notch 3	Induced
NR3C1	nuclear receptor subfamily 3, group C, member 1 (glucocorticoid receptor)	Induced
NRAS	neuroblastoma RAS viral (v-ras) oncogene homolog	Induced
NSF	N-ethylmaleimide-sensitive factor	Induced
NSMCE2	NSE2/MMS21 homolog, SMC5-SMC6 complex SUMO ligase	Induced
NUDT21	nudix (nucleoside diphosphate linked moiety X)-type motif 21	Induced
NUP153	nucleoporin 153kDa	Induced
NXF1	nuclear RNA export factor 1	Induced
OAS3	2'-5'-oligoadenylate synthetase 3, 100kDa	Induced
PABPC4	poly(A) binding protein, cytoplasmic 4 (inducible form)	Induced
PARP1	poly (ADP-ribose) polymerase 1	Induced
PBK	PDZ binding kinase	Input
PCNA	proliferating cell nuclear antigen	Induced

## APPENDIX II

**Supplementary Table II-5 (continued): G1-X-G2 Analysis-Induced EGFR1 Resistance Network Members that interact with CK2 $\alpha$  or CK2 $\alpha'$  within one or two edges.**

<b>SYMBOL</b>	<b>GENE NAME</b>	<b>TYPE</b>
PDGFRB	platelet-derived growth factor receptor, beta polypeptide	Induced
PEX19	peroxisomal biogenesis factor 19	Induced
PEX5	peroxisomal biogenesis factor 5	Induced
PFAS	phosphoribosylformylglycinamide synthase	Input
PIK3C2A	phosphatidylinositol-4-phosphate 3-kinase, catalytic subunit type 2 alpha	Induced
PIP5K1A	phosphatidylinositol-4-phosphate 5-kinase, type I, alpha	Induced
PLK1	polo-like kinase 1	Induced
PLK2	polo-like kinase 2	Induced
PLK3	polo-like kinase 3	Induced
PLK4	polo-like kinase 4	Induced
PML	promyelocytic leukemia	Induced
POLB	polymerase (DNA directed), beta	Induced
POLR1C	polymerase (RNA) I polypeptide C, 30kDa	Induced
POMZP3	POM121 and ZP3 fusion	Input
PPP2CA	protein phosphatase 2, catalytic subunit, alpha isozyme	Induced
PPP3CA	protein phosphatase 3, catalytic subunit, alpha isozyme	Induced
PPP3CC	protein phosphatase 3, catalytic subunit, gamma isozyme	Input
PRDX1	peroxiredoxin 1	Induced
PRKACA	protein kinase, cAMP-dependent, catalytic, alpha	Induced
PRKCA	protein kinase C, alpha	Induced
PRKCB	protein kinase C, beta	Induced
PRKCD	protein kinase C, delta	Induced
PRKCZ	protein kinase C, zeta	Induced
PRKD1	protein kinase D1	Induced

**Supplementary Table II-5 (continued): G1-X-G2 Analysis-Induced EGFR1 Resistance Network Members that interact with CK2 $\alpha$  or CK2 $\alpha'$  within one or two edges.**

<b>SYMBOL</b>	<b>GENE NAME</b>	<b>TYPE</b>
PRKDC	protein kinase, DNA-activated, catalytic polypeptide	Induced
PROCR	protein C receptor, endothelial	Input
PSMA2	proteasome subunit alpha 2	Induced
PSMA3	proteasome subunit alpha 3	Induced
PSMA4	proteasome subunit alpha 4	Induced
PSMA7	proteasome subunit alpha 7	Induced
PSMA8	proteasome subunit alpha 8	Induced
PSMB1	proteasome subunit beta 1	Induced
PSMB2	proteasome subunit beta 2	Induced
PSMB4	proteasome subunit beta 4	Induced
PSMD4	proteasome 26S subunit, non-ATPase 4	Induced
PSMD6	proteasome 26S subunit, non-ATPase 6	Induced
PTEN	phosphatase and tensin homolog	Input
PTK2	protein tyrosine kinase 2	Induced
PTMA	prothymosin, alpha, prothymosin alpha-like	Induced
PTPN1	protein tyrosine phosphatase, non-receptor type 1	Induced
PTPN11	protein tyrosine phosphatase, non-receptor type 11	Induced
PWP1	PWP1 homolog, endonuclein	Input
RAB11A	RAB11A, member RAS oncogene family	Induced
RAB11B	RAB11B, member RAS oncogene family	Induced
RAB7A	RAB7A, member RAS oncogene family	Induced
RAC3	ras-related C3 botulinum toxin substrate 3 (rho family, small GTP binding protein Rac3)	Induced
RAD23B	RAD23 homolog B, nucleotide excision repair protein	Induced
RAD51	RAD51 recombinase	Induced

## APPENDIX II

**Supplementary Table II-5 (continued): G1-X-G2 Analysis-Induced EGFR1 Resistance Network Members that interact with CK2 $\alpha$  or CK2 $\alpha'$  within one or two edges.**

<b>SYMBOL</b>	<b>GENE NAME</b>	<b>TYPE</b>
RAF1	Raf-1 proto-oncogene, serine/threonine kinase	Induced
RAN	RAN, member RAS oncogene family	Induced
RANGRF	RAN guanine nucleotide release factor	Input
RASA1	RAS p21 protein activator (GTPase activating protein) 1	Induced
RBM3	RNA binding motif (RNP1, RRM) protein 3	Input
RBX1	ring-box 1, E3 ubiquitin protein ligase	Induced
RIPK1	receptor (TNFRSF)-interacting serine-threonine kinase 1	Induced
RPL17	ribosomal protein L17	Induced
RPL5	ribosomal protein L5	Induced
RPS20	ribosomal protein S20	Induced
RPS23	ribosomal protein S23	Induced
RPS27A	ribosomal protein S27a	Induced
RPS7	ribosomal protein S7	Induced
RPTOR	regulatory associated protein of MTOR, complex 1	Induced
RQCD1	RCD1 required for cell differentiation1 homolog (S. pombe)	Induced
RUVBL1	RuvB-like AAA ATPase 1	Induced
S100A1	S100 calcium binding protein A1	Induced
S100B	S100 calcium binding protein B	Induced
SACS	sacsin molecular chaperone	Input
SEC23A	Sec23 homolog A, COPII coat complex component	Induced
SGTA	small glutamine-rich tetratricopeptide repeat (407)-containing, alpha	Induced
SHARPN	SHANK-associated RH domain interactor	Induced
SIN3A	SIN3 transcription regulator family member A	Induced
SIRT1	sirtuin 1	Induced

**Supplementary Table II-5 (continued): G1-X-G2 Analysis-Induced EGFR1 Resistance Network Members that interact with CK2 $\alpha$  or CK2 $\alpha'$  within one or two edges.**

<b>SYMBOL</b>	<b>GENE NAME</b>	<b>TYPE</b>
SKP1	S-phase kinase-associated protein 1	Induced
SLC25A3	solute carrier family 25 (mitochondrial carrier; phosphate carrier), member 3	Induced
SLC9A3R1	solute carrier family 9, subfamily A (NHE3, cation proton antiporter 3), member 3 regulator 1	Induced
SMAD1	SMAD family member 1	Induced
SMAD 2	SMAD family member 2	Induced
SMAD 3	SMAD family member 3	Induced
SMAD 4	SMAD family member 4	Induced
SMC1A	structural maintenance of chromosomes 1A	Input
SMS	spermine synthase	Induced
SMURF1	SMAD specific E3 ubiquitin protein ligase 1	Induced
SNCA	synuclein, alpha (non A4 component of amyloid precursor)	Induced
SNRPA	small nuclear ribonucleoprotein polypeptide A	Induced
SPTAN1	spectrin, alpha, non-erythrocytic 1	Induced
SRC	SRC proto-oncogene, non-receptor tyrosine kinase	Induced
SSU72	SSU72 homolog, RNA polymerase II CTD phosphatase	Induced
STAT5A	signal transducer and activator of transcription 5A	Induced
STUB1	STIP1 homology and U-box containing protein 1, E3 ubiquitin protein ligase	Induced
STX2	syntaxin 2	Input
SUMO1	small ubiquitin-like modifier 1	Induced
SUMO2	small ubiquitin-like modifier 2	Induced
SUMO3	small ubiquitin-like modifier 3	Induced
TCP1	t-complex 1	Induced
TERT	telomerase reverse transcriptase	Induced

APPENDIX II

**Supplementary Table II-5 (continued): G1-X-G2 Analysis-Induced EGFR1 Resistance Network Members that interact with CK2 $\alpha$  or CK2 $\alpha'$  within one or two edges.**

<b>SYMBOL</b>	<b>GENE NAME</b>	<b>TYPE</b>
TJP1	tight junction protein 1	Induced
TLR4	toll-like receptor 4	Induced
TNFRSF1A	tumor necrosis factor receptor superfamily, member 1A	Induced
TNPO1	transportin 1	Input
TOM1L1	target of myb1 like 1 membrane trafficking protein	Induced
TOMM40	translocase of outer mitochondrial membrane 40 homolog (yeast)	Induced
TOP2A	topoisomerase (DNA) II alpha	Induced
TOP2B	topoisomerase (DNA) II beta	Induced
TOP3B	topoisomerase (DNA) III beta	Induced
TP53	tumor protein p53	Induced
TP53BP1	tumor protein p53 binding protein 1	Induced
TPR	translocated promoter region, nuclear basket protein	Induced
TRAF1	TNF receptor-associated factor 1	Induced
TRAF2	TNF receptor-associated factor 2	Induced
TTC28	tetratricopeptide repeat domain 28	Input
TUBA1A	tubulin, alpha 1a	Induced
TUBA4A	tubulin, alpha 4a	Induced
TUBGCP2	tubulin, gamma complex associated protein 2	Input
TUBGCP4	tubulin, gamma complex associated protein 4	Induced
TXN	Thioredoxin	Induced
UBA52	ubiquitin A-52 residue ribosomal protein fusion product 1	Induced
UBB	ubiquitin B	Induced
UBC	ubiquitin C	Induced

## APPENDIX II

**Supplementary Table II-5 (continued): G1-X-G2 Analysis-Induced EGFR1 Resistance Network Members that interact with CK2 $\alpha$  or CK2 $\alpha'$  within one or two edges.**

<b>SYMBOL</b>	<b>GENE NAME</b>	<b>TYPE</b>
UBE2D1	ubiquitin-conjugating enzyme E2D 1	Induced
UBE2D2	ubiquitin-conjugating enzyme E2D 2	Induced
UBE2I	ubiquitin-conjugating enzyme E2I	Induced
UBE2L3	ubiquitin-conjugating enzyme E2L 3	Induced
UBE2N	ubiquitin-conjugating enzyme E2N	Induced
UBE2V2	ubiquitin-conjugating enzyme E2 variant 2	Induced
UBL4A	ubiquitin-like 4A	Induced
UBQLN1	ubiquilin 1	Induced
UBQLN2	ubiquilin 2	Induced
UBQLN4	ubiquilin 4	Induced
UBQLNL	ubiquilin-like	Induced
UBR4	ubiquitin protein ligase E3 component n-recognin 4	Induced
UBR7	ubiquitin protein ligase E3 component n-recognin 7 (putative)	Induced
UBXN7	UBX domain protein 7	Induced
UCHL3	ubiquitin carboxyl-terminal esterase L3 (ubiquitin thiolesterase)	Induced
UIMC1	ubiquitin interaction motif containing 1	Input
USP10	ubiquitin specific peptidase 10	Induced
USP14	ubiquitin specific peptidase 14 (tRNA-guanine transglycosylase)	Induced
USP34	ubiquitin specific peptidase 34	Induced
USP39	ubiquitin specific peptidase 39	Induced
USP7	ubiquitin specific peptidase 7 (herpes virus-associated)	Induced
USP8	ubiquitin specific peptidase 8	Induced
USP9X	ubiquitin specific peptidase 9, X-linked	Input
UVRAG	UV radiation resistance associated	Induced

## APPENDIX II

**Supplementary Table II-5 (continued): G1-X-G2 Analysis-Induced EGFR1 Resistance Network Members that interact with CK2 $\alpha$  or CK2 $\alpha'$  within one or two edges.**

<b>SYMBOL</b>	<b>GENE NAME</b>	<b>TYPE</b>
VIM	Vimentin	Input
VPS16	vacuolar protein sorting 16 homolog (S. cerevisiae)	Induced
VPS33B	vacuolar protein sorting 33 homolog B (yeast)	Input
WASL	Wiskott-Aldrich syndrome-like	Induced
WDHD1	WD repeat and HMG-box DNA binding protein 1	Induced
WDR48	WD repeat domain 48	Induced
WRN	Werner syndrome, RecQ helicase-like	Input
WWP1	WW domain containing E3 ubiquitin protein ligase 1	Induced
WWP2	WW domain containing E3 ubiquitin protein ligase 2	Induced
XIAP	X-linked inhibitor of apoptosis, E3 ubiquitin protein ligase	Induced
XRCC5	X-ray repair complementing defective repair in Chinese hamster cells 5 (double-strand-break rejoining)	Induced
XRCC6	X-ray repair complementing defective repair in Chinese hamster cells 6	Induced
YAP1	Yes-associated protein 1	Induced
YBX1	Y box binding protein 1	Induced
YEATS4	YEATS domain containing 4	Induced
YKT6	YKT6 v-SNARE homolog (S. cerevisiae)	Induced
YWHAB	tyrosine 3-monooxygenase/tryptophan 5-monooxygenase activation protein, beta	Induced
YWHAE	tyrosine 3-monooxygenase/tryptophan 5-monooxygenase activation protein, epsilon	Induced
YWHAH	tyrosine 3-monooxygenase/tryptophan 5-monooxygenase activation protein, eta	Induced
YWHAZ	tyrosine 3-monooxygenase/tryptophan 5-monooxygenase activation protein, zeta	Induced
ZC3H14	zinc finger CCCH-type containing 14	Input
ZEB1	zinc finger E-box binding homeobox 1	Input
ZYX	Zyxin	Induced

**Supplementary Table II-6: G1-X-G2 Analysis-Induced EGFR1 Resistance Network Members that do not interact with CK2 $\alpha$  or CK2 $\alpha'$ .** Table members were generated using the 85 independent Ensembl IDs identified by the FS analysis. Table members generated by the STRING analysis considering the scenario G1-X-G2 where G1 and G2 are from the original list of 85 Ensembl IDs of mRNA found to be upregulated in EGFR1 resistant NSCLC cells and X is any other node that connects them. Table members are from the complete network of 385 proteins that do not interact with CK2 $\alpha$  or CK2 $\alpha'$  within one or two edges.

<b>SYMBOL</b>	<b>GENE NAME</b>	<b>TYPE</b>
ARHGEF9	Cdc42 guanine nucleotide exchange factor 9	Input
DHRS4 DHRS4L2 DHRS4L1	dehydrogenase/reductase (SDR family) member 4, dehydrogenase/reductase (SDR family) member 4 like 2, dehydrogenase/reductase (SDR family) member 4 like 1	Input
EGF	epidermal growth factor	Induced
FANCF	Fanconi anemia, complementation group F	Input
FBXO31	F-box protein 31	Input
GAB1	GRB2-associated binding protein 1	Induced
GNG11	guanine nucleotide binding protein (G protein), gamma 11	Input
KNG1	kininogen 1	Induced
LDHAL6B	lactate dehydrogenase A-like 6B	Induced
MINOS1	mitochondrial inner membrane organizing system 1	Induced
NRG1	neuregulin 1	Input
NUBP2	nucleotide binding protein 2	Input
PLK5	polo-like kinase 5	Induced
PMP22	peripheral myelin protein 22	Input
RAB11FIP2	RAB11 family interacting protein 2 (class I)	Input
RNMTL1	RNA methyltransferase like 1	Input
S100A3	S100 calcium binding protein A3	Input
TFE3	transcription factor binding to IGHM enhancer 3	Input
TNFSF9	tumor necrosis factor (ligand) superfamily, member 9	Input

APPENDIX II

**Supplementary Table II-7: Induced network members sorted by putative collective activity of community members.** Communities of genes were determined from the induced network using the cluster\_walktrap function in igraph v1.0.1 (Described in Appendix IV) (385, 386).

**Supplementary Table II-7, Community #1: (Putative hallmark/functions: genomic instability, replicative immortality)**

<b>SYMBOL</b>	<b>GENE NAME</b>	<b>TYPE</b>
ATM	ATM serine/threonine kinase	Induced
BARD1	BRCA1 associated RING domain 1	Induced
BLM	Bloom syndrome, RecQ helicase-like	Induced
BRE	brain and reproductive organ-expressed (TNFRSF1A modulator)	Induced
CHAF1A	chromatin assembly factor 1, subunit A (p150)	Induced
DKC1	dyskeratosis congenita 1, dyskerin	Induced
FAM175A	family with sequence similarity 175, member A	Induced
FANCA	Fanconi anemia, complementation group A	Induced
FANCF	Fanconi anemia, complementation group F	Input
FANCG	Fanconi anemia, complementation group G	Induced
FANCM	Fanconi anemia, complementation group M	Induced
H2AFX	H2A histone family, member X	Induced
HES1	hes family bHLH transcription factor 1	Induced
LIG3	ligase III, DNA, ATP-dependent	Input
MDC1	mediator of DNA-damage checkpoint 1	Induced
MLH3	mutL homolog 3	Induced
MSH2	mutS homolog 2	Induced
NSMCE2	NSE2/MMS21 homolog, SMC5-SMC6 SUMO ligase	Induced
PARP1	poly (ADP-ribose) polymerase 1	Induced
PCNA	proliferating cell nuclear antigen	Induced
POLB	polymerase (DNA directed), beta	Induced

## APPENDIX II

**Supplementary Table II-7, Community #1 (continued): (Putative hallmark/functions: genomic instability, replicative immortality)**

<b>SYMBOL</b>	<b>GENE NAME</b>	<b>TYPE</b>
POLR1C	polymerase (RNA) I polypeptide C, 30kDa	Induced
PWP1	PWP1 homolog, endonuclein	Input
RAD51	RAD51 recombinase	Induced
SMC1A	structural maintenance of chromosomes 1A	Input
SUMO2	small ubiquitin-like modifier 2	Induced
SUMO3	small ubiquitin-like modifier 3	Induced
TOP2A	topoisomerase (DNA) II alpha	Induced
TOP2B	topoisomerase (DNA) II beta	Induced
TOP3B	topoisomerase (DNA) III beta	Induced
TP53BP1	tumor protein p53 binding protein 1	Induced
UIMC1	ubiquitin interaction motif containing 1	Input
WDHD1	WD repeat and HMG-box DNA binding protein 1	Induced
WRN	Werner syndrome, RecQ helicase-like	Input
XRCC5	X-ray repair complementing defective repair in Chinese hamster cells 5 (double-strand-break rejoining)	Induced
XRCC6	X-ray repair complementing defective repair in Chinese hamster cells 6	Induced

## APPENDIX II

**Supplementary Table II-7, Community #2: (Putative hallmark/functions: growth signal autonomy, invasion and metastasis, proteomic instability, EGFR/ RESISTANCE MECHANISMS)**

<b>SYMBOL</b>	<b>GENE NAME</b>	<b>TYPE</b>
DVL2	dishevelled segment polarity protein 2	Induced
EGF	epidermal growth factor	Induced
ERBB2	erb-b2 receptor tyrosine kinase 2	Induced
ERBB3	erb-b2 receptor tyrosine kinase 3	Induced
ERBB4	erb-b2 receptor tyrosine kinase 4	Induced
FBXL15	F-box and leucine-rich repeat protein 15	Input
ID2	inhibitor of DNA binding 2, dominant negative helix-loop-helix protein	Input
ITCH	itchy E3 ubiquitin protein ligase	Induced
KRAS	Kirsten rat sarcoma viral oncogene homolog	Induced
LIN7C	lin-7 homolog C (C. elegans)	Induced
NDFIP1	Nedd4 family interacting protein 1	Induced
NDFIP2	Nedd4 family interacting protein 2	Induced
NEDD4	neural precursor cell expressed, developmentally down-regulated 4, E3 ubiquitin protein ligase	Induced
NOTCH1	notch 1	Induced
NOTCH2	notch 2	Induced
NOTCH3	notch 3	Induced
NRAS	neuroblastoma RAS viral (v-ras) oncogene homolog	Induced
NRG1	neuregulin 1	Input
RASA1	RAS p21 protein activator (GTPase activating protein) 1	Induced
SMURF1	SMAD specific E3 ubiquitin protein ligase 1	Induced
WWP1	WW domain containing E3 ubiquitin protein ligase 1	Induced
WWP2	WW domain containing E3 ubiquitin protein ligase 2	Induced

APPENDIX II

**Supplementary Table II-7, Community #3: (Putative hallmark/functions: genomic instability, deregulating cellular energetics)**

<b>SYMBOL</b>	<b>GENE NAME</b>	<b>TYPE</b>
GRSF1	G-rich RNA sequence binding factor 1	Induced
MRPS7	mitochondrial ribosomal protein S7	Induced
RNMTL1	RNA methyltransferase like 1	Input
USP39	ubiquitin specific peptidase 39	Induced

**Supplementary Table II-7, Community #4: (Putative hallmark/functions: growth signal autonomy, proteomic instability, EGFR RESISTANCE MECHANISMS)**

<b>SYMBOL</b>	<b>GENE NAME</b>	<b>TYPE</b>
AKT1	v-akt murine thymoma viral oncogene homolog 1	Induced
AKT2	v-akt murine thymoma viral oncogene homolog 2	Induced
AP2A1	adaptor-related protein complex 2, alpha 1 subunit	Induced
APC	adenomatous polyposis coli	Induced
ARHGEF40	Rho guanine nucleotide exchange factor (406) 40	Input
ARRB2	arrestin, beta 2	Induced
BCL2	B-cell CLL/lymphoma 2	Induced
CAV1	caveolin 1, caveolae protein, 22kDa	Induced
CBL	Cbl proto-oncogene, E3 ubiquitin protein ligase	Induced
CDC37	cell division cycle 37	Induced
EGFR	epidermal growth factor receptor	Input
EIF2AK2	eukaryotic translation initiation factor 2-alpha kinase 2	Induced
EPN1	epsin 1	Induced
EPS15	epidermal growth factor receptor pathway substrate 15	Induced
GAB1	GRB2-associated binding protein 1	Induced

## APPENDIX II

**Supplementary Table II-7, Community #4 (continued): (Putative hallmark/functions: growth signal autonomy, proteomic instability, EGFR RESISTANCE MECHANISMS)**

<b>SYMBOL</b>	<b>GENE NAME</b>	<b>TYPE</b>
GAPDH	glyceraldehyde-3-phosphate dehydrogenase	Induced
GLRX	glutaredoxin (thioltransferase)	Input
HGS	hepatocyte growth factor-regulated tyrosine kinase substrate	Induced
HRAS	Harvey rat sarcoma viral oncogene homolog	Induced
HSP90AA1	heat shock protein 90kDa alpha (cytosolic), class A member 1	Induced
HSP90AB1	heat shock protein 90kDa alpha (cytosolic), class B member 1	Induced
HSP90B1	heat shock protein 90kDa beta (Grp94), member 1	Induced
HSPA12A	heat shock 70kDa protein 12A	Input
HSPA4	heat shock 70kDa protein 4	Induced
HSPA5	heat shock 70kDa protein 5 (glucose-regulated protein, 78kDa)	Induced
HSPB1	heat shock 27kDa protein 1	Induced
HTT	Huntingtin	Induced
IGF1R	insulin-like growth factor 1 receptor	Induced
IRS1	insulin receptor substrate 1	Induced
IRS2	insulin receptor substrate 2	Induced
IRS4	insulin receptor substrate 4	Induced
KCTD9	potassium channel tetramerization domain containing 9	Input
LRRK2	leucine-rich repeat kinase 2	Induced
MAP1LC3A	microtubule-associated protein 1 light chain 3 alpha	Induced
MAP3K3	mitogen-activated protein kinase kinase kinase 3	Induced
MAP3K5	mitogen-activated protein kinase kinase kinase 5	Induced
MAPK1	mitogen-activated protein kinase 1	Induced
MAPT	microtubule-associated protein tau	Induced
MARK2	MAP/microtubule affinity-regulating kinase 2	Induced

## APPENDIX II

**Supplementary Table II-7, Community #4 (continued): (Putative hallmark/functions: growth signal autonomy, proteomic instability, EGFR RESISTANCE MECHANISMS)**

<b>SYMBOL</b>	<b>GENE NAME</b>	<b>TYPE</b>
MET	MET proto-oncogene, receptor tyrosine kinase	Induced
MTOR	mechanistic target of rapamycin (serine/threonine kinase)	Induced
MVP	major vault protein	Induced
PDGFRB	platelet-derived growth factor receptor, beta polypeptide	Induced
PRKACA	protein kinase, cAMP-dependent, catalytic, alpha	Induced
PRKCA	protein kinase C, alpha	Induced
PRKCB	protein kinase C, beta	Induced
PRKCD	protein kinase C, delta	Induced
PRKCZ	protein kinase C, zeta	Induced
PRKD1	protein kinase D1	Induced
PTK2	protein tyrosine kinase 2	Induced
PTPN1	protein tyrosine phosphatase, non-receptor type 1	Induced
PTPN11	protein tyrosine phosphatase, non-receptor type 11	Induced
RAF1	Raf-1 proto-oncogene, serine/threonine kinase	Induced
RPTOR	regulatory associated protein of MTOR, complex 1	Induced
SNCA	synuclein, $\alpha$ (non A4 component of amyloid precursor)	Induced
SRC	SRC proto-oncogene, non-receptor tyrosine kinase	Induced
STAT5A	signal transducer and activator of transcription 5A	Induced
STUB1	STIP1 homology and U-box containing protein 1, E3 ubiquitin ligase	Induced
TTC28	tetratricopeptide repeat domain 28	Input
TUBA1A	tubulin, alpha 1a	Induced
TUBA4A	tubulin, alpha 4a	Induced
USP8	ubiquitin specific peptidase 8	Induced
YAP1	Yes-associated protein 1	Induced
YWHAB	tyrosine 3-monooxygenase/tryptophan 5-monooxygenase activation protein, beta	Induced

APPENDIX II

**Supplementary Table II-7, Community #4 (continued): (Putative hallmark/functions: growth signal autonomy, proteomic instability, EGFR RESISTANCE MECHANISMS)**

YWHAE	tyrosine 3-monooxygenase/tryptophan 5-monooxygenase activation protein, epsilon	Induced
YWHAH	tyrosine 3-monooxygenase/tryptophan 5-monooxygenase activation protein, eta	Induced
YWHAZ	tyrosine 3-monooxygenase/tryptophan 5-monooxygenase activation protein, zeta	Induced

**Supplementary Table II-7, Community #5: (Putative hallmark/functions: invasion and metastasis, proteomic instability, replicative immortality)**

<b>SYMBOL</b>	<b>GENE NAME</b>	<b>TYPE</b>
ACTA1	actin, alpha 1, skeletal muscle	Induced
ACTA2	actin, alpha 2, smooth muscle, aorta	Input
ADSS	adenylosuccinate synthase	Induced
CALM1 CALM2	calmodulin 1 (phosphorylase kinase, delta), calmodulin 2 (phosphorylase kinase, delta)	Induced
CALM2	calmodulin 2 (phosphorylase kinase, delta)	Induced
CAMK1	calcium/calmodulin-dependent protein kinase I	Input
CAPZA1	capping protein (actin filament) muscle Z-line, alpha 1	Induced
CAPZB	capping protein (actin filament) muscle Z-line, beta	Induced
CD2AP	CD2-associated protein	Induced
CFL1	cofilin 1 (non-muscle)	Induced
DLG1	discs, large homolog 1 (Drosophila)	Induced
EEF1A1	eukaryotic translation elongation factor 1 alpha 1	Induced
EIF3A	eukaryotic translation initiation factor 3, subunit A	Input
ELAVL1	ELAV like RNA binding protein 1	Induced
H2AFV	H2A histone family, member V	Induced
HECW2	HECT, C2 and WW domain containing E3 ubiquitin protein ligase 2	Induced

## APPENDIX II

**Supplementary Table II-7, Community #5 (continued): (Putative hallmark/functions: invasion and metastasis, proteomic instability, replicative immortality)**

<b>SYMBOL</b>	<b>GENE NAME</b>	<b>TYPE</b>
HNRNPA1	heterogeneous nuclear ribonucleoprotein A1	Induced
HNRNPF	heterogeneous nuclear ribonucleoprotein F	Induced
HSPA9	heat shock 70kDa protein 9 (mortalin)	Induced
IQGAP1	IQ motif containing GTPase activating protein 1	Induced
MYH11	myosin, heavy chain 11, smooth muscle	Induced
MYH9	myosin, heavy chain 9, non-muscle	Induced
NUDT21	nudix (nucleoside diphosphate linked moiety X)-type motif 21	Induced
PIK3C2A	phosphatidylinositol-4-phosphate 3-kinase, catalytic subunit type 2 alpha	Induced
PRDX1	peroxiredoxin 1	Induced
SGTA	small glutamine-rich tetratricopeptide repeat-containing, alpha	Induced
SLC25A3	solute carrier family 25 (mitochondrial carrier; phosphate carrier), member 3	Induced
SPTAN1	spectrin, alpha, non-erythrocytic 1	Induced
SSU72	SSU72 homolog, RNA polymerase II CTD phosphatase	Induced
TJP1	tight junction protein 1	Induced
TXN	Thioredoxin	Induced
UBC	ubiquitin C	Induced
VIM	Vimentin	Input
WASL	Wiskott-Aldrich syndrome-like	Induced
WDR48	WD repeat domain 48	Induced
YBX1	Y box binding protein 1	Induced
YEATS4	YEATS domain containing 4	Induced

APPENDIX II

**Supplementary Table II-7, Community #6: (Putative hallmark/functions: invasion and metastasis, growth and proliferation, cytoskeletal requirements)**

<b>SYMBOL</b>	<b>GENE NAME</b>	<b>TYPE</b>
C1QBP	complement component 1, q subcomponent binding protein	Input
CKAP5	cytoskeleton associated protein 5	Induced
MAD2L1	MAD2 mitotic arrest deficient-like 1 (yeast)	Induced
MINOS1	mitochondrial inner membrane organizing system 1	Induced
PLK2	polo-like kinase 2	Induced
PLK3	polo-like kinase 3	Induced
PLK4	polo-like kinase 4	Induced
PLK5	polo-like kinase 5	Induced
TOMM40	translocase of outer mitochondrial membrane 40 homolog (yeast)	Induced
TUBGCP2	tubulin, gamma complex associated protein 2	Input
TUBGCP4	tubulin, gamma complex associated protein 4	Induced

**Supplementary Table II-7, Community #7: (Putative hallmark/functions: evasion of growth suppressors, proteomic instability, evasion of apoptosis)**

<b>SYMBOL</b>	<b>GENE NAME</b>	<b>TYPE</b>
ACACB	acetyl-CoA carboxylase beta	Induced
BABAM1	BRISC and BRCA1 A complex member 1	Induced
BRCC3	BRCA1/BRCA2-containing complex, subunit 3	Input
CAD	carbamoyl-phosphate synthetase 2, aspartate transcarbamylase, and dihydroorotase	Induced
CCT4	chaperonin containing TCP1, subunit 4 (delta)	Induced
COPS5	COP9 signalosome subunit 5	Induced
CUL1	cullin 1	Induced
DPYSL3	dihydropyrimidinase-like 3	Input

## APPENDIX II

**Supplementary Table II-7, Community #7 (continued): (Putative hallmark/functions: evasion of growth suppressors, proteomic instability, evasion of apoptosis)**

<b>SYMBOL</b>	<b>GENE NAME</b>	<b>TYPE</b>
ERP44	endoplasmic reticulum protein 44	Induced
FAM175B	family with sequence similarity 175, member B	Induced
HUWE1	HECT, UBA and WWE domain containing 1, E3 ubiquitin protein ligase	Induced
IGBP1	immunoglobulin (CD79A) binding protein 1	Induced
IKBKAP	inhibitor of kappa light polypeptide gene enhancer in B-cells, kinase complex-associated protein	Induced
NEDD8	neural precursor cell expressed, developmentally down-regulated 8	Induced
NUBP2	nucleotide binding protein 2	Input
OAS3	2'-5'-oligoadenylate synthetase 3, 100kDa	Induced
PABPC4	poly(A) binding protein, cytoplasmic 4 (inducible form)	Induced
PFAS	phosphoribosylformylglycinamide synthase	Input
PLK1	polo-like kinase 1	Induced
PPP2CA	protein phosphatase 2, catalytic subunit, alpha isozyme	Induced
PSMD4	proteasome 26S subunit, non-ATPase 4	Induced
RAD23B	RAD23 homolog B, nucleotide excision repair protein	Induced
RPL17	ribosomal protein L17	Induced
RPL5	ribosomal protein L5	Induced
RPS20	ribosomal protein S20	Induced
RPS23	ribosomal protein S23	Induced
RPS27A	ribosomal protein S27a	Induced
RPS7	ribosomal protein S7	Induced
SEC23A	Sec23 homolog A, COPII coat complex component	Induced
SIN3A	SIN3 transcription regulator family member A	Induced
TCP1	t-complex 1	Induced
UBA52	ubiquitin A-52 residue ribosomal protein fusion product 1	Induced

APPENDIX II

**Supplementary Table II-7, Community #7 (continued): (Putative hallmark/functions: evasion of growth suppressors, proteomic instability, evasion of apoptosis)**

<b>SYMBOL</b>	<b>GENE NAME</b>	<b>TYPE</b>
UBB	ubiquitin B	Induced
UBE2D1	ubiquitin-conjugating enzyme E2D 1	Induced
UBE2D2	ubiquitin-conjugating enzyme E2D 2	Induced
UBE2L3	ubiquitin-conjugating enzyme E2L 3	Induced
UBE2V2	ubiquitin-conjugating enzyme E2 variant 2	Induced
UBL4A	ubiquitin-like 4A	Induced
UBQLN1	ubiquilin 1	Induced
UBQLN2	ubiquilin 2	Induced
UBQLN4	ubiquilin 4	Induced
UBQLNL	ubiquilin-like	Induced
UBR4	ubiquitin protein ligase E3 component n-recognin 4	Induced
UBXN7	UBX domain protein 7	Induced
UCHL3	ubiquitin carboxyl-terminal esterase L3 (ubiquitin thiolesterase)	Induced
USP10	ubiquitin specific peptidase 10	Induced
USP14	ubiquitin specific peptidase 14 (tRNA-guanine transglycosylase)	Induced
USP34	ubiquitin specific peptidase 34	Induced
USP7	ubiquitin specific peptidase 7 (herpes virus-associated)	Induced
USP9X	ubiquitin specific peptidase 9, X-linked	Input
ZYX	Zyxin	Induced

APPENDIX II

**Supplementary Table II-7, Community #8: (Putative hallmark/functions: tumor promoting inflammation, evasion of apoptosis)**

<b>SYMBOL</b>	<b>GENE NAME</b>	<b>TYPE</b>
BIRC2	baculoviral IAP repeat containing 2	Induced
BIRC3	baculoviral IAP repeat containing 3	Induced
CASP8	caspase 8, apoptosis-related cysteine peptidase	Induced
MAP3K1	mitogen-activated protein kinase kinase kinase 1, E3 ubiquitin protein ligase	Induced
MAP4K4	mitogen-activated protein kinase kinase kinase kinase 4	Induced
MAVS	mitochondrial antiviral signaling protein	Induced
RIPK1	receptor (TNFRSF)-interacting serine-threonine kinase 1	Induced
SHARPIN	SHANK-associated RH domain interactor	Induced
TLR4	toll-like receptor 4	Induced
TNFRSF1A	tumor necrosis factor receptor superfamily, member 1A	Induced
TNFSF9	tumor necrosis factor (ligand) superfamily, member 9	Input
TRAF1	TNF receptor-associated factor 1	Induced
TRAF2	TNF receptor-associated factor 2	Induced
UBE2N	ubiquitin-conjugating enzyme E2N	Induced
XIAP	X-linked inhibitor of apoptosis, E3 ubiquitin protein ligase	Induced

## APPENDIX II

**Supplementary Table II-7, Community #9: (Putative hallmark/functions: proteomic instability, evasion of apoptosis)**

<b>SYMBOL</b>	<b>GENE NAME</b>	<b>TYPE</b>
CNOT4	CCR4-NOT transcription complex, subunit 4	Induced
NSF	N-ethylmaleimide-sensitive factor	Induced
PSMA2	proteasome subunit alpha 2	Induced
PSMA3	proteasome subunit alpha 3	Induced
PSMA4	proteasome subunit alpha 4	Induced
PSMA7	proteasome subunit alpha 7	Induced
PSMA8	proteasome subunit alpha 8	Induced
PSMB1	proteasome subunit beta 1	Induced
PSMB2	proteasome subunit beta 2	Induced
PSMB4	proteasome subunit beta 4	Induced
PSMD6	proteasome 26S subunit, non-ATPase 6	Induced
RQCD1	RCD1 required for cell differentiation1 homolog (S. pombe)	Induced
SACS	sacsin molecular chaperone	Input

APPENDIX II

**Supplementary Table II-7, Community #10: (Putative hallmark/functions: genomic instability)**

<b>SYMBOL</b>	<b>GENE NAME</b>	<b>TYPE</b>
EIF4A3	eukaryotic translation initiation factor 4A3	Induced
EXOSC10	exosome component 10	Induced
MAGOH	mago homolog, exon junction complex core component	Induced
NUP153	nucleoporin 153kDa	Induced
NXF1	nuclear RNA export factor 1	Induced
RAN	RAN, member RAS oncogene family	Induced
RANGRF	RAN guanine nucleotide release factor	Input
RBM3	RNA binding motif (RNP1, RRM) protein 3	Input
SNRPA	small nuclear ribonucleoprotein polypeptide A	Induced
TNPO1	transportin 1	Input
TPR	translocated promoter region, nuclear basket protein	Induced

**Supplementary Table II-7, Community #11: (Putative hallmark/functions: evasion of growth suppressors, evasion of apoptosis)**

<b>SYMBOL</b>	<b>GENE NAME</b>	<b>TYPE</b>
ANXA6	annexin A6	Input
IMPA1	inositol(myo)-1(or 4)-monophosphatase 1	Input
S100B	S100 calcium binding protein B	Induced

APPENDIX II

**Supplementary Table II-7, Community #12: (Putative hallmark/functions: growth signal autonomy, evasion of growth suppressors)**

<b>SYMBOL</b>	<b>GENE NAME</b>	<b>TYPE</b>
PIP5K1A	phosphatidylinositol-4-phosphate 5-kinase, type I, alpha	Induced
PPP3CA	protein phosphatase 3, catalytic subunit, alpha isozyme	Induced
PPP3CC	protein phosphatase 3, catalytic subunit, gamma isozyme	Input
RAB11A	RAB11A, member RAS oncogene family	Induced
RAB11B	RAB11B, member RAS oncogene family	Induced
RAB11FIP2	RAB11 family interacting protein 2 (class I)	Input

**Supplementary Table II-7, Community #13: (Putative hallmark/functions: deregulating cellular energetics)**

<b>SYMBOL</b>	<b>GENE NAME</b>	<b>TYPE</b>
ATP5C1	ATP synthase, H <sup>+</sup> transporting, mitochondrial F1 complex, gamma polypeptide 1	Induced
ATP5G1	ATP synthase, H <sup>+</sup> transporting, mitochondrial Fo complex, subunit C1 (subunit 9)	Input

**Supplementary Table II-7, Community #14: (Putative hallmark/functions: deregulating cellular energetics)**

<b>SYMBOL</b>	<b>GENE NAME</b>	<b>TYPE</b>
COX15	cytochrome c oxidase assembly homolog 15 (yeast)	Input
LAMTOR3	late endosomal/lysosomal adaptor, MAPK and MTOR activator 3	Induced

APPENDIX II

**Supplementary Table II-7, Community #15: (Putative hallmark/functions: tumor promoting inflammation)**

<b>SYMBOL</b>	<b>GENE NAME</b>	<b>TYPE</b>
MTMR9	myotubularin related protein 9	Input
NMI	N-myc (and STAT) interactor	Induced
POMZP3	POM121 and ZP3 fusion	Input

**Supplementary Table II-7, Community #16: (Putative hallmark/functions: tumor promoting inflammation, angiogenesis, tumor microenvironment influence)**

<b>SYMBOL</b>	<b>GENE NAME</b>	<b>TYPE</b>
CTSL	cathepsin L	Input
KNG1	kininogen 1	Induced

**Supplementary Table II-7, Community #17: (Putative hallmark/functions: deregulating cellular energetics)**

<b>SYMBOL</b>	<b>GENE NAME</b>	<b>TYPE</b>
BCCIP	BRCA2 and CDKN1A interacting protein	Input
CHORDC1	cysteine and histidine-rich domain (CHORD) containing 1	Induced
GDA	guanine deaminase	Induced
KYNU	Kynureninase	Input
LDHA	lactate dehydrogenase A	Induced
SMS	spermine synthase	Induced

APPENDIX II

**Supplementary Table II-7, Community #18: (Putative hallmark/functions: deregulating cellular energetics)**

<b>SYMBOL</b>	<b>GENE NAME</b>	<b>TYPE</b>
DARS2	aspartyl-tRNA synthetase 2, mitochondrial	Input
DCP2	decapping mRNA 2	Induced

**Supplementary Table II-7, Community #19: (Putative hallmark/functions: growth signal autonomy, invasion and metastasis, genomic instability)**

<b>SYMBOL</b>	<b>GENE NAME</b>	<b>TYPE</b>
AR	androgen receptor	Induced
AURKA	aurora kinase A	Induced
BRCA1	breast cancer 1, early onset	Induced
BTRC	beta-transducin repeat containing E3 ubiquitin protein ligase	Induced
CCND1	cyclin D1	Induced
CDH1	cadherin 1, type 1	Induced
CDK1	cyclin-dependent kinase 1	Induced
CDK2	cyclin-dependent kinase 2	Induced
CDKN1A	cyclin-dependent kinase inhibitor 1A (p21, Cip1)	Induced
CDKN1B	cyclin-dependent kinase inhibitor 1B (p27, Kip1)	Induced
CHUK	conserved helix-loop-helix ubiquitous kinase	Input
CREBBP	CREB binding protein	Induced
CSNK2A1	casein kinase 2, alpha 1 polypeptide	Induced
CSNK2A2	casein kinase 2, alpha prime polypeptide	Induced
CTNNB1	catenin (cadherin-associated protein), beta 1, 88kDa	Induced
EP300	E1A binding protein p300	Induced
ESR1	estrogen receptor 1	Induced

## APPENDIX II

**Supplementary Table II-7, Community #19 (continued): (Putative hallmark/functions: growth signal autonomy, invasion and metastasis, genomic instability)**

<b>SYMBOL</b>	<b>GENE NAME</b>	<b>TYPE</b>
FBXO31	F-box protein 31	Input
FBXW7	F-box and WD repeat domain containing 7, E3 ubiquitin protein ligase	Induced
HDAC1	histone deacetylase 1	Induced
HIST3H3	histone cluster 3, H3	Induced
KEAP1	kelch-like ECH-associated protein 1	Induced
NCOA3	nuclear receptor coactivator 3	Induced
NR3C1	nuclear receptor subfamily 3, group C, member 1 (glucocorticoid receptor)	Induced
PBK	PDZ binding kinase	Input
PML	promyelocytic leukemia	Induced
PRKDC	protein kinase, DNA-activated, catalytic polypeptide	Induced
PTEN	phosphatase and tensin homolog	Input
PTMA	prothymosin, alpha, prothymosin alpha-like	Induced
RAC3	ras-related C3 botulinum toxin substrate 3 (rho family, small GTP binding protein Rac3)	Induced
RBX1	ring-box 1, E3 ubiquitin protein ligase	Induced
RUVBL1	RuvB-like AAA ATPase 1	Induced
SIRT1	sirtuin 1	Induced
SKP1	S-phase kinase-associated protein 1	Induced
SMAD1	SMAD family member 1	Induced
SMAD 2	SMAD family member 2	Induced
SMAD 3	SMAD family member 3	Induced
SMAD 4	SMAD family member 4	Induced
SUMO1	small ubiquitin-like modifier 1	Induced
TERT	telomerase reverse transcriptase	Induced
TP53	tumor protein p53	Induced

APPENDIX II

**Supplementary Table II-7, Community #19 (continued): (Putative hallmark/functions: growth signal autonomy, invasion and metastasis, genomic instability)**

UBE2I	ubiquitin-conjugating enzyme E2I	Induced
ZEB1	zinc finger E-box binding homeobox 1	Input

**Supplementary Table II-7, Community #20: (Putative hallmark/functions: genomic instability, proteomic instability)**

<b>SYMBOL</b>	<b>GENE NAME</b>	<b>TYPE</b>
RAB7A	RAB7A, member RAS oncogene family	Induced
UVRAG	UV radiation resistance associated	Induced
VPS16	vacuolar protein sorting 16 homolog (S. cerevisiae)	Induced
VPS33B	vacuolar protein sorting 33 homolog B (yeast)	Input

**Supplementary Table II-7, Community #21: (Putative hallmark/functions: growth signal autonomy, deregulating cellular energetics, Endo/Exocytosis)**

<b>SYMBOL</b>	<b>GENE NAME</b>	<b>TYPE</b>
STX2	syntaxin 2	Input
YKT6	YKT6 v-SNARE homolog (S. cerevisiae)	Induced

APPENDIX II

**Supplementary Table II-7, Community #22: (Putative hallmark/functions: growth signal autonomy, proteomic instability)**

<b>SYMBOL</b>	<b>GENE NAME</b>	<b>TYPE</b>
CRTAP	cartilage associated protein	Input
TOM1L1	target of myb1 like 1 membrane trafficking protein	Induced

**Supplementary Table II-7, Community #23: (Putative hallmark/functions: post-translational gene regulation, proteomic instability)**

<b>SYMBOL</b>	<b>GENE NAME</b>	<b>TYPE</b>
DAZAP1	DAZ associated protein 1	Induced
MSI1	musashi RNA-binding protein 1	Induced
MSI2	musashi RNA-binding protein 2	Induced
ZC3H14	zinc finger CCCH-type containing 14	Input

**Supplementary Table II-7, Community #24: (Putative hallmark/functions: genomic instability)**

<b>SYMBOL</b>	<b>GENE NAME</b>	<b>TYPE</b>
CSE1L	CSE1 chromosome segregation 1-like (yeast)	Induced
SLC9A3R1	solute carrier family 9, subfamily A (NHE3, cation proton antiporter 3), member 3 regulator 1	Induced

APPENDIX II

**Supplementary Table II-7, Community #25: (Putative hallmark/functions: deregulating cellular energetics, proteomic instability)**

<b>SYMBOL</b>	<b>GENE NAME</b>	<b>TYPE</b>
ALDH1B1	aldehyde dehydrogenase 1 family, member B1	Input
UBR7	ubiquitin protein ligase E3 component n-recognin 7 (putative)	Induced

**Supplementary Table II-7, Community #26: (Putative hallmark/functions: deregulating cellular energetics)**

<b>SYMBOL</b>	<b>GENE NAME</b>	<b>TYPE</b>
GNS	glucosamine (N-acetyl)-6-sulfatase	Induced
LDHAL6B	lactate dehydrogenase A-like 6B	Induced
NAGK	N-acetylglucosamine kinase	Induced

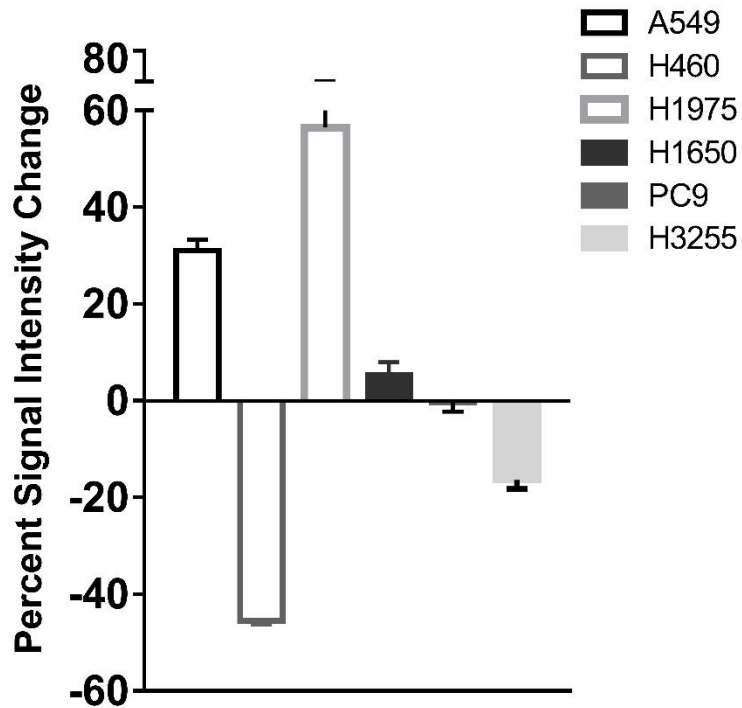
APPENDIX II

**Supplementary Table II-7, Proteins with no community affiliation:**

<b>SYMBOL</b>	<b>GENE NAME</b>	<b>TYPE</b>
PROCR	protein C receptor, endothelial	Input
GNG11	guanine nucleotide binding protein (G protein), gamma 11	Input
ARHGEF9	Cdc42 guanine nucleotide exchange factor (406) 9	Input
DOCK10	dedicator of cytokinesis 10	Input
INVS	Inversin	Input
DIP2C	disco-interacting protein 2 homolog C	Input
S100A1	S100 calcium binding protein A1	Induced
ADCY9	adenylate cyclase 9	Input
HS1BP3	HCLS1 binding protein 3	Input
PMP22	peripheral myelin protein 22	Input
TFE3	transcription factor binding to IGHM enhancer 3	Input
DHRS4:D HRS4L2: DHRS4L1	dehydrogenase/reductase (SDR family) member 4, dehydrogenase/reductase (SDR family) member 4 like 2, dehydrogenase/reductase (SDR family) member 4 like 1	Input
MID1IP1	MID1 interacting protein 1	Input
ANGEL2	angel homolog 2 (Drosophila)	Input
PEX19	peroxisomal biogenesis factor 19	Induced
S100A3	S100 calcium binding protein A3	Input
CUTC	cutC copper transporter	Input
IGFBP3	insulin-like growth factor binding protein 3	Induced
DIXDC1	DIX domain containing 1	Input
FASTKD1	FAST kinase domains 1	Input
PEX5	peroxisomal biogenesis factor 5	Induced
GPHN	Gephyrin	Induced

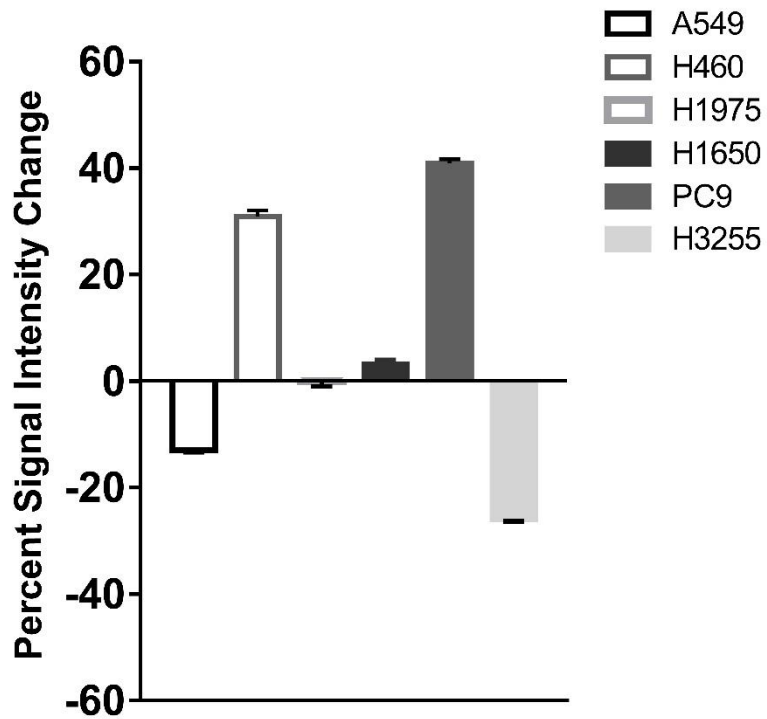
**Supplementary Figure II-1: NSCLC cells most sensitive to CX-4945 have decreased CSNK2B expression.** U133A Affymetrix signal intensity values for **(A)** CSNK2A1 (Averaged of three probesets: 212072\_s\_at, 206075\_s\_at, and 212075\_s\_at), **(B)** CSNK2A2 (203575\_at), and **(C)** CSNK2B (201390\_s\_at) probesets were generated from untreated NSCLC cell lines (n=3) with using Affymetrix MAS v5.0 software [Balco, 2006 #238]. Values for each gene set were normalized to corresponding expression in Small Airway Epithelial Cells (SAEC) and is shown as percent change.

A



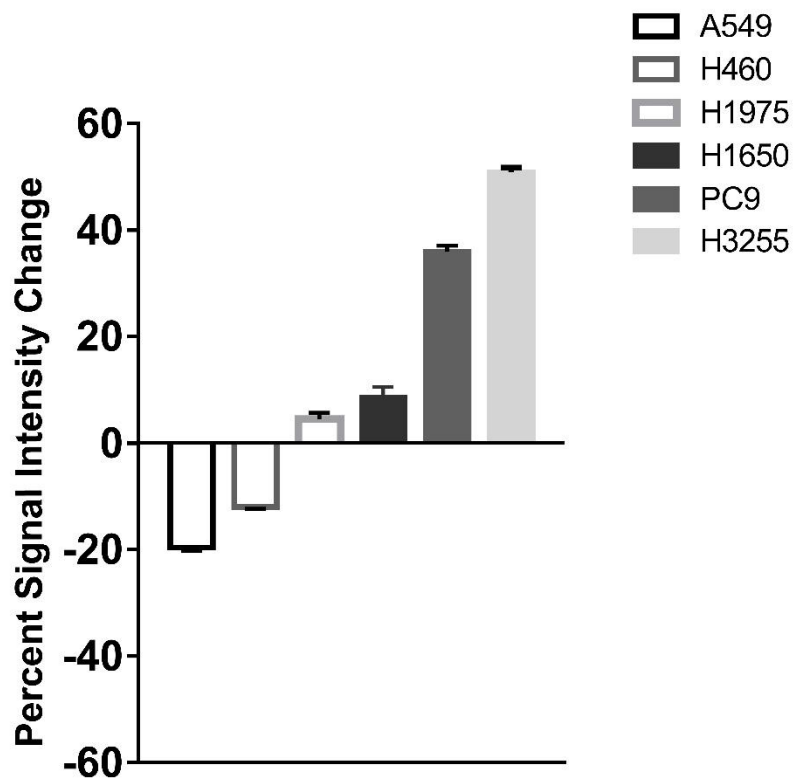
**Supplementary Figure II-1 (continued): NSCLC cells most sensitive to CX-4945 have decreased CSNK2B expression.** U133A Affymetrix signal intensity values for (A) CSNK2A1 (Averaged of three probesets: 212072\_s\_at, 206075\_s\_at, and 212075\_s\_at), (B) CSNK2A2 (203575\_at), and (C) CSNK2B (201390\_s\_at) probesets were generated from untreated NSCLC cell lines (n=3) with using Affymetrix MAS v5.0 software [Balko, 2006 #238]. Values for each gene set were normalized to corresponding expression in Small Airway Epithelial Cells (SAEC) and is shown as percent change.

**B**



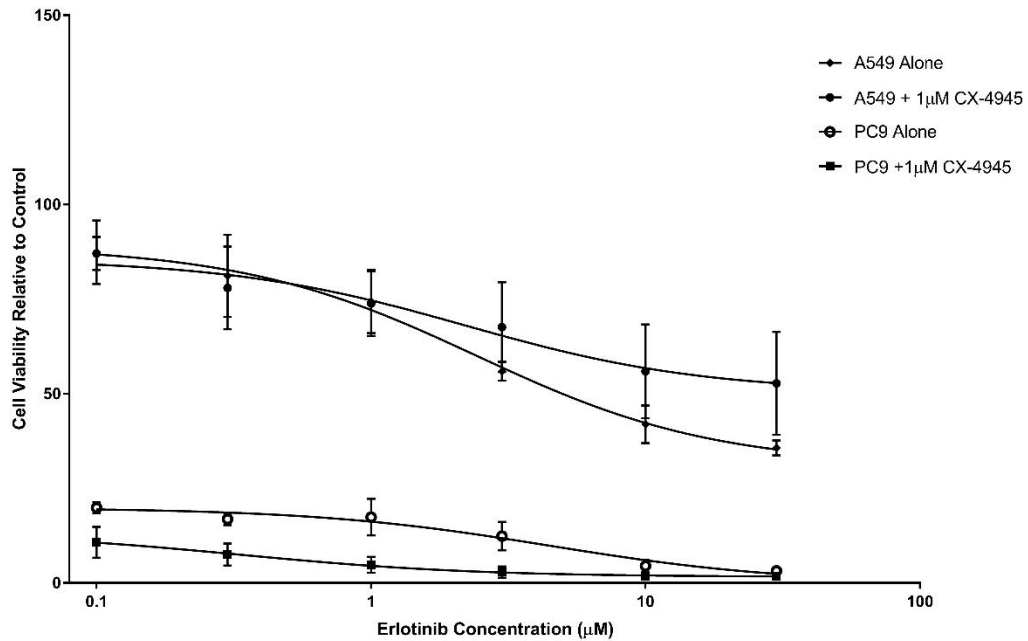
**Supplementary Figure II-1 (continued): NSCLC cells most sensitive to CX-4945 have decreased CSNK2B expression.** U133A Affymetrix signal intensity values for **(A)** CSNK2A1 (Averaged of three probesets: 212072\_s\_at, 206075\_s\_at, and 212075\_s\_at), **(B)** CSNK2A2 (203575\_at), and **(C)** CSNK2B (201390\_s\_at) probesets were generated from untreated NSCLC cell lines (n=3) with using Affymetrix MAS v5.0 software [Balko, 2006 #238]. Values for each gene set were normalized to corresponding expression in Small Airway Epithelial Cells (SAEC) and is shown as percent change.

**C**



APPENDIX III: SUPPLEMENTARY FIGURES FOR CHAPTER 5

**Supplementary Figure III-1: Comparison of CX-4945 treatment on erlotinib response.** A549 and PC9 samples treated only with  $\pm 1\mu\text{M}$  CX-4945 from Figures 3 and 5 to determine the impact of 7-day incubation of CX-4945 on erlotinib sensitivity in cells not modulated with TGF $\beta$ , LY-2109761, or SB-431542. Unpaired t-test comparing untreated and CX-4945 treated curves indicates that the differences between the curves are not significant.



## REFERENCES

### REFERENCES:

1. Hanahan D, Weinberg RA. Hallmarks of cancer: the next generation. *Cell*. 2011;144(5):646-74. doi: 10.1016/j.cell.2011.02.013. PubMed PMID: 21376230.
2. Klein G. Oncogenes and tumor suppressor genes. *Acta oncologica (Stockholm, Sweden)*. 1988;27(4):427-37. Epub 1988/01/01. PubMed PMID: 2849463.
3. Lynch TJ, Bell DW, Sordella R, Gurubhagavatula S, Okimoto RA, Brannigan BW, Harris PL, Haserlat SM, Supko JG, Haluska FG, Louis DN, Christiani DC, Settleman J, Haber DA. Activating mutations in the epidermal growth factor receptor underlying responsiveness of non-small-cell lung cancer to gefitinib. *N Engl J Med*. 2004;350(21):2129-39. Epub 2004/05/01. doi: 10.1056/NEJMoa040938. PubMed PMID: 15118073.
4. Weinstein IB. Cancer. Addiction to oncogenes--the Achilles heel of cancer. *Science*. 2002;297(5578):63-4. Epub 2002/07/06. doi: 10.1126/science.1073096. PubMed PMID: 12098689.
5. Pecorino L. *Molecular biology of cancer: mechanisms, targets, and therapeutics*: Oxford university press; 2012.
6. Torre LA, Siegel RL, Jemal A. Lung Cancer Statistics. *Advances in experimental medicine and biology*. 2016;893:1-19. Epub 2015/12/17. doi: 10.1007/978-3-319-24223-1\_1. PubMed PMID: 26667336.
7. Hecht SS. Lung carcinogenesis by tobacco smoke. *Int J Cancer*. 2012;131(12):2724-32. Epub 2012/09/05. doi: 10.1002/ijc.27816. PubMed PMID: 22945513; PMCID: PMC3479369.
8. Siegel RL, Miller KD, Jemal A. Cancer statistics, 2016. *CA: a cancer journal for clinicians*. 2016;66(1):7-30.
9. Mokdad AH, Dwyer-Lindgren L, Fitzmaurice C, Stubbs RW, Bertozzi-Villa A, Morozoff C, Charara R, Allen C, Naghavi M, Murray CJ. Trends and Patterns of Disparities in Cancer Mortality Among US Counties, 1980-2014. *Jama*. 2017;317(4):388-406. Epub 2017/01/25. doi: 10.1001/jama.2016.20324. PubMed PMID: 28118455.
10. Health UDo, Services H. *The health consequences of smoking—50 years of progress: a report of the Surgeon General*. Atlanta, GA: US Department of Health and Human Services, Centers for Disease Control and Prevention, National Center for Chronic Disease Prevention and Health Promotion, Office on Smoking and Health. 2014;17.
11. Alberg AJ, Brock MV, Ford JG, Samet JM, Spivack SD. *Epidemiology of lung cancer: Diagnosis and management of lung cancer, 3rd ed: American College of Chest Physicians evidence-based clinical practice guidelines*. *Chest*. 2013;143(5 Suppl):e1S-29S. Epub 2013/05/10. doi: 10.1378/chest.12-2345. PubMed PMID: 23649439; PMCID: PMC4694610.
12. Sethi TK, El-Ghamry MN, Kloecker GH. Radon and lung cancer. *Clinical advances in hematology & oncology : H&O*. 2012;10(3):157-64. Epub 2012/03/10. PubMed PMID: 22402423.
13. Hahn EJ, Gokun Y, Andrews WM, Overfield BL, Robertson H, Wiggins A, Rayens MK. Radon potential, geologic formations, and lung cancer risk. *Preventive medicine reports*. 2015;2:342-6.
14. Alberg AJ, Samet JM. Epidemiology of lung cancer. *Chest*. 2003;123(1 Suppl):21s-49s. Epub 2003/01/16. PubMed PMID: 12527563.
15. Hecht SS. Tobacco carcinogens, their biomarkers and tobacco-induced cancer. *Nature Reviews Cancer*. 2003;3(10):733-44.
16. Greenman C, Stephens P, Smith R, Dalgliesh GL, Hunter C, Bignell G, Davies H, Teague J, Butler A, Stevens C, Edkins S, O'Meara S, Vastrik I, Schmidt EE, Avis T, Barthorpe S, Bhamra G, Buck

## REFERENCES

- G, Choudhury B, Clements J, Cole J, Dicks E, Forbes S, Gray K, Halliday K, Harrison R, Hills K, Hinton J, Jenkinson A, Jones D, Menzies A, Mironenko T, Perry J, Raine K, Richardson D, Shepherd R, Small A, Tofts C, Varian J, Webb T, West S, Widaa S, Yates A, Cahill DP, Louis DN, Goldstraw P, Nicholson AG, Brasseur F, Looijenga L, Weber BL, Chiew YE, DeFazio A, Greaves MF, Green AR, Campbell P, Birney E, Easton DF, Chenevix-Trench G, Tan MH, Khoo SK, Teh BT, Yuen ST, Leung SY, Wooster R, Futreal PA, Stratton MR. Patterns of somatic mutation in human cancer genomes. *Nature*. 2007;446(7132):153-8. Epub 2007/03/09. doi: 10.1038/nature05610. PubMed PMID: 17344846; PMCID: PMC2712719.
17. Larsen JE, Minna JD. Molecular biology of lung cancer: clinical implications. *Clinics in chest medicine*. 2011;32(4):703-40. Epub 2011/11/08. doi: 10.1016/j.ccm.2011.08.003. PubMed PMID: 22054881; PMCID: PMC3367865.
18. Hiley CT, Le Quesne J, Santis G, Sharpe R, de Castro DG, Middleton G, Swanton C. Challenges in molecular testing in non-small-cell lung cancer patients with advanced disease. *Lancet (London, England)*. 2016;388(10048):1002-11. Epub 2016/09/07. doi: 10.1016/s0140-6736(16)31340-x. PubMed PMID: 27598680.
19. Cooper WA, Lam DC, O'Toole SA, Minna JD. Molecular biology of lung cancer. *Journal of thoracic disease*. 2013;5 Suppl 5:S479-90. Epub 2013/10/29. doi: 10.3978/j.issn.2072-1439.2013.08.03. PubMed PMID: 24163741; PMCID: PMC3804875.
20. Yip PY, Yu B, Cooper WA, Selinger CI, Ng CC, Kennedy CW, Kohonen-Corish MR, McCaughan BC, Trent RJ, Boyer MJ, Kench JG, Horvath LG, O'Toole SA. Patterns of DNA mutations and ALK rearrangement in resected node negative lung adenocarcinoma. *Journal of thoracic oncology : official publication of the International Association for the Study of Lung Cancer*. 2013;8(4):408-14. Epub 2013/02/09. doi: 10.1097/JTO.0b013e318283558e. PubMed PMID: 23392229.
21. Karnoub AE, Weinberg RA. Ras oncogenes: split personalities. *Nature reviews Molecular cell biology*. 2008;9(7):517-31. Epub 2008/06/24. doi: 10.1038/nrm2438. PubMed PMID: 18568040; PMCID: PMC3915522.
22. Ding L, Getz G, Wheeler DA, Mardis ER, McLellan MD, Cibulskis K, Sougnez C, Greulich H, Muzny DM, Morgan MB, Fulton L, Fulton RS, Zhang Q, Wendl MC, Lawrence MS, Larson DE, Chen K, Dooling DJ, Sabo A, Hawes AC, Shen H, Jhangiani SN, Lewis LR, Hall O, Zhu Y, Mathew T, Ren Y, Yao J, Scherer SE, Clerc K, Metcalf GA, Ng B, Milosavljevic A, Gonzalez-Garay ML, Osborne JR, Meyer R, Shi X, Tang Y, Koboldt DC, Lin L, Abbott R, Miner TL, Pohl C, Fewell G, Haipek C, Schmidt H, Dunford-Shore BH, Kraja A, Crosby SD, Sawyer CS, Vickery T, Sander S, Robinson J, Winckler W, Baldwin J, Chirieac LR, Dutt A, Fennell T, Hanna M, Johnson BE, Onofrio RC, Thomas RK, Tonon G, Weir BA, Zhao X, Ziaugra L, Zody MC, Giordano T, Orringer MB, Roth JA, Spitz MR, Wistuba II, Ozenberger B, Good PJ, Chang AC, Beer DG, Watson MA, Ladanyi M, Broderick S, Yoshizawa A, Travis WD, Pao W, Province MA, Weinstock GM, Varmus HE, Gabriel SB, Lander ES, Gibbs RA, Meyerson M, Wilson RK. Somatic mutations affect key pathways in lung adenocarcinoma. *Nature*. 2008;455(7216):1069-75. Epub 2008/10/25. doi: 10.1038/nature07423. PubMed PMID: 18948947; PMCID: PMC2694412.
23. Linardou H, Dahabreh IJ, Kanaloupiti D, Siannis F, Bafaloukos D, Kosmidis P, Papadimitriou CA, Murray S. Assessment of somatic k-RAS mutations as a mechanism associated with resistance to EGFR-targeted agents: a systematic review and meta-analysis of studies in advanced non-small-cell lung cancer and metastatic colorectal cancer. *The Lancet Oncology*. 2008;9(10):962-72. Epub 2008/09/23. doi: 10.1016/s1470-2045(08)70206-7. PubMed PMID: 18804418.
24. Rodenhuis S, Slebos RJ. Clinical significance of ras oncogene activation in human lung cancer. *Cancer Res*. 1992;52(9 Suppl):2665s-9s. Epub 1992/05/01. PubMed PMID: 1562997.

## REFERENCES

25. Shigematsu H, Lin L, Takahashi T, Nomura M, Suzuki M, Wistuba II, Fong KM, Lee H, Toyooka S, Shimizu N, Fujisawa T, Feng Z, Roth JA, Herz J, Minna JD, Gazdar AF. Clinical and biological features associated with epidermal growth factor receptor gene mutations in lung cancers. *Journal of the National Cancer Institute*. 2005;97(5):339-46. Epub 2005/03/03. doi: 10.1093/jnci/dji055. PubMed PMID: 15741570.
26. Tam IY, Chung LP, Suen WS, Wang E, Wong MC, Ho KK, Lam WK, Chiu SW, Girard L, Minna JD, Gazdar AF, Wong MP. Distinct epidermal growth factor receptor and KRAS mutation patterns in non-small cell lung cancer patients with different tobacco exposure and clinicopathologic features. *Clin Cancer Res*. 2006;12(5):1647-53. Epub 2006/03/15. doi: 10.1158/1078-0432.ccr-05-1981. PubMed PMID: 16533793.
27. Schmid K, Oehl N, Wrba F, Pirker R, Pirker C, Filipits M. EGFR/KRAS/BRAF mutations in primary lung adenocarcinomas and corresponding locoregional lymph node metastases. *Clin Cancer Res*. 2009;15(14):4554-60. Epub 2009/07/09. doi: 10.1158/1078-0432.ccr-09-0089. PubMed PMID: 19584155.
28. Millington GW. Mutations of the BRAF gene in human cancer, by Davies et al. (*Nature* 2002; 417: 949-54). *Clinical and experimental dermatology*. 2013;38(2):222-3. Epub 2013/02/13. doi: 10.1111/ced.12015. PubMed PMID: 23397951.
29. Stinchcombe TE. Targeted Therapies for Lung Cancer. In: Reckamp KL, editor. *Lung Cancer: Treatment and Research*. Cham: Springer International Publishing; 2016. p. 165-82.
30. Marchetti A, Felicioni L, Malatesta S, Grazia Sciarrotta M, Guetti L, Chella A, Viola P, Pullara C, Mucilli F, Buttitta F. Clinical features and outcome of patients with non-small-cell lung cancer harboring BRAF mutations. *Journal of clinical oncology : official journal of the American Society of Clinical Oncology*. 2011;29(26):3574-9. Epub 2011/08/10. doi: 10.1200/jco.2011.35.9638. PubMed PMID: 21825258.
31. Downward J. Targeting RAS signalling pathways in cancer therapy. *Nat Rev Cancer*. 2003;3(1):11-22. Epub 2003/01/02. doi: 10.1038/nrc969. PubMed PMID: 12509763.
32. Marks JL, Gong Y, Chitale D, Golas B, McLellan MD, Kasai Y, Ding L, Mardis ER, Wilson RK, Solit D, Levine R, Michel K, Thomas RK, Rusch VW, Ladanyi M, Pao W. Novel MEK1 mutation identified by mutational analysis of epidermal growth factor receptor signaling pathway genes in lung adenocarcinoma. *Cancer Res*. 2008;68(14):5524-8. Epub 2008/07/18. doi: 10.1158/0008-5472.can-08-0099. PubMed PMID: 18632602; PMCID: PMC2586155.
33. Yarden Y. Biology of HER2 and its importance in breast cancer. *Oncology*. 2001;61 Suppl 2:1-13. Epub 2001/11/06. doi: 55396. PubMed PMID: 11694782.
34. Tzahar E, Waterman H, Chen X, Levkowitz G, Karunakaran D, Lavi S, Ratzkin BJ, Yarden Y. A hierarchical network of interreceptor interactions determines signal transduction by Neu differentiation factor/neuregulin and epidermal growth factor. *Molecular and cellular biology*. 1996;16(10):5276-87. Epub 1996/10/01. PubMed PMID: 8816440; PMCID: PMC231527.
35. Graus-Porta D, Beerli RR, Daly JM, Hynes NE. ErbB-2, the preferred heterodimerization partner of all ErbB receptors, is a mediator of lateral signaling. *The EMBO journal*. 1997;16(7):1647-55. Epub 1997/04/01. doi: 10.1093/emboj/16.7.1647. PubMed PMID: 9130710; PMCID: PMC1169769.
36. Heinmoller P, Gross C, Beyser K, Schmidtgen C, Maass G, Pedrocchi M, Ruschoff J. HER2 status in non-small cell lung cancer: results from patient screening for enrollment to a phase II study of herceptin. *Clin Cancer Res*. 2003;9(14):5238-43. Epub 2003/11/14. PubMed PMID: 14614004.
37. Stephens P, Hunter C, Bignell G, Edkins S, Davies H, Teague J, Stevens C, O'Meara S, Smith R, Parker A, Barthorpe A, Blow M, Brackenbury L, Butler A, Clarke O, Cole J, Dicks E, Dike A, Drozd A, Edwards K, Forbes S, Foster R, Gray K, Greenman C, Halliday K, Hills K, Kosmidou V, Lugg R,

## REFERENCES

- Menzies A, Perry J, Petty R, Raine K, Ratford L, Shepherd R, Small A, Stephens Y, Tofts C, Varian J, West S, Widaa S, Yates A, Basseur F, Cooper CS, Flanagan AM, Knowles M, Leung SY, Louis DN, Looijenga LH, Malkowicz B, Pierotti MA, Teh B, Chenevix-Trench G, Weber BL, Yuen ST, Harris G, Goldstraw P, Nicholson AG, Futreal PA, Wooster R, Stratton MR. Lung cancer: intragenic ERBB2 kinase mutations in tumours. *Nature*. 2004;431(7008):525-6. Epub 2004/10/01. doi: 10.1038/431525b. PubMed PMID: 15457249.
38. Sadiq AA, Salgia R. MET as a possible target for non-small-cell lung cancer. *Journal of clinical oncology : official journal of the American Society of Clinical Oncology*. 2013;31(8):1089-96. Epub 2013/02/13. doi: 10.1200/jco.2012.43.9422. PubMed PMID: 23401458; PMCID: PMC3589702.
39. Engelman JA, Zejnullahu K, Mitsudomi T, Song Y, Hyland C, Park JO, Lindeman N, Gale CM, Zhao X, Christensen J, Kosaka T, Holmes AJ, Rogers AM, Cappuzzo F, Mok T, Lee C, Johnson BE, Cantley LC, Janne PA. MET amplification leads to gefitinib resistance in lung cancer by activating ERBB3 signaling. *Science*. 2007;316(5827):1039-43. Epub 2007/04/28. doi: 10.1126/science.1141478. PubMed PMID: 17463250.
40. Cappuzzo F, Marchetti A, Skokan M, Rossi E, Gajapathy S, Felicioni L, Del Grammastro M, Sciarrotta MG, Buttitta F, Incarbone M, Toschi L, Finocchiaro G, Destro A, Terracciano L, Roncalli M, Alloisio M, Santoro A, Varella-Garcia M. Increased MET gene copy number negatively affects survival of surgically resected non-small-cell lung cancer patients. *Journal of clinical oncology : official journal of the American Society of Clinical Oncology*. 2009;27(10):1667-74. Epub 2009/03/04. doi: 10.1200/jco.2008.19.1635. PubMed PMID: 19255323; PMCID: PMC3341799.
41. Bean J, Brennan C, Shih JY, Riely G, Viale A, Wang L, Chitale D, Motoi N, Szoke J, Broderick S, Balak M, Chang WC, Yu CJ, Gazdar A, Pass H, Rusch V, Gerald W, Huang SF, Yang PC, Miller V, Ladanyi M, Yang CH, Pao W. MET amplification occurs with or without T790M mutations in EGFR mutant lung tumors with acquired resistance to gefitinib or erlotinib. *Proceedings of the National Academy of Sciences of the United States of America*. 2007;104(52):20932-7. Epub 2007/12/21. doi: 10.1073/pnas.0710370104. PubMed PMID: 18093943; PMCID: PMC2409244.
42. Beau-Faller M, Ruppert AM, Voegeli AC, Neuville A, Meyer N, Guerin E, Legrain M, Mennecier B, Wihlm JM, Massard G, Quoix E, Oudet P, Gaub MP. MET gene copy number in non-small cell lung cancer: molecular analysis in a targeted tyrosine kinase inhibitor naive cohort. *Journal of thoracic oncology : official publication of the International Association for the Study of Lung Cancer*. 2008;3(4):331-9. Epub 2008/04/02. doi: 10.1097/JTO.0b013e318168d9d4. PubMed PMID: 18379349.
43. Brognard J, Clark AS, Ni Y, Dennis PA. Akt/protein kinase B is constitutively active in non-small cell lung cancer cells and promotes cellular survival and resistance to chemotherapy and radiation. *Cancer Res*. 2001;61(10):3986-97. Epub 2001/05/19. PubMed PMID: 11358816.
44. Papadimitrakopoulou V. Development of PI3K/AKT/mTOR pathway inhibitors and their application in personalized therapy for non-small-cell lung cancer. *Journal of thoracic oncology : official publication of the International Association for the Study of Lung Cancer*. 2012;7(8):1315-26. Epub 2012/06/01. doi: 10.1097/JTO.0b013e31825493eb. PubMed PMID: 22648207.
45. Vivanco I, Sawyers CL. The phosphatidylinositol 3-Kinase AKT pathway in human cancer. *Nat Rev Cancer*. 2002;2(7):489-501. Epub 2002/07/03. doi: 10.1038/nrc839. PubMed PMID: 12094235.
46. Choi YL, Takeuchi K, Soda M, Inamura K, Togashi Y, Hatano S, Enomoto M, Hamada T, Haruta H, Watanabe H, Kurashina K, Hatanaka H, Ueno T, Takada S, Yamashita Y, Sugiyama Y, Ishikawa Y, Mano H. Identification of novel isoforms of the EML4-ALK transforming gene in non-small cell lung cancer. *Cancer Res*. 2008;68(13):4971-6. Epub 2008/07/03. doi: 10.1158/0008-5472.can-07-6158. PubMed PMID: 18593892.

## REFERENCES

47. Koivunen JP, Mermel C, Zejnullahu K, Murphy C, Lifshits E, Holmes AJ, Choi HG, Kim J, Chiang D, Thomas R, Lee J, Richards WG, Sugarbaker DJ, Ducko C, Lindeman N, Marcoux JP, Engelman JA, Gray NS, Lee C, Meyerson M, Janne PA. EML4-ALK fusion gene and efficacy of an ALK kinase inhibitor in lung cancer. *Clin Cancer Res*. 2008;14(13):4275-83. Epub 2008/07/03. doi: 10.1158/1078-0432.ccr-08-0168. PubMed PMID: 18594010; PMCID: PMC3025451.
48. Soda M, Choi YL, Enomoto M, Takada S, Yamashita Y, Ishikawa S, Fujiwara S, Watanabe H, Kurashina K, Hatanaka H, Bando M, Ohno S, Ishikawa Y, Aburatani H, Niki T, Sohara Y, Sugiyama Y, Mano H. Identification of the transforming EML4-ALK fusion gene in non-small-cell lung cancer. *Nature*. 2007;448(7153):561-6. Epub 2007/07/13. doi: 10.1038/nature05945. PubMed PMID: 17625570.
49. Choi YL, Soda M, Yamashita Y, Ueno T, Takashima J, Nakajima T, Yatabe Y, Takeuchi K, Hamada T, Haruta H, Ishikawa Y, Kimura H, Mitsudomi T, Tanio Y, Mano H. EML4-ALK mutations in lung cancer that confer resistance to ALK inhibitors. *N Engl J Med*. 2010;363(18):1734-9. Epub 2010/10/29. doi: 10.1056/NEJMoa1007478. PubMed PMID: 20979473.
50. Rikova K, Guo A, Zeng Q, Possemato A, Yu J, Haack H, Nardone J, Lee K, Reeves C, Li Y, Hu Y, Tan Z, Stokes M, Sullivan L, Mitchell J, Wetzell R, Macneill J, Ren JM, Yuan J, Bakalarski CE, Villen J, Kornhauser JM, Smith B, Li D, Zhou X, Gygi SP, Gu TL, Polakiewicz RD, Rush J, Comb MJ. Global survey of phosphotyrosine signaling identifies oncogenic kinases in lung cancer. *Cell*. 2007;131(6):1190-203. Epub 2007/12/18. doi: 10.1016/j.cell.2007.11.025. PubMed PMID: 18083107.
51. Shaw AT, Solomon B. Targeting anaplastic lymphoma kinase in lung cancer. *Clin Cancer Res*. 2011;17(8):2081-6. Epub 2011/02/04. doi: 10.1158/1078-0432.ccr-10-1591. PubMed PMID: 21288922.
52. Soda M, Takada S, Takeuchi K, Choi YL, Enomoto M, Ueno T, Haruta H, Hamada T, Yamashita Y, Ishikawa Y, Sugiyama Y, Mano H. A mouse model for EML4-ALK-positive lung cancer. *Proceedings of the National Academy of Sciences of the United States of America*. 2008;105(50):19893-7. Epub 2008/12/10. doi: 10.1073/pnas.0805381105. PubMed PMID: 19064915; PMCID: PMC2605003.
53. Solomon B, Varella-Garcia M, Camidge DR. ALK gene rearrangements: a new therapeutic target in a molecularly defined subset of non-small cell lung cancer. *Journal of thoracic oncology : official publication of the International Association for the Study of Lung Cancer*. 2009;4(12):1450-4. Epub 2009/12/17. doi: 10.1097/JTO.0b013e3181c4dedb. PubMed PMID: 20009909.
54. Chin LP, Soo RA, Soong R, Ou SH. Targeting ROS1 with anaplastic lymphoma kinase inhibitors: a promising therapeutic strategy for a newly defined molecular subset of non-small-cell lung cancer. *Journal of thoracic oncology : official publication of the International Association for the Study of Lung Cancer*. 2012;7(11):1625-30. Epub 2012/10/17. doi: 10.1097/JTO.0b013e31826baf83. PubMed PMID: 23070242.
55. Bergethon K, Shaw AT, Ou SH, Katayama R, Lovly CM, McDonald NT, Massion PP, Siwak-Tapp C, Gonzalez A, Fang R, Mark EJ, Batten JM, Chen H, Wilner KD, Kwak EL, Clark JW, Carbone DP, Ji H, Engelman JA, Mino-Kenudson M, Pao W, Iafrate AJ. ROS1 rearrangements define a unique molecular class of lung cancers. *Journal of clinical oncology : official journal of the American Society of Clinical Oncology*. 2012;30(8):863-70. Epub 2012/01/05. doi: 10.1200/jco.2011.35.6345. PubMed PMID: 22215748; PMCID: PMC3295572.
56. Takeuchi K, Soda M, Togashi Y, Suzuki R, Sakata S, Hatano S, Asaka R, Hamanaka W, Ninomiya H, Uehara H, Lim Choi Y, Satoh Y, Okumura S, Nakagawa K, Mano H, Ishikawa Y. RET, ROS1 and ALK fusions in lung cancer. *Nature medicine*. 2012;18(3):378-81. Epub 2012/02/14. doi: 10.1038/nm.2658. PubMed PMID: 22327623.

## REFERENCES

57. Ju YS, Lee WC, Shin JY, Lee S, Bleazard T, Won JK, Kim YT, Kim JI, Kang JH, Seo JS. A transforming KIF5B and RET gene fusion in lung adenocarcinoma revealed from whole-genome and transcriptome sequencing. *Genome research*. 2012;22(3):436-45. Epub 2011/12/24. doi: 10.1101/gr.133645.111. PubMed PMID: 22194472; PMCID: PMC3290779.
58. Kohno T, Ichikawa H, Totoki Y, Yasuda K, Hiramoto M, Nammo T, Sakamoto H, Tsuta K, Furuta K, Shimada Y, Iwakawa R, Ogiwara H, Oike T, Enari M, Schetter AJ, Okayama H, Haugen A, Skaug V, Chiku S, Yamanaka I, Arai Y, Watanabe S, Sekine I, Ogawa S, Harris CC, Tsuda H, Yoshida T, Yokota J, Shibata T. KIF5B-RET fusions in lung adenocarcinoma. *Nature medicine*. 2012;18(3):375-7. Epub 2012/02/14. doi: 10.1038/nm.2644. PubMed PMID: 22327624.
59. Lipson D, Capelletti M, Yelensky R, Otto G, Parker A, Jarosz M, Curran JA, Balasubramanian S, Bloom T, Brennan KW, Donahue A, Downing SR, Frampton GM, Garcia L, Juhn F, Mitchell KC, White E, White J, Zwirko Z, Peretz T, Nechushtan H, Soussan-Gutman L, Kim J, Sasaki H, Kim HR, Park SI, Ercan D, Sheehan CE, Ross JS, Cronin MT, Janne PA, Stephens PJ. Identification of new ALK and RET gene fusions from colorectal and lung cancer biopsies. *Nature medicine*. 2012;18(3):382-4. Epub 2012/02/14. doi: 10.1038/nm.2673. PubMed PMID: 22327622; PMCID: PMC3916180.
60. Knudson AG. Antioncogenes and human cancer. *Proceedings of the National Academy of Sciences of the United States of America*. 1993;90(23):10914-21. Epub 1993/12/01. PubMed PMID: 7902574; PMCID: PMC47892.
61. Wistuba II, Berry J, Behrens C, Maitra A, Shivapurkar N, Milchgrub S, Mackay B, Minna JD, Gazdar AF. Molecular changes in the bronchial epithelium of patients with small cell lung cancer. *Clin Cancer Res*. 2000;6(7):2604-10. Epub 2000/07/29. PubMed PMID: 10914700; PMCID: PMC5164924.
62. D'Amico D, Carbone D, Mitsudomi T, Nau M, Fedorko J, Russell E, Johnson B, Buchhagen D, Bodner S, Phelps R, et al. High frequency of somatically acquired p53 mutations in small-cell lung cancer cell lines and tumors. *Oncogene*. 1992;7(2):339-46. Epub 1992/02/01. PubMed PMID: 1312696.
63. Mogi A, Kuwano H. TP53 mutations in nonsmall cell lung cancer. *Journal of biomedicine & biotechnology*. 2011;2011:583929. Epub 2011/02/19. doi: 10.1155/2011/583929. PubMed PMID: 21331359; PMCID: PMC3035360.
64. Pfeifer GP, Denissenko MF, Olivier M, Tretyakova N, Hecht SS, Hainaut P. Tobacco smoke carcinogens, DNA damage and p53 mutations in smoking-associated cancers. *Oncogene*. 2002;21(48):7435-51. Epub 2002/10/16. doi: 10.1038/sj.onc.1205803. PubMed PMID: 12379884.
65. Vazquez A, Bond EE, Levine AJ, Bond GL. The genetics of the p53 pathway, apoptosis and cancer therapy. *Nature reviews Drug discovery*. 2008;7(12):979-87. Epub 2008/12/02. doi: 10.1038/nrd2656. PubMed PMID: 19043449.
66. Husgafvel-Pursiainen K, Boffetta P, Kannio A, Nyberg F, Pershagen G, Mukeria A, Constantinescu V, Fortes C, Benhamou S. p53 mutations and exposure to environmental tobacco smoke in a multicenter study on lung cancer. *Cancer Res*. 2000;60(11):2906-11. Epub 2000/06/13. PubMed PMID: 10850436.
67. Kosaka T, Yatabe Y, Endoh H, Kuwano H, Takahashi T, Mitsudomi T. Mutations of the epidermal growth factor receptor gene in lung cancer: biological and clinical implications. *Cancer Res*. 2004;64(24):8919-23. Epub 2004/12/18. doi: 10.1158/0008-5472.can-04-2818. PubMed PMID: 15604253.
68. Cully M, You H, Levine AJ, Mak TW. Beyond PTEN mutations: the PI3K pathway as an integrator of multiple inputs during tumorigenesis. *Nat Rev Cancer*. 2006;6(3):184-92. Epub 2006/02/03. doi: 10.1038/nrc1819. PubMed PMID: 16453012.

## REFERENCES

69. Marignani PA. LKB1, the multitasking tumour suppressor kinase. *Journal of clinical pathology*. 2005;58(1):15-9. Epub 2004/12/30. doi: 10.1136/jcp.2003.015255. PubMed PMID: 15623475; PMCID: PMC1770539.
70. Koivunen JP, Kim J, Lee J, Rogers AM, Park JO, Zhao X, Naoki K, Okamoto I, Nakagawa K, Yeap BY, Meyerson M, Wong KK, Richards WG, Sugarbaker DJ, Johnson BE, Janne PA. Mutations in the LKB1 tumour suppressor are frequently detected in tumours from Caucasian but not Asian lung cancer patients. *Br J Cancer*. 2008;99(2):245-52. Epub 2008/07/03. doi: 10.1038/sj.bjc.6604469. PubMed PMID: 18594528; PMCID: PMC2480968.
71. Matsumoto S, Iwakawa R, Takahashi K, Kohno T, Nakanishi Y, Matsuno Y, Suzuki K, Nakamoto M, Shimizu E, Minna JD, Yokota J. Prevalence and specificity of LKB1 genetic alterations in lung cancers. *Oncogene*. 2007;26(40):5911-8. Epub 2007/03/27. doi: 10.1038/sj.onc.1210418. PubMed PMID: 17384680; PMCID: PMC3457639.
72. Wikman H, Kettunen E. Regulation of the G1/S phase of the cell cycle and alterations in the RB pathway in human lung cancer. *Expert review of anticancer therapy*. 2006;6(4):515-30. Epub 2006/04/15. doi: 10.1586/14737140.6.4.515. PubMed PMID: 16613540.
73. Harbour JW, Lai SL, Whang-Peng J, Gazdar AF, Minna JD, Kaye FJ. Abnormalities in structure and expression of the human retinoblastoma gene in SCLC. *Science*. 1988;241(4863):353-7. Epub 1988/07/15. PubMed PMID: 2838909.
74. Raso MG, Wistuba, II. Molecular pathogenesis of early-stage non-small cell lung cancer and a proposal for tissue banking to facilitate identification of new biomarkers. *Journal of thoracic oncology : official publication of the International Association for the Study of Lung Cancer*. 2007;2(7 Suppl 3):S128-35. Epub 2007/07/19. doi: 10.1097/JTO.0b013e318074fe42. PubMed PMID: 17603309.
75. Trimarchi JM, Lees JA. Sibling rivalry in the E2F family. *Nature reviews Molecular cell biology*. 2002;3(1):11-20. Epub 2002/02/02. doi: 10.1038/nrm714. PubMed PMID: 11823794.
76. Otterson GA, Kratzke RA, Coxon A, Kim YW, Kaye FJ. Absence of p16INK4 protein is restricted to the subset of lung cancer lines that retains wildtype RB. *Oncogene*. 1994;9(11):3375-8. Epub 1994/11/01. PubMed PMID: 7936665.
77. Brambilla E, Moro D, Gazzeri S, Brambilla C. Alterations of expression of Rb, p16(INK4A) and cyclin D1 in non-small cell lung carcinoma and their clinical significance. *The Journal of pathology*. 1999;188(4):351-60. Epub 1999/08/10. doi: 10.1002/(sici)1096-9896(199908)188:4<351::aid-path385>3.0.co;2-w. PubMed PMID: 10440744.
78. Govindan R, Page N, Morgensztern D, Read W, Tierney R, Vlahiotis A, Spitznagel EL, Piccirillo J. Changing epidemiology of small-cell lung cancer in the United States over the last 30 years: analysis of the surveillance, epidemiologic, and end results database. *Journal of clinical oncology : official journal of the American Society of Clinical Oncology*. 2006;24(28):4539-44. Epub 2006/09/30. doi: 10.1200/jco.2005.04.4859. PubMed PMID: 17008692.
79. Breathnach OS, Freidlin B, Conley B, Green MR, Johnson DH, Gandara DR, O'Connell M, Shepherd FA, Johnson BE. Twenty-two years of phase III trials for patients with advanced non-small-cell lung cancer: sobering results. *Journal of clinical oncology : official journal of the American Society of Clinical Oncology*. 2001;19(6):1734-42. Epub 2001/03/17. doi: 10.1200/jco.2001.19.6.1734. PubMed PMID: 11251004.
80. Pylayeva-Gupta Y, Grabocka E, Bar-Sagi D. RAS oncogenes: weaving a tumorigenic web. *Nat Rev Cancer*. 2011;11(11):761-74. Epub 2011/10/14. doi: 10.1038/nrc3106. PubMed PMID: 21993244; PMCID: PMC3632399.
81. Naidoo J, Drilon A. KRAS-Mutant Lung Cancers in the Era of Targeted Therapy. *Advances in experimental medicine and biology*. 2016;893:155-78. Epub 2015/12/17. doi: 10.1007/978-3-319-24223-1\_8. PubMed PMID: 26667343.

## REFERENCES

82. Kris MG, Johnson BE, Berry LD, et al. Using multiplexed assays of oncogenic drivers in lung cancers to select targeted drugs. *JAMA*. 2014;311(19):1998-2006. doi: 10.1001/jama.2014.3741.
83. Kwak EL, Bang YJ, Camidge DR, Shaw AT, Solomon B, Maki RG, Ou SH, Dezube BJ, Janne PA, Costa DB, Varella-Garcia M, Kim WH, Lynch TJ, Fidias P, Stubbs H, Engelman JA, Sequist LV, Tan W, Gandhi L, Mino-Kenudson M, Wei GC, Shreeve SM, Ratain MJ, Settleman J, Christensen JG, Haber DA, Wilner K, Salgia R, Shapiro GI, Clark JW, Iafrate AJ. Anaplastic lymphoma kinase inhibition in non-small-cell lung cancer. *N Engl J Med*. 2010;363(18):1693-703. Epub 2010/10/29. doi: 10.1056/NEJMoa1006448. PubMed PMID: 20979469; PMCID: PMC3014291.
84. Shaw AT, Kim DW, Mehra R, Tan DS, Felip E, Chow LQ, Camidge DR, Vansteenkiste J, Sharma S, De Pas T, Riely GJ, Solomon BJ, Wolf J, Thomas M, Schuler M, Liu G, Santoro A, Lau YY, Goldwasser M, Boral AL, Engelman JA. Ceritinib in ALK-rearranged non-small-cell lung cancer. *N Engl J Med*. 2014;370(13):1189-97. Epub 2014/03/29. doi: 10.1056/NEJMoa1311107. PubMed PMID: 24670165; PMCID: PMC4079055.
85. Paik PK, Arcila ME, Fara M, Sima CS, Miller VA, Kris MG, Ladanyi M, Riely GJ. Clinical characteristics of patients with lung adenocarcinomas harboring BRAF mutations. *Journal of clinical oncology : official journal of the American Society of Clinical Oncology*. 2011;29(15):2046-51. Epub 2011/04/13. doi: 10.1200/jco.2010.33.1280. PubMed PMID: 21483012; PMCID: PMC3107760.
86. Rubinstein JC, Sznol M, Pavlick AC, Ariyan S, Cheng E, Bacchiocchi A, Kluger HM, Narayan D, Halaban R. Incidence of the V600K mutation among melanoma patients with BRAF mutations, and potential therapeutic response to the specific BRAF inhibitor PLX4032. *J Transl Med*. 2010;8:67. doi: 10.1186/1479-5876-8-67. PubMed PMID: 20630094; PMCID: PMC2917408.
87. Robinson SD, O'Shaughnessy JA, Cowey CL, Konduri K. BRAF V600E-mutated lung adenocarcinoma with metastases to the brain responding to treatment with vemurafenib. *Lung Cancer*. 2014;85(2):326-30. Epub 2014/06/04. doi: 10.1016/j.lungcan.2014.05.009. PubMed PMID: 24888229.
88. Peters S, Michielin O, Zimmermann S. Dramatic response induced by vemurafenib in a BRAF V600E-mutated lung adenocarcinoma. *Journal of clinical oncology : official journal of the American Society of Clinical Oncology*. 2013;31(20):e341-4. Epub 2013/06/05. doi: 10.1200/jco.2012.47.6143. PubMed PMID: 23733758.
89. Brower V. NCI-MATCH pairs tumor mutations with matching drugs. *Nature Research*; 2015.
90. Kumar R, Collins D, Dolly S, McDonald F, O'Brien ME, Yap TA. Targeting the PD-1/PD-L1 axis in non-small cell lung cancer. *Current problems in cancer*. 2016. Epub 2017/02/19. doi: 10.1016/j.currproblcancer.2016.12.002. PubMed PMID: 28214087.
91. Ohaegbulam KC, Assal A, Lazar-Molnar E, Yao Y, Zang X. Human cancer immunotherapy with antibodies to the PD-1 and PD-L1 pathway. *Trends in molecular medicine*. 2015;21(1):24-33. Epub 2014/12/03. doi: 10.1016/j.molmed.2014.10.009. PubMed PMID: 25440090; PMCID: PMC4282825.
92. Scapin G, Yang X, Prosis WW, McCoy M, Reichert P, Johnston JM, Kashi RS, Strickland C. Structure of full-length human anti-PD1 therapeutic IgG4 antibody pembrolizumab. *Nature structural & molecular biology*. 2015;22(12):953-8. Epub 2015/11/26. doi: 10.1038/nsmb.3129. PubMed PMID: 26595420.
93. Wang C, Thudium KB, Han M, Wang XT, Huang H, Feingersh D, Garcia C, Wu Y, Kuhne M, Srinivasan M, Singh S, Wong S, Garner N, Leblanc H, Bunch RT, Blanset D, Selby MJ, Korman AJ. In vitro characterization of the anti-PD-1 antibody nivolumab, BMS-936558, and in vivo toxicology in non-human primates. *Cancer immunology research*. 2014;2(9):846-56. Epub 2014/05/30. doi: 10.1158/2326-6066.cir-14-0040. PubMed PMID: 24872026.

## REFERENCES

94. Fehrenbacher L, Spira A, Ballinger M, Kowanetz M, Vansteenkiste J, Mazieres J, Park K, Smith D, Artal-Cortes A, Lewanski C, Braiteh F, Waterkamp D, He P, Zou W, Chen DS, Yi J, Sandler A, Rittmeyer A. Atezolizumab versus docetaxel for patients with previously treated non-small-cell lung cancer (POPLAR): a multicentre, open-label, phase 2 randomised controlled trial. *Lancet* (London, England). 2016;387(10030):1837-46. Epub 2016/03/14. doi: 10.1016/s0140-6736(16)00587-0. PubMed PMID: 26970723.
95. Prenzel N, Fischer OM, Streit S, Hart S, Ullrich A. The epidermal growth factor receptor family as a central element for cellular signal transduction and diversification. *Endocr Relat Cancer*. 2001;8(1):11-31. Epub 2001/05/15. PubMed PMID: 11350724.
96. Garrett TP, McKern NM, Lou M, Elleman TC, Adams TE, Lovrecz GO, Zhu HJ, Walker F, Frenkel MJ, Hoyne PA, Jorissen RN, Nice EC, Burgess AW, Ward CW. Crystal structure of a truncated epidermal growth factor receptor extracellular domain bound to transforming growth factor alpha. *Cell*. 2002;110(6):763-73. Epub 2002/09/26. PubMed PMID: 12297049.
97. Bertolini G, D'Amico L, Moro M, Landoni E, Perego P, Miceli R, Gatti L, Andriani F, Wong D, Caserini R, Tortoreto M, Milione M, Ferracini R, Mariani L, Pastorino U, Roato I, Sozzi G, Roz L. Microenvironment-Modulated Metastatic CD133+/CXCR4+/EpCAM- Lung Cancer-Initiating Cells Sustain Tumor Dissemination and Correlate with Poor Prognosis. *Cancer Research*. 2015;75(17):3636-49. doi: 10.1158/0008-5472.can-14-3781.
98. Hynes NE, Horsch K, Olayioye MA, Badache A. The ErbB receptor tyrosine family as signal integrators. *Endocr Relat Cancer*. 2001;8(3):151-9. Epub 2001/09/22. PubMed PMID: 11566606.
99. Scagliotti GV, Selvaggi G, Novello S, Hirsch FR. The biology of epidermal growth factor receptor in lung cancer. *Clin Cancer Res*. 2004;10(12 Pt 2):4227s-32s. Epub 2004/06/26. doi: 10.1158/1078-0432.ccr-040007. PubMed PMID: 15217963.
100. Yarden Y, Sliwkowski MX. Untangling the ErbB signalling network. *Nature reviews Molecular cell biology*. 2001;2(2):127-37. Epub 2001/03/17. doi: 10.1038/35052073. PubMed PMID: 11252954.
101. Kestler HA, Wawra C, Kracher B, Kuhl M. Network modeling of signal transduction: establishing the global view. *BioEssays : news and reviews in molecular, cellular and developmental biology*. 2008;30(11-12):1110-25. Epub 2008/10/22. doi: 10.1002/bies.20834. PubMed PMID: 18937364.
102. Blume-Jensen P, Hunter T. Oncogenic kinase signalling. *Nature*. 2001;411(6835):355-65. Epub 2001/05/18. doi: 10.1038/35077225. PubMed PMID: 11357143.
103. Sasaoka T, Langlois WJ, Leitner JW, Draznin B, Olefsky JM. The signaling pathway coupling epidermal growth factor receptors to activation of p21ras. *J Biol Chem*. 1994;269(51):32621-5. Epub 1994/12/23. PubMed PMID: 7798267.
104. Wasylyk B, Hagman J, Gutierrez-Hartmann A. Ets transcription factors: nuclear effectors of the Ras-MAP-kinase signaling pathway. *Trends Biochem Sci*. 1998;23(6):213-6. Epub 1998/06/30. PubMed PMID: 9644975.
105. Hsieh YS, Chu SC, Yang SF, Chen PN, Liu YC, Lu KH. Silibinin suppresses human osteosarcoma MG-63 cell invasion by inhibiting the ERK-dependent c-Jun/AP-1 induction of MMP-2. *Carcinogenesis*. 2007;28(5):977-87. Epub 2006/11/23. doi: 10.1093/carcin/bgl221. PubMed PMID: 17116726.
106. Al-azawi D, Ilroy MM, Kelly G, Redmond AM, Bane FT, Cocchiglia S, Hill AD, Young LS. Ets-2 and p160 proteins collaborate to regulate c-Myc in endocrine resistant breast cancer. *Oncogene*. 2008;27(21):3021-31. Epub 2007/12/07. doi: 10.1038/sj.onc.1210964. PubMed PMID: 18059336.
107. Datta SR, Dudek H, Tao X, Masters S, Fu H, Gotoh Y, Greenberg ME. Akt phosphorylation of BAD couples survival signals to the cell-intrinsic death machinery. *Cell*. 1997;91(2):231-41. Epub 1997/11/05. PubMed PMID: 9346240.

## REFERENCES

108. Laplante M, Sabatini DM. mTOR signaling in growth control and disease. *Cell*. 2012;149(2):274-93. doi: 10.1016/j.cell.2012.03.017. PubMed PMID: PMC3331679.
109. Giannopoulou E, Nikolakopoulos A, Kotsirilou D, Lampropoulou A, Raftopoulou S, Papadimitriou E, Theocharis AD, Makatsoris T, Fasseas K, Kalofonos HP. Epidermal growth factor receptor status and Notch inhibition in non-small cell lung cancer cells. *Journal of Biomedical Science*. 2015;22:98. doi: 10.1186/s12929-015-0196-1. PubMed PMID: PMC4619334.
110. Pellegrini S, Dusanter-Fourt I. The structure, regulation and function of the Janus kinases (JAKs) and the signal transducers and activators of transcription (STATs). *European journal of biochemistry*. 1997;248(3):615-33. Epub 1997/10/28. PubMed PMID: 9342212.
111. O'Shea JJ, Schwartz DM, Villarino AV, Gadina M, McInnes IB, Laurence A. The JAK-STAT pathway: impact on human disease and therapeutic intervention. *Annual review of medicine*. 2015;66:311-28. Epub 2015/01/15. doi: 10.1146/annurev-med-051113-024537. PubMed PMID: 25587654.
112. Quesnelle KM, Boehm AL, Grandis JR. STAT-mediated EGFR signaling in cancer. *J Cell Biochem*. 2007;102(2):311-9. Epub 2007/07/31. doi: 10.1002/jcb.21475. PubMed PMID: 17661350.
113. Grandis JR, Sok JC. Signaling through the epidermal growth factor receptor during the development of malignancy. *Pharmacology & therapeutics*. 2004;102(1):37-46. Epub 2004/04/02. doi: 10.1016/j.pharmthera.2004.01.002. PubMed PMID: 15056497.
114. Lui VW, Grandis JR. EGFR-mediated cell cycle regulation. *Anticancer research*. 2002;22(1a):1-11. Epub 2002/05/23. PubMed PMID: 12017269.
115. Tokumo M, Toyooka S, Kiura K, Shigematsu H, Tomii K, Aoe M, Ichimura K, Tsuda T, Yano M, Tsukuda K, Tabata M, Ueoka H, Tanimoto M, Date H, Gazdar AF, Shimizu N. The relationship between epidermal growth factor receptor mutations and clinicopathologic features in non-small cell lung cancers. *Clin Cancer Res*. 2005;11(3):1167-73. Epub 2005/02/15. PubMed PMID: 15709185.
116. Marchetti A, Ardizzone A, Papotti M, Crino L, Rossi G, Gridelli C, Barberis M, Maiorano E, Normanno N, Taddei GL, Scagliotti G, Clemente C, Pinto C. Recommendations for the analysis of ALK gene rearrangements in non-small-cell lung cancer: a consensus of the Italian Association of Medical Oncology and the Italian Society of Pathology and Cytopathology. *Journal of thoracic oncology : official publication of the International Association for the Study of Lung Cancer*. 2013;8(3):352-8. Epub 2013/02/15. doi: 10.1097/JTO.0b013e31827d5280. PubMed PMID: 23407559.
117. Sordella R, Bell DW, Haber DA, Settleman J. Gefitinib-sensitizing EGFR mutations in lung cancer activate anti-apoptotic pathways. *Science*. 2004;305(5687):1163-7. Epub 2004/07/31. doi: 10.1126/science.1101637. PubMed PMID: 15284455.
118. Sasaki H, Kawano O, Endo K, Yukiue H, Yano M, Fujii Y. EGFRvIII mutation in lung cancer correlates with increased EGFR copy number. *Oncology reports*. 2007;17(2):319-23. Epub 2007/01/05. PubMed PMID: 17203167.
119. Heist RS, Sequist LV, Engelman JA. Genetic changes in squamous cell lung cancer: a review. *Journal of thoracic oncology : official publication of the International Association for the Study of Lung Cancer*. 2012;7(5):924-33. Epub 2012/06/23. doi: 10.1097/JTO.0b013e31824cc334. PubMed PMID: 22722794; PMCID: PMC3404741.
120. Balak MN, Gong Y, Riely GJ, Somwar R, Li AR, Zakowski MF, Chiang A, Yang G, Ouerfelli O, Kris MG, Ladanyi M, Miller VA, Pao W. Novel D761Y and common secondary T790M mutations in epidermal growth factor receptor-mutant lung adenocarcinomas with acquired resistance to kinase inhibitors. *Clin Cancer Res*. 2006;12(21):6494-501. Epub 2006/11/07. doi: 10.1158/1078-0432.ccr-06-1570. PubMed PMID: 17085664.

## REFERENCES

121. Hirsch FR, Herbst RS, Olsen C, Chansky K, Crowley J, Kelly K, Franklin WA, Bunn PA, Jr., Varella-Garcia M, Gandara DR. Increased EGFR gene copy number detected by fluorescent in situ hybridization predicts outcome in non-small-cell lung cancer patients treated with cetuximab and chemotherapy. *Journal of clinical oncology : official journal of the American Society of Clinical Oncology*. 2008;26(20):3351-7. Epub 2008/07/10. doi: 10.1200/jco.2007.14.0111. PubMed PMID: 18612151; PMCID: PMC3368372.
122. Zandi R, Larsen AB, Andersen P, Stockhausen MT, Poulsen HS. Mechanisms for oncogenic activation of the epidermal growth factor receptor. *Cellular signalling*. 2007;19(10):2013-23. Epub 2007/08/08. doi: 10.1016/j.cellsig.2007.06.023. PubMed PMID: 17681753.
123. Pedersen MW, Pedersen N, Damstrup L, Villingshoj M, Sonder SU, Rieneck K, Bovin LF, Spang-Thomsen M, Poulsen HS. Analysis of the epidermal growth factor receptor specific transcriptome: effect of receptor expression level and an activating mutation. *J Cell Biochem*. 2005;96(2):412-27. Epub 2005/08/03. doi: 10.1002/jcb.20554. PubMed PMID: 16075456.
124. Fujimoto N, Wislez M, Zhang J, Iwanaga K, Dackor J, Hanna AE, Kalyankrishna S, Cody DD, Price RE, Sato M, Shay JW, Minna JD, Peyton M, Tang X, Massarelli E, Herbst R, Threadgill DW, Wistuba II, Kurie JM. High expression of ErbB family members and their ligands in lung adenocarcinomas that are sensitive to inhibition of epidermal growth factor receptor. *Cancer Res*. 2005;65(24):11478-85. Epub 2005/12/17. doi: 10.1158/0008-5472.can-05-1977. PubMed PMID: 16357156.
125. Rusch V, Baselga J, Cordon-Cardo C, Orazem J, Zaman M, Hoda S, McIntosh J, Kurie J, Dmitrovsky E. Differential expression of the epidermal growth factor receptor and its ligands in primary non-small cell lung cancers and adjacent benign lung. *Cancer Res*. 1993;53(10 Suppl):2379-85. Epub 1993/05/15. PubMed PMID: 7683573.
126. Zhou BB, Peyton M, He B, Liu C, Girard L, Caudler E, Lo Y, Baribaud F, Mikami I, Reguart N, Yang G, Li Y, Yao W, Vaddi K, Gazdar AF, Friedman SM, Jablons DM, Newton RC, Fridman JS, Minna JD, Scherle PA. Targeting ADAM-mediated ligand cleavage to inhibit HER3 and EGFR pathways in non-small cell lung cancer. *Cancer cell*. 2006;10(1):39-50. Epub 2006/07/18. doi: 10.1016/j.ccr.2006.05.024. PubMed PMID: 16843264; PMCID: PMC4451119.
127. Lin Y, Wang X, Jin H. EGFR-TKI resistance in NSCLC patients: mechanisms and strategies. *American Journal of Cancer Research*. 2014;4(5):411-35. PubMed PMID: 25232485; PMCID: PMC4163608.
128. Honegger AM, Dull TJ, Felder S, Van Obberghen E, Bellot F, Szapary D, Schmidt A, Ullrich A, Schlessinger J. Point mutation at the ATP binding site of EGF receptor abolishes protein-tyrosine kinase activity and alters cellular routing. *Cell*. 1987;51(2):199-209. Epub 1987/10/23. PubMed PMID: 3499230.
129. Redemann N, Holzmann B, von Ruden T, Wagner EF, Schlessinger J, Ullrich A. Anti-oncogenic activity of signalling-defective epidermal growth factor receptor mutants. *Molecular and cellular biology*. 1992;12(2):491-8. Epub 1992/02/01. PubMed PMID: 1346334; PMCID: PMC364201.
130. Wakeling AE, Guy SP, Woodburn JR, Ashton SE, Curry BJ, Barker AJ, Gibson KH. ZD1839 (Iressa): an orally active inhibitor of epidermal growth factor signaling with potential for cancer therapy. *Cancer Res*. 2002;62(20):5749-54. Epub 2002/10/18. PubMed PMID: 12384534.
131. Hidalgo M, Siu LL, Nemunaitis J, Rizzo J, Hammond LA, Takimoto C, Eckhardt SG, Tolcher A, Britten CD, Denis L, Ferrante K, Von Hoff DD, Silberman S, Rowinsky EK. Phase I and pharmacologic study of OSI-774, an epidermal growth factor receptor tyrosine kinase inhibitor, in patients with advanced solid malignancies. *Journal of clinical oncology : official journal of the American Society of Clinical Oncology*. 2001;19(13):3267-79. Epub 2001/07/04. doi: 10.1200/jco.2001.19.13.3267. PubMed PMID: 11432895.

## REFERENCES

132. Miller VA, Riely GJ, Zakowski MF, Li AR, Patel JD, Heelan RT, Kris MG, Sandler AB, Carbone DP, Tsao A, Herbst RS, Heller G, Ladanyi M, Pao W, Johnson DH. Molecular characteristics of bronchioloalveolar carcinoma and adenocarcinoma, bronchioloalveolar carcinoma subtype, predict response to erlotinib. *Journal of clinical oncology : official journal of the American Society of Clinical Oncology*. 2008;26(9):1472-8. Epub 2008/03/20. doi: 10.1200/jco.2007.13.0062. PubMed PMID: 18349398.
133. Paez JG, Janne PA, Lee JC, Tracy S, Greulich H, Gabriel S, Herman P, Kaye FJ, Lindeman N, Boggon TJ, Naoki K, Sasaki H, Fujii Y, Eck MJ, Sellers WR, Johnson BE, Meyerson M. EGFR mutations in lung cancer: correlation with clinical response to gefitinib therapy. *Science*. 2004;304(5676):1497-500. Epub 2004/05/01. doi: 10.1126/science.1099314. PubMed PMID: 15118125.
134. Mok TS, Wu YL, Thongprasert S, Yang CH, Chu DT, Saijo N, Sunpaweravong P, Han B, Margono B, Ichinose Y, Nishiwaki Y, Ohe Y, Yang JJ, Chewaskulyong B, Jiang H, Duffield EL, Watkins CL, Armour AA, Fukuoka M. Gefitinib or carboplatin-paclitaxel in pulmonary adenocarcinoma. *N Engl J Med*. 2009;361(10):947-57. Epub 2009/08/21. doi: 10.1056/NEJMoa0810699. PubMed PMID: 19692680.
135. Fukuoka M, Wu YL, Thongprasert S, Sunpaweravong P, Leong SS, Sriuranpong V, Chao TY, Nakagawa K, Chu DT, Saijo N, Duffield EL, Rukazenzov Y, Speake G, Jiang H, Armour AA, To KF, Yang JC, Mok TS. Biomarker analyses and final overall survival results from a phase III, randomized, open-label, first-line study of gefitinib versus carboplatin/paclitaxel in clinically selected patients with advanced non-small-cell lung cancer in Asia (IPASS). *Journal of clinical oncology : official journal of the American Society of Clinical Oncology*. 2011;29(21):2866-74. Epub 2011/06/15. doi: 10.1200/jco.2010.33.4235. PubMed PMID: 21670455.
136. Mitsudomi T, Morita S, Yatabe Y, Negoro S, Okamoto I, Tsurutani J, Seto T, Satouchi M, Tada H, Hirashima T, Asami K, Katakami N, Takada M, Yoshioka H, Shibata K, Kudoh S, Shimizu E, Saito H, Toyooka S, Nakagawa K, Fukuoka M. Gefitinib versus cisplatin plus docetaxel in patients with non-small-cell lung cancer harbouring mutations of the epidermal growth factor receptor (WJTOG3405): an open label, randomised phase 3 trial. *The Lancet Oncology*. 2010;11(2):121-8. Epub 2009/12/22. doi: 10.1016/s1470-2045(09)70364-x. PubMed PMID: 20022809.
137. Rosell R, Carcereny E, Gervais R, Vergnenegre A, Massuti B, Felip E, Palmero R, Garcia-Gomez R, Pallares C, Sanchez JM, Porta R, Cobo M, Garrido P, Longo F, Moran T, Insa A, De Marinis F, Corre R, Bover I, Illiano A, Dansin E, de Castro J, Milella M, Reguart N, Altavilla G, Jimenez U, Provencio M, Moreno MA, Terrasa J, Munoz-Langa J, Valdivia J, Isla D, Domine M, Molinier O, Mazieres J, Baize N, Garcia-Campelo R, Robinet G, Rodriguez-Abreu D, Lopez-Vivanco G, Gebbia V, Ferrera-Delgado L, Bombaron P, Bernabe R, Bearz A, Artal A, Cortesi E, Rolfo C, Sanchez-Ronco M, Drozdowskyj A, Queralt C, de Aguirre I, Ramirez JL, Sanchez JJ, Molina MA, Taron M, Paz-Ares L. Erlotinib versus standard chemotherapy as first-line treatment for European patients with advanced EGFR mutation-positive non-small-cell lung cancer (EURTAC): a multicentre, open-label, randomised phase 3 trial. *The Lancet Oncology*. 2012;13(3):239-46. Epub 2012/01/31. doi: 10.1016/s1470-2045(11)70393-x. PubMed PMID: 22285168.
138. Zhou C, Wu YL, Chen G, Feng J, Liu XQ, Wang C, Zhang S, Wang J, Zhou S, Ren S, Lu S, Zhang L, Hu C, Hu C, Luo Y, Chen L, Ye M, Huang J, Zhi X, Zhang Y, Xiu Q, Ma J, Zhang L, You C. Erlotinib versus chemotherapy as first-line treatment for patients with advanced EGFR mutation-positive non-small-cell lung cancer (OPTIMAL, CTONG-0802): a multicentre, open-label, randomised, phase 3 study. *The Lancet Oncology*. 2011;12(8):735-42. Epub 2011/07/26. doi: 10.1016/s1470-2045(11)70184-x. PubMed PMID: 21783417.
139. Thongprasert S, Duffield E, Saijo N, Wu YL, Yang JC, Chu DT, Liao M, Chen YM, Kuo HP, Negoro S, Lam KC, Armour A, Magill P, Fukuoka M. Health-related quality-of-life in a randomized

## REFERENCES

- phase III first-line study of gefitinib versus carboplatin/paclitaxel in clinically selected patients from Asia with advanced NSCLC (IPASS). *Journal of thoracic oncology : official publication of the International Association for the Study of Lung Cancer*. 2011;6(11):1872-80. Epub 2011/10/21. doi: 10.1097/JTO.0b013e31822adaf7. PubMed PMID: 22011650.
140. Sequist LV, Yang JC, Yamamoto N, O'Byrne K, Hirsh V, Mok T, Geater SL, Orlov S, Tsai CM, Boyer M, Su WC, Bennouna J, Kato T, Gorbunova V, Lee KH, Shah R, Massey D, Zazulina V, Shahidi M, Schuler M. Phase III study of afatinib or cisplatin plus pemetrexed in patients with metastatic lung adenocarcinoma with EGFR mutations. *Journal of clinical oncology : official journal of the American Society of Clinical Oncology*. 2013;31(27):3327-34. Epub 2013/07/03. doi: 10.1200/jco.2012.44.2806. PubMed PMID: 23816960.
141. Yang JC, Wu YL, Schuler M, Sebastian M, Popat S, Yamamoto N, Zhou C, Hu CP, O'Byrne K, Feng J, Lu S, Huang Y, Geater SL, Lee KY, Tsai CM, Gorbunova V, Hirsh V, Bennouna J, Orlov S, Mok T, Boyer M, Su WC, Lee KH, Kato T, Massey D, Shahidi M, Zazulina V, Sequist LV. Afatinib versus cisplatin-based chemotherapy for EGFR mutation-positive lung adenocarcinoma (LUX-Lung 3 and LUX-Lung 6): analysis of overall survival data from two randomised, phase 3 trials. *The Lancet Oncology*. 2015;16(2):141-51. Epub 2015/01/16. doi: 10.1016/s1470-2045(14)71173-8. PubMed PMID: 25589191.
142. Park K, Tan EH, O'Byrne K, Zhang L, Boyer M, Mok T, Hirsh V, Yang JC, Lee KH, Lu S, Shi Y, Kim SW, Laskin J, Kim DW, Arvis CD, Kolbeck K, Laurie SA, Tsai CM, Shahidi M, Kim M, Massey D, Zazulina V, Paz-Ares L. Afatinib versus gefitinib as first-line treatment of patients with EGFR mutation-positive non-small-cell lung cancer (LUX-Lung 7): a phase 2B, open-label, randomised controlled trial. *The Lancet Oncology*. 2016;17(5):577-89. Epub 2016/04/17. doi: 10.1016/s1470-2045(16)30033-x. PubMed PMID: 27083334.
143. Lynch JA, Berse B, Chun D, Rivera D, Filipinski KK, Kulich S, Viernes B, DuVall SL, Kelley MJ. Epidermal Growth Factor Receptor Mutational Testing and Erlotinib Treatment Among Veterans Diagnosed With Lung Cancer in the United States Department of Veterans Affairs. *Clinical lung cancer*. doi: <http://dx.doi.org/10.1016/j.clcc.2016.11.018>.
144. Shepherd FA, Rodrigues Pereira J, Ciuleanu T, Tan EH, Hirsh V, Thongprasert S, Campos D, Maoleekoonpiroj S, Smylie M, Martins R, van Kooten M, Dediu M, Findlay B, Tu D, Johnston D, Bezjak A, Clark G, Santabarbara P, Seymour L. Erlotinib in previously treated non-small-cell lung cancer. *N Engl J Med*. 2005;353(2):123-32. Epub 2005/07/15. doi: 10.1056/NEJMoa050753. PubMed PMID: 16014882.
145. Rivera G, Wakelee HA. Resistance to Therapy. *Cancer treatment and research*. 2016;170:183-202. Epub 2016/08/19. doi: 10.1007/978-3-319-40389-2\_9. PubMed PMID: 27535395.
146. Kazandjian D, Blumenthal GM, Yuan W, He K, Keegan P, Pazdur R. FDA Approval of Gefitinib for the Treatment of Patients with Metastatic EGFR Mutation-Positive Non-Small Cell Lung Cancer. *Clin Cancer Res*. 2016;22(6):1307-12. Epub 2016/03/17. doi: 10.1158/1078-0432.ccr-15-2266. PubMed PMID: 26980062.
147. Sullivan I, Planchard D. Next-Generation EGFR Tyrosine Kinase Inhibitors for Treating EGFR-Mutant Lung Cancer beyond First Line. *Frontiers in medicine*. 2016;3:76. Epub 2017/02/06. doi: 10.3389/fmed.2016.00076. PubMed PMID: 28149837; PMCID: PMC5241298.
148. Gainor JF, Shaw AT. Emerging paradigms in the development of resistance to tyrosine kinase inhibitors in lung cancer. *Journal of clinical oncology : official journal of the American Society of Clinical Oncology*. 2013;31(31):3987-96. Epub 2013/10/09. doi: 10.1200/jco.2012.45.2029. PubMed PMID: 24101047; PMCID: PMC3805932.
149. Sequist LV, Besse B, Lynch TJ, Miller VA, Wong KK, Gitlitz B, Eaton K, Zacharchuk C, Freyman A, Powell C, Ananthkrishnan R, Quinn S, Soria JC. Neratinib, an irreversible pan-ErbB

## REFERENCES

- receptor tyrosine kinase inhibitor: results of a phase II trial in patients with advanced non-small-cell lung cancer. *Journal of clinical oncology : official journal of the American Society of Clinical Oncology*. 2010;28(18):3076-83. Epub 2010/05/19. doi: 10.1200/jco.2009.27.9414. PubMed PMID: 20479403.
150. Miller VA, Hirsh V, Cadranel J, Chen YM, Park K, Kim SW, Zhou C, Su WC, Wang M, Sun Y, Heo DS, Crino L, Tan EH, Chao TY, Shahidi M, Cong XJ, Lorence RM, Yang JC. Afatinib versus placebo for patients with advanced, metastatic non-small-cell lung cancer after failure of erlotinib, gefitinib, or both, and one or two lines of chemotherapy (LUX-Lung 1): a phase 2b/3 randomised trial. *The Lancet Oncology*. 2012;13(5):528-38. Epub 2012/03/29. doi: 10.1016/s1470-2045(12)70087-6. PubMed PMID: 22452896.
151. Reckamp KL, Giaccone G, Camidge DR, Gadgeel SM, Khuri FR, Engelman JA, Koczywas M, Rajan A, Campbell AK, Gernhardt D, Ruiz-Garcia A, Letrent S, Liang J, Taylor I, O'Connell JP, Janne PA. A phase 2 trial of dacomitinib (PF-00299804), an oral, irreversible pan-HER (human epidermal growth factor receptor) inhibitor, in patients with advanced non-small cell lung cancer after failure of prior chemotherapy and erlotinib. *Cancer*. 2014;120(8):1145-54. Epub 2014/02/07. doi: 10.1002/cncr.28561. PubMed PMID: 24501009; PMCID: PMC4164026.
152. Joshi M, Rizvi SM, Belani CP. Afatinib for the treatment of metastatic non-small cell lung cancer. *Cancer management and research*. 2015;7:75-82. Epub 2015/03/04. doi: 10.2147/cmar.s51808. PubMed PMID: 25733926; PMCID: PMC4340466.
153. Khozin S, Weinstock C, Blumenthal GM, Cheng J, He K, Zhuang L, Zhao H, Orbach RC, Fan I, Keegan P, Pazdur R. Osimertinib for the Treatment of Metastatic Epidermal Growth Factor T970M Positive Non-Small Cell Lung Cancer. *Clin Cancer Res*. 2016. Epub 2016/12/08. doi: 10.1158/1078-0432.ccr-16-1773. PubMed PMID: 27923840.
154. Song HN, Jung KS, Yoo KH, Cho J, Lee JY, Lim SH, Kim HS, Sun JM, Lee SH, Ahn JS, Park K, Choi YL, Park W, Ahn MJ. Acquired C797S Mutation upon Treatment with a T790M-Specific Third-Generation EGFR Inhibitor (HM61713) in Non-Small Cell Lung Cancer. *Journal of thoracic oncology : official publication of the International Association for the Study of Lung Cancer*. 2016;11(4):e45-7. Epub 2016/01/11. doi: 10.1016/j.jtho.2015.12.093. PubMed PMID: 26749488.
155. Chabon JJ, Simmons AD, Lovejoy AF, Esfahani MS, Newman AM, Haringsma HJ, Kurtz DM, Stehr H, Scherer F, Karlovich CA, Harding TC, Durkin KA, Otterson GA, Purcell WT, Camidge DR, Goldman JW, Sequist LV, Piotrowska Z, Wakelee HA, Neal JW, Alizadeh AA, Diehn M. Circulating tumour DNA profiling reveals heterogeneity of EGFR inhibitor resistance mechanisms in lung cancer patients. *Nature communications*. 2016;7:11815. Epub 2016/06/11. doi: 10.1038/ncomms11815. PubMed PMID: 27283993; PMCID: PMC4906406.
156. Bersanelli M, Minari R, Bordi P, Gnetti L, Bozzetti C, Squadrilli A, Lagrasta CA, Bottarelli L, Osipova G, Capelletto E, Mor M, Tiseo M. L718Q Mutation as New Mechanism of Acquired Resistance to AZD9291 in EGFR-Mutated NSCLC. *Journal of thoracic oncology : official publication of the International Association for the Study of Lung Cancer*. 2016;11(10):e121-3. Epub 2016/06/04. doi: 10.1016/j.jtho.2016.05.019. PubMed PMID: 27257132.
157. Eberlein CA, Stetson D, Markovets AA, Al-Kadhimi KJ, Lai Z, Fisher PR, Meador CB, Spitzler P, Ichihara E, Ross SJ, Ahdesmaki MJ, Ahmed A, Ratcliffe LE, O'Brien EL, Barnes CH, Brown H, Smith PD, Dry JR, Beran G, Thress KS, Dougherty B, Pao W, Cross DA. Acquired Resistance to the Mutant-Selective EGFR Inhibitor AZD9291 Is Associated with Increased Dependence on RAS Signaling in Preclinical Models. *Cancer Res*. 2015;75(12):2489-500. Epub 2015/04/15. doi: 10.1158/0008-5472.can-14-3167. PubMed PMID: 25870145; PMCID: PMC4605607.
158. Thress KS, Paweletz CP, Felip E, Cho BC, Stetson D, Dougherty B, Lai Z, Markovets A, Vivancos A, Kuang Y, Ercan D, Matthews SE, Cantarini M, Barrett JC, Janne PA, Oxnard GR. Acquired EGFR C797S mutation mediates resistance to AZD9291 in non-small cell lung cancer

## REFERENCES

- harboring EGFR T790M. *Nature medicine*. 2015;21(6):560-2. Epub 2015/05/06. doi: 10.1038/nm.3854. PubMed PMID: 25939061; PMCID: PMC4771182.
159. Pirker R, Filipits M. Monoclonal antibodies against EGFR in non-small cell lung cancer. *Critical reviews in oncology/hematology*. 2011;80(1):1-9. Epub 2010/11/27. doi: 10.1016/j.critrevonc.2010.10.008. PubMed PMID: 21109448.
160. Pirker R. Epidermal growth factor receptor-directed monoclonal antibodies in nonsmall cell lung cancer: an update. *Current opinion in oncology*. 2015;27(2):87-93. Epub 2015/01/31. doi: 10.1097/cco.000000000000162. PubMed PMID: 25636162.
161. Kurai J, Chikumi H, Hashimoto K, Yamaguchi K, Yamasaki A, Sako T, Touge H, Makino H, Takata M, Miyata M, Nakamoto M, Burioka N, Shimizu E. Antibody-dependent cellular cytotoxicity mediated by cetuximab against lung cancer cell lines. *Clin Cancer Res*. 2007;13(5):1552-61. Epub 2007/03/03. doi: 10.1158/1078-0432.ccr-06-1726. PubMed PMID: 17332301.
162. Thienelt CD, Bunn PA, Jr., Hanna N, Rosenberg A, Needle MN, Long ME, Gustafson DL, Kelly K. Multicenter phase I/II study of cetuximab with paclitaxel and carboplatin in untreated patients with stage IV non-small-cell lung cancer. *Journal of clinical oncology : official journal of the American Society of Clinical Oncology*. 2005;23(34):8786-93. Epub 2005/10/26. doi: 10.1200/jco.2005.03.1997. PubMed PMID: 16246975.
163. Robert F, Blumenschein G, Herbst RS, Fossella FV, Tseng J, Saleh MN, Needle M. Phase I/IIa study of cetuximab with gemcitabine plus carboplatin in patients with chemotherapy-naive advanced non-small-cell lung cancer. *Journal of clinical oncology : official journal of the American Society of Clinical Oncology*. 2005;23(36):9089-96. Epub 2005/11/23. doi: 10.1200/jco.2004.00.1438. PubMed PMID: 16301597.
164. Belani CP, Schreeder MT, Steis RG, Guidice RA, Marsland TA, Butler EH, Ramalingam SS. Cetuximab in combination with carboplatin and docetaxel for patients with metastatic or advanced-stage nonsmall cell lung cancer: a multicenter phase 2 study. *Cancer*. 2008;113(9):2512-7. Epub 2008/09/26. doi: 10.1002/cncr.23902. PubMed PMID: 18816622.
165. Pirker R, Pereira JR, Szczesna A, von Pawel J, Krzakowski M, Ramlau R, Vynnychenko I, Park K, Yu CT, Ganul V, Roh JK, Bajetta E, O'Byrne K, de Marinis F, Eberhardt W, Goddemeier T, Emig M, Gatzemeier U. Cetuximab plus chemotherapy in patients with advanced non-small-cell lung cancer (FLEX): an open-label randomised phase III trial. *Lancet (London, England)*. 2009;373(9674):1525-31. Epub 2009/05/05. doi: 10.1016/s0140-6736(09)60569-9. PubMed PMID: 19410716.
166. Lynch TJ, Patel T, Dreisbach L, McCleod M, Heim WJ, Hermann RC, Paschold E, Iannotti NO, Dakhil S, Gorton S, Pautret V, Weber MR, Woytowicz D. Cetuximab and first-line taxane/carboplatin chemotherapy in advanced non-small-cell lung cancer: results of the randomized multicenter phase III trial BMS099. *Journal of clinical oncology : official journal of the American Society of Clinical Oncology*. 2010;28(6):911-7. Epub 2010/01/27. doi: 10.1200/jco.2009.21.9618. PubMed PMID: 20100966.
167. Pirker R, Pereira JR, von Pawel J, Krzakowski M, Ramlau R, Park K, de Marinis F, Eberhardt WE, Paz-Ares L, Storkel S, Schumacher KM, von Heydebreck A, Celik I, O'Byrne KJ. EGFR expression as a predictor of survival for first-line chemotherapy plus cetuximab in patients with advanced non-small-cell lung cancer: analysis of data from the phase 3 FLEX study. *The Lancet Oncology*. 2012;13(1):33-42. Epub 2011/11/08. doi: 10.1016/s1470-2045(11)70318-7. PubMed PMID: 22056021.
168. O'Byrne KJ, Gatzemeier U, Bondarenko I, Barrios C, Eschbach C, Martens UM, Hotko Y, Kortsik C, Paz-Ares L, Pereira JR, von Pawel J, Ramlau R, Roh JK, Yu CT, Stroh C, Celik I, Schueler A, Pirker R. Molecular biomarkers in non-small-cell lung cancer: a retrospective analysis of data from

## REFERENCES

- the phase 3 FLEX study. *The Lancet Oncology*. 2011;12(8):795-805. Epub 2011/07/26. doi: 10.1016/s1470-2045(11)70189-9. PubMed PMID: 21782507.
169. Khambata-Ford S, Harbison CT, Hart LL, Awad M, Xu LA, Horak CE, Dakhil S, Hermann RC, Lynch TJ, Weber MR. Analysis of potential predictive markers of cetuximab benefit in BMS099, a phase III study of cetuximab and first-line taxane/carboplatin in advanced non-small-cell lung cancer. *Journal of clinical oncology : official journal of the American Society of Clinical Oncology*. 2010;28(6):918-27. Epub 2010/01/27. doi: 10.1200/jco.2009.25.2890. PubMed PMID: 20100958.
170. Paz-Ares L, Mezger J, Ciuleanu TE, Fischer JR, von Pawel J, Provencio M, Kazarnowicz A, Losonczy G, de Castro G, Jr., Szczesna A, Crino L, Reck M, Ramlau R, Ulsperger E, Schumann C, Miziara JE, Lessa AE, Dediu M, Balint B, Depenbrock H, Soldatenkova V, Kurek R, Hirsch FR, Thatcher N, Socinski MA. Necitumumab plus pemetrexed and cisplatin as first-line therapy in patients with stage IV non-squamous non-small-cell lung cancer (INSPIRE): an open-label, randomised, controlled phase 3 study. *The Lancet Oncology*. 2015;16(3):328-37. Epub 2015/02/24. doi: 10.1016/s1470-2045(15)70046-x. PubMed PMID: 25701171.
171. Thatcher N, Hirsch FR, Luft AV, Szczesna A, Ciuleanu TE, Dediu M, Ramlau R, Galiulin RK, Balint B, Losonczy G, Kazarnowicz A, Park K, Schumann C, Reck M, Depenbrock H, Nanda S, Kruljac-Letunic A, Kurek R, Paz-Ares L, Socinski MA. Necitumumab plus gemcitabine and cisplatin versus gemcitabine and cisplatin alone as first-line therapy in patients with stage IV squamous non-small-cell lung cancer (SQUIRE): an open-label, randomised, controlled phase 3 trial. *The Lancet Oncology*. 2015;16(7):763-74. Epub 2015/06/06. doi: 10.1016/s1470-2045(15)00021-2. PubMed PMID: 26045340.
172. Garnock-Jones KP. Necitumumab: First Global Approval. *Drugs*. 2016;76(2):283-9. Epub 2016/01/06. doi: 10.1007/s40265-015-0537-0. PubMed PMID: 26729188.
173. Greillier L, Tomasini P, Barlesi F. Necitumumab for non-small cell lung cancer. Expert opinion on biological therapy. 2015;15(8):1231-9. Epub 2015/06/09. doi: 10.1517/14712598.2015.1055243. PubMed PMID: 26051700.
174. Smith AL, Robin TP, Ford HL. Molecular Pathways: Targeting the TGF-beta Pathway for Cancer Therapy. *Clin Cancer Res*. 2012;18(17):4514-21. doi: 10.1158/1078-0432.CCR-11-3224. PubMed PMID: 22711703.
175. Tian M, Neil JR, Schiemann WP. Transforming growth factor-beta and the hallmarks of cancer. *Cellular signalling*. 2011;23(6):951-62. doi: 10.1016/j.cellsig.2010.10.015. PubMed PMID: 20940046; PMCID: 3076078.
176. Derynck R, Akhurst RJ. Differentiation plasticity regulated by TGF-beta family proteins in development and disease. *Nat Cell Biol*. 2007;9(9):1000-4. Epub 2007/09/01. doi: 10.1038/ncb434. PubMed PMID: 17762890.
177. Roberts AB, Wakefield LM. The two faces of transforming growth factor beta in carcinogenesis. *Proceedings of the National Academy of Sciences of the United States of America*. 2003;100(15):8621-3. Epub 2003/07/16. doi: 10.1073/pnas.1633291100. PubMed PMID: 12861075; PMCID: PMC166359.
178. Shi Y, Massague J. Mechanisms of TGF-beta signaling from cell membrane to the nucleus. *Cell*. 2003;113(6):685-700. Epub 2003/06/18. PubMed PMID: 12809600.
179. Massague J. TGFbeta in Cancer. *Cell*. 2008;134(2):215-30. doi: 10.1016/j.cell.2008.07.001. PubMed PMID: 18662538.
180. Galliher AJ, Neil JR, Schiemann WP. Role of transforming growth factor-beta in cancer progression. *Future oncology*. 2006;2(6):743-63. Epub 2006/12/13. doi: 10.2217/14796694.2.6.743. PubMed PMID: 17155901.

## REFERENCES

181. Derynck R, Zhang YE. Smad-dependent and Smad-independent pathways in TGF-beta family signalling. *Nature*. 2003;425(6958):577-84. Epub 2003/10/10. doi: 10.1038/nature02006. PubMed PMID: 14534577.
182. Sankar S, Mahooti-Brooks N, Centrella M, McCarthy TL, Madri JA. Expression of transforming growth factor type III receptor in vascular endothelial cells increases their responsiveness to transforming growth factor beta 2. *J Biol Chem*. 1995;270(22):13567-72. Epub 1995/06/02. PubMed PMID: 7768960.
183. Massague J, Wotton D. Transcriptional control by the TGF-beta/Smad signaling system. *The EMBO journal*. 2000;19(8):1745-54. Epub 2000/04/25. doi: 10.1093/emboj/19.8.1745. PubMed PMID: 10775259; PMCID: PMC302010.
184. Dennler S, Itoh S, Vivien D, ten Dijke P, Huet S, Gauthier JM. Direct binding of Smad3 and Smad4 to critical TGF beta-inducible elements in the promoter of human plasminogen activator inhibitor-type 1 gene. *The EMBO journal*. 1998;17(11):3091-100. doi: 10.1093/emboj/17.11.3091. PubMed PMID: 9606191; PMCID: 1170648.
185. Tsukazaki T, Chiang TA, Davison AF, Attisano L, Wrana JL. SARA, a FYVE domain protein that recruits Smad2 to the TGFbeta receptor. *Cell*. 1998;95(6):779-91. Epub 1998/12/29. PubMed PMID: 9865696.
186. Miura S, Takeshita T, Asao H, Kimura Y, Murata K, Sasaki Y, Hanai JI, Beppu H, Tsukazaki T, Wrana JL, Miyazono K, Sugamura K. Hgs (Hrs), a FYVE domain protein, is involved in Smad signaling through cooperation with SARA. *Molecular and cellular biology*. 2000;20(24):9346-55. Epub 2000/11/30. PubMed PMID: 11094085; PMCID: PMC102191.
187. Hocevar BA, Smine A, Xu XX, Howe PH. The adaptor molecule Disabled-2 links the transforming growth factor beta receptors to the Smad pathway. *The EMBO journal*. 2001;20(11):2789-801. Epub 2001/06/02. doi: 10.1093/emboj/20.11.2789. PubMed PMID: 11387212; PMCID: PMC125498.
188. Hayashi H, Abdollah S, Qiu Y, Cai J, Xu YY, Grinnell BW, Richardson MA, Topper JN, Gimbrone MA, Jr., Wrana JL, Falb D. The MAD-related protein Smad7 associates with the TGFbeta receptor and functions as an antagonist of TGFbeta signaling. *Cell*. 1997;89(7):1165-73. Epub 1997/06/27. PubMed PMID: 9215638.
189. Kavsak P, Rasmussen RK, Causing CG, Bonni S, Zhu H, Thomsen GH, Wrana JL. Smad7 binds to Smurf2 to form an E3 ubiquitin ligase that targets the TGF beta receptor for degradation. *Molecular cell*. 2000;6(6):1365-75. Epub 2001/02/13. PubMed PMID: 11163210.
190. Derynck R, Muthusamy BP, Saeteurn KY. Signaling pathway cooperation in TGF-beta-induced epithelial-mesenchymal transition. *Current opinion in cell biology*. 2014;31:56-66. Epub 2014/09/23. doi: 10.1016/j.ceb.2014.09.001. PubMed PMID: 25240174.
191. Lin X, Duan X, Liang YY, Su Y, Wrighton KH, Long J, Hu M, Davis CM, Wang J, Brunicardi FC, Shi Y, Chen YG, Meng A, Feng XH. PPM1A functions as a Smad phosphatase to terminate TGFbeta signaling. *Cell*. 2006;125(5):915-28. Epub 2006/06/06. doi: 10.1016/j.cell.2006.03.044. PubMed PMID: 16751101.
192. Lo RS, Massague J. Ubiquitin-dependent degradation of TGF-beta-activated smad2. *Nat Cell Biol*. 1999;1(8):472-8. Epub 1999/12/10. doi: 10.1038/70258. PubMed PMID: 10587642.
193. Choy L, Derynck R. The type II transforming growth factor (TGF)-beta receptor-interacting protein TRIP-1 acts as a modulator of the TGF-beta response. *J Biol Chem*. 1998;273(47):31455-62. Epub 1998/11/13. PubMed PMID: 9813058.
194. Massague J, Gomis RR. The logic of TGFbeta signaling. *FEBS letters*. 2006;580(12):2811-20. Epub 2006/05/09. doi: 10.1016/j.febslet.2006.04.033. PubMed PMID: 16678165.
195. Frederick JP, Liberati NT, Waddell DS, Shi Y, Wang XF. Transforming growth factor beta-mediated transcriptional repression of c-myc is dependent on direct binding of Smad3 to a novel

## REFERENCES

- repressive Smad binding element. *Molecular and cellular biology*. 2004;24(6):2546-59. Epub 2004/03/03. PubMed PMID: 14993291; PMCID: PMC355825.
196. Kang Y, Chen CR, Massague J. A self-enabling TGFbeta response coupled to stress signaling: Smad engages stress response factor ATF3 for Id1 repression in epithelial cells. *Molecular cell*. 2003;11(4):915-26. Epub 2003/04/30. PubMed PMID: 12718878.
197. Seoane J, Pouponnot C, Staller P, Schader M, Eilers M, Massague J. TGFbeta influences Myc, Miz-1 and Smad to control the CDK inhibitor p15INK4b. *Nat Cell Biol*. 2001;3(4):400-8. Epub 2001/04/03. doi: 10.1038/35070086. PubMed PMID: 11283614.
198. Moustakas A, Kardassis D. Regulation of the human p21/WAF1/Cip1 promoter in hepatic cells by functional interactions between Sp1 and Smad family members. *Proceedings of the National Academy of Sciences of the United States of America*. 1998;95(12):6733-8. Epub 1998/06/17. PubMed PMID: 9618481; PMCID: PMC22615.
199. Perlman R, Schiemann WP, Brooks MW, Lodish HF, Weinberg RA. TGF-beta-induced apoptosis is mediated by the adapter protein Daxx that facilitates JNK activation. *Nat Cell Biol*. 2001;3(8):708-14. Epub 2001/08/03. doi: 10.1038/35087019. PubMed PMID: 11483955.
200. Bakin AV, Rinehart C, Tomlinson AK, Arteaga CL. p38 mitogen-activated protein kinase is required for TGFbeta-mediated fibroblastic transdifferentiation and cell migration. *J Cell Sci*. 2002;115(Pt 15):3193-206. Epub 2002/07/16. PubMed PMID: 12118074.
201. Yue J, Mulder KM. Activation of the mitogen-activated protein kinase pathway by transforming growth factor-beta. *Methods in molecular biology*. 2000;142:125-31. Epub 2000/05/12. doi: 10.1385/1-59259-053-5:125. PubMed PMID: 10806618.
202. Lamouille S, Derynck R. Cell size and invasion in TGF-beta-induced epithelial to mesenchymal transition is regulated by activation of the mTOR pathway. *The Journal of cell biology*. 2007;178(3):437-51. Epub 2007/07/25. doi: 10.1083/jcb.200611146. PubMed PMID: 17646396; PMCID: PMC2064840.
203. Bakin AV, Tomlinson AK, Bhowmick NA, Moses HL, Arteaga CL. Phosphatidylinositol 3-kinase function is required for transforming growth factor beta-mediated epithelial to mesenchymal transition and cell migration. *J Biol Chem*. 2000;275(47):36803-10. Epub 2000/09/02. doi: 10.1074/jbc.M005912200. PubMed PMID: 10969078.
204. Azuma M, Motegi K, Aota K, Yamashita T, Yoshida H, Sato M. TGF-beta1 inhibits NF-kappaB activity through induction of IkappaB-alpha expression in human salivary gland cells: a possible mechanism of growth suppression by TGF-beta1. *Experimental cell research*. 1999;250(1):213-22. Epub 1999/07/02. doi: 10.1006/excr.1999.4503. PubMed PMID: 10388535.
205. Horowitz JC, Rogers DS, Sharma V, Vittal R, White ES, Cui Z, Thannickal VJ. Combinatorial activation of FAK and AKT by transforming growth factor-beta1 confers an anoikis-resistant phenotype to myofibroblasts. *Cellular signalling*. 2007;19(4):761-71. Epub 2006/11/23. doi: 10.1016/j.cellsig.2006.10.001. PubMed PMID: 17113264; PMCID: PMC1820832.
206. Galliher-Beckley AJ, Schiemann WP. Grb2 binding to Tyr284 in TbetaR-II is essential for mammary tumor growth and metastasis stimulated by TGF-beta. *Carcinogenesis*. 2008;29(2):244-51. Epub 2008/01/05. doi: 10.1093/carcin/bgm245. PubMed PMID: 18174260; PMCID: PMC2615477.
207. Park SS, Eom YW, Kim EH, Lee JH, Min DS, Kim S, Kim SJ, Choi KS. Involvement of c-Src kinase in the regulation of TGF-beta1-induced apoptosis. *Oncogene*. 2004;23(37):6272-81. Epub 2004/06/23. doi: 10.1038/sj.onc.1207856. PubMed PMID: 15208664.
208. Schrantz N, Bourgeade MF, Mouhamad S, Leca G, Sharma S, Vazquez A. p38-mediated regulation of an Fas-associated death domain protein-independent pathway leading to caspase-8 activation during TGFbeta-induced apoptosis in human Burkitt lymphoma B cells BL41. *Mol Biol Cell*. 2001;12(10):3139-51. Epub 2001/10/13. PubMed PMID: 11598198; PMCID: PMC60162.

## REFERENCES

209. Sanchez-Capelo A. Dual role for TGF-beta1 in apoptosis. *Cytokine & growth factor reviews*. 2005;16(1):15-34. Epub 2005/03/01. doi: 10.1016/j.cytogfr.2004.11.002. PubMed PMID: 15733830.
210. Finger EC, Turley RS, Dong M, How T, Fields TA, Blobel GC. TbetaRIII suppresses non-small cell lung cancer invasiveness and tumorigenicity. *Carcinogenesis*. 2008;29(3):528-35. Epub 2008/01/05. doi: 10.1093/carcin/bgm289. PubMed PMID: 18174241.
211. Blobel GC, Schiemann WP, Lodish HF. Role of transforming growth factor beta in human disease. *N Engl J Med*. 2000;342(18):1350-8. Epub 2000/05/04. doi: 10.1056/nejm200005043421807. PubMed PMID: 10793168.
212. Takagi Y, Koumura H, Futamura M, Aoki S, Ymaguchi K, Kida H, Tanemura H, Shimokawa K, Saji S. Somatic alterations of the SMAD-2 gene in human colorectal cancers. *Br J Cancer*. 1998;78(9):1152-5. Epub 1998/11/20. PubMed PMID: 9820171; PMCID: PMC2063002.
213. Tian M, Schiemann WP. The TGF-beta paradox in human cancer: an update. *Future oncology*. 2009;5(2):259-71. doi: 10.2217/14796694.5.2.259. PubMed PMID: 19284383; PMCID: 2710615.
214. Petrocca F, Visone R, Onelli MR, Shah MH, Nicoloso MS, de Martino I, Iliopoulos D, Pilozi E, Liu CG, Negrini M, Cavazzini L, Volinia S, Alder H, Ruco LP, Baldassarre G, Croce CM, Vecchione A. E2F1-regulated microRNAs impair TGFbeta-dependent cell-cycle arrest and apoptosis in gastric cancer. *Cancer cell*. 2008;13(3):272-86. Epub 2008/03/11. doi: 10.1016/j.ccr.2008.02.013. PubMed PMID: 18328430.
215. Smith AL, Iwanaga R, Drasin DJ, Micalizzi DS, Vartuli RL, Tan AC, Ford HL. The miR-106b-25 cluster targets Smad7, activates TGF-beta signaling, and induces EMT and tumor initiating cell characteristics downstream of Six1 in human breast cancer. *Oncogene*. 2012;31(50):5162-71. Epub 2012/01/31. doi: 10.1038/onc.2012.11. PubMed PMID: 22286770; PMCID: PMC3342483.
216. Brier B, Moses HL. Tumour microenvironment: TGFbeta: the molecular Jekyll and Hyde of cancer. *Nat Rev Cancer*. 2006;6(7):506-20. Epub 2006/06/24. doi: 10.1038/nrc1926. PubMed PMID: 16794634.
217. Lin WW, Karin M. A cytokine-mediated link between innate immunity, inflammation, and cancer. *The Journal of clinical investigation*. 2007;117(5):1175-83. Epub 2007/05/04. doi: 10.1172/jci31537. PubMed PMID: 17476347; PMCID: PMC1857251.
218. Li MO, Wan YY, Sanjabi S, Robertson AK, Flavell RA. Transforming growth factor-beta regulation of immune responses. *Annual review of immunology*. 2006;24:99-146. Epub 2006/03/23. doi: 10.1146/annurev.immunol.24.021605.090737. PubMed PMID: 16551245.
219. Neuzillet C, Tijeras-Raballand A, Cohen R, Cros J, Faivre S, Raymond E, de Gramont A. Targeting the TGFβ pathway for cancer therapy. *Pharmacology & therapeutics*. 2015;147:22-31. doi: <http://dx.doi.org/10.1016/j.pharmthera.2014.11.001>.
220. Brenner C, Deplus R, Didelot C, Lorient A, Vire E, De Smet C, Gutierrez A, Danovi D, Bernard D, Boon T, Pelicci PG, Amati B, Kouzarides T, de Launoit Y, Di Croce L, Fuks F. Myc represses transcription through recruitment of DNA methyltransferase corepressor. *The EMBO journal*. 2005;24(2):336-46. Epub 2004/12/24. doi: 10.1038/sj.emboj.7600509. PubMed PMID: 15616584; PMCID: PMC545804.
221. Lo RS, Wotton D, Massague J. Epidermal growth factor signaling via Ras controls the Smad transcriptional co-repressor TGIF. *The EMBO journal*. 2001;20(1-2):128-36. Epub 2001/02/28. doi: 10.1093/emboj/20.1.128. PubMed PMID: 11226163; PMCID: PMC140192.
222. Wu S, Cetinkaya C, Munoz-Alonso MJ, von der Lehr N, Bahram F, Beuger V, Eilers M, Leon J, Larsson LG. Myc represses differentiation-induced p21CIP1 expression via Miz-1-dependent interaction with the p21 core promoter. *Oncogene*. 2003;22(3):351-60. Epub 2003/01/25. doi: 10.1038/sj.onc.1206145. PubMed PMID: 12545156.

## REFERENCES

223. Luo J, Manning BD, Cantley LC. Targeting the PI3K-Akt pathway in human cancer: rationale and promise. *Cancer cell*. 2003;4(4):257-62. Epub 2003/10/31. PubMed PMID: 14585353.
224. Taylor MA, Lee YH, Schiemann WP. Role of TGF-beta and the tumor microenvironment during mammary tumorigenesis. *Gene expression*. 2011;15(3):117-32. Epub 2012/01/25. PubMed PMID: 22268294; PMCID: PMC3723115.
225. Condeelis J, Pollard JW. Macrophages: obligate partners for tumor cell migration, invasion, and metastasis. *Cell*. 2006;124(2):263-6. Epub 2006/01/28. doi: 10.1016/j.cell.2006.01.007. PubMed PMID: 16439202.
226. Yang L, Pang Y, Moses HL. TGF-beta and immune cells: an important regulatory axis in the tumor microenvironment and progression. *Trends in immunology*. 2010;31(6):220-7. Epub 2010/06/12. doi: 10.1016/j.it.2010.04.002. PubMed PMID: 20538542; PMCID: PMC2891151.
227. Teicher BA. Transforming growth factor-beta and the immune response to malignant disease. *Clin Cancer Res*. 2007;13(21):6247-51. Epub 2007/11/03. doi: 10.1158/1078-0432.ccr-07-1654. PubMed PMID: 17975134.
228. Wrzesinski SH, Wan YY, Flavell RA. Transforming growth factor-beta and the immune response: implications for anticancer therapy. *Clin Cancer Res*. 2007;13(18 Pt 1):5262-70. Epub 2007/09/19. doi: 10.1158/1078-0432.ccr-07-1157. PubMed PMID: 17875754.
229. Thomas DA, Massague J. TGF-beta directly targets cytotoxic T cell functions during tumor evasion of immune surveillance. *Cancer cell*. 2005;8(5):369-80. Epub 2005/11/16. doi: 10.1016/j.ccr.2005.10.012. PubMed PMID: 16286245.
230. Gorelik L, Flavell RA. Transforming growth factor-beta in T-cell biology. *Nature reviews Immunology*. 2002;2(1):46-53. Epub 2002/03/22. doi: 10.1038/nri704. PubMed PMID: 11905837.
231. Pertovaara L, Kaipainen A, Mustonen T, Orpana A, Ferrara N, Saksela O, Alitalo K. Vascular endothelial growth factor is induced in response to transforming growth factor-beta in fibroblastic and epithelial cells. *J Biol Chem*. 1994;269(9):6271-4. Epub 1994/03/04. PubMed PMID: 8119973.
232. Kang Y, Siegel PM, Shu W, Drobnjak M, Kakonen SM, Cordon-Cardo C, Guise TA, Massague J. A multigenic program mediating breast cancer metastasis to bone. *Cancer cell*. 2003;3(6):537-49. Epub 2003/07/05. PubMed PMID: 12842083.
233. Goumans MJ, Valdimarsdottir G, Itoh S, Lebrin F, Larsson J, Mummery C, Karlsson S, ten Dijke P. Activin receptor-like kinase (ALK)1 is an antagonistic mediator of lateral TGFbeta/ALK5 signaling. *Molecular cell*. 2003;12(4):817-28. Epub 2003/10/29. PubMed PMID: 14580334.
234. Paszek MJ, Weaver VM. The tension mounts: mechanics meets morphogenesis and malignancy. *Journal of mammary gland biology and neoplasia*. 2004;9(4):325-42. Epub 2005/04/20. doi: 10.1007/s10911-004-1404-x. PubMed PMID: 15838603.
235. Shirakihara T, Saitoh M, Miyazono K. Differential regulation of epithelial and mesenchymal markers by deltaEF1 proteins in epithelial mesenchymal transition induced by TGF-beta. *Mol Biol Cell*. 2007;18(9):3533-44. Epub 2007/07/07. doi: 10.1091/mbc.E07-03-0249. PubMed PMID: 17615296; PMCID: PMC1951739.
236. Xu J, Lamouille S, Derynck R. TGF-beta-induced epithelial to mesenchymal transition. *Cell research*. 2009;19(2):156-72. Epub 2009/01/21. doi: 10.1038/cr.2009.5. PubMed PMID: 19153598; PMCID: PMC4720263.
237. Zhang J, Tian XJ, Xing J. Signal Transduction Pathways of EMT Induced by TGF-beta, SHH, and WNT and Their Crosstalks. *Journal of clinical medicine*. 2016;5(4). Epub 2016/04/05. doi: 10.3390/jcm5040041. PubMed PMID: 27043642; PMCID: PMC4850464.
238. Lantermann AB, Chen D, McCutcheon K, Hoffman G, Frias E, Ruddy D, Rakiec D, Korn J, McAllister G, Stegmeier F, Meyer MJ, Sharma SV. Inhibition of Casein Kinase 1 Alpha Prevents Acquired Drug Resistance to Erlotinib in EGFR-Mutant Non-Small Cell Lung Cancer. *Cancer Research*. 2015;75(22):4937-48. doi: 10.1158/0008-5472.can-15-1113.

## REFERENCES

239. Kim J, Hwan Kim S. CK2 Inhibitor CX-4945 Blocks TGF- $\beta$ 1-Induced Epithelial-to-Mesenchymal Transition in A549 Human Lung Adenocarcinoma Cells. *PLoS ONE*. 2013;8(9):e74342. doi: 10.1371/journal.pone.0074342.
240. Siddiqui-Jain A, Drygin D, Streiner N, Chua P, Pierre F, O'Brien SE, Bliesath J, Omori M, Huser N, Ho C, Proffitt C, Schwaebe MK, Ryckman DM, Rice WG, Anderes K. CX-4945, an orally bioavailable selective inhibitor of protein kinase CK2, inhibits prosurvival and angiogenic signaling and exhibits antitumor efficacy. *Cancer Res*. 2010;70(24):10288-98. Epub 2010/12/17. doi: 10.1158/0008-5472.can-10-1893. PubMed PMID: 21159648.
241. Montenarh M. Protein kinase CK2 and angiogenesis. *Adv Clin Exp Med*. 2014;23(2):153-8. Epub 2014/06/11. PubMed PMID: 24913104.
242. Trembley JH, Wang G, Unger G, Slaton J, Ahmed K. Protein kinase CK2 in health and disease: CK2: a key player in cancer biology. *Cell Mol Life Sci*. 2009;66(11-12):1858-67. Epub 2009/04/24. doi: 10.1007/s00018-009-9154-y. PubMed PMID: 19387548; PMCID: PMC4385580.
243. Romero-Oliva F, Jacob G, Allende JE. Dual effect of lysine-rich polypeptides on the activity of protein kinase CK2. *J Cell Biochem*. 2003;89(2):348-55. Epub 2003/04/22. doi: 10.1002/jcb.10493. PubMed PMID: 12704797.
244. Chua MM, Ortega CE, Sheikh A, Lee M, Abdul-Rassoul H, Hartshorn KL, Dominguez I. CK2 in Cancer: Cellular and Biochemical Mechanisms and Potential Therapeutic Target. *Pharmaceuticals (Basel, Switzerland)*. 2017;10(1). Epub 2017/01/31. doi: 10.3390/ph10010018. PubMed PMID: 28134850.
245. Filhol O, Nueda A, Martel V, Gerber-Scokaert D, Benitez MJ, Souchier C, Saoudi Y, Cochet C. Live-cell fluorescence imaging reveals the dynamics of protein kinase CK2 individual subunits. *Molecular and cellular biology*. 2003;23(3):975-87. Epub 2003/01/17. PubMed PMID: 12529402; PMCID: PMC140707.
246. Lolli G, Ranchio A, Battistutta R. Active form of the protein kinase CK2 alpha2beta2 holoenzyme is a strong complex with symmetric architecture. *ACS chemical biology*. 2014;9(2):366-71. Epub 2013/11/02. doi: 10.1021/cb400771y. PubMed PMID: 24175891.
247. Escalier D, Silvius D, Xu X. Spermatogenesis of mice lacking CK2alpha<sup>1</sup>: failure of germ cell survival and characteristic modifications of the spermatid nucleus. *Molecular reproduction and development*. 2003;66(2):190-201. Epub 2003/09/02. doi: 10.1002/mrd.10346. PubMed PMID: 12950107.
248. Buchou T, Vernet M, Blond O, Jensen HH, Pointu H, Olsen BB, Cochet C, Issinger OG, Boldyreff B. Disruption of the regulatory beta subunit of protein kinase CK2 in mice leads to a cell-autonomous defect and early embryonic lethality. *Molecular and cellular biology*. 2003;23(3):908-15. Epub 2003/01/17. PubMed PMID: 12529396; PMCID: PMC140710.
249. Lou DY, Dominguez I, Toselli P, Landesman-Bollag E, O'Brien C, Seldin DC. The alpha catalytic subunit of protein kinase CK2 is required for mouse embryonic development. *Molecular and cellular biology*. 2008;28(1):131-9. Epub 2007/10/24. doi: 10.1128/mcb.01119-07. PubMed PMID: 17954558; PMCID: PMC2223292.
250. Schneider HR, Reichert GH, Issinger OG. Enhanced casein kinase II activity during mouse embryogenesis. Identification of a 110-kDa phosphoprotein as the major phosphorylation product in mouse embryos and Krebs II mouse ascites tumor cells. *European journal of biochemistry*. 1986;161(3):733-8. Epub 1986/12/15. PubMed PMID: 3466791.
251. Filhol O, Cochet C. Protein kinase CK2 in health and disease: Cellular functions of protein kinase CK2: a dynamic affair. *Cell Mol Life Sci*. 2009;66(11-12):1830-9. Epub 2009/04/24. doi: 10.1007/s00018-009-9151-1. PubMed PMID: 19387551.

## REFERENCES

252. Franchin C, Borgo C, Zaramella S, Cesaro L, Arrigoni G, Salvi M, Pinna LA. Exploring the CK2 Paradox: Restless, Dangerous, Dispensable. *Pharmaceuticals* (Basel, Switzerland). 2017;10(1). Epub 2017/01/25. doi: 10.3390/ph10010011. PubMed PMID: 28117670.
253. Graham KC, Litchfield DW. The regulatory beta subunit of protein kinase CK2 mediates formation of tetrameric CK2 complexes. *J Biol Chem*. 2000;275(7):5003-10. Epub 2000/02/15. PubMed PMID: 10671540.
254. Meggio F, Boldyreff B, Issinger OG, Pinna LA. Casein kinase 2 down-regulation and activation by polybasic peptides are mediated by acidic residues in the 55-64 region of the beta-subunit. A study with calmodulin as phosphorylatable substrate. *Biochemistry*. 1994;33(14):4336-42. Epub 1994/04/12. PubMed PMID: 8155651.
255. Montenarh M. Cellular regulators of protein kinase CK2. *Cell and tissue research*. 2010;342(2):139-46. Epub 2010/10/27. doi: 10.1007/s00441-010-1068-3. PubMed PMID: 20976471.
256. Litchfield DW. Protein kinase CK2: structure, regulation and role in cellular decisions of life and death. *The Biochemical journal*. 2003;369(Pt 1):1-15. Epub 2002/10/25. doi: 10.1042/bj20021469. PubMed PMID: 12396231; PMCID: PMC1223072.
257. Guerra B, Issinger OG. Protein kinase CK2 and its role in cellular proliferation, development and pathology. *Electrophoresis*. 1999;20(2):391-408. Epub 1999/04/10. doi: 10.1002/(sici)1522-2683(19990201)20:2<391::aid-elps391>3.0.co;2-n. PubMed PMID: 10197447.
258. Faust M, Montenarh M. Subcellular localization of protein kinase CK2. A key to its function? *Cell and tissue research*. 2000;301(3):329-40. Epub 2000/09/20. PubMed PMID: 10994779.
259. Tawfic S, Davis AT, Faust RA, Gapany M, Ahmed K. Association of protein kinase CK2 with nuclear matrix: influence of method of preparation of nuclear matrix. *J Cell Biochem*. 1997;64(3):499-504. Epub 1997/03/01. PubMed PMID: 9057107.
260. Faust M, Jung M, Gunther J, Zimmermann R, Montenarh M. Localization of individual subunits of protein kinase CK2 to the endoplasmic reticulum and to the Golgi apparatus. *Molecular and cellular biochemistry*. 2001;227(1-2):73-80. Epub 2002/02/06. PubMed PMID: 11827177.
261. Filhol O, Martiel JL, Cochet C. Protein kinase CK2: a new view of an old molecular complex. *EMBO reports*. 2004;5(4):351-5. Epub 2004/04/03. doi: 10.1038/sj.embor.7400115. PubMed PMID: 15060571; PMCID: PMC1299026.
262. Ahmed K. Nuclear matrix and protein kinase CK2 signaling. *Critical reviews in eukaryotic gene expression*. 1999;9(3-4):329-36. Epub 2000/01/29. PubMed PMID: 10651249.
263. Ahmed K, Gerber DA, Cochet C. Joining the cell survival squad: an emerging role for protein kinase CK2. *Trends Cell Biol*. 2002;12(5):226-30. Epub 2002/06/14. PubMed PMID: 12062170.
264. Filhol O, Cochet C, Chambaz EM. Cytoplasmic and nuclear distribution of casein kinase II: characterization of the enzyme uptake by bovine adrenocortical nuclear preparation. *Biochemistry*. 1990;29(42):9928-36. Epub 1990/10/23. PubMed PMID: 2271631.
265. Pinna LA, Allende JE. Protein kinase CK2 in health and disease: Protein kinase CK2: an ugly duckling in the kinome pond. *Cell Mol Life Sci*. 2009;66(11-12):1795-9. Epub 2009/04/24. doi: 10.1007/s00018-009-9148-9. PubMed PMID: 19387554.
266. Kelliher MA, Seldin DC, Leder P. Tal-1 induces T cell acute lymphoblastic leukemia accelerated by casein kinase IIalpha. *The EMBO journal*. 1996;15(19):5160-6. Epub 1996/10/01. PubMed PMID: 8895560; PMCID: PMC452259.

## REFERENCES

267. Seldin DC, Leder P. Casein kinase II alpha transgene-induced murine lymphoma: relation to theileriosis in cattle. *Science*. 1995;267(5199):894-7. Epub 1995/02/10. PubMed PMID: 7846532.
268. Landesman-Bollag E, Channavajhala PL, Cardiff RD, Seldin DC. p53 deficiency and misexpression of protein kinase CK2alpha collaborate in the development of thymic lymphomas in mice. *Oncogene*. 1998;16(23):2965-74. Epub 1998/07/14. doi: 10.1038/sj.onc.1201854. PubMed PMID: 9662328.
269. Ortega CE, Seidner Y, Dominguez I. Mining CK2 in cancer. *PLoS One*. 2014;9(12):e115609. Epub 2014/12/30. doi: 10.1371/journal.pone.0115609. PubMed PMID: 25541719; PMCID: PMC4277308.
270. Bae JS, Park SH, Kim KM, Kwon KS, Kim CY, Lee HK, Park BH, Park HS, Lee H, Moon WS, Chung MJ, Sylvester KG, Jang KY. CK2alpha phosphorylates DBC1 and is involved in the progression of gastric carcinoma and predicts poor survival of gastric carcinoma patients. *Int J Cancer*. 2015;136(4):797-809. Epub 2014/06/26. doi: 10.1002/ijc.29043. PubMed PMID: 24962073.
271. Ruzzene M, Pinna LA. Addiction to protein kinase CK2: a common denominator of diverse cancer cells? *Biochimica et biophysica acta*. 2010;1804(3):499-504. Epub 2009/08/12. doi: 10.1016/j.bbapap.2009.07.018. PubMed PMID: 19665589.
272. Venerando A, Ruzzene M, Pinna LA. Casein kinase: the triple meaning of a misnomer. *The Biochemical journal*. 2014;460(2):141-56. Epub 2014/05/16. doi: 10.1042/bj20140178. PubMed PMID: 24825444.
273. Vazquez F, Grossman SR, Takahashi Y, Rokas MV, Nakamura N, Sellers WR. Phosphorylation of the PTEN tail acts as an inhibitory switch by preventing its recruitment into a protein complex. *J Biol Chem*. 2001;276(52):48627-30. Epub 2001/11/15. doi: 10.1074/jbc.C100556200. PubMed PMID: 11707428.
274. Torres J, Pulido R. The tumor suppressor PTEN is phosphorylated by the protein kinase CK2 at its C terminus. Implications for PTEN stability to proteasome-mediated degradation. *J Biol Chem*. 2001;276(2):993-8. Epub 2000/10/18. doi: 10.1074/jbc.M009134200. PubMed PMID: 11035045.
275. Di Maira G, Salvi M, Arrigoni G, Marin O, Sarno S, Brustolon F, Pinna LA, Ruzzene M. Protein kinase CK2 phosphorylates and upregulates Akt/PKB. Cell death and differentiation. 2005;12(6):668-77. Epub 2005/04/09. doi: 10.1038/sj.cdd.4401604. PubMed PMID: 15818404.
276. Park JH, Kim JJ, Bae YS. Involvement of PI3K-AKT-mTOR pathway in protein kinase CKII inhibition-mediated senescence in human colon cancer cells. *Biochem Biophys Res Commun*. 2013;433(4):420-5. Epub 2013/03/26. doi: 10.1016/j.bbrc.2013.02.108. PubMed PMID: 23523798.
277. Ritt DA, Zhou M, Conrads TP, Veenstra TD, Copeland TD, Morrison DK. CK2 is a component of the KSR1 scaffold complex that contributes to Raf kinase activation. *Current biology : CB*. 2007;17(2):179-84. Epub 2006/12/19. doi: 10.1016/j.cub.2006.11.061. PubMed PMID: 17174095.
278. Zheng Y, Qin H, Frank SJ, Deng L, Litchfield DW, Tefferi A, Pardanani A, Lin FT, Li J, Sha B, Benveniste EN. A CK2-dependent mechanism for activation of the JAK-STAT signaling pathway. *Blood*. 2011;118(1):156-66. Epub 2011/04/30. doi: 10.1182/blood-2010-01-266320. PubMed PMID: 21527517; PMCID: PMC3139382.
279. Dominguez I, Sonenshein GE, Seldin DC. Protein kinase CK2 in health and disease: CK2 and its role in Wnt and NF-kappaB signaling: linking development and cancer. *Cell Mol Life Sci*. 2009;66(11-12):1850-7. Epub 2009/04/24. doi: 10.1007/s00018-009-9153-z. PubMed PMID: 19387549; PMCID: PMC3905806.
280. Bailly K, Soulet F, Leroy D, Amalric F, Bouche G. Uncoupling of cell proliferation and differentiation activities of basic fibroblast growth factor. *FASEB journal : official publication of*

## REFERENCES

- the Federation of American Societies for Experimental Biology. 2000;14(2):333-44. Epub 2000/02/05. PubMed PMID: 10657989.
281. Bonnet H, Filhol O, Truchet I, Brethenou P, Cochet C, Amalric F, Bouche G. Fibroblast growth factor-2 binds to the regulatory beta subunit of CK2 and directly stimulates CK2 activity toward nucleolin. *J Biol Chem.* 1996;271(40):24781-7. Epub 1996/10/04. PubMed PMID: 8798749.
282. Dominguez I, Mizuno J, Wu H, Imbrie GA, Symes K, Seldin DC. A role for CK2alpha/beta in *Xenopus* early embryonic development. *Molecular and cellular biochemistry.* 2005;274(1-2):125-31. Epub 2005/12/14. PubMed PMID: 16342412.
283. Jia H, Liu Y, Xia R, Tong C, Yue T, Jiang J, Jia J. Casein kinase 2 promotes Hedgehog signaling by regulating both smoothed and *Cubitus interruptus*. *J Biol Chem.* 2010;285(48):37218-26. Epub 2010/09/30. doi: 10.1074/jbc.M110.174565. PubMed PMID: 20876583; PMCID: PMC2988328.
284. Ji H, Wang J, Nika H, Hawke D, Keezer S, Ge Q, Fang B, Fang X, Fang D, Litchfield DW, Aldape K, Lu Z. EGF-induced ERK activation promotes CK2-mediated disassociation of alpha-Catenin from beta-Catenin and transactivation of beta-Catenin. *Molecular cell.* 2009;36(4):547-59. Epub 2009/11/28. doi: 10.1016/j.molcel.2009.09.034. PubMed PMID: 19941816; PMCID: PMC2784926.
285. Gotz C, Kartarius S, Schwar G, Montenarh M. Phosphorylation of mdm2 at serine 269 impairs its interaction with the retinoblastoma protein. *International journal of oncology.* 2005;26(3):801-8. Epub 2005/02/11. PubMed PMID: 15703839.
286. Prowald A, Schuster N, Montenarh M. Regulation of the DNA binding of p53 by its interaction with protein kinase CK2. *FEBS letters.* 1997;408(1):99-104. Epub 1997/05/12. PubMed PMID: 9180277.
287. Cox ML, Meek DW. Phosphorylation of serine 392 in p53 is a common and integral event during p53 induction by diverse stimuli. *Cellular signalling.* 2010;22(3):564-71. Epub 2009/11/26. doi: 10.1016/j.cellsig.2009.11.014. PubMed PMID: 19932175.
288. Keller DM, Lu H. p53 serine 392 phosphorylation increases after UV through induction of the assembly of the CK2.hSPT16.SSRP1 complex. *J Biol Chem.* 2002;277(51):50206-13. Epub 2002/10/24. doi: 10.1074/jbc.M209820200. PubMed PMID: 12393879.
289. St-Denis NA, Litchfield DW. Protein kinase CK2 in health and disease: From birth to death: the role of protein kinase CK2 in the regulation of cell proliferation and survival. *Cell Mol Life Sci.* 2009;66(11-12):1817-29. Epub 2009/04/24. doi: 10.1007/s00018-009-9150-2. PubMed PMID: 19387552.
290. Guo C, Davis AT, Yu S, Tawfic S, Ahmed K. Role of protein kinase CK2 in phosphorylation nucleosomal proteins in relation to transcriptional activity. *Molecular and cellular biochemistry.* 1999;191(1-2):135-42. Epub 1999/03/27. PubMed PMID: 10094402.
291. Barz T, Ackermann K, Dubois G, Eils R, Pyerin W. Genome-wide expression screens indicate a global role for protein kinase CK2 in chromatin remodeling. *J Cell Sci.* 2003;116(Pt 8):1563-77. Epub 2003/03/18. PubMed PMID: 12640040.
292. Alghisi GC, Roberts E, Cardenas ME, Gasser SM. The regulation of DNA topoisomerase II by casein kinase II. *Cellular & molecular biology research.* 1994;40(5-6):563-71. Epub 1994/01/01. PubMed PMID: 7735331.
293. Trembley JH, Tatsumi S, Sakashita E, Loyer P, Slaughter CA, Suzuki H, Endo H, Kidd VJ, Mayeda A. Activation of pre-mRNA splicing by human RNPS1 is regulated by CK2 phosphorylation. *Molecular and cellular biology.* 2005;25(4):1446-57. Epub 2005/02/03. doi: 10.1128/mcb.25.4.1446-1457.2005. PubMed PMID: 15684395; PMCID: PMC547998.
294. Panova TB, Panov KI, Russell J, Zomerdiik JC. Casein kinase 2 associates with initiation-competent RNA polymerase I and has multiple roles in ribosomal DNA transcription. *Molecular*

## REFERENCES

- and cellular biology. 2006;26(16):5957-68. Epub 2006/08/02. doi: 10.1128/mcb.00673-06. PubMed PMID: 16880508; PMCID: PMC1592790.
295. Escargueil AE, Plisov SY, Filhol O, Cochet C, Larsen AK. Mitotic phosphorylation of DNA topoisomerase II alpha by protein kinase CK2 creates the MPM-2 phosphoepitope on Ser-1469. *J Biol Chem*. 2000;275(44):34710-8. Epub 2000/08/16. doi: 10.1074/jbc.M005179200. PubMed PMID: 10942766.
296. Tawfic S, Yu S, Wang H, Faust R, Davis A, Ahmed K. Protein kinase CK2 signal in neoplasia. *Histology and histopathology*. 2001;16(2):573-82. Epub 2001/05/03. PubMed PMID: 11332713.
297. Strom CE, Mortusewicz O, Finch D, Parsons JL, Lagerqvist A, Johansson F, Schultz N, Erixon K, Dianov GL, Helleday T. CK2 phosphorylation of XRCC1 facilitates dissociation from DNA and single-strand break formation during base excision repair. *DNA repair*. 2011;10(9):961-9. Epub 2011/08/16. doi: 10.1016/j.dnarep.2011.07.004. PubMed PMID: 21840775.
298. Scaglioni PP, Yung TM, Cai LF, Erdjument-Bromage H, Kaufman AJ, Singh B, Teruya-Feldstein J, Tempst P, Pandolfi PP. A CK2-dependent mechanism for degradation of the PML tumor suppressor. *Cell*. 2006;126(2):269-83. Epub 2006/07/29. doi: 10.1016/j.cell.2006.05.041. PubMed PMID: 16873060.
299. Fragoso R, Barata JT. Kinases, tails and more: regulation of PTEN function by phosphorylation. *Methods (San Diego, Calif)*. 2015;77-78:75-81. Epub 2014/12/03. doi: 10.1016/j.ymeth.2014.10.015. PubMed PMID: 25448482.
300. Lu H, Yan C, Quan XX, Yang X, Zhang J, Bian Y, Chen Z, Van Waes C. CK2 phosphorylates and inhibits TAp73 tumor suppressor function to promote expression of cancer stem cell genes and phenotype in head and neck cancer. *Neoplasia*. 2014;16(10):789-800. Epub 2014/11/08. doi: 10.1016/j.neo.2014.08.014. PubMed PMID: 25379016; PMCID: PMC4212254.
301. Kim KJ, Cho KD, Jang KY, Kim HA, Kim HK, Lee HK, Im SY. Platelet-activating factor enhances tumour metastasis via the reactive oxygen species-dependent protein kinase casein kinase 2-mediated nuclear factor-kappaB activation. *Immunology*. 2014;143(1):21-32. Epub 2014/03/19. doi: 10.1111/imm.12283. PubMed PMID: 24628121; PMCID: PMC4137952.
302. Drygin D, Ho CB, Omori M, Bliesath J, Proffitt C, Rice R, Siddiqui-Jain A, O'Brien S, Padgett C, Lim JK, Anderes K, Rice WG, Ryckman D. Protein kinase CK2 modulates IL-6 expression in inflammatory breast cancer. *Biochem Biophys Res Commun*. 2011;415(1):163-7. Epub 2011/10/27. doi: 10.1016/j.bbrc.2011.10.046. PubMed PMID: 22027148.
303. Su YW, Xie TX, Sano D, Myers JN. IL-6 stabilizes Twist and enhances tumor cell motility in head and neck cancer cells through activation of casein kinase 2. *PLoS One*. 2011;6(4):e19412. Epub 2011/05/12. doi: 10.1371/journal.pone.0019412. PubMed PMID: 21559372; PMCID: PMC3084854.
304. Aparicio-Siegmund S, Sommer J, Monhasery N, Schwanbeck R, Keil E, Finkenstadt D, Pfeiffer K, Rose-John S, Scheller J, Garbers C. Inhibition of protein kinase II (CK2) prevents induced signal transducer and activator of transcription (STAT) 1/3 and constitutive STAT3 activation. *Oncotarget*. 2014;5(8):2131-48. Epub 2014/04/20. doi: 10.18632/oncotarget.1852. PubMed PMID: 24742922; PMCID: PMC4039151.
305. Koch S, Capaldo CT, Hilgarth RS, Fournier B, Parkos CA, Nusrat A. Protein kinase CK2 is a critical regulator of epithelial homeostasis in chronic intestinal inflammation. *Mucosal immunology*. 2013;6(1):136-45. Epub 2012/07/06. doi: 10.1038/mi.2012.57. PubMed PMID: 22763408; PMCID: PMC3517934.
306. Ponce DP, Yefi R, Cabello P, Maturana JL, Niechi I, Silva E, Galindo M, Antonelli M, Marcelain K, Armisen R, Tapia JC. CK2 functionally interacts with AKT/PKB to promote the beta-catenin-dependent expression of survivin and enhance cell survival. *Molecular and cellular*

## REFERENCES

- biochemistry. 2011;356(1-2):127-32. Epub 2011/07/08. doi: 10.1007/s11010-011-0965-4. PubMed PMID: 21735093.
307. Ravi R, Bedi A. Sensitization of tumor cells to Apo2 ligand/TRAIL-induced apoptosis by inhibition of casein kinase II. *Cancer Res.* 2002;62(15):4180-5. Epub 2002/08/03. PubMed PMID: 12154014.
308. Wang G, Ahmad KA, Ahmed K. Role of protein kinase CK2 in the regulation of tumor necrosis factor-related apoptosis inducing ligand-induced apoptosis in prostate cancer cells. *Cancer Res.* 2006;66(4):2242-9. Epub 2006/02/21. doi: 10.1158/0008-5472.can-05-2772. PubMed PMID: 16489027.
309. Zheng Y, McFarland BC, Drygin D, Yu H, Bellis SL, Kim H, Bredel M, Benveniste EN. Targeting protein kinase CK2 suppresses prosurvival signaling pathways and growth of glioblastoma. *Clin Cancer Res.* 2013;19(23):6484-94. Epub 2013/09/17. doi: 10.1158/1078-0432.ccr-13-0265. PubMed PMID: 24036851; PMCID: PMC3932633.
310. Ulges A, Klein M, Reuter S, Gerlitzki B, Hoffmann M, Grebe N, Staudt V, Stergiou N, Bohn T, Bruhl TJ, Muth S, Yurugi H, Rajalingam K, Bellinghausen I, Tuettenberg A, Hahn S, Reissig S, Haben I, Zipp F, Waisman A, Probst HC, Beilhack A, Buchou T, Filhol-Cochet O, Boldyreff B, Breloer M, Jonuleit H, Schild H, Schmitt E, Bopp T. Protein kinase CK2 enables regulatory T cells to suppress excessive TH2 responses in vivo. *Nature immunology.* 2015;16(3):267-75. Epub 2015/01/20. doi: 10.1038/ni.3083. PubMed PMID: 25599562.
311. Sawant DV, Dent AL. It takes CK2 to suppress TH2. *Nature immunology.* 2015;16(3):224-5. Epub 2015/02/18. doi: 10.1038/ni.3104. PubMed PMID: 25689435.
312. Romero-Oliva F, Allende JE. Protein p21(WAF1/CIP1) is phosphorylated by protein kinase CK2 in vitro and interacts with the amino terminal end of the CK2 beta subunit. *J Cell Biochem.* 2001;81(3):445-52. Epub 2001/03/20. PubMed PMID: 11255227.
313. Tapia JC, Bolanos-Garcia VM, Sayed M, Allende CC, Allende JE. Cell cycle regulatory protein p27KIP1 is a substrate and interacts with the protein kinase CK2. *J Cell Biochem.* 2004;91(5):865-79. Epub 2004/03/23. doi: 10.1002/jcb.20027. PubMed PMID: 15034923.
314. Dixit D, Sharma V, Ghosh S, Mehta VS, Sen E. Inhibition of Casein kinase-2 induces p53-dependent cell cycle arrest and sensitizes glioblastoma cells to tumor necrosis factor (TNFalpha)-induced apoptosis through SIRT1 inhibition. *Cell death & disease.* 2012;3:e271. Epub 2012/02/10. doi: 10.1038/cddis.2012.10. PubMed PMID: 22318540; PMCID: PMC3288342.
315. Krock BL, Skuli N, Simon MC. Hypoxia-Induced Angiogenesis: Good and Evil. *Genes & Cancer.* 2011;2(12):1117-33. doi: 10.1177/1947601911423654. PubMed PMID: PMC3411127.
316. Hubert A, Paris S, Piret JP, Ninane N, Raes M, Michiels C. Casein kinase 2 inhibition decreases hypoxia-inducible factor-1 activity under hypoxia through elevated p53 protein level. *J Cell Sci.* 2006;119(Pt 16):3351-62. Epub 2006/08/03. doi: 10.1242/jcs.03069. PubMed PMID: 16882692.
317. Mottet D, Ruys SP, Demazy C, Raes M, Michiels C. Role for casein kinase 2 in the regulation of HIF-1 activity. *Int J Cancer.* 2005;117(5):764-74. Epub 2005/06/16. doi: 10.1002/ijc.21268. PubMed PMID: 15957168.
318. Noy P, Sawasdichai A, Jayaraman PS, Gaston K. Protein kinase CK2 inactivates PRH/Hhex using multiple mechanisms to de-repress VEGF-signalling genes and promote cell survival. *Nucleic acids research.* 2012;40(18):9008-20. Epub 2012/07/31. doi: 10.1093/nar/gks687. PubMed PMID: 22844093; PMCID: PMC3467080.
319. An S, Kyoung M, Allen JJ, Shokat KM, Benkovic SJ. Dynamic regulation of a metabolic multi-enzyme complex by protein kinase CK2. *J Biol Chem.* 2010;285(15):11093-9. Epub 2010/02/17. doi: 10.1074/jbc.M110.101139. PubMed PMID: 20157113; PMCID: PMC2856985.

## REFERENCES

320. Al Quobaili F, Montenarh M. CK2 and the regulation of the carbohydrate metabolism. *Metabolism: clinical and experimental*. 2012;61(11):1512-7. Epub 2012/08/25. doi: 10.1016/j.metabol.2012.07.011. PubMed PMID: 22917893.
321. Taylor KM, Hiscox S, Nicholson RI, Hogstrand C, Kille P. Protein kinase CK2 triggers cytosolic zinc signaling pathways by phosphorylation of zinc channel ZIP7. *Science signaling*. 2012;5(210):ra11. Epub 2012/02/10. doi: 10.1126/scisignal.2002585. PubMed PMID: 22317921; PMCID: PMC3428905.
322. Filhol O, Giacosa S, Wallez Y, Cochet C. Protein kinase CK2 in breast cancer: the CK2beta regulatory subunit takes center stage in epithelial plasticity. *Cell Mol Life Sci*. 2015;72(17):3305-22. Epub 2015/05/21. doi: 10.1007/s00018-015-1929-8. PubMed PMID: 25990538.
323. Chon HJ, Bae KJ, Lee Y, Kim J. The casein kinase 2 inhibitor, CX-4945, as an anti-cancer drug in treatment of human hematological malignancies. *Frontiers in pharmacology*. 2015;6:70. Epub 2015/04/16. doi: 10.3389/fphar.2015.00070. PubMed PMID: 25873900; PMCID: PMC4379896.
324. Borgo C, Franchin C, Scalco S, Bosello-Travain V, Donella-Deana A, Arrigoni G, Salvi M, Pinna LA. Generation and quantitative proteomics analysis of CK2alpha/alpha'(-/-) cells. *Scientific reports*. 2017;7:42409. Epub 2017/02/18. doi: 10.1038/srep42409. PubMed PMID: 28209983.
325. Liu B, Bernard B, Wu JH. Impact of EGFR point mutations on the sensitivity to gefitinib: insights from comparative structural analyses and molecular dynamics simulations. *Proteins*. 2006;65(2):331-46. Epub 2006/08/24. doi: 10.1002/prot.21111. PubMed PMID: 16927343.
326. Eberhard DA, Johnson BE, Amler LC, Goddard AD, Heldens SL, Herbst RS, Ince WL, Janne PA, Januario T, Johnson DH, Klein P, Miller VA, Ostland MA, Ramies DA, Sebisano D, Stinson JA, Zhang YR, Seshagiri S, Hillan KJ. Mutations in the epidermal growth factor receptor and in KRAS are predictive and prognostic indicators in patients with non-small-cell lung cancer treated with chemotherapy alone and in combination with erlotinib. *Journal of clinical oncology : official journal of the American Society of Clinical Oncology*. 2005;23(25):5900-9. Epub 2005/07/27. doi: 10.1200/jco.2005.02.857. PubMed PMID: 16043828.
327. Bryant JL, Britson J, Balko JM, William M, Timmons R, Frolov A, Black EP. A microRNA gene expression signature predicts response to erlotinib in epithelial cancer cell lines and targets EMT. *Br J Cancer*. 2012;106(1):148-56. doi: 10.1038/bjc.2011.465. PubMed PMID: 22045191; PMCID: 3251842.
328. Balko JM, Potti A, Saunders C, Stromberg A, Haura EB, Black EP. Gene expression patterns that predict sensitivity to epidermal growth factor receptor tyrosine kinase inhibitors in lung cancer cell lines and human lung tumors. *BMC genomics*. 2006;7:289. Epub 2006/11/14. doi: 10.1186/1471-2164-7-289. PubMed PMID: 17096850; PMCID: Pmc1660550.
329. Balko JM, Jones BR, Coakley VL, Black EP. MEK and EGFR inhibition demonstrate synergistic activity in EGFR-dependent NSCLC. *Cancer biology & therapy*. 2009;8(6):522-30. Epub 2009/03/24. doi: 10.4161/cbt.8.6.7690. PubMed PMID: 19305165.
330. Britson JS, Barton F, Balko JM, Black EP. Deregulation of DUSP activity in EGFR-mutant lung cancer cell lines contributes to sustained ERK1/2 signaling. *Biochem Biophys Res Commun*. 2009;390(3):849-54. Epub 2009/10/20. doi: 10.1016/j.bbrc.2009.10.061. PubMed PMID: 19836351.
331. Stamatkin C, Ratermann KL, Overley CW, Black EP. Inhibition of class IA PI3K enzymes in non-small cell lung cancer cells uncovers functional compensation among isoforms. *Cancer biology & therapy*. 2015;16(9):1341-52. Epub 2015/07/16. doi: 10.1080/15384047.2015.1070986. PubMed PMID: 26176612; PMCID: PMC4622503.
332. Gregory PA, Bracken CP, Smith E, Bert AG, Wright JA, Roslan S, Morris M, Wyatt L, Farshid G, Lim Y-Y, Lindeman GJ, Shannon MF, Drew PA, Khew-Goodall Y, Goodall GJ. An autocrine TGF-

## REFERENCES

- $\beta$ /ZEB/miR-200 signaling network regulates establishment and maintenance of epithelial-mesenchymal transition. *Molecular Biology of the Cell*. 2011;22(10):1686-98. doi: 10.1091/mbc.E11-02-0103.
333. Kasai H, Allen JT, Mason RM, Kamimura T, Zhang Z. TGF-beta1 induces human alveolar epithelial to mesenchymal cell transition (EMT). *Respir Res*. 2005;6:56. doi: 10.1186/1465-9921-6-56. PubMed PMID: 15946381; PMCID: 1177991.
334. The Cancer Genome Atlas Research N. Comprehensive molecular profiling of lung adenocarcinoma. *Nature*. 2014;511(7511):543-50. doi: 10.1038/nature13385  
<http://www.nature.com/nature/journal/v511/n7511/abs/nature13385.html#supplementary-information>.
335. Kim ES, Herbst RS, Wistuba II, Lee JJ, Blumenschein GR, Jr., Tsao A, Stewart DJ, Hicks ME, Erasmus J, Jr., Gupta S, Alden CM, Liu S, Tang X, Khuri FR, Tran HT, Johnson BE, Heymach JV, Mao L, Fossella F, Kies MS, Papadimitrakopoulou V, Davis SE, Lippman SM, Hong WK. The BATTLE trial: personalizing therapy for lung cancer. *Cancer discovery*. 2011;1(1):44-53. Epub 2012/05/16. doi: 10.1158/2159-8274.cd-10-0010. PubMed PMID: 22586319.
336. Pao W, Miller VA. Epidermal growth factor receptor mutations, small-molecule kinase inhibitors, and non-small-cell lung cancer: current knowledge and future directions. *Journal of clinical oncology : official journal of the American Society of Clinical Oncology*. 2005;23(11):2556-68. doi: 10.1200/JCO.2005.07.799. PubMed PMID: 15767641.
337. Bartel DP. MicroRNAs: target recognition and regulatory functions. *Cell*. 2009;136(2):215-33. doi: 10.1016/j.cell.2009.01.002. PubMed PMID: 19167326.
338. Meyer-Rochow GY, Jackson NE, Conaglen JV, Whittle DE, Kunnimalaiyaan M, Chen H, Westin G, Sandgren J, Stalberg P, Khanafshar E, Shibru D, Duh QY, Clark OH, Kebebew E, Gill AJ, Clifton-Bligh R, Robinson BG, Benn DE, Sidhu SB. MicroRNA profiling of benign and malignant pheochromocytomas identifies novel diagnostic and therapeutic targets. *Endocr Relat Cancer*. 2010;17(3):835-46. doi: 10.1677/ERC-10-0142. PubMed PMID: 20621999.
339. Burk U, Schubert J, Wellner U, Schmalhofer O, Vincan E, Spaderna S, Brabletz T. A reciprocal repression between ZEB1 and members of the miR-200 family promotes EMT and invasion in cancer cells. *EMBO reports*. 2008;9(6):582-9. doi: 10.1038/embor.2008.74. PubMed PMID: 18483486; PMCID: 2396950.
340. Xue L, Su D, Li D, Gao W, Yuan R, Pang W. miR-200 Regulates Epithelial-Mesenchymal Transition in Anaplastic Thyroid Cancer via EGF/EGFR Signaling. *Cell biochemistry and biophysics*. 2014. Epub 2014/12/30. doi: 10.1007/s12013-014-0435-1. PubMed PMID: 25542369.
341. Rajabi H, Alam M, Takahashi H, Kharbanda A, Guha M, Ahmad R, Kufe D. MUC1-C oncoprotein activates the ZEB1/miR-200c regulatory loop and epithelial-mesenchymal transition. *Oncogene*. 2014;33(13):1680-9. Epub 2013/04/16. doi: 10.1038/onc.2013.114. PubMed PMID: 23584475; PMCID: Pmc3783575.
342. Wong N, Wang X. miRDB: an online resource for microRNA target prediction and functional annotations. *Nucleic acids research*. 2015;43(Database issue):D146-52. Epub 2014/11/08. doi: 10.1093/nar/gku1104. PubMed PMID: 25378301; PMCID: PMC4383922.
343. Katsuno Y, Lamouille S, Derynck R. TGF-beta signaling and epithelial-mesenchymal transition in cancer progression. *Current opinion in oncology*. 2013;25(1):76-84. Epub 2012/12/01. doi: 10.1097/CCO.0b013e32835b6371. PubMed PMID: 23197193.
344. Blahna MT, Hata A. Smad-mediated regulation of microRNA biosynthesis. *FEBS letters*. 2012;586(14):1906-12. doi: 10.1016/j.febslet.2012.01.041. PubMed PMID: 22306316.
345. Ren S, Su C, Wang Z, Li J, Fan L, Li B, Li X, Zhao C, Wu C, Hou L, He Y, Gao G, Chen X, Ren J, Li A, Xu G, Zhou X, Zhou C, Schmid-Bindert G. Epithelial phenotype as a predictive marker for

## REFERENCES

- response to EGFR-TKIs in non-small cell lung cancer patients with wild-type EGFR. *Int J Cancer*. 2014. Epub 2014/04/29. doi: 10.1002/ijc.28925. PubMed PMID: 24771540.
346. Camara J, Jarai G. Epithelial-mesenchymal transition in primary human bronchial epithelial cells is Smad-dependent and enhanced by fibronectin and TNF-alpha. *Fibrogenesis & tissue repair*. 2010;3(1):2. Epub 2010/01/07. doi: 10.1186/1755-1536-3-2. PubMed PMID: 20051102; PMCID: Pmc2821296.
347. Marinescu VD, Kohane IS, Riva A. MAPPER: a search engine for the computational identification of putative transcription factor binding sites in multiple genomes. *BMC Bioinformatics*. 2005;6:79. doi: 10.1186/1471-2105-6-79. PubMed PMID: 15799782; PMCID: 1131891.
348. Marinescu VD, Kohane IS, Riva A. The MAPPER database: a multi-genome catalog of putative transcription factor binding sites. *Nucleic acids research*. 2005;33(suppl 1):D91-D7. doi: 10.1093/nar/gki103.
349. Zawel L, Le Dai J, Buckhaults P, Zhou S, Kinzler KW, Vogelstein B, Kern SE. Human Smad3 and Smad4 Are Sequence-Specific Transcription Activators. *Molecular cell*. 1998;1(4):611-7. doi: [http://dx.doi.org/10.1016/S1097-2765\(00\)80061-1](http://dx.doi.org/10.1016/S1097-2765(00)80061-1).
350. Long X, Miano JM. Transforming growth factor-beta1 (TGF-beta1) utilizes distinct pathways for the transcriptional activation of microRNA 143/145 in human coronary artery smooth muscle cells. *J Biol Chem*. 2011;286(34):30119-29. doi: 10.1074/jbc.M111.258814. PubMed PMID: 21712382; PMCID: 3191051.
351. Taniguchi C, Maitra A. It's a SMAD/SMAD World. *Cell*. 161(6):1245-6. doi: 10.1016/j.cell.2015.05.030.
352. Xu J, Acharya S, Sahin O, Zhang Q, Saito Y, Yao J, Wang H, Li P, Zhang L, Lowery FJ, Kuo WL, Xiao Y, Ensor J, Sahin AA, Zhang XH, Hung MC, Zhang JD, Yu D. 14-3-3zeta turns TGF-beta's function from tumor suppressor to metastasis promoter in breast cancer by contextual changes of Smad partners from p53 to Gli2. *Cancer cell*. 2015;27(2):177-92. doi: 10.1016/j.ccell.2014.11.025. PubMed PMID: 25670079; PMCID: 4325275.
353. Jolly MK, Tripathi SC, Jia D, Mooney SM, Celiktas M, Hanash SM, Mani SA, Pienta KJ, Ben-Jacob E, Levine H. Stability of the hybrid epithelial/mesenchymal phenotype. *Oncotarget*. 2016;7(19):27067-84. Epub 2016/03/24. doi: 10.18632/oncotarget.8166. PubMed PMID: 27008704.
354. Miettinen PJ, Ebner R, Lopez AR, Derynck R. TGF-beta induced transdifferentiation of mammary epithelial cells to mesenchymal cells: involvement of type I receptors. *The Journal of cell biology*. 1994;127(6 Pt 2):2021-36. Epub 1994/12/01. PubMed PMID: 7806579; PMCID: PMC2120317.
355. David CJ, Huang YH, Chen M, Su J, Zou Y, Bardeesy N, Iacobuzio-Donahue CA, Massague J. TGF-beta Tumor Suppression through a Lethal EMT. *Cell*. 2016;164(5):1015-30. doi: 10.1016/j.cell.2016.01.009. PubMed PMID: 26898331; PMCID: PMC4801341.
356. Lei L, Huang Y, Gong W. miR-205 promotes the growth, metastasis and chemoresistance of NSCLC cells by targeting PTEN. *Oncology reports*. 2013;30(6):2897-902. Epub 2013/10/03. doi: 10.3892/or.2013.2755. PubMed PMID: 24084898.
357. Cui R, Meng W, Sun H-L, Kim T, Ye Z, Fassan M, Jeon Y-J, Li B, Vicentini C, Peng Y, Lee TJ, Luo Z, Liu L, Xu D, Tili E, Jin V, Middleton J, Chakravarti A, Lautenschlaeger T, Croce CM. MicroRNA-224 promotes tumor progression in nonsmall cell lung cancer. *Proceedings of the National Academy of Sciences*. 2015. doi: 10.1073/pnas.1502068112.
358. O'Connor JW, Gomez EW. Biomechanics of TGFbeta-induced epithelial-mesenchymal transition: implications for fibrosis and cancer. *Clinical and translational medicine*. 2014;3:23.

## REFERENCES

- Epub 2014/08/07. doi: 10.1186/2001-1326-3-23. PubMed PMID: 25097726; PMCID: Pmc4114144.
359. Ribeiro AS, Paredes J. P-Cadherin Linking Breast Cancer Stem Cells and Invasion: A Promising Marker to Identify an "Intermediate/Metastable" EMT State. *Frontiers in oncology*. 2014;4:371. Epub 2015/01/21. doi: 10.3389/fonc.2014.00371. PubMed PMID: 25601904; PMCID: Pmc4283504.
360. Maeda M, Johnson K, Wheelock M. Cadherin switching is essential for behavioral but not morphological changes during and epithelial-mesenchyme transition. *J Cell Sci*. 2005;118:873 - 87. PubMed PMID: doi:10.1242/jcs.01634.
361. Mizuguchi Y, Specht S, Lunz JG, 3rd, Isse K, Corbitt N, Takizawa T, Demetris AJ. Cooperation of p300 and PCAF in the control of microRNA 200c/141 transcription and epithelial characteristics. *PLoS One*. 2012;7(2):e32449. Epub 2012/03/03. doi: 10.1371/journal.pone.0032449. PubMed PMID: 22384255; PMCID: Pmc3284570.
362. Inman GJ, Nicolas FJ, Callahan JF, Harling JD, Gaster LM, Reith AD, Laping NJ, Hill CS. SB-431542 is a potent and specific inhibitor of transforming growth factor-beta superfamily type I activin receptor-like kinase (ALK) receptors ALK4, ALK5, and ALK7. *Molecular pharmacology*. 2002;62(1):65-74. PubMed PMID: 12065756.
363. Pardali K, Kowanetz M, Heldin CH, Moustakas A. Smad pathway-specific transcriptional regulation of the cell cycle inhibitor p21(WAF1/Cip1). *J Cell Physiol*. 2005;204(1):260-72. Epub 2005/02/04. doi: 10.1002/jcp.20304. PubMed PMID: 15690394.
364. Mukherjee P, Winter SL, Alexandrow MG. Cell Cycle Arrest by Transforming Growth Factor  $\beta$ 1 near G1/S Is Mediated by Acute Abrogation of Prereplication Complex Activation Involving an Rb-MCM Interaction. *Molecular and cellular biology*. 2010;30(3):845-56. doi: 10.1128/mcb.01152-09.
365. Robinson KW, Sandler AB. EGFR tyrosine kinase inhibitors: difference in efficacy and resistance. *Current oncology reports*. 2013;15(4):396-404. Epub 2013/05/16. doi: 10.1007/s11912-013-0323-7. PubMed PMID: 23674236.
366. Ren S, Su C, Wang Z, Li J, Fan L, Li B, Li X, Zhao C, Wu C, Hou L, He Y, Gao G, Chen X, Ren J, Li A, Xu G, Zhou X, Zhou C, Schmid-Bindert G. Epithelial phenotype as a predictive marker for response to EGFR-TKIs in non-small cell lung cancer patients with wild-type EGFR. *Int J Cancer*. 2014;135(12):2962-71. Epub 2014/04/29. doi: 10.1002/ijc.28925. PubMed PMID: 24771540.
367. Gober MK, Collard JP, Thompson K, Black EP. A microRNA signature of response to erlotinib is descriptive of TGF $\beta$  behaviour in NSCLC. *Scientific reports*. 2017;7(1):s41598-017. doi: 10.1038/s41598-017-04097-7.
368. Izumchenko E, Chang X, Michailidi C, Kagohara L, Ravi R, Paz K, Brait M, Hoque M, Ling S, Bedi A, Sidransky D. The TGFbeta-miR200-MIG6 pathway orchestrates the EMT-associated kinase switch that induces resistance to EGFR inhibitors. *Cancer Res*. 2014;74(14):3995-4005. Epub 2014/05/17. doi: 10.1158/0008-5472.can-14-0110. PubMed PMID: 24830724; PMCID: Pmc4122100.
369. Melisi D, Ishiyama S, Scwabas GM, Fleming JB, Xia Q, Tortora G, Abbruzzese JL, Chiao PJ. LY2109761, a novel transforming growth factor beta receptor type I and type II dual inhibitor, as a therapeutic approach to suppressing pancreatic cancer metastasis. *Mol Cancer Ther*. 2008;7(4):829-40. Epub 2008/04/17. doi: 10.1158/1535-7163.mct-07-0337. PubMed PMID: 18413796; PMCID: PMC3088432.
370. Schliekelman MJ, Taguchi A, Zhu J, Dai X, Rodriguez J, Celiktaş M, Zhang Q, Chin A, Wong C-H, Wang H, McFerrin L, Selamat SA, Yang C, Kroh EM, Garg KS, Behrens C, Gazdar AF, Laird-Offringa IA, Tewari M, Wistuba II, Thiery JP, Hanash SM. Molecular Portraits of Epithelial,

## REFERENCES

- Mesenchymal, and Hybrid States in Lung Adenocarcinoma and Their Relevance to Survival. *Cancer Research*. 2015;75(9):1789-800. doi: 10.1158/0008-5472.can-14-2535.
371. Zarzynska JM. Two faces of TGF-beta1 in breast cancer. *Mediators of inflammation*. 2014;2014:141747. Epub 2014/06/04. doi: 10.1155/2014/141747. PubMed PMID: 24891760; PMCID: Pmc4033515.
372. Cox AD, Der CJ, Philips MR. Targeting RAS Membrane Association: Back to the Future for Anti-RAS Drug Discovery? *Clin Cancer Res*. 2015;21(8):1819-27. Epub 2015/04/17. doi: 10.1158/1078-0432.ccr-14-3214. PubMed PMID: 25878363; PMCID: PMC4400837.
373. Correll RN, Pang C, Finlin BS, Dailey AM, Satin J, Andres DA. Plasma membrane targeting is essential for Rem-mediated Ca<sup>2+</sup> channel inhibition. *J Biol Chem*. 2007;282(39):28431-40. Epub 2007/08/10. doi: 10.1074/jbc.M706176200. PubMed PMID: 17686775; PMCID: PMC3063359.
374. Acunzo M, Romano G, Nigita G, Veneziano D, Fattore L, Lagana A, Zanesi N, Fadda P, Fassan M, Rizzotto L, Kladney R, Coppola V, Croce CM. Selective targeting of point-mutated KRAS through artificial microRNAs. *Proceedings of the National Academy of Sciences of the United States of America*. 2017;114(21):E4203-e12. Epub 2017/05/10. doi: 10.1073/pnas.1620562114. PubMed PMID: 28484014.
375. Bournet B, Buscail C, Muscari F, Cordelier P, Buscail L. Targeting KRAS for diagnosis, prognosis, and treatment of pancreatic cancer: Hopes and realities. *European journal of cancer (Oxford, England : 1990)*. 2016;54:75-83. Epub 2016/01/07. doi: 10.1016/j.ejca.2015.11.012. PubMed PMID: 26735353.
376. Ohm AM, Tan AC, Heasley LE, Reyland ME. Co-dependency of PKCdelta and K-Ras: inverse association with cytotoxic drug sensitivity in KRAS mutant lung cancer. *Oncogene*. 2017. Epub 2017/04/04. doi: 10.1038/onc.2017.27. PubMed PMID: 28368426.
377. Stewart EL, Tan SZ, Liu G, Tsao MS. Known and putative mechanisms of resistance to EGFR targeted therapies in NSCLC patients with EGFR mutations-a review. *Transl Lung Cancer Res*. 2015;4(1):67-81. Epub 2015/03/26. doi: 10.3978/j.issn.2218-6751.2014.11.06. PubMed PMID: 25806347; PMCID: PMC4367712.
378. Balko JM, Black EP. Do the genes tell us the path of most resistance? *Cancer biology & therapy*. 2011;11(2):213-5. Epub 2011/01/26. doi: 10.4161/cbt.11.2.13922. PubMed PMID: 21263213.
379. Rodon J, Carducci M, Sepulveda-Sanchez JM, Azaro A, Calvo E, Seoane J, Brana I, Sicart E, Gueorguieva I, Cleverly A, Pillay NS, Desai D, Estrem ST, Paz-Ares L, Holdhoff M, Blakeley J, Lahn MM, Baselga J. Pharmacokinetic, pharmacodynamic and biomarker evaluation of transforming growth factor-beta receptor I kinase inhibitor, galunisertib, in phase 1 study in patients with advanced cancer. *Investigational new drugs*. 2015;33(2):357-70. Epub 2014/12/23. doi: 10.1007/s10637-014-0192-4. PubMed PMID: 25529192; PMCID: PMC4387272.
380. Gray GK, McFarland BC, Rowse AL, Gibson SA, Benveniste EN. Therapeutic CK2 inhibition attenuates diverse prosurvival signaling cascades and decreases cell viability in human breast cancer cells. *Oncotarget*. 2014;5(15):6484-96. Epub 2014/08/26. PubMed PMID: 25153725; PMCID: PMC4171645.
381. Franceschini A, Szklarczyk D, Frankild S, Kuhn M, Simonovic M, Roth A, Lin J, Minguez P, Bork P, von Mering C, Jensen LJ. STRING v9.1: protein-protein interaction networks, with increased coverage and integration. *Nucleic acids research*. 2013;41(Database issue):D808-15. doi: 10.1093/nar/gks1094. PubMed PMID: 23203871; PMCID: 3531103.
382. Gentleman RC, Carey VJ, Bates DM, Bolstad B, Dettling M, Dudoit S, Ellis B, Gautier L, Ge Y, Gentry J, Hornik K, Hothorn T, Huber W, Iacus S, Irizarry R, Leisch F, Li C, Maechler M, Rossini AJ, Sawitzki G, Smith C, Smyth G, Tierney L, Yang JY, Zhang J. Bioconductor: open software development for computational biology and bioinformatics. *Genome biology*. 2004;5(10):R80.

## REFERENCES

- Epub 2004/10/06. doi: 10.1186/gb-2004-5-10-r80. PubMed PMID: 15461798; PMCID: PMC545600.
383. Shannon P, Markiel A, Ozier O, Baliga NS, Wang JT, Ramage D, Amin N, Schwikowski B, Ideker T. Cytoscape: a software environment for integrated models of biomolecular interaction networks. *Genome research*. 2003;13(11):2498-504. Epub 2003/11/05. doi: 10.1101/gr.1239303. PubMed PMID: 14597658; PMCID: PMC403769.
384. Longabaugh WJ. Combing the hairball with BioFabric: a new approach for visualization of large networks. *BMC Bioinformatics*. 2012;13(1):275. doi: 10.1186/1471-2105-13-275.
385. Csardi G, Nepusz T. The igraph software package for complex network research. *InterJournal, Complex Systems*. 2006;1695(5):1-9.
386. Pons P, Latapy M, editors. Computing communities in large networks using random walks. *International Symposium on Computer and Information Sciences*; 2005: Springer.
387. Szklarczyk D, Franceschini A, Wyder S, Forslund K, Heller D, Huerta-Cepas J, Simonovic M, Roth A, Santos A, Tsafou KP, Kuhn M, Bork P, Jensen LJ, von Mering C. STRING v10: protein-protein interaction networks, integrated over the tree of life. *Nucleic acids research*. 2015;43(Database issue):D447-52. Epub 2014/10/30. doi: 10.1093/nar/gku1003. PubMed PMID: 25352553; PMCID: PMC4383874.
388. Bian Y, Han J, Kannabiran V, Mohan S, Cheng H, Friedman J, Zhang L, VanWaes C, Chen Z. MEK inhibitor PD-0325901 overcomes resistance to CK2 inhibitor CX-4945 and exhibits anti-tumor activity in head and neck cancer. *International journal of biological sciences*. 2015;11(4):411-22. Epub 2015/03/24. doi: 10.7150/ijbs.10745. PubMed PMID: 25798061; PMCID: PMC4366640.
389. Naeger LK, Goodwin EC, Hwang ES, DeFilippis RA, Zhang H, DiMaio D. Bovine papillomavirus E2 protein activates a complex growth-inhibitory program in p53-negative HT-3 cervical carcinoma cells that includes repression of cyclin A and cdc25A phosphatase genes and accumulation of hypophosphorylated retinoblastoma protein. *Cell growth & differentiation : the molecular biology journal of the American Association for Cancer Research*. 1999;10(6):413-22. Epub 1999/07/07. PubMed PMID: 10392903.
390. Ma L, Huang Y, Zhu W, Zhou S, Zhou J, Zeng F, Liu X, Zhang Y, Yu J. An integrated analysis of miRNA and mRNA expressions in non-small cell lung cancers. *PLoS One*. 2011;6(10):e26502. Epub 2011/11/03. doi: 10.1371/journal.pone.0026502. PubMed PMID: 22046296; PMCID: PMC3203153.
391. Stabile LP, Lyker JS, Gubish CT, Zhang W, Grandis JR, Siegfried JM. Combined targeting of the estrogen receptor and the epidermal growth factor receptor in non-small cell lung cancer shows enhanced antiproliferative effects. *Cancer Res*. 2005;65(4):1459-70. Epub 2005/03/01. doi: 10.1158/0008-5472.can-04-1872. PubMed PMID: 15735034.
392. Li J, Sordella R, Powers S. Effectors and potential targets selectively upregulated in human KRAS-mutant lung adenocarcinomas. *Scientific reports*. 2016;6:27891. Epub 2016/06/16. doi: 10.1038/srep27891. PubMed PMID: 27301828; PMCID: PMC4908391.
393. Kalathur M, Toso A, Chen J, Revandkar A, Danzer-Baltzer C, Guccini I, Alajati A, Sarti M, Pinton S, Brambilla L, Di Mitri D, Carbone G, Garcia-Escudero R, Padova A, Magnoni L, Tarditi A, Maccari L, Malusa F, Kalathur RK, L AP, Cozza G, Ruzzene M, Delaleu N, Catapano CV, Frew IJ, Alimonti A. A chemogenomic screening identifies CK2 as a target for pro-senescence therapy in PTEN-deficient tumours. *Nature communications*. 2015;6:7227. Epub 2015/06/19. doi: 10.1038/ncomms8227. PubMed PMID: 26085373.
394. Ohashi K, Sequist LV, Arcila ME, Moran T, Chmielecki J, Lin YL, Pan Y, Wang L, de Stanchina E, Shien K, Aoe K, Toyooka S, Kiura K, Fernandez-Cuesta L, Fidias P, Yang JCH, Miller VA, Riely GJ, Kris MG, Engelman JA, Vnencak-Jones CL, Dias-Santagata D, Ladanyi M, Pao W. Lung cancers with acquired resistance to EGFR inhibitors occasionally harbor BRAF gene mutations but lack

## REFERENCES

- mutations in KRAS, NRAS, or MEK1. *Proceedings of the National Academy of Sciences of the United States of America*. 2012;109(31):E2127-33. doi: 10.1073/pnas.1203530109. PubMed PMID: 22773810; PMCID: PMC3411967.
395. So KS, Kim CH, Rho JK, Kim SY, Choi YJ, Song JS, Kim WS, Choi CM, Chun YJ, Lee JC. Autophagosome-mediated EGFR down-regulation induced by the CK2 inhibitor enhances the efficacy of EGFR-TKI on EGFR-mutant lung cancer cells with resistance by T790M. *PLoS One*. 2014;9(12):e114000. Epub 2014/12/09. doi: 10.1371/journal.pone.0114000. PubMed PMID: 25486409; PMCID: PMC4259313.
396. Bliesath J, Huser N, Omori M, Bunag D, Proffitt C, Streiner N, Ho C, Siddiqui-Jain A, O'Brien SE, Lim JK, Ryckman DM, Anderes K, Rice WG, Drygin D. Combined inhibition of EGFR and CK2 augments the attenuation of PI3K-Akt-mTOR signaling and the killing of cancer cells. *Cancer Lett*. 2012;322(1):113-8. Epub 2012/03/06. doi: 10.1016/j.canlet.2012.02.032. PubMed PMID: 22387988.
397. Migliore C, Giordano S. Resistance to targeted therapies: a role for microRNAs? *Trends in molecular medicine*. 2013;19(10):633-42. doi: 10.1016/j.molmed.2013.08.002. PubMed PMID: 24012193.
398. Huang L, Fu L. Mechanisms of resistance to EGFR tyrosine kinase inhibitors. *Acta Pharmaceutica Sinica B*. 2015;5(5):390-401. doi: 10.1016/j.apsb.2015.07.001. PubMed PMID: PMC4629442.
399. Misumi K, Sun J, Kinomura A, Miyata Y, Okada M, Tashiro S. Enhanced gefitinib-induced repression of the epidermal growth factor receptor pathway by ataxia telangiectasia-mutated kinase inhibition in non-small-cell lung cancer cells. *Cancer science*. 2016;107(4):444-51. Epub 2016/01/31. doi: 10.1111/cas.12899. PubMed PMID: 26825989; PMCID: PMC4832868.
400. Hoellein A, Pickhard A, von Keitz F, Schoeffmann S, Piontek G, Rudelius M, Baumgart A, Wagenpfeil S, Peschel C, Dechow T, Bier H, Keller U. Aurora kinase inhibition overcomes cetuximab resistance in squamous cell cancer of the head and neck. *Oncotarget*. 2011;2(8):599-609. Epub 2011/08/26. doi: 10.18632/oncotarget.311. PubMed PMID: 21865609; PMCID: PMC3248211.
401. Foster SA, Whalen DM, Ozen A, Wongchenko MJ, Yin J, Yen I, Schaefer G, Mayfield JD, Chmielecki J, Stephens PJ, Albacker LA, Yan Y, Song K, Hatzivassiliou G, Eigenbrot C, Yu C, Shaw AS, Manning G, Skelton NJ, Hymowitz SG, Malek S. Activation Mechanism of Oncogenic Deletion Mutations in BRAF, EGFR, and HER2. *Cancer cell*. 2016;29(4):477-93. Epub 2016/03/22. doi: 10.1016/j.ccell.2016.02.010. PubMed PMID: 26996308.
402. Dempke WC, Heinemann V. Ras mutational status is a biomarker for resistance to EGFR inhibitors in colorectal carcinoma. *Anticancer research*. 2010;30(11):4673-7. Epub 2010/12/01. PubMed PMID: 21115922.
403. van der Veeken J, Oliveira S, Schiffelers RM, Storm G, van Bergen En Henegouwen PM, Roovers RC. Crosstalk between epidermal growth factor receptor- and insulin-like growth factor-1 receptor signaling: implications for cancer therapy. *Current cancer drug targets*. 2009;9(6):748-60. Epub 2009/09/17. PubMed PMID: 19754359.
404. Yoo J, Rodriguez Perez CE, Nie W, Edwards RA, Sinnett-Smith J, Rozengurt E. TNF-alpha induces upregulation of EGFR expression and signaling in human colonic myofibroblasts. *American journal of physiology Gastrointestinal and liver physiology*. 2012;302(8):G805-14. Epub 2012/02/04. doi: 10.1152/ajpgi.00522.2011. PubMed PMID: 22301110; PMCID: PMC3355565.
405. Shostak K, Chariot A. EGFR and NF- $\kappa$ B: partners in cancer. *Trends in molecular medicine*. 21(6):385-93. doi: 10.1016/j.molmed.2015.04.001.
406. Ungefroren H, Groth S, Sebens S, Lehnert H, Gieseler F, Fandrich F. Differential roles of Smad2 and Smad3 in the regulation of TGF-beta1-mediated growth inhibition and cell migration

## REFERENCES

- in pancreatic ductal adenocarcinoma cells: control by Rac1. *Molecular cancer*. 2011;10:67. doi: 10.1186/1476-4598-10-67. PubMed PMID: 21624123; PMCID: 3112431.
407. Boutet M, Gauthier L, Leclerc M, Gros G, de Montpreville V, Théret N, Donnadiou E, Mami-Chouaib F. TGF $\beta$  Signaling Intersects with CD103 Integrin Signaling to Promote T-Lymphocyte Accumulation and Antitumor Activity in the Lung Tumor Microenvironment. *Cancer Research*. 2016;76(7):1757-69. doi: 10.1158/0008-5472.can-15-1545.

**Madeline Krentz Gober**

**EDUCATION:**

**The University of Georgia, Athens, GA**

*Bachelors of Science in Genetics (May 2012)*

**POSITIONS HELD:**

**Department of Pharmaceutical Sciences – The University of Kentucky**

From Aug. 2012 to Present

*Doctoral Candidate (Mentor: Dr. Esther P. Black)*

**Department of Pharmaceutical and Biomedical Sciences - The University of Georgia**

From Jan. 2010 to July 2012

*Undergraduate Researcher (Mentor: Dr. Raj Govindarajan)*

**AWARDS AND HONORS:**

- Awarded the 2016-2017 AAPS Foundation Fellowship
- Awarded the 2016-2017 Kentucky Opportunity Fellowship
- Awarded the 2015-2016 AAPS Foundation Graduate Student Fellowship
- Awarded the 2015-2016 UK Graduate School Academic Year Fellowship
- Awarded the 2015 S. Elizabeth Helton Memorial Fellowship
- Selected for podia presentation entitled “A microRNA signature of response to erlotinib is impacted by the EMT- inducing cytokine TGF $\beta$ 1” given at 2015 Experimental Biology Conference (March 2015)
- Awarded First Place in Annual “Two-Minute Elevator Speech” Competition (UK Drug Discovery and Development Symposium – September 2014)
- Awarded Third Place in Drug Discovery and Development Symposium Poster Competition (September 2014)
- Selected for podia presentation entitled “Interacting miRNA and mRNA genes identify potential therapeutic targets for NSCLC” given at PGSRM Conference (June 2014)
- Awarded the 2014-2015 Kentucky Opportunity Fellowship
- Awarded the 2014 S. Elizabeth Helton Memorial Fellowship
- Awarded Second Place in Annual “Two-Minute Elevator Speech” Competition (October 2013)

**PROFESSIONAL ASSOCIATIONS:**

## VITA

- The American Association for Cancer Research (AACR) – Associate Member
- The American Association of Pharmaceutical Scientists (AAPS) – Graduate Student Member
- **The American Society for Pharmacology and Experimental Therapeutics (ASPET) – Graduate Student Member**

## **PUBLICATIONS:**

- **Krentz Gober M**, Collard JP, Thompson K, Black EP. A microRNA signature of response to erlotinib is descriptive of TGF $\beta$  behaviour in NSCLC. *Scientific Reports*. Manuscript in Accepted and in Editorial Review.
- Bhutia YD, Hung SW, **Krentz M**, Patel D, Lovin D, et al. (2013) Differential Processing of let-7a Precursors Influences RRM2 Expression and Chemosensitivity in Pancreatic Cancer: Role of LIN-28 and SET Oncoprotein. *PLoS ONE* 8(1): e53436. doi:10.1371/journal.pone.0053436